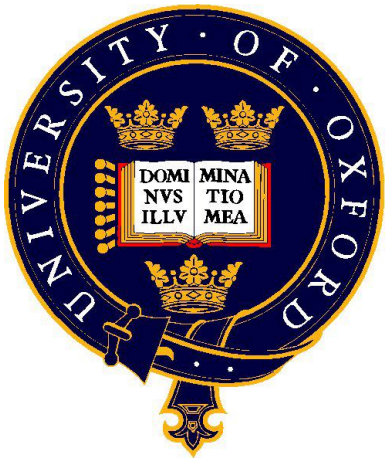

Evaluation of Immune Correlates to TB Vaccines

Thesis submitted for the degree of Doctor of Philosophy

Leanne Marsay

Wolfson College, Michaelmas Term 2011

Word count 41,082

Evaluation of Immune Correlates to TB Vaccines

Leanne Marsay, Wolfson College, University of Oxford

Thesis submitted for the degree of Doctor of Philosophy, Michaelmas Term 2011

Abstract

Development of an improved TB vaccine is hindered by the lack of a correlate of protection. Efficacy of TB vaccines in humans can only be assessed by expensive and time consuming trials within TB endemic areas, which are limited; therefore, it is critical that vaccines with the greatest potential to protect are selected for these trials. Mycobacterial growth inhibition assays (MGIAs) have been developed with the hope that these *in vitro* functional assays will correlate with protection, which could aid in the selection of the best vaccine candidates. Work in this thesis describes the development and evaluation of different MGIAs for their ability to detect TB vaccine induced mycobacterial growth inhibition. The mycobacterial growth indicator tube (MGIT) MGIA reproducibly demonstrated mycobacterial growth inhibition in splenocytes from BCG vaccinated compared with naïve mice, which corresponded with *in vivo* protection from *M. tb* challenge. This assay also discriminated between PBMC from naïve and BCG/BCG-MVA85A vaccinated macaques. Microarray data showed extensive differential gene expression in splenocyte responses to *ex-vivo* BCG stimulation between naïve and BCG vaccinated mice. T_H1 responses including IFN-γ with NOS2 expression were enhanced in BCG vaccinated mice, indicating a possible mechanism for mycobacterial growth inhibition in BCG vaccinated mice. Further investigation into whether the MGIT assay can be used as a correlate of protection from *M. tb* in humans and animals is warranted.

Acknowledgements

I would like to thank my supervisors Prof Helen McShane and Dr Sally Sharpe for creating this challenging but ultimately rewarding project. They were always encouraging and supportive of my ideas, including the creation of the “Marassay” (admittedly not one of my better ideas), and their advice and guidance was invaluable. Dr Helen Fletcher provided substantial technical and emotional support throughout my studies. Thank you Fletch for everything, not least for being a friend. I also received help in performing some of my experiments. Chapter 6 would not exist were it not for the efforts of Magali Kostov. Hazel Poyntz, Elena Stylianou and Kristin Griffiths helped with all my mouse work. Rachel Tanner kindly let me use her stocks of BCG for the MGIT assay and performed all of the ground work that enabled me to perform this assay. There were also a number of people who helped me out on numerous occasions, Iman Satti, Steph Harris, Ruth Thom, Simon Clark, Karen Gooch, Andrew white, Laura Sibley, Alice Marriott, Julie Furze, Phil Marsh, Ann Rawkins, Marcus Morgan and staff from the John Radcliffe hospital and Drew Worth all made my life that little bit easier. I thank Katharine Collins, Dusty McDusterson, Sumi Biswas, Sajid Javed, Jennie Latham, Slummers, Steve Welch, Debbie and Barry Atkinson and even my nemesis Checkers for making this process actually enjoyable at times. Special thanks go to Simone de Cassan who has been so helpful and so supportive, you were great. I thank my family for the happy upbringing they provided me with, and for all of their support over the last 29 years. And last but especially not least I thank poor long suffering Kevin, who bore the brunt of my foul moods and ill temper with great dignity. You made the bad times bearable, and the good times even better. Thank you.

Funding was from Oxford Biomedical Research Centre and the Health Protection Agency

Table of Contents

Table of Figures

Table of Tables

List of Abbreviations

ADC	Albumin, dextrose, and catalase
APC	Antigen presenting cells
BCG	Bacillus Calmette-Guérin
BSA	Bovine serum albumin
CD	Cluster of differentiation
CFP-10	Culture filtrate protein-10
CFSE	Carboxyfluorescein succinimidyl Ester
CFU	Colony forming units
CL3	Containment level 3
DC	Dendritic cells
DGE	Differential gene expression
DMSO	Dimethyl Sulfoxide
DNA	Deoxyribonucleic acid
DTH	Delayed type hypersensitivity
EDTA	Ethylenediaminetetraacetic acid
ELISpot	Enzyme-linked immunosorbent spot
ESAT-6	Early secretory antigen target 6
FC	Fold change
FCS	Fetal calf serum
FGF	Functional genetics facility
g	The acceleration due to gravity
GR	Growth ratio
h	Hour
HIV	Human immunodeficiency virus
HPRT	Hypoxanthine-guanine phosphoribosyltransferase
i.d.	Intra-dermal
i.m.	Intra-muscular
ICS	Intracellular cytokine staining
IFN	Interferon
IL	Interleukin
KEGG	Kyoto encyclopaedia of genes and genomes

LAM	lipoarabinomannan
LPS	Lipopolysaccharide
M. tb	Mycobacterium tuberculosis
ManLAM	Manosylated lipoarabinomannan
MDR-TB	Multi-drug resistant tuberculosis
MFI	Median fluorescent intensity
MGIA	Mycobacterial growth inhibition assay
MGIT	Mycobacterial growth indicator tube
MHC	Major histocompatibility complex
MOI	Multiplicity of infection
mRNA	Messenger ribonucleic acid
MVA	Modified vaccinia virus Ankara
NHP	Non-human primate
NK	Natural killer
NO	Nitric oxide
OADC	Oleic acid, albumin, dextrose, and catalase
OD	Optical density
PAMP	Pathogen-associated molecular patterns
PBMC	Peripheral blood mononuclear cells
PBS	Phosphate buffered saline
PCR	Polymerase chain reaction
pfu	Plaque forming units
PPD	Purified protein derivative
PRR	Pattern recognition receptors
q-PCR	Quantitative polymerase chain reaction
RBC	Red blood cell
RNA	Ribonucleic acid
RNS	Reactive nitrogen species
ROS	Reactive oxygen species
RPM	Revolutions per minute
RT	Room temperature
s.c.	Subcutaneous
SDS	Sodium Dodecyl Sulfate

SPICE	Simplified presentation of incredibly complex evaluations
ssRNA	Single stranded ribonucleic acid
TB	Tuberculosis
TCR	T-cell Receptor
T_H	T helper cell
TLR	Toll-like receptor
TNF	Tumour necrosis factor
TST	Tuberculin skin test
TTP	Time to positivity
WB	Whole blood
WHO	World Health Organisation
XDR-TB	Extensively drug resistant tuberculosis

Chapter 1

Introduction

1. Introduction

1.1 Tuberculosis

1.1.1 History of Tuberculosis

The white plague, phthisis and consumption are just some of the names used throughout history for Tuberculosis (TB), a contagious disease that has affected mankind for at least 9000 years [1]. It is estimated that during the 18th century in western Europe, 1 in every 4 deaths was due to TB [2]. Very little was known about the disease until the causative agent was discovered by Robert Koch in 1882. The agent was called the Tubercle bacillus; now known as *Mycobacterium tuberculosis* (*M. tb*).

In 1908 Leon Calmette and Camille Guérin began an epic experiment at the Pasteur Institute in Lille. They began culturing *Mycobacterium bovis (M. bovis)* in broth containing bile, potato starch and glycerol to create an attenuated form of the bacteria that could be used for vaccination against human TB. After 13 years and 230 passages, they had created Bacillus Calmette-Guérin (BCG). The bacterium was shown to be avirulent in a number of laboratory animals including guinea pigs, and was first tested in humans in 1921.

Even though the causative agent of TB disease and a vaccine had now been discovered, there was still no cure, other than the idea that fresh air and a healthy diet would help self-healing. It was not until 1943 that Schatz and Waksman discovered the drug streptomycin, which they proved was effective in halting the growth of *M. tb*. Finally, the dawn of antibiotic treatment for TB had arrived, but since then, efforts to eliminate this devastating disease have played out through the decades, and the struggle is still far from over today.

1.1.2 Outcomes of infection with M. tb

A small percentage of people exposed to *M. tb* do not become infected, although no one knows exactly what proportion of the population this is true of [3]. These individuals do not develop adaptive immune responses against *M. tb*, despite prolonged exposure to household contacts who have TB. It is likely that these individuals mount extensive innate immune responses that result in sterile clearance of *M. tb* without the involvement of cellular immunity. Other individuals may clear *M. tb* with the involvement of adaptive immune responses; this situation is complicated by the fact that these individuals do respond to *M. tb* antigen stimulation so it is clear that they have been exposed to *M. tb,* but we cannot tell whether they have cleared the infection or not.

The vast majority of individuals (90%) who become infected with *M. tb* will not entirely clear the bacteria, but their adaptive immune response is capable of walling off the infection resulting in latent infection. These individuals have a 10% chance of reactivation of the disease over the course of their lifetime, although human immunodeficiency virus (HIV) positive individuals stand a far greater chance of developing active disease at 10% per annum [4, 5]. Around 10% of those exposed to *M. tb* will not mount an adequate innate or adaptive response, so the bacteria are not effectively contained; this leads to primary TB disease.

1.1.3 Infectious cycle

M. tb is spread via aerosolised droplets that quickly dry out in air producing infectious particles containing a small number of bacteria. These particles are very small at <5µm in diameter and are easily drawn into the alveoli of the lungs. In people suffering from primary or reactivated TB, the bacteria are actively causing disease and are capable of replicating extracellularly in damaged tissues, resulting in the spread of bacteria throughout the lung and formation of cavities. If a cavity erodes into an airway, the host becomes highly contagious and is capable of transmitting TB through coughing, sneezing and speaking. It is estimated that an individual with active TB will spread the disease to 10-15 people each year [6].

1.1.4 Clinical manifestations

Although pulmonary TB is by far the most common and contagious form of the disease, most parts of the body can be affected. The symptoms of pulmonary TB generally include a persistent cough lasting more than 3 weeks, coughing up blood and or sputum, night sweats, low grade fever/chills, anorexia and wasting.

A small percentage of TB patients will develop a disseminated form of the disease known as miliary TB, which can spread throughout the body in the blood stream or lymphatics, causing distinctively small (<5mm) and numerous lesions. Infants are more likely to suffer from disseminated disease than adults. The symptoms are very similar to pulmonary TB, however, disseminated TB is a more serious condition that can lead to the infection of the heart, lungs, liver and spleen, which, if not treated will almost certainly result in death. Up to 30% of miliary TB patients will have involvement of the central nervous system [7, 8], resulting in tuberculomas and/or meningitis. Symptoms include headaches, hemiplegia, seizures, coma and eventually death if not treated.

1.1.5 Drug resistance

Treating a patient who has TB is a long and expensive process. An example of a typical course of treatment is 2 months of drug therapy with isoniazid, rifampicin, pyrazinamide, and ethambutol; then a further 4 months of just isoniazid and rifampicin alone, after which

most patients will be cured. The complicated regimen and lengthy treatment duration ultimately leads to some patients not taking the full course of antibiotics as they are prescribed, as well as some doctors not being able to give out the correct prescriptions, particularly in poor countries. This partial treatment of TB has contributed to the emergence of drug resistant strains of *M. tb*. In 1990, multi-drug resistant tuberculosis (MDR-TB) was first defined as *M. tb* strains which were resistant to both isoniazid and rifampicin *in vitro*. In 2009 there were an estimated 440,000 cases of MDR-TB worldwide.

Efforts were made to treat MDR-TB using second line drugs, but this brought about the emergence of extensively drug resistant *M. tb* (XDR-TB). In 2007, XDR-TB was quickly identified as a major challenge to global health [9-12]. XDR-TB is defined by resistance to rifampicin, isoniazid and a fluoroquinalone along with an injectable drug such as Kanamycin; it has so far been detected in 58 countries. Most recently strains have been identified that are resistant to all anti-tuberculosis drugs and as such, the nightmare scenario of totally untreatable TB has become a grim reality [13, 14].

1.1.6 HIV-TB co-infections

HIV was discovered in 1983 and was found to be the etiologic agent for acquired immunodeficiency syndrome (AIDS). Since its discovery, it is estimated by the World Health Organisation (WHO) to have killed over 25 million people. In 2009 approximately

33.3 million people were living with HIV, of these, 2.6 million were new cases. HIV is considered to be pandemic, but the majority of cases occur in sub-Saharan Africa, which unfortunately, is also a region with the highest incidence of TB.

HIV displays tropism for cells that express CD4 receptors on their surface, which means that it infects $CD4^+$ T cells, macrophages and dendritic cells (DCs). These cells are integral to the adaptive immune response and essential for controlling *M. tb* infection; once infected, the virus inserts its genome into the host cell chromosomes so that it effectively hijacks the host cell's machinery, resulting in production of more virus particles. HIV infection causes death of $CD4^+$ cells by increasing the rate of apoptosis, inducing $CD8^+$ T cell killing of infected cells and direct killing of the cells by the virus.

The loss of $CD4^+$ cells is a diagnostic marker of HIV infection and once the cell count drops to <500/µl blood, cellular immunity begins to wane resulting in opportunistic infections. Once the $CD4^+$ count is <200/µl blood, the patient is classified as having AIDS, and for patients in sub Saharan Africa it is highly likely that this will result in death from TB. Of the 1.1 million HIV-infected TB patients globally in 2009, 80% of cases were in sub-Saharan Africa. HIV is the leading cause of failure to meet TB control targets in areas of high HIV prevalence and a leading cause of death in this group.

1.1.7 Epidemiology

One third of the world's population is infected with *M. tb* (90% latent infections); in 2009 there were 9.4 million new cases or relapses of TB and 1.7 million deaths [15]. South East Asia and Africa accounted for 35% and 30% of global cases respectively; Africa has the highest incidence per capita which is almost double that of South East Asia (Fig. 1-1). The WHO estimates that of the 1.7 million deaths in 2009, 1.3 million were in HIV- patients, 380,000 were in HIV+ patients and 150,000 were caused by MDR-TB.

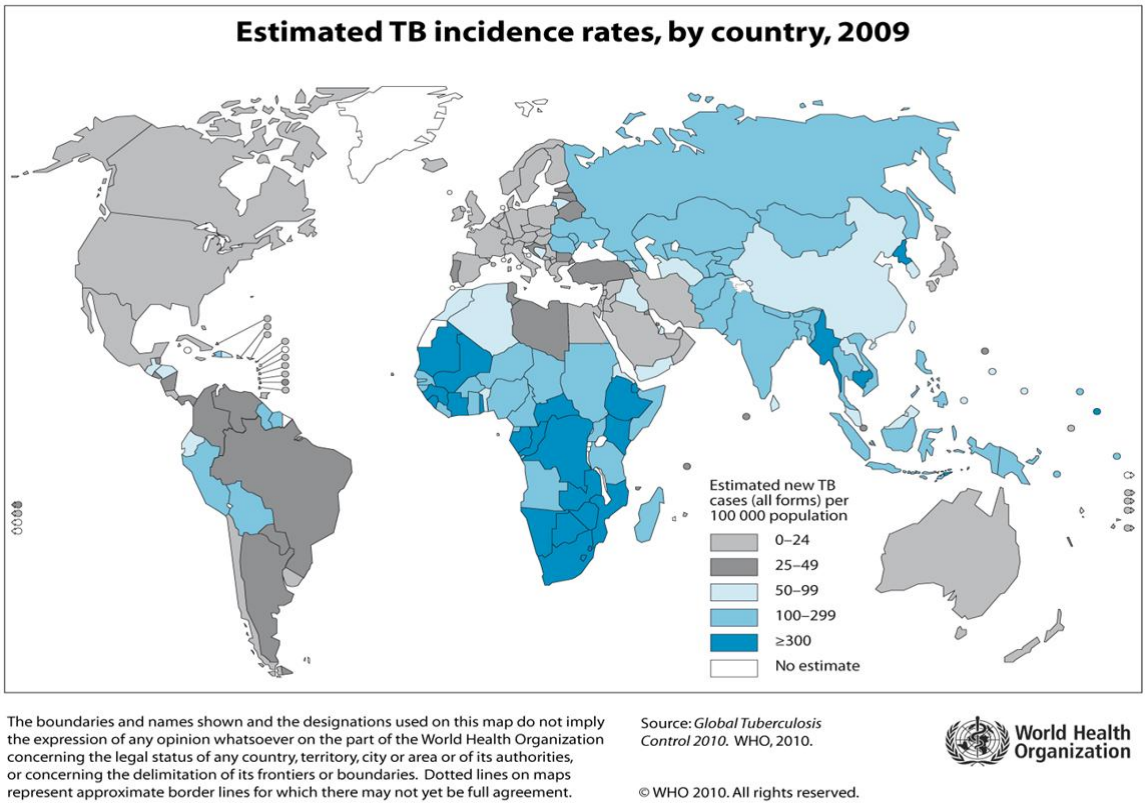

Fig. 1-1 Global incidence rates by country for 2009.
Taken from the WHO website [15]. The incidence of TB in regions of Africa and South East Asia are greater than anywhere else in the world. TB is a disease of poverty, and it is due to the lack of medical resources, prevalence of HIV and low efficacy of the BCG vaccine that these regions are suffering the most.

1.2 Mycobacteria

1.2.1 Physical attributes

All mycobacteria share a similar structure and have distinct properties that make them easily distinguishable from other types of bacteria. Mycobacteria are quite small at ~ 0.4μm wide and 1-4μm long. Their cell wall is waxy, hydrophobic, very thick and rich in mycolic acids, all of which contribute to their hardiness and impermeable nature. It is because of these attributes that there is so much difficulty in antibiotic treatment and chemical killing of these bacteria (Fig. 1-2).

Fig. 1-2 Structure of the cell wall of mycobacteria.
Adapted from Toda's Bacteriology 2007 [16]. The cytoplasmic membrane is surrounded by a layer of peptidoglycan, which is itself surrounded by a layer of arabinogalactan. Mycolic acid chains attach to the arabinogalactan and are responsible for the hydrophobicity of the bacteria. Lipoarabinomannan is an immunogenic molecule which attaches to the cytoplasmic membrane through a phosphatidylinositol anchor. Porins create water filled channels by which hydrophilic molecules can diffuse through the cell wall. Whereas lipid soluble molecules are likely to diffuse across lipid layers

All mycobacteria replicate at a relatively slow rate, however, generally speaking this family of bacteria can be divided into fast or slow growing organisms. Slow growers can take between 2-3 weeks to reach visible colonies on 7H10 agar plates, although *M. leprae* (the causative agent of leprosy) is totally uncultivable in artificial media; fast growers on the other hand are visible after only 1 week.

1.2.2 Mycobacterium tuberculosis complex

The mycobacterium tuberculosis complex is the name given to the group of mycobacteria that are capable of causing TB in either humans or animals. The complex contains *M. tb*, *M. africanum, and M. bovis* as well as a number of other species. Members of the complex are all very closely related, sharing 99% DNA sequence identity with each other; there is direct evidence that *M. tb* and *M. bovis* most likely co-evolved from a common ancestor [17]. These bacteria are all slow growers and it is believed that this property contributes to their pathogenicity. Humans are the only reservoir for *M. tb* whereas *M. bovis* is capable of causing disease in humans as well as its primary host which is cattle. *M. africanum* is only found in Western Africa and can cause TB although it is not as virulent as *M. tb* [18].

1.2.3 Mycobacterium tuberculosis

M. tb is a facultative aerobe that is capable of altering its metabolism to adapt to the environment, enabling it to grow in highly aerated liquid/solid media, but also inside host

cells under hypoxic conditions. The genome of *M. tb* is $4.4x10^6$ bp long and contains roughly 4000 different genes [19]. *M. tb* is able to change to a latent state; where it does not divide and reduces cellular functions to a minimum, resulting in less stimulation of the host immune system and survival within the granuloma.

1.2.4 Bacillus Calmette-Guérin

Although BCG is a relatively recent member of the mycobacterial family there are now many different strains that have diverged from the primary isolate of 1921. When BCG was created, there were no freezing and lyophilising processes to properly store and maintain seed stocks of the vaccine; so rolling cultures were propagated in different laboratories using the same media that had attenuated BCG in the first place.

After a total of 1173 passages (including the 230 by Calmette and Guérin) a stock of the Pasteur strain was lyophilised in 1961 [20]. This means that the bacteria had undergone a further 943 passages. Considering that Calmette had reported attenuation of the original *M. bovis* after only 15 passages, and considerably more had occurred after another 215; it is reasonable to assume that attenuation continued over the next 943 passages as well [21]. The result of this rather haphazard method of maintaining vaccine stocks is that a number of different strains are currently used to vaccinate people in different geographic locations.

Although the different strains of BCG used throughout the world are genetically different, it is unclear what effect these differences have on protective immunity. In some animal models different BCG strains confer similar levels of protection, but in others they confer varying levels of protection [22-25]. Different strains of BCG used in the same clinical trial have been shown to induce varying levels of protection and adverse effects [26-28]. All BCG strains are lacking some of the virulence factors of *M. tb*, most notably the RD1 locus, and there is clear evidence that different strains of BCG have varying virulence [29].

1.2.5 Non-tuberculous mycobacteria

Any mycobacterium that does not cause TB or leprosy is considered to be a non-tuberculous mycobacterium (NTM) otherwise known as environmental mycobacteria. Although some NTM can cause disease, usually this is only in immunosuppressed people or those with damaged lungs. There have been no documented cases of either human to human or animal to human spread of NTM. Members of this group are generally rapid growers and there are many more of them, than there are in the *M. tb* complex; also many NTM are saprophytic and live in soil or water, which means that the majority of people will encounter these bacteria throughout their daily lives. Some common NTM include *M. smegmatis and M. fortuitum.*

1.3 The innate immune response to TB

1.3.1 The first line of host defence

In vertebrates, infections result in activation of the innate immune system within minutes, this generally leads to the killing and removal of the organism. The majority of infections that a person acquires throughout their life are imperceptible due to this response. In instances where the innate response is incapable of killing the organism, it still plays an important role in delaying the spread of infection, allowing time for the adaptive immune response to become established.

1.3.2 Pathogen-associated molecular patterns

Pathogens can be identified as non-self by the repetitive structure of their surface, these structures are known collectively as pathogen-associated molecular patterns (PAMPs); receptors that recognise them are termed pattern recognition receptors (PRRs). An example of a PRR is pulmonary surfactant protein A, an antimicrobial protein of the collectin family. This PRR is present in the fluid coating the epithelial surfaces of lungs, and has been shown to opsonise *M. tb* [30, 31]. Phagocytic cells including macrophages and neutrophils have specialised cell surface receptors that bind to, and recognise pathogens, such as macrophage mannose receptor and scavenger receptors, both of which induce phagocytosis of *M. tb* [32].

1.3.3 Toll like receptors

These receptors are membrane bound PRRs that can be present on either the cell surface or the surface of endosomes. So far, 11 different toll-like receptors (TLRs) have been discovered, each binding to a different pathogen associated molecule such as single stranded RNA (ssRNA) or lipopolysaccharide (LPS). Certain TLRs are only found in specific cell types, so their activation will direct the immune response in a particular way towards the elimination of specific pathogens [33]. LAM, which is present in the cell wall of all mycobacteria has been shown to activate tumour necrosis factor-α (TNF-α) secretion in macrophages [34] via interactions between TLR-2 and CD14. The exact mechanism by which whole *M. tb* interacts with TLRs is unknown, although it is thought to involve TLR-2, TLR-6 and TLR-4 [35, 36].

1.3.4 NFκB

Binding of TLRs and other PRRs results in activation of the transcription factor NFκB via MyD88 interactions. NFκB activates the transcription of inflammatory mediators such as cytokines and chemokines; as well as up-regulating the expression of co-stimulatory molecules (CD80 and CD86) on the surface of macrophages and dendritic cells. These molecules are essential for activating naïve $CD4^+$ T cells and initiating the adaptive immune response. The cytosolic proteins nucleotide-binding oligomerization domain (NOD1 and NOD2) are capable of binding the same ligands as TLRs and can directly activate the

NFκB pathway. There is debate as to how important NOD2 is for controlling *M. tb* in mice [37, 38].

1.3.5 Complement system

The complement system is a group of plasma proteins that interact with each other and bind to pathogens aiding their phagocytosis and inducing inflammatory responses. The complement system works by sequential cleavage and activation of proteases, so from a small stimulus a rapid and successively large response is generated. The cascade can be activated by the classical, lectin or alternative pathways. *M. tb* interacts with complement via the alternative pathway, binding to spontaneously activated complement component C3 in the plasma, leading to its opsonisation and phagocytosis.

1.3.6 Monocytes/macrophages

These cells are integral to the host immune response against *M. tb*, but their involvement can be advantageous both to the host and to *M. tb*. The relationship between macrophages and *M. tb* can be thought of as a biological arms race, where they have both evolved towards a stalemate. Macrophages phagocytose *M. tb* and deploy an arsenal of antimicrobial products and processes to eliminate the bacterium; but *M. tb* is both tolerant of, and actively suppresses these mechanisms.

1.3.6.1 Phagocytosis of M. tb

Both monocytes and macrophages are capable of phagocytosing mycobacteria [39]. *M. tb* enters the alveoli of the lungs where it comes into contact with a macrophage. The complement receptors CR3, CR1 and CR4, as well as receptors for mannose, CD14 and scavenger receptors are all thought to be used by *M. tb* to gain entry into macrophages via phagocytosis [32, 40]. *In vitro* studies show accumulation of cholesterol at the site of phagocytosis that seems to permit the entry of *M. tb*, as macrophages depleted of cholesterol do not take up the bacteria [41]; it is uncertain of the relevance of this finding *in vivo.*

1.3.6.2 Phagosome maturation

Once *M. tb* is taken up by a macrophage it is contained within a vacuole called the phagosome, which usually enters a maturation process by fusing with sub-compartments of the endocytic pathway. This very complex maturation process results in a gradual increase in the inhospitable nature of the phagosome, culminating in fusion with lysosomes to create a phagolysosome (Fig. 1-3).

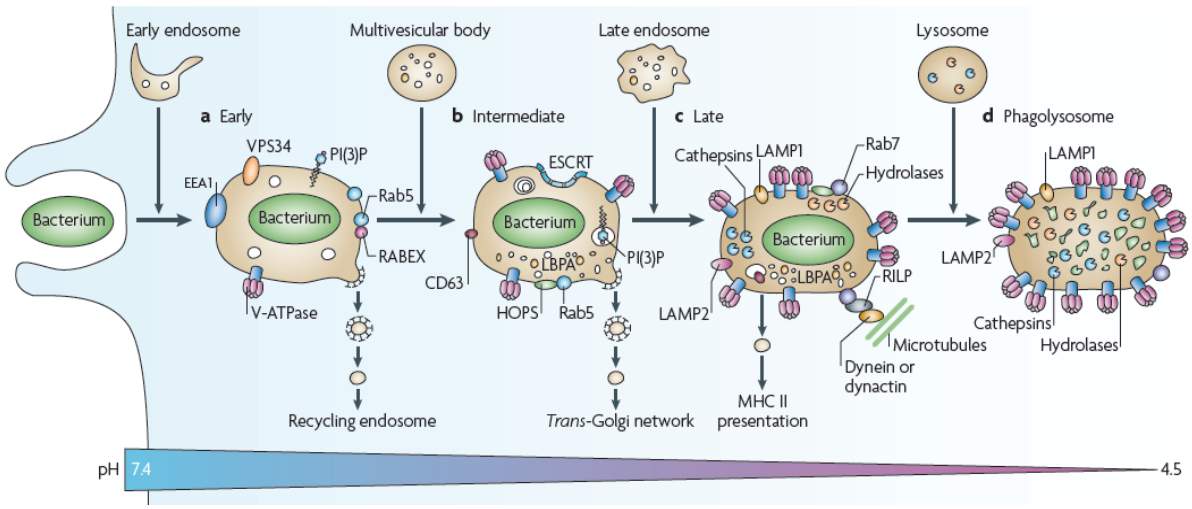

Fig. 1-3 Phagosome maturation pathway.
Taken from (Flannagan et al 2009) [42]. The maturation of the phagosome can be divided into 4 distinct stages being early, intermediate, late and finally the phagolysosome. Throughout the process there is increasing acidification of the phagosome which is achieved through proton pumping and an accumulation of hydrolases and proteases. Fusion of the phagosome with endosomes is mediated by the GTPases Rab5 and Rab7. The conditions inside the phagolysosome are practically uninhabitable for many micro-organisms.

However, as with the adaptive immune response (discussed in section 1.4), *M. tb* has evolved to subvert the killing mechanisms of the macrophage. In the early 1970s it was discovered that *M. tb* inhibits fusion of the lysosome with the phagosome [43, 44]. A lot of work has been done to elucidate the mechanisms behind this inhibition. There is evidence that early trafficking of *M. tb* infected phagosomes is normal, as iron [45, 46] and glycosphingolipids [47] are associated with the early phagosome. In phagosomes arrested by *M. tb*, there is a lack of lysosomal hydrolases and vacuolar ATPase [48], this discovery led to further investigation of this process. It was found that the *M. tb* phagosome was associated with the small GTPase Rab5 that is involved in fusion of vesicles with early

endosomes, but they were not associated with Rab7 that is involved in the late endocytic pathway and formation of lysosomes [49, 50].

There are many suppositions as to how *M. tb* blocks phagosome maturation, which include the disturbance of the Ca^{2+} signalling pathway [51], and the action of Manosylated lipoarabinomannan (ManLAM) an *M. tb* homologue of phosphatidylinositol-3 phosphate [52, 53], resulting in the lack of lysosomal hydrolases and vacuolar ATPases. Other possible mechanisms could include iron acquisition and actin disturbances caused by *M. tb* within the early phagosome. Inhibition of phagolysosome formation results in uncontrolled growth of *M. tb* within macrophages, unless they become activated by an effector T cell.

1.3.6.3 Reactive nitrogen species

Nitric oxide ($NO^{\cdot}$) and other reactive nitrogen species (RNS) derived from it, are important antimicrobial molecules that are prominent in macrophages and to a lesser extent in neutrophils. They are produced by the enzyme nitric oxide synthase (NOS2; iNOS) from L-arginine. Synthesised in the cytoplasm, they diffuse across phagosomal membranes to act on internal targets [54]. A study in 2004 demonstrated that mycobacteria are able to inhibit recruitment of NOS2 to phagosomes [55]. Inside the endosome $NO^{\cdot}$ may come into contact with reactive oxygen species (ROS) to form a number of RNS such as nitrogen dioxide

($NO_2^{\cdot}$). ROS and RNS synergise to produce highly toxic compounds that damage DNA and lipids leading to decreased replication and death of microorganisms.

It is worth noting that there has been controversy over whether human macrophages produce NO or not. Current opinion seems to be that IFN-γ induces NOS2 expression in mouse macrophages [56] whereas IFN-$\alpha\beta$, IL-4 and anti-CD23 induce NOS2 production in human macrophages [57].

1.3.7 Neutrophils

1.3.7.1 Reactive oxygen species

Neutrophils phagocytose mycobacteria but they do not produce phagolysosomes like macrophages; instead NOX2 NADPH oxidase produces ROS [58] which are synthesised inside the lumen of phagosomes and have antimicrobial properties.

1.3.7.2 Antimicrobial proteins and peptides

Neutrophils also have the capacity to degranulate, releasing preformed oxidants and proteolytic enzymes [59] that are bactericidal. The acquisition of antimicrobial proteins and peptides in phagosomes augments the killing abilities of phagocytes. Broadly, these molecules can be divided by their properties into bacteriostatic or bactericidal groups. An example of a bacteriostatic protein is lactoferrin which scavenges Fe^{2+} out of the phagosome [60], so that it is unavailable for *M. tb* house-keeping enzymes. Neutrophils

also deploy bactericidal peptides such as defensins, cathelicidins and lysozymes which damage bacterial membranes, there is evidence that these molecules are also expressed in macrophages [61].

1.3.7.3 Neutrophils and M. tb - a help or a hindrance?

The role of neutrophils in controlling *M. tb* is unclear as there are conflicting data concerning the anti-mycobacterial capabilities of these cells. One study found that greater numbers of neutrophils in blood correlate with increased restriction of mycobacterial growth *in vitro,* and circulating neutrophil numbers inversely correlated with the risk of becoming infected with *M. tb* in a cohort of TB contacts [62]. In stark contrast, Eruslanov *et al* found that neutrophils demonstrated limited capacity to control mycobacterial growth compared to macrophages. Further investigations using genetically susceptible mice showed that they displayed increased resistance to *M. tb* infection upon neutrophil depletion [63]. In agreement with this finding, D'Avila *et al* demonstrated that BCG induces profound apoptosis of neutrophils; phagocytosis of apoptotic neutrophils by macrophages elicits increased synthesis of prostaglandin E2 (PGE2) and transforming growth factor β1 (TGFβ1), and these mediators may possibly deactivate macrophages allowing bacterial persistence [64].

1.3.8 Dendritic Cells

DCs are specialised antigen presenting cells (APC) that play a vital role in linking the innate and adaptive immune responses. As with macrophages, DCs express CR3 and mannose receptors that bind to and mediate uptake of *M. tb* within lung alveoli. However, unlike macrophages, DCs also express a unique C-type lectin, DC-specific intracellular adhesion molecule-grabbing non-integrin (DC-SIGN) receptor that binds *M. tb* through ManLAM. Studies have also shown that DCs do not provide a suitable environment for the replication of mycobacteria [65, 66]. DCs are essential for activation of the adaptive immune response via delivery of *M. tb* and *M. tb* antigens to draining lymph nodes, where they present those antigens to circulating T cells.

1.3.9 Natural Killer cells

Natural killer cells (NK) are able to recognise infected or damaged self-cells. They release cytotoxic granules onto the surface of infected cells that they are bound to, inducing apoptosis, thereby, preventing further replication of intracellular pathogens. They also mediate killing of *M. tb* via granule-independent mechanisms [67] such as the expression of INF-γ and can lyse T_{regs} proliferating in response to intracellular pathogens [68].

1.3.10 $\gamma\delta$ T cells

$\gamma\delta^+$ T cells have both innate and adaptive properties. They undergo receptor gene rearrangement, which is a defining feature of the T cells of the adaptive immune response,

but their gene rearrangement is limited. They do not need to undergo clonal expansion to response to antigens they encounter; nor do they need antigens to be presented by MHC molecules. Mouse studies have shown that these cells are implicated in early control of *M. tb* infection [69] and that they are capable of secreting IFN-γ [70] and IL-17 [71]. $\gamma\delta^+$ T cells have also been implicated in controlling *M. tb* infection in macaques [72] and in *in vitro* mycobacterial growth inhibition assays (MGIA) [73].

1.3.11 CD1 restricted T cells

CD1 molecules are similar to major histocompatibility complex (MHC) class I molecules but they lie outside of the MHC region genetically. These molecules bind to and present glycolipids to CD1 restricted T cells that are αβ T cells that lack CD4 and CD8 receptors. Mycolic acids [74] and LAM [75] which are abundant in the cell wall of mycobacteria, have been shown to bind to CD1 molecules, resulting in activation of CD1 restricted T cells.

1.3.12 Autophagy

Autophagy can be considered as a cytoplasmic clean-up function in cells where surplus or damaged organelles and other macromolecular cell components, are degraded and recycled via endocytic pathways. Recently, autophagy has been studied in the context of innate immunity against intracellular pathogens. Work by Gutierrez *et al.* in 2004 demonstrated a role for autophagy in elimination of *M. tb* [76]; furthermore, IFN-γ was shown to induce

autophagy in *M. tb* infected macrophages leading to destruction of the bacterium, whist the T_H2 cytokines IL-4 and IL-13 inhibited autophagy, permitting intracellular growth of *M. tb.*

1.3.13 Cytokines and chemokines

Cytokines are small proteins released by many cells of the body in response to microbial stimulus. There are two major families of cytokines; the hematopoietin family includes growth hormones and interleukins including IFN-γ, whereas the TNF family consists of many membrane-bound molecules including TNF-α, CD40L and Fas ligand (FasL). Cytokines contribute to both innate and adaptive immune responses. Some of the earliest cytokines to be released during an infection are the chemokines, which induce chemotaxis of nearby responsive cells to the site of infection.

1.4 The adaptive immune response to *M. tb*

1.4.1 Antigen presentation

If the innate immune system is unable to control an invading pathogen there is an accumulation of antigen and a change in the cellular environment around the focus of infection. At this point, cells of the adaptive immune response become activated. Antigen presenting cells have engulfed the invading organism or antigen and are now able to activate T cells by presenting antigenic peptides bound to a MHC receptor on their surface.

The different classes of MHC receptors, MHC class I and MHC class II, have a role in directing the type of immune response produced against an infection. MHC class I molecules bind peptides found in the cytosol of host cells leading to activation of $CD8^+$ T cells; whereas MHC class II molecules obtain peptides from cellular vesicles that stimulate $CD4^+$ T cells. Because of the phagosomal localisation of *M. tb*, the majority of antigen presentation occurs via the MHC class II route, predominantly resulting in a $CD4^+$ T cell response.

1.4.2 Naïve T cell activation

T cells that have not yet encountered their specific antigen are called naïve T cells. Once inside lymphoid organs, T cells leave the blood and pass through lymphoid tissue, where they may encounter an APC displaying the specific antigen for that T cell bound to a MHC molecule.

The APC also presents the necessary co-stimulatory molecules such as B7, which binds to CD28 and CD40 which binds CD40L on T cells. This co-stimulation results in the T cell entering the cell cycle whilst producing IL-2 that promotes proliferation and cell survival. The APC also provides a signal for the differentiation of the naïve T cell into effector T cells. This whole process is termed a primary cell-mediated immune response and these antigen primed T cells leave the lymphoid organ and progress to the site of the infection.

1.4.3 Effector T cells

There are 5 major types of effector T cell, each with its own specific function. All effector T cells still require binding of peptide:MHC complexes for them to act upon another cell and thus illicit their protective effects. However, unlike naïve T cells, they do not require the interaction of co-receptors and therefore, they rapidly respond to contact with specific antigen.

1.4.3.1 Differentiation of $CD4^+$ effector cells

Naïve $CD4^+$ T cells can develop into any of 4 different types of effector cell called T helper 1, T helper 2, T helper 17 and regulatory T cells (T_H1, T_H2, T_H17 and T_{reg} respectively). Cytokines present in the environment where $CD4^+$ cells are initially primed with antigen play an important role in T helper cell differentiation [77]. T_H1 cells secrete IFN-γ that inhibits activation of T_H2 cells; which by contrast secrete IL-4, IL-5 and IL-13 [78-80] that inhibit the development of a T_H1 response, resulting in positive feed-back loops [81-84].

Studies have also shown that surface molecules on APC bind to TCR with variable strength and duration, resulting in the dominance of one T helper cell subset over the others [85]. In 2004 it was discovered that the Notch ligands Delta and Jagged that are present on APC, induce T_H1 and T_H2 cell differentiation respectively [86].

Differentiation of $CD4^+$ cells into T_H1 or T_H2 cells results in macrophage activation or antibody production respectively. When DCs are stimulated by *M. tb*, they secrete IL-12 which in turn induces IFN-γ secretion in nearby NK cells. If a $CD4^+$ T cell is primed in the presence of IL-12 and IFN-γ, it will become a T_H1 cell, therefore, TB usually induces a T_H1 response.

1.4.3.2 T_H1 cells

T_H1 cells are major producers of IFN-γ and TNF-α, they can also express CD40L; a cell activating molecule which provides a secondary signal to activate macrophages that bear CD40 receptors on their surface. This activation drives the maturation of phagosomes containing *M. tb*, into phagolysosomes that destroy the *M. tb* inside them.

1.4.3.3 T_H2, T_H17 and T_{reg} cells

T_H2 cells can activate naïve B cells and induce antibody class switching, they are particularly important for switching production of antibodies to class IgE in order to combat parasitic infections. T_H17 cells have only recently been described, but it is understood that their function is to recruit neutrophils to the site of extracellular bacterial infections by producing IL-17.

The final type of effector T cell is the T_{reg} subset, which unlike the other types of T helper cell, has an inhibitory effect on other $CD4^+$ T cells. Some T_{regs} develop in the thymus and

are termed natural regulatory T cells, whereas others differentiate from naïve $CD4^+$ T cells in the periphery and are called adaptive regulatory T cells.

1.4.4 $CD8^+$ effector T cells

All $CD8^+$ effector cells are cytotoxic lymphocytes (CTL), capable of killing host cells that are infected or display markers that indicate the cell is abnormal. The role of $CD8^+$ T cells in the immune response to TB has been controversial; but there is strong evidence that mycobacteria specific $CD8^+$ T cells are induced in TB and these cells are capable of recognising *M. tb* infected macrophages [87, 88].

$CD8^+$ effector T cells are capable of producing IFN-γ, TNF-α and FASL just as T_H1 do, but they can also release cytotoxic enzymes that are stored in granules onto target cells. Perforin aids in the delivery of granule contents across cell membranes, allowing granzymes which are pro-proteases to enter the cell, whereupon they are activated and induce apoptosis. Granulysin which is expressed by humans but not mice, is antimicrobial and in high concentrations is able to induce apoptosis. There is evidence to suggest that $CD8^+$ T cells that express IFN-γ do not produce perforin [89, 90] and so a polarisation of the response may be skewed towards cytotoxicity or cytokine production.

1.4.5 The role of B cells

B cells are involved in the humoral immune response to infection; they produce antibodies against specific antigens and can act as APCs. The receptors on these lymphocytes are immunoglobulins that are capable of recognising native antigens that do not require MHC complex presentation. Activated B cells that have encountered their cognitive antigen are able to differentiate into either plasma cells that secrete vast quantities of antibody, or they become memory B cells that respond rapidly to a secondary encounter with their specific antigen.

Not without good reason, the majority of TB vaccine research has been focused on T cell responses and their functions, however, recent studies point towards there being a role for B cells in the process of eliminating *M. tb*. $B220^{+}$ cells have been found to constitute the majority of cells within granulomas; these cells are most likely B cells [91]. The function of these immune cells in TB is still unclear with some studies indicating that they are important in mice given high dose aerosol challenges of *M. tb* [92-94] but a study in guinea pigs perhaps indicates that a response that is predominated by B cells is linked to increased susceptibility to TB [95].

1.4.6 Granulomas

In humans, infection with *M. tb* leads to the formation of granulomas, which are a hallmark of protection against active disease. Individuals with latent TB have granulomas within their lungs that contain *M. tb* and prevent it from multiplying and spreading throughout the lung. The exact mechanisms for how granulomas are formed, maintained and broken down are not yet fully understood.

Alveolar macrophages infected with *M. tb* secrete large quantities of cytokines and chemokines, including TNF-α, CCL2 and CXCL10 which results in recruitment of more macrophages to the site of infection; positive feedback loops lead to increased levels of TNF-α, producing a greater inflammatory response. Under the influence of increased expression of CXCR3 binding cytokines [96, 97], NK cells are the first lymphoid cells to migrate to the granuloma, followed by $CD3^+$ T cells and B cells. The dampening down of this response coincides with the secretion of IFN-γ by lymphocytes; mice that are deficient in IFN-γ quickly succumb to gross pathology of the lungs [98]. It should be noted that mice do not develop caseation of granulomas as humans do.

The tightly controlled sequential recruitment of the different types of immune cell results in formation of a highly ordered structure; containing *M. tb* infected macrophages in the centre,

surrounded by foamy macrophages (macrophages with high lipid content) that are in turn surrounded by uninfected macrophages and finally lymphocytes on the outer edge. To begin with, granulomas are well vascularised, but as they mature they lose much of their vasculature and develop a fibrous outer layer that delineates a boundary between macrophages and lymphocytes. The mature granuloma is therefore hypoxic within its centre and the structure can be maintained for many years.

Perturbation of the $CD4^+$ immune response in an individual can lead to breakdown of granulomas, resulting in caseation of the centre, which turns into a liquid that is filled with dead cells and their by-products. In this environment *M. tb* is able to replicate uncontrollably, ultimately resulting in release of the organism and its spread throughout the lungs and eventually the airways of the infected individual.

1.4.7 Immunological memory

In 1796 the first vaccination as we now know it, was carried out by Edward Jenner, who realised that once a person had encountered a pathogen or a closely related pathogen, they were less likely to suffer from the same illness a second time. We now know the mechanism behind this protection is immunological memory, which can involve either memory T or B cells. Upon infection or vaccination, antigen specific T or B cells undergo clonal expansion to clear the stimulus; after the challenge has been dealt with the vast

majority of effector cells die off, leaving behind a small subset of memory cells [92, 99]. These memory cells are better equipped and faster at responding to their cognitive antigen than naïve cells, and so the adaptive response is mounted more rapidly and robustly upon a second encounter.

1.4.7.1 What constitutes a memory cell?

There has been a concerted effort to define exactly what a memory T cell is, and to answer the questions, what cell surface markers do they possess, and what drives these few cells to become memory cells? In the case of $CD8^+$ T cells these questions were able to be answered successfully, probably due to the fact that large numbers of these cells are present after antigenic stimulation. The same cannot be said for $CD4^+$ cells, in fact, the very existence of memory $CD4^+$ T cells has been a matter of contention [91, 100].

In humans CD45RA and CD45RO expression are used to differentiate between naïve and memory cells respectively [92]. T cell activation results in the down regulation of CD62L and CCR7 which permit entry into the lymph nodes and the T cell zone of lymph nodes respectively; the loss of these surface molecules means that these cells will remain in the circulation and can be delivered to a site of infection. Unlike the expression of CD45, it is thought that some activated T cells regain expression CD62L and CCR7 leading to the idea that there are two distinct populations of memory T cell [101]. Central memory T cells

(T_{CM}) have similar surface markers to naïve cells, expressing CCR7 and CD62L and producing IL-2 upon re-stimulation, whereas effector memory T cells (T_{EM}) express much lower levels of these lymph node homing molecules and secrete effector cytokines such as IFN-γ and IL-4 [101].

1.4.7.2 BCG vaccination

BCG is the only licensed vaccine we have against TB, having been administered for over 70 years, some 3 billion doses have been given worldwide. There are however some issues with this vaccine. The efficacy of BCG against adult pulmonary TB is estimated to be between 0-80% [102] with the lowest efficacies found in the tropics where TB incidence is greatest [102]. The exact cause of this variation is unknown but is likely to be a combination of host genetics, prevalence of NTM in the environment, nutritional status, and the sub-strain of BCG used for vaccination. BCG is widely thought to protect against TB disease but not against infection with *M. tb* [103], although there is some evidence to suggest that BCG can provide protection against *M. tb* infection in some settings [104].

Despite the variable efficacy of BCG to prevent adult pulmonary disease, it is highly effective at preventing the more severe disseminated forms of TB (miliary TB and TB meningitis), especially in infants [105]. Unfortunately, in neonates where HIV infection is

suspected, the use of BCG is now contraindicated as the possibility of them developing disseminated BCG infection is considered too great.

1.4.7.3 Memory responses to M. tb

Although we do not know the exact mechanisms behind BCG protection from disseminated TB, it is thought to be mediated by the production of $CD4^+$ T cells expressing IFN-γ, which in turn activate *M. tb* infected macrophages [98]. The argument for a sustained population of memory $CD4^+$ T cells is further backed by the delayed type hypersensitivity (DTH) response seen in the tuberculin skin test (TST) after BCG vaccination, although it is not known whether this is caused by persistent stimulation by antigens present in the environment. We also know that the TST response induced by BCG vaccination does not correlate with protection against TB [106].

One theory for the apparent lack of ability of BCG to prevent pulmonary TB is the kinetic of T cell mediated immunity. Studies performed by A. Cooper and colleagues suggest that during an un-primed response to *M. tb* in mice, it takes between 18-20 days for *M. tb* specific T cells to migrate to the lungs; when mice have been BCG vaccinated, this delay in effector T cell arrival is reduced to 12-15 days after infection [107]. Although reduced, this is still a long enough period for *M. tb* to establish infection within alveolar phagocytes. However, the reduced time taken for memory T cells to arrive in the lung could enable

them to limit *M. tb* replication during the early stages of infection. This could therefore account for the widely held view that BCG fails to prevent latent TB infections whilst protecting against TB disease.

1.4.7.4 Mycobacterial antigens

As BCG is an attenuated strain of *M. bovis,* it has lost many genes associated with virulence; most notably the RD1 locus is missing in all strains of BCG but is present in both *M. tb* and *M. bovis*. The RD1 locus contains several secreted antigens that are recognised by the mammalian immune system. The antigens that illicit the strongest responses in most individuals are culture filtrate protein-10 (CFP-10) and early secretory antigenic target-6 (ESAT-6). These proteins form heterodimers that are thought to disrupt the immune response by direct interaction with TLR-2 [108]. TB10.4 is a member of the ESAT-6 family which is also immunogenic though it is not as immunodominant as ESAT-6. The fact that these antigens are not present in BCG but are present in *M. tb* and *M. bovis,* means that they can be used as diagnostic markers in tests such as ELIspot and QuantiFERON gold to discriminate between BCG vaccine memory responses and responses to *M. tb/M. bovis* infection.

Other secreted antigens include those of the Ag85 complex (Ag85A, Ag85B and Ag85C) which are important for mycobacterial cell wall maintenance through mycolyltransferase

activity. The Ag85 complex is present in both virulent *M. tb* and environmentals/BCG. There are also the PE and PPE families of proteins which get their names from their highly conserved Proline-Glutamate and Proline-Proline-Glutamate sequences respectively. These proteins were discovered just over a decade ago and their exact functions have yet to be established, however, there is some evidence that they can modulate innate immune responses to mycobacteria, including disruption of phagosome trafficking [109]. These proteins are particularly abundant in pathogenic mycobacteria and account for around 10% of the genome.

1.5 Novel vaccination strategies

1.5.1 BCG is good, but not good enough

In spite of global vaccination with BCG, 1/3rd of the world's population is infected with *M. tb* and nearly 2 million people die of TB every year. It is clear that we need an improved vaccine but as previously mentioned in section 1.4.7.2, BCG is protective against disseminated disease, and is recommended for infants shortly after birth in TB endemic countries; therefore withdrawing BCG vaccination in infancy may be unethical. An obvious strategy to improve the protection afforded by BCG is to administer boosting doses, however this has proven to be ineffective [110]. So a number of novel vaccination

strategies incorporate the use of BCG as a priming agent, boosted with a subunit vaccine delivering recombinant proteins in the presence of adjuvant, or a viral vector expressing one or more *M. tb* antigens in a heterologous prime boost regime.

1.5.1.1 Heterologous BCG prime-boost

A number of subunit vaccines have been proven to be efficacious in animal models of TB and have excellent safety records. M.tb72F is a leading fusion protein vaccine containing PPE protein and a serine protease that is common to both *M. tb* and BCG [111, 112]; it has entered phase IIa safety and immunogenicity trials in Africa (NCT00146744). Other promising subunit vaccines include the secreted antigen fusion proteins Hybrid I and HyVac IV from SSI, which contain Ag85B with ESAT-6 and Ag85B with TB10.4 respectively [113, 114]. The use of ESAT-6 however, could potentially confound diagnostic tests such as Elispot that test for responses against *M. tb* specific antigens such as ESAT-6. HyVac IV entered a phase I trial in Sweden in 2007.

The most clinically advanced viral vector candidate is a modified vaccinia Ankara expressing the *M. tb* antigen 85A (MVA85A); it has been shown to illicit strong and long lasting $CD4^+$ T cell responses [115, 116] and has proved to be safe for use in infants, healthy adults and adults infected with HIV. MVA85A is currently being evaluated in phase IIb efficacy trials in infants in South Africa and HIV-infected adults in South Africa and Senegal

(NCT01151189). Another promising viral vectored vaccine is the Aeras 402 (AdHu35) vaccine expressing Ag85A, Ag85B and TB10.4 [117]. This vaccine has shown to be efficacious in the mouse model of TB, and elicits strong $CD4^+$ and $CD8^+$ T cell responses in adults in South Africa [118].

1.5.1.2 Attenuated viable mycobacteria

Researchers have also produced novel mutants of BCG that are more immunogenic and effective at protecting against *M. tb* challenge in animal models. A number of different approaches have been taken in this field, including promotion of endosomal escape of BCG; which aids MHC class I presentation of antigens and so inducing a greater $CD8^+$ T cell response to vaccination [119]. Recombinant BCG strains (rBCG) over expressing key *M. tb* antigens such as 85A and 85B have also been developed and entered phase I trials to test safety and immunogenicity [120]. The Aeras 422 rBCG over expresses Ag85A, Ag85B and Rv3407 and has an endosomal escape mechanism, this vaccine has entered phase I trials in the USA (NCT01340820).

Some groups have used genetic sequence data to rationally design an attenuated strain of *M. tb* suitable for use as a vaccine. The leading candidates in this field include the phoP mutant SO2 and panC and panD mutants that maintain infectivity, but are limited in their capacity to replicate within the host. Preclinical safety data so far show these vaccines are

safer than BCG in immunocompromised animals, and most importantly, they are more efficacious [121-123]. It is possible that these attenuated mycobacterial vaccines could be used alone, or in a prime boost regime with/instead of BCG.

1.5.1.3 Other novel TB vaccine candidates

Other vaccines that are much earlier stage concepts and are being evaluated as proof-of-concept in mice include DCs that are pre-loaded with mycobacterial peptides. It is thought that because DCs are the most potent stimulators of cell mediated immunity, this vaccine will increase activation of naïve T cells. This type of vaccine has been shown to protect mice against high dose intravenous challenge with *M. tb* [124].

Another promising candidate is the DNA/viral vector combination encoding HSP65 and IL-12 encapsulated inside haemagglutination virus of Japan (HVJ) liposomes. Studies have shown it to be more protective than BCG when administered alone or when boosting BCG in macaques [125]. Fulkerson *et al.* have been developing a shigella vectored vaccine that is able to be administered orally, delivering capsids containing dsRNA encoding *M. tb* antigens into the cytoplasm. Researchers have been looking to boost the effect of previous vaccination with BCG in HIV patients by vaccinating with whole killed *M. vaccae* in the hope that it will prevent these patients from developing TB. This strategy has shown some promise in clinical trials [126].

1.6 Searching for a surrogate of protection

1.6.1 Why do we need a surrogate of protection?

One of the most challenging aspects of developing an improved TB vaccine is efficacy testing. To begin with, vaccine candidates are tested in animal models of TB, generally testing first in mice and then in guinea pigs, followed by macaques or possibly cows. Even though all new vaccines must be tested for safety in animals before clinical trials can commence, we are still unsure of how representative any of these models are of human TB disease.

At present, the only reliable measure of efficacy are large scale field trials in TB endemic areas; these trials take years to carry out, in thousands of subjects and cost millions of pounds to perform. Because of these constrictions, screening novel TB vaccines for efficacy is a very protracted process. Correlates of protection expedite the process of assessing vaccines for immunogenicity in animal models and early clinical trials, but do not necessarily imply protection; whereas it has been suggested that a surrogate of protection could be taken to mean that a vaccine is protective [127].

If a robust and validated surrogate of protection is identified, it could potentially greatly increase the rate at which we can assess TB vaccine candidates, as it could aid in the

selection of vaccines that are chosen to go into large scale efficacy trials at limited sites within TB endemic countries. There is also the possibility that large scale field trials and animal challenge studies may become unnecessary for licensure, as was the case with the meningococcal C conjugate vaccine [128]. At present BCG vaccination is being used as the gold standard to identify surrogates of protection, the obvious problem with this is, a new TB vaccine is needed because BCG is not very protective, so the responses being analysed are probably not optimal.

1.6.2 Correlates of protection

1.6.2.1 $CD4^+$ and $CD8^+$ T cells

So far, no single parameter has been found to robustly correlate with protection against TB in various preclinical or clinical models [129, 130]. Even IFN-γ, which is known to be essential for immunity against TB and is the primary readout of many immunological assays assessing vaccines, does not correlate with protection [131]. The search for correlates/surrogates of protection seems to be complicated by the fact that such correlates appear to be vaccine or species specific, for example, early $CD8^+$ T cell influx into the lungs of mice [132] or cultured ELIspot responses in cattle [133]. However, there is a large body of evidence from gene knockout, cell depletion and adoptive transfer studies in mice that proves T_H1, MHC class-II restricted $CD4^+$ T cells are essential for protection against *M. tb* disease [134-140]. Evidence for the importance of $CD4^+$ cells in humans is provided by

the direct association of increased incidence of TB in HIV patients as $CD4^+$ T cell counts decrease [141]. However, Kagina *et al*. recently reported that specific $CD4^+$ T cell responses 10 weeks after BCG vaccination in new-borns do not correlate with ultimate risk of tuberculosis disease [129]. Importantly, $CD4^+$ T cell expression of IFN-γ, co-expression of IFN-γ, TNF and IL-2 (by polyfunctional $CD4^+$ T cells) or $CD8^+$ T cell responses did not correlate with risk of disease during the first 2 years of life. By contrast studies in macaques have suggested an importance for $CD8^+$ T cells in the control of M. tuberculosis [142]. There is also the possibility that PBMCs may not be the optimal cells to assess correlates of protection. Some studies have pointed towards improved correlations of antigen specific $CD4^+$ T cell responses with protection in the lungs [143] and spleens [144] of animals; although these measurements are not likely to be feasible in large scale clinical trials.

1.6.2.2 Memory responses

Immunological memory is essential for successful vaccination. A relatively recent discovery that responses against RD1 antigens (ESAT-6/CFP-10) in patients who have been successfully treated for TB are detectable by cultured but not *ex vivo* ELIspot, highlights the importance of central memory $CD4^+$ T cells over effector cells in the immune response to *M. tb* [145].

1.6.2.3 Other cell types correlating with protection

T_H17 T cells are another member of the $CD4^+$ T cell family that have been implicated in protection from development of *M. tb* disease. These cells, under the influence of IL-23, produce IL-17 which is a potent inflammatory cytokine that induces chemokine expression and migration of responsive cells to sites of infection including the lung [146]. Upon infection with *M. tb,* both IL-17 and T_H17 cells are induced and in vaccinated animals, the loss of memory T_H17 cells results in a loss of the accelerated T_H1 response and protection [147-149]. Recently, Lockhart *et al.* reported that $\gamma\delta^+$ T cells were major producers of IL-17 in *M. tb* infected mice [150] and have been shown to have a role in granuloma formation in the lungs of mice with pulmonary BCG infection [151].

1.6.2.4 Multi-parametric measures

It is currently thought that systems measuring large numbers of immunological readouts such as microarrays could provide us with a panel of biomarkers, which may be predictive of vaccine efficacy. Such studies have been conducted in mice, looking at gene expression within the lungs of BCG vaccinated animals, where changes in the connective tissue structure and function, along with a T_H17 cytokine profile correlated with protection from *M. bovis* challenge [152]. Functional assays that take into account a whole host of cellular mechanisms might provide the elusive surrogate of protection. One such functional assay

is the mycobacterial growth inhibition assay (MGIA), which is the principle subject of this thesis.

1.7 Mycobacterial growth inhibition assays

These assays can be thought of as *in vitro* challenge models for assessing vaccine efficacy. A number of MGIAs have been published for a variety of sample types obtained from humans and mice. All MGIAs have one principle in common, which is, samples taken after vaccination against TB should be better able to inhibit growth of mycobacteria in cell culture, as compared to samples from unvaccinated controls. Summarised below, are the main details of existing published MGIAs, highlighting the logistics and key findings for each one and a schematic of the three different MGIAs used throughout this project (

Fig. 1-4).

a

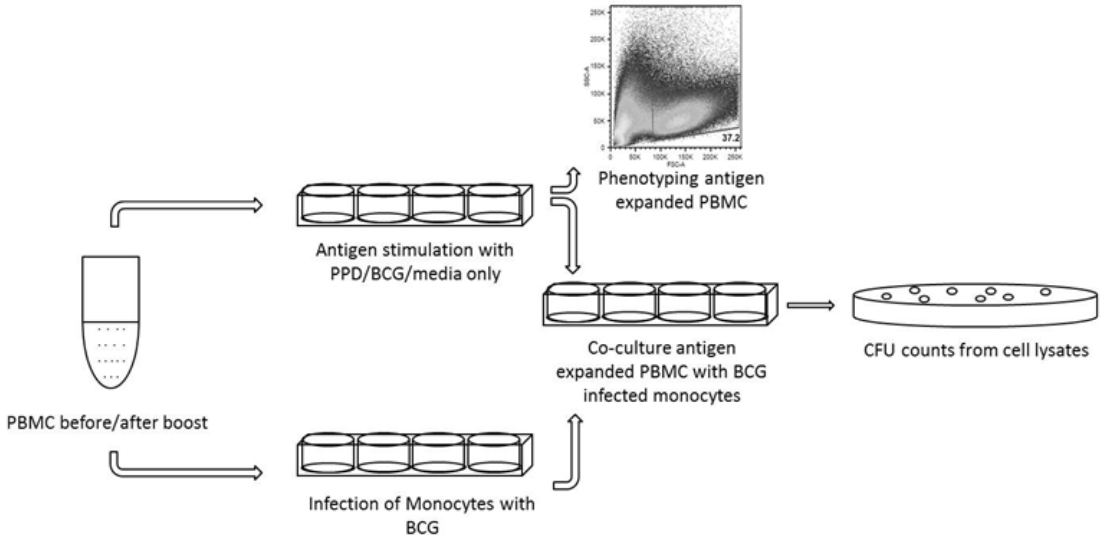
Phenotyping antigen expanded PBMC
Antigen stimulation with PPD/BCG/media only
PBMC before/after boost
Co-culture antigen expanded PBMC with BCG infected monocytes
CFU counts from cell lysates
Infection of Monocytes with BCG

b

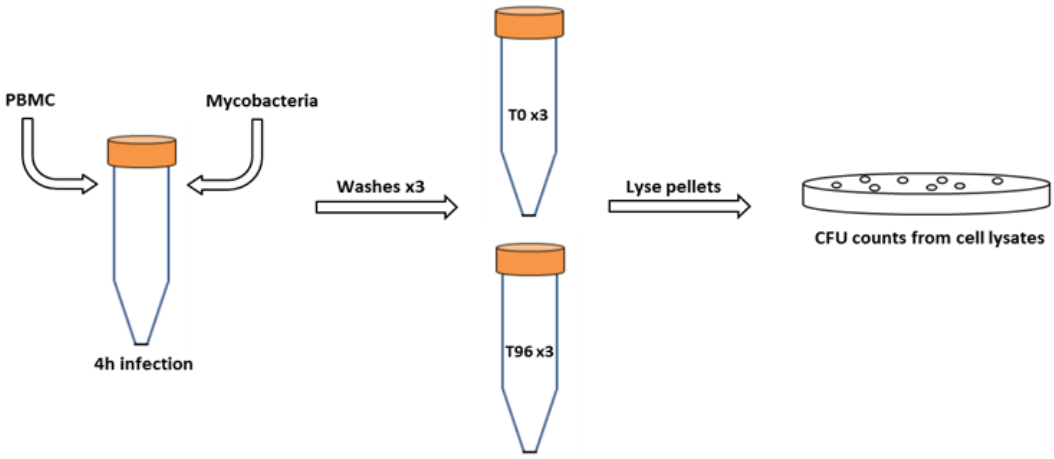
PBMC
Mycobacteria
Washes x3
T0 x3
Lyse pellets
CFU counts from cell lysates
4h infection
T96 x3

c

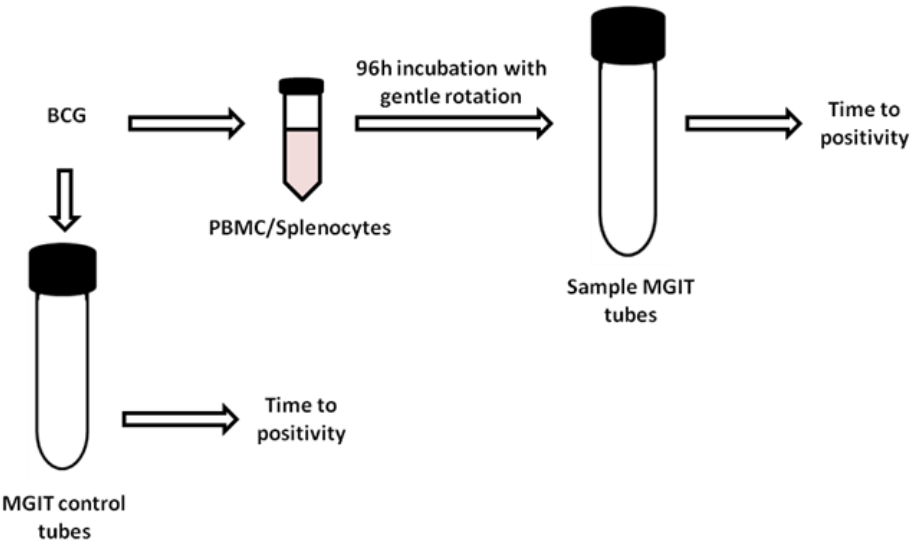
BCG
96h incubation with gentle rotation
Time to positivity
PBMC/Splenocytes
Sample MGIT tubes
Time to positivity
MGIT control tubes

Fig. 1-4 Comparison of the three MGIAs used throughout this project

(a) The cultured MGIA; PBMC taken from volunteers before and after BCG vaccination are stimulated with mycobacterial antigens or media alone for 7 days, after which a proportion of the PBMC are analysed by flow cytometry. Autologous monocytes are infected with BCG after 6 days culture. Antigen expanded PBMC and BCG infected monocytes are co-cultured together to assess the ability of the PBMCs to inhibit BCG growth in monocytes as measured by CFU counts. (b) A whole PBMC infection MGIA; PBMC taken from volunteers/animals are infected for 4 hours at an estimated MOI of 3:1 mycobacteria to monocyte. Cultures are washed x 3 to remove non-phagocytosed bacteria. Samples are split equally into 6 cultures each. T0 cultures are harvested immediately before cell pellet lysis and serial dilution for CFU quantification. T96 samples are cultured for 4 days before harvest. (c) The mycobacterial growth indicator tube (MGIT) MGIA; MGIT tubes are directly inoculated with BCG on day 0 with the same stock of bacteria used to infect PBMC/splenocyte cultures. Cultures are incubated for 96h with rotation before cell pellets are harvested and used to inoculate sample MGIT tubes. MGIT tubes must be placed in a BACTEC machine until they register as positive. The time to positivity is the primary readout of this assay.

1.7.1 Ex vivo MGIA in humans

In 1998 Silver *et al.* developed a MGIA that tested the ability of lymphocytes taken from TST+ and TST- volunteers to inhibit growth of H37Rv within monocytes [153]. They found that $CD4^+$ T cells were required for inhibition in TST+ but not TST- volunteers. Possibly the most interesting finding was that TST- volunteers appeared to inhibit mycobacterial growth better than individuals who were TST+ (10.6 and 6 fold respectively). It is not clear whether the TST+ volunteers are latently infected or BCG vaccinated, but it could be the case that lymphocytes from latently infected individuals are less able to control *in vitro* growth of H37Rv, than those taken from non-reactive individuals. This study also found that IFN-γ induced a 1.9 fold reduction but TNF-α failed to inhibit intracellular growth of *M. tb* in the absence of lymphocytes.

1.7.2 Cultured MGIA in humans

This MGIA used antigens to expand populations of mycobacteria specific T cells for 6 days that were then co-cultured with autologous monocytes infected with BCG. The studies performed by Worku *et al.* in 2003 demonstrated the enhanced killing of BCG by PBMC expanded with a wide range of *M. tb* antigens, but not media rested or tetanus toxoid stimulated PBMC [73]. They found $\gamma\delta^+$ T cells to be the most potent inhibitors of BCG growth and that cell-cell contact was required for this perceived inhibition; a finding that supported the results from the Silver MGIA.

1.7.3 Whole blood assay in infants

As BCG takes around 3 weeks to grow on solid media, B. Kampmann and colleagues utilised a strain of BCG expressing a fluorescent reporter gene (BCG *lux*) that can be quantified by luminescence. This strain was used to infect whole blood taken from neonates both before, and after BCG vaccination. In this study whole blood (WB) taken after BCG vaccination was found to inhibit BCG *lux* growth more than naïve blood samples, growth ratio (GR) GR=3.9 compared to GR=9.6 respectively [154]. Increased secretion of IFN-γ was also seen in BCG vaccinated infants blood as compared to pre vaccination samples.

1.7.4 Mycobacterial growth indicator tube (MGIT) assay

This MGIA uses whole blood culture in much the same way as the assay published by Kampmann *et al.* except that the MGIT system was used to quantify the CFU. MGIT tubes contain Middlebrook 7H9 liquid media plus an oxygen-quenched fluorochrome (tris 4, 7-diphenyl-1, 10-phenonthroline ruthenium chloride pentahydrate) embedded in silicone at the bottom of the tube. During bacterial growth within the tube, the free oxygen is utilized and is replaced with carbon dioxide. With depletion of free oxygen, the fluorochrome is no longer inhibited, resulting in fluorescence within the MGIT tube when visualized under ultra violet light. The intensity of fluorescence is directly proportional to the extent of oxygen depletion. MGIT tubes placed in a MGIT 960 instrument are incubated and monitored for increasing fluorescence every 60 minutes. Growth of bacteria as well as mycobacterial metabolism increases the fluorescence. In the case of *M. tuberculosis*, at the time of positivity, there are approximately 10^5-10^6 CFU/ml of medium. The instrument reports the time to positivity of specimens that reach a predetermined level of fluorescence.

WB taken before and after BCG vaccination was co-cultured with BCG for 4 days. These co-cultures were used to inoculate MGIT tubes, which were placed in a BACTEC™ machine to incubate until they registered positive for bacterial growth. The readout of this assay is

time to positivity of the sample MGIT tubes, which is compared with that of control tubes and can be converted to CFU from a standard curve.

Again blood taken from volunteers after vaccination with BCG resulted in increased mycobacterial growth inhibition in comparison with pre vaccination blood samples [155]. Interestingly this study also points towards the need for $CD4^+$ T cells for inhibition in blood from TST+ volunteers but not in TST- ones, however as with the ex *vivo* MGIA it is impossible to know whether individuals were latently infected with *M. tb* or not, but again these findings point towards innate mechanisms being involved in mycobacterially naïve samples and a requirement for cellular immunity in blood taken from mycobacterially exposed individuals.

1.7.5 Murine MGIA

So far, all of the MGIA that I have discussed have been performed using WB or PBMC samples that are readily available in humans. In the mouse model of TB it is difficult to obtain sufficient blood volumes with which to perform such an assay. Parra and colleagues solved this problem by developing an assay that tested mycobacterial growth inhibition elicited by splenocytes in bone marrow derived macrophages infected with *M. tb* or BCG [156, 157].

As with all of the previously mentioned MGIA, splenocytes taken from mice vaccinated with BCG induced greater levels of mycobacterial growth inhibition in macrophages than splenocytes taken from naïve mice. Importantly, as this assay was performed in mice, the authors were able to correlate the *in vitro* growth inhibition with *in vivo* efficacy as measured by protection against *M. tb* challenge in the lungs and spleens of animals 28 days post challenge. This is the only example to date of an MGIA correlating with protection, albeit in the mouse model.

1.8 Study Aims

As there are several MGIA methodologies that have been published over the last decade, a number of these MGIAs were to be assessed for their suitability for use with human and NHP PBMC (both fresh and cryopreserved), as well as splenocytes taken from mice. This would include evaluation of the ability of the different MGIAs to discriminate between naïve and BCG vaccinated individuals/animals. The MGIA that was capable of providing the best results would be used to evaluate whether *in vitro* mycobacterial growth inhibition correlates with protection from *M. tb* challenge in mice and NHP. The final aim of this study was to investigate the mechanisms behind mycobacterial growth inhibition. This would include microarray experiments to identify differential gene expression between naïve and BCG

vaccinated animals and cell depletion experiments to identify which cell types are responsible for mycobacterial growth inhibition.

Chapter 2

Materials and Methods

2. Materials and Methods

2.1 Materials

2.1.1 Reagents

Table 2-1 details the commercially available reagents and consumables used throughout this study.

Material	**Supplier**	**Catalogue Number**
0.2μm syringe filter	Sartorius	16534
12 well plates	Costar	3513
15ml centrifuge tubes	Fisher, Inc.	FB55950
2-β Mercaptoethanol (50μm)	Gibco	31350-010
24 well plates	Nunc	142475
5μm syringe filter	Millipore	SLSV025LS
50ml centrifuge tubes	Greiner	227261
5ml syringe	BD plastipak	302187
60mm petri dishes	Corning	430166
6-well tissue culture plates	Fisher, Inc.	TKT-520-030T
7H10 agar	Becton Dickinson UK	262710

7H9 Media	Becton Dickinson UK	271310
96 well plates lightcycler 480	Roche diagnostics UK	4729692001
AIM V medium CTS	Invitrogen UK	0870112DK
Alexafluor 700 isotype control	Beckton Dickinson UK	557882
Anti-biotin microbeads	Miltenyi biotech	130-090-485
Anti-human CD14 ECD	Beckman coulter UK	IM2707U
Anti-human CD14 Pacific blue	Invitrogen UK	MHCD1428
Anti-human CD19 Pacific blue	Invitrogen UK	MHCD1928
Anti-human CD20 ECD	Beckman coulter UK	IM3607U
Anti-human CD3 AF700	Beckton Dickinson UK	557917
Anti-human CD3 PerCPCy5.5	Beckton Dickinson UK	332771
Anti-human CD4 APC	ebioscience	170047
Anti-human CD4 PE	Beckton Dickinson UK	550630
Anti-human CD8 APC-AF780	ebioscience	47008842
Anti-human CD8 pe-cy7	Beckton Dickinson UK	335822
Anti-human IFN-γ FITC	Beckton Dickinson UK	552887
Anti-human TCR$\gamma\delta$ PE	Beckton Dickinson UK	333141
Anti-human TCR$\alpha\beta$ PE	Beckton Dickinson UK	555548

Anti-human TNF 450	ebioscience Ltd	48734942
Anti-mouse B220 AF700	Ebioscience	56-0452-80
Anti-mouse CD14 PE	Ebioscience	12-0141-81
Anti-mouse CD4 Dynabeads	Invitrogen	11445D
Anti-mouse CD4 EF650	Ebioscience	95-0041-42
Anti-mouse CD8 APC-EF780	Ebioscience	47-0081-81
Anti-mouse CD8 Dynabeads	Invitrogen	11447D
Anti-mouse compensation beads	Beckton Dickinson UK	552843
Anti-mouse NK biotinylated	Biolegend	115703
Anti-mouse NK FITC	Ebioscience	11-3351-80
Anti-mouse TCR-$\gamma\delta$ biotinylated	Ebioscience	13-5811-81
Anti-mouse TCR-$\gamma\delta$ PerCP-EF710	Ebioscience	46-5711-80
Anti-mouse TCR-$\alpha\beta$ Pacific blue	Invitrogen	HM3628
Anti-NHP IL-2 APC	Miltenyi biotech UK	130091644
Anti-rat/hamster compensation beads	Beckton Dickinson UK	552845
Benzonase ® Nuclease	Novagen	706643
Bijou container	Sigma Aldrich UK	Z645338700EA
Bioanalyzer RNA nano kit	Agilent	5067-1511

Brefeldin A	Sigma Aldrich, UK	B7651
Casy cups	Roche diagnostics	43003
Casyton	Roche diagnostics	43001
CD16/32 (Fc block)	Ebioscience	14-0161-82
Cell strainers	BD Falcon	352350
CFSE	ebioscience	65085084
Cytofix/Cytoperm™ fixation/permeabilization solution kit	Becton Dickinson Ltd	555028
DMSO	Sigma Aldrich, UK	D2650
DNase digest kit	Qiagen	79254
Ethanol	Sigma Aldrich UK	32221
Fetal calf serum	Biosera Ltd, UK	S8130
Gas permeable plate sealers	Thermo Fisher	TUL98060V
Glycerol	Sigma Aldrich UK	G5516
Homogenisation tubes	Stretton Scientific UK	CK28R
Human AB pooled serum	Sera Labs international Ltd	S112F19887
Immersion Oil	Sigma-Aldrich, UK	10890
LD columns	Miltenyi biotech	130-042-901
Leucosep tubes	Greiner	227290

L-glutamine (4mM)	Sigma Aldrich, UK	G7513
Lymphoprep	Axis shield	NYC1114547
MGIT PANTA supplement	BD bioscience	245124
MGIT Tube	BD bioscience	245122
Micro tube	Sarstedt UK	72694006
Micro-fine Insulin Syringe with needle 1mL 29gx12.7mm	Nu-care products	M4891
MouseRef-8 v2.0 Expression BeadChip Kit	Illumina	202-0202
Oligo dt (15mer)	eurofins	N/A
Omniscript RT kit	Qiagen	205111
Pastettes	Appleton woods Ltd	KC244
PBS	Sigma Aldrich, UK	D8537
pen/strep (100U penicillin 100μg strep)	Sigma Aldrich, UK	P0781
Plastipak syringe 1ml Luer slip	Nu-care products	M0013
PPD tuberculin	Statens serum institute	2390
QuantiTect SYBR green master mix	Qiagen	204143
Recombinant human IL-2	R&D UK	202IL010
Recombinant human IL-7	R&D UK	207IL025
Red live/dead	Invitrogen UK	L23102

RNeasy mini kit	Qiagen	74104
RPMI with HEPES	Sigma Aldrich, UK	R5886
RPMI-1640	Sigma Aldrich, UK	R0883
SDS 10%	Sigma Aldrich UK	71736
Streptavidin-Cy3	Amasham	PA43001
TB quick stain	Becton Dickinson UK	212315
Totalprep kit	Ambion	AMIL1791
Trypan blue 0.4%	Sigma Aldrich UK	T8154
Tween 80	Becton Dickinson UK	231181
U bottom plates, with lid, 96-well	Jencons	7340027
Universal 25ml tube	Sigma Aldrich UK	Z645362400
Vaccutainer tubes heparin	Becton Dickinson UK	367526
Violet live dead	Invitrogen UK	L34955

Table 2-1 Reagents and consumables

2.1.2 Solutions

- **R10 media:** RPMI 1640 media supplemented with 10% serum (can be human pooled AB serum or fetal calf serum), 2mM L-glutamine; with/without 100U/ml penicillin and 100ug/ml streptomycin sulphate as stated and 1.7mM sodium glutamate.

- **MGIT RPMI:** RPMI media with HEPES supplemented with 2mM L-glutamine and 10% FCS
- **Cryopreservation media:** 90% fetal calf serum with 10% DMSO.
- **7H9 media:** 4.7g/l 7H9 powder made up with water and 0.05% Tween 80 and supplemented with 10% ADC after autoclaving and cooling below 55°C.
- **7H10 agar:** 19g/l of 7H10 powder made up with water and 5ml glycerol supplemented with 10% OADC after autoclaving and cooling below 55°C.
- **PBS:** 0.01M: NaCl 0.138M, KCl 0.0027M, pH 7.4: made by dissolving tablets in dH_2O.
- **Lysis buffer:** 0.067% SDS in 7H9 media and filtered through 0.2µm syringe filter.
- **FACS buffer:** 0.1% BSA in PBS.
- **MACS buffer:** PBS with 2mM EDTA and 0.5% FCS

2.1.3 Mycobacteria

- BCG Pasteur was kindly donated by Ann Rawkins at the HPA Porton Down, UK.
- Clinical grade BCG Danish was obtained from Statens Serum Institute.
- *M. tb* H37Rv strain was kindly donated by Simon Clark at the HPA Porton Down, UK.
- *M. tb* Erdman was obtained from Amy Yang at the FDA, Bethesda, USA

2.2 Microbiology

2.2.1 Liquid culture of BCG

BCG Pasteur was grown in 7H9 media in 250ml glass flasks for bulk preparations or in 25ml universal tubes for individual experiments. Cultures were incubated at 37°C at 240 RPM until an OD540nm of around 0.6 was obtained using a spectrophotometer. Purity of bulk cultures were assessed using the BD TB quick stain kit according to the manufacturer's instructions. Aliquots were frozen at -80°C and stored until use, some were kept as seed stocks for growing future batches of BCG.

2.2.2 Liquid culture of M. tb

M. tb was cultured in 7H9 media in 25ml plastic universal tubes at 37°C with shaking at 240rpm within a bio-secure plastic transport pot inside a CL3 laboratory. Cultures were incubated for 72h before being used in MGIAs.

2.3 NHP experiments

The animals used in this study were obtained from an established United Kingdom breeding colony. Monkeys were housed according to Home Office (United Kingdom) guidelines for the care and maintenance of primates and were sedated by intramuscular (i.m.) injection with ketamine hydrochloride (10 mg/kg of body weight) (Ketaset; Fort Dodge Animal Health

Ltd. Southampton, United Kingdom) for all procedures requiring removal from their cages. All procedures involving animals were approved by the Ethical Review Committee of the Centre for Emergency Preparedness and Response (CEPR), Salisbury, United Kingdom. None of the animals had been used previously for experimental procedures. All procedures carried out in NHP were performed by Dr M. Dennis and colleagues in the biological investigations unit at CEPR.

2.3.1 Vaccination of rhesus macaques with BCG and MVA85A

This work was not carried out by my-self as I performed my studies on cryopreserved PBMC taken from these NHP, detailed methods can be found in the published paper from this study [158]. BCG vaccinations were performed by immunising 12 animals intradermally (i.d) in the left upper arm with 100µl of BCG Danish strain 1331 (titre 4.25-7.55 $x10^6$ CFU/ml). At 12 weeks post BCG, 6 animals were immunised i.d with 100µl of MVA85A into their right upper arm (5 $x10^8$ PFU).

2.3.2 NHP aerosol challenge with M. tb Erdman

All animals were 4 years old at the time of challenge and naïve in terms of prior exposure to mycobacterial antigens (*M. tb* infection or environmental mycobacteria) apart from BCG vaccination, as demonstrated by a negative TST while in their original breeding colony, and by the gamma interferon (IFNγ)-based Primagam test kit (Biocor; CSL) just prior to the start of the study. Mono-dispersed bacteria in particles were generated using a three-jet Collison

nebulizer (BGI) and, in conjunction with a modified Henderson apparatus, delivered to the nose of each sedated primate via a modified veterinary anesthesia mask (estimated dose of 40-65 CFU). Challenge was performed on sedated animals placed within a "head-out" plethysmography chamber (Buxco, Wilmington, NC) to enable the aerosol to be delivered simultaneously with the measurement of the respiration rate.

2.4 Human/NHP immunology

2.4.1 PBMC isolation and Cryopreservation

PBMC were separated from Buffy coats (National Blood Service) or from fresh heparinised blood obtained from healthy volunteers/NHP using Leucosep tubes and Lymphoprep or Ficoll according to manufacturer's instructions. All PBMC were frozen in cryopreservation media and stored in liquid nitrogen until use, whereupon they were quickly thawed and washed x 2 in excess R10 media before being left for at least 2 hours at 37°C with 5% CO_2 and Benzonase 2µl/ml.

2.4.2 Surface staining of PBMC for flow cytometry

PBMC taken from MGIAs were phenotyped and assessed for proliferation by flow cytometry. PBMC were stained with 0.1µM CFSE prior to culture according to the manufacturer's instructions, to detect proliferation by dilution of fluorescent signal. All antibodies had been

previously titrated to determine the optimum amount of each antibody to use. PBMC were stained in 100µl of FACS buffer in the dark for 10mins with live/dead, before final staining with various combinations of surface antibodies (CD8, CD4, CD14, CD19, CD20, TCRαβ, and TCRγδ). Cells were washed with 1ml of FACS buffer and finally re-suspended in 250µl of FACS buffer and kept in the fridge until acquisition.

2.4.3 Intracellular staining of NHP PBMC for flow cytometry

All antibodies had been previously titrated to determine the optimum amount of each antibody to use. Cells were incubated with *M. tb* H37Rv ($3x10^5$ CFU/$1x10^6$ PBMC) in polypropylene facs tubes with 10µg/ml of Brefeldin A for 16h at 37°C with 5% CO_2, then washed with FACS buffer before being stained. Firstly, surface labelling antibodies (CD8, CD4, CD14, CD20, TCRαβ, TCRγδ and live/dead) were added at RT in the dark for 30 mins. Cells were washed with FACS buffer then treated with 250µl of cytofix/cytoperm solution for 15mins at RT in the dark, whereupon they were then washed with 1ml of perm wash solution. The cells were then ready for intracellular staining (IL-2, TNFα, IFNγ and CD3) at RT for 30mins in the dark. Finally the cells were washed with 1ml of perm wash and re-suspended in 250µl of FACS buffer with 4% formalin.

2.4.4 Flow cytometry of human/NHP PBMC

Stained cells were used for acquisition on the day of staining using an LSRII flow cytometer with FACS Diva software (BD bioscience). Compensation was performed using

unstained PBMC, CFSE stained PBMC (if used during culture) and single stained anti-Mouse Ig/κ, compensation beads (BD biosciences). Data were analysed using Flow Jo V 8.3 (Tree Star, inc). To assess polyfunctionality the Boolean gate platform in FlowJo was used with individual function gates to create all possible combinations of response patterns. Pestle version 1.3 (Mario Roederer, National Institutes of Health) was used to prepare data for the subsequent analysis of response profiles. The data analysis program, simplified presentation of incredibly complex evaluations (SPICE) (Mario Roederer, National Institute of Health) was used to analyse data and to generate graphical representations of functional T cell responses.

2.5 Mouse experiments

All procedures were performed in accordance with the terms of the UK Animals (Scientific Procedures) Act Project Licence (PPL 30/2414) and were approved by the University of Oxford Animal Care and Ethical Review Committee. All mice were housed in the Wellcome Trust Centre for Human Genetics Animal Facility (Functional Genomics Facility (FGF)) under Specific Pathogen Free (SPF) conditions. Female C57BL/6 mice (Harlan Laboratories, Oxfordshire, UK) were 6-8 weeks old at the start of experiments.

2.5.1 BCG vaccinations

All vaccinations were performed using BCG Pasteur by subcutaneous (s.c) injection in a volume of 100µl to the base of the tail using an insulin syringe (29G). The vast majority of vaccinations were kindly performed by Hazel Poyntz and Dr E. Stylianou. The dose of BCG is detailed in the relevant experiment sections.

2.5.2 *Mouse aerosol challenge with M. tb* Erdman

M. tb Erdman was defrosted and sonicated in a water bath for 1 minute then rested on ice for 1 minute, this was repeated 3 times. A sample of *M. tb* was plated out on 7H10 agar plates for estimation of CFU/ml. Animals were challenged using the Biaera aeroMP nose only challenge equipment in the CL3 suite at the FGF. Briefly, mice were loaded into individual nose only exposure restrainers that were fitted to the exposure apparatus. Mono-dispersed bacteria in particles were generated using a collision nebuliser which were delivered to the mice. The mice were challenged for 10 minutes followed by a purge cycle of 5 minutes, at which point mice were unloaded from the challenge apparatus and placed into CL3 housing units until they were sacrificed. The day after challenge, 2 naïve mice were sacrificed for calculation of the mean challenge dose, which was found to be 231 CFU/mouse. All other animals were sacrificed 4 weeks after challenge.

2.5.3 Estimation of M. tb burden in lungs/spleen

Mice were sacrificed by cervical dislocation and lungs/spleens removed aseptically by dissection to calculate the number of CFU/ml in these organs. Whole lungs/spleen from each animal were homogenised in 1ml of PBS using the Precellys 24 machine with ceramic beads (2.8mm) for 15s at 5500 rpm. The homogenates were serially diluted before being plated onto 7H10 agar and were counted after 2-3 weeks.

2.6 Mouse immunology

2.6.1 Splenocyte preparation

Mice were sacrificed by cervical dislocation and spleens removed aseptically by dissection. Spleens were crushed in PBS, passed through a sterile 70µm cell strainer and centrifuged (500xg, 5min). Supernatants were discarded and splenocytes re-suspended in complete R10 medium before being immediately centrifuged again (500xg, 5min). Splenocytes were finally re-suspended in R10 medium and counted using a CASY counter (Schärfe Systems, Germany).

2.6.2 T cell depletions

$CD4^+$ and $CD8^+$ T cells were depleted from splenocytes using Dynabeads in MACS buffer according to the manufacturer's instructions. The efficiency of depletion was assessed by flow cytometry using the methods in the section below.

2.6.3 Cellular staining of splenocytes for flow cytometry

All antibodies had been previously titrated to determine the optimum amount of each antibody to use and cells were stained in FACS buffer. Firstly, red live/dead stain was added to the cells in the dark for 10mins before the surface labelling antibody cocktail (CD8, CD4, CD14, NK, TCR$\alpha\beta$, TCR$\gamma\delta$ and B220) was added at 4^{o}C in the dark for 30 mins. Cells were washed with FACS buffer and finally the cells were re-suspended in 250µl of FACS buffer. Stained cells were used for acquisition in the same way as described in section 2.4.4; the only difference being that compensation was performed using unstained splenocytes and single stained anti-rat/hampster Ig/κ, compensation beads (BD biosciences).

2.7 Mycobacterial growth inhibition assays

2.7.1 Cultured mycobacterial growth inhibition assay

2.7.1.1 Preparation of BCG for use in cultured MGIA

Upon thawing, BCG was washed using a method adapted from one developed by T.H.M. Ottenhoff's team at Leiden University Medical Centre, Dept. of Infectious Diseases. Briefly BCG was pelleted, thoroughly washed and re-suspended (x3) in 7H9 media containing 0.05% Tween 80 to disaggregate clumps. The BCG was then re-suspended in 1.3ml of media, vortexed and left to sediment for exactly 1 minute whereupon the top 1ml was carefully aspirated off for use. Test vials were thawed after 48h to assess viability of the frozen BCG; serial dilutions were plated on 7H10 agar plates. Resulting CFU counts were used to calculate the mean CFU/ml for each batch after washing and disaggregation.

Due to the very large number of CFU counts needed for the MGIA, a 24 or 12 well agar plate technique was adopted, whereby approximately 1-2ml of 7H10 agar was pipetted into the wells of 24/12 well cell culture plates respectively. The agar containing wells were spotted with 20µl of bacteria, and counted after 2 weeks using a dissection microscope for the 24 well plates.

2.7.1.2 Origin of PBMC used for cultured MGIA

The cultured MGIA method used, was adapted from the assay published by S. Worku and D. Hoft 2003 [73]. Archived PBMC from a clinical trial previously performed by the Jenner group were used to see if we could replicate their results in our laboratory. Details of the trial are described elsewhere [159], briefly, healthy volunteers that had been previously vaccinated with BCG were enrolled to be revaccinated with a second dose of BCG, ClinicalTrials.gov NCT00654316, after obtaining ethical approval. Bloods were taken pre BCG boost and at defined time points post boost.

2.7.1.3 7 day antigen stimulation of PBMC

Unless otherwise stated, PBMC were cultured in 24 well plates at a density of $2x10^6$/ml of R10 with antibiotics or AIM V media, and incubated in 5% CO_2 at 37°C for 7 days. Where sufficient PBMC were available, each condition was tested with and without the addition of 20U IL-7 on day 0 and 20U IL-7 & IL-2 on day 3. Cultures were stimulated with BCG at an MOI of 6000 CFU/ $2x10^5$ PBMC, PPD 5μg/ml or media alone. To study proliferation of antigen specific cell populations, PBMC were stained with 0.1μM CFSE according to the manufacturer's instructions, prior to culture.

2.7.1.4 Co-culture of PBMC with BCG infected monocytes

Autologous monocytes were simultaneously selected for by adherence to 96 well plates after 2 hours incubation at 37°C in 5% CO_2. Monocytes were cultured and washed with warm

R10 media (human serum). Adhered monocytes were incubated for 6 days in media only, prior to infection with BCG. BCG infection was performed by removing the supernatant and adding disaggregated BCG in antibiotic free R10 at an MOI of 3:1 for 16 hours before carefully washing away non phagocytosed BCG. There were approximately 15,000 monocytes/well and monocyte layers were plated in triplicate. Three wells were included as positive controls to test for monocyte alone inhibition and three for negative controls to check for contamination.

On day 7, antigen stimulated PBMC were harvested, counted and $6x10^5$ were incubated in excess R10 without antibiotic. Cells were re-suspended in 600µl of antibiotic free R10 and 200µl of PBMC were added to each of the triplicate wells containing BCG infected monocytes. Cells were co-cultured for a further 3 days at 37°C in 5% CO_2 to assess the ability of antigen stimulated/media rested PBMC to inhibit growth of BCG within the monocytes. Remaining PBMC were analysed by flow cytometry for phenotypic and cell proliferation analysis as detailed in section 2.4.2.

On day 10 supernatants from co-cultures were removed by aspiration and 100µl of lysis buffer was added to each well. Plates were incubated at 37°C in 5% CO_2 for 1 hour to ensure complete lysis of monocytes, then 100µl of 7H9 media was added to each well and

cell lysates were serially diluted and plated out to determine the CFU of BCG/well. For each triplicate well, neat, 1:10 and 1:100 dilutions were plated in duplicate. Agar plates were incubated for 2-3 weeks before colony counting. To calculate growth inhibition the dilution which gave the most reproducible CFU counts across all replicates was used to calculate the mean CFU/ml. Percentage inhibition was calculated using the equation given by S. Worku and D. Hoft 2003 as follows; % inhibition = 100 - (100 x (CFU antigen stimulated/CFU media rested)).

2.7.2 Novel mycobacterial growth inhibition assay

2.7.2.1 Preparation of mycobacteria for novel MGIA

Three test vials of frozen stocks of BCG Pasteur or *M. tb* H37Rv were grown to mid log phase (OD540nm ~ 1.0), by inoculating 9ml of 7H9 media with 1ml of thawed bacteria in a universal tube, and shaking vigorously at 37°C for 72 hours. The bacteria were filtered using a 5µm syringe filter to remove clumps. The resulting suspensions were serially diluted in 7H9 media for plating out on 7H10 agar for enumeration. The mean CFU/ml from these cultures was then used to calculate all future CFU/ml for starter cultures after 72h.

2.7.2.2 The novel MGIA

All cell culture was performed using R10 media without antibiotics and all incubations were at 37°C with 5% CO_2. Mycobacteria that had been prepared as stated above were used to

infect human/NHP PBMC or murine splenocytes. Two varying methods for infecting the mammalian cells were utilised during this project but were always performed in polypropylene tubes to limit monocyte adherence. The first method involved infecting the PBMC/splenocytes at an MOI of 3:1 bacteria to monocytes (10% of total cell count) for 4h, before washing away non-phagocytosed bacteria by pelleting at 1800rpm for 5mins 3 times. The second method involved infecting PBMC/splenocytes with ~ $5x10^3$ mycobacteria/$1x10^6$ cells without washing. All infected cells were divided into 2 lots of triplicate test conditions for each subject/animal. On day 0 (D0) 3 tubes/wells for each subject/animal were harvested by centrifugation at 3000rpm for 15mins to pellet both the mammalian cells and extracellular mycobacteria; cell pellets were lysed immediately with lysis buffer at RT for at least 10mins. The remaining 3 tubes/wells were incubated for 4 or 7 days before being harvested and lysed. Cell lysates were serially diluted in 7H9 media and plated out in triplicate on 7H10 agar, the median CFU/ml was determined. The growth ratio was calculated as GR= CFU day 4 or 7/ CFU day 0.

2.7.3 MGIT mycobacterial growth inhibition assay

2.7.3.1 Preparation of mycobacteria for MGIT MGIA

This work was performed by R. Tanner at the Jenner Institute. A 1:200 dilution of BCG Pasteur seed stock was prepared by mixing 20µl of seed stock (at $1x10^7$ CFU/ml) with 4ml of 7H9 media with PANTA/enrichment (10%) in a 50ml tube. The solution was vortexed

thoroughly, and then clumped bacteria were allowed to settle for 10 minutes. The top 3ml was then transferred to a new 50ml tube without disturbing the sediment; 400µl of this diluted stock was added to 6 MGIT tubes with PANTA/enrichment which were placed in the MGIT 960 instrument (BD) at the John Radcliffe hospital, Oxford. The MGIT tubes were removed from the 960 instrument 1-2 days after they were all recorded as positive (this was 6-16 days after inoculation). If the cultures were not positive within this time frame, the process of stock preparation was repeated.

The positive MGIT tubes were mixed by inversion and again clumps were allowed to settle for 10 minutes; all but the bottom 0.5ml was transferred to a single 50ml tube and mixed thoroughly by vortexing. The bacteria were stored in 1.2 ml and mainly 500µl aliquots in microtubes at -80^{o}C before being used to create a standard curve; for this, 12 MGIT tubes were supplemented with PANTA/enrichment. A 1.2ml aliquot of BCG was used to prepare 5 serial 10-fold dilutions of stock in 7H9 media (with added PANTA/enrichment). MGIT tubes were inoculated in duplicate with 500µl of serially diluted BCG from Neat to 1x10^{-5} before being placed in the MGIT 960 instrument. Each dilution also had CFU counts performed using 7H10 agar plates so that Time to positivity (TTP) could be plotted against known CFU counts for serial dilutions, and provide the standard curve from which all TTP

values could be transformed into inoculum values (i.e. the volume in µl of neat BCG required to produce a certain TTP).

2.7.3.2 The MGIT mycobacterial growth inhibition assay using Splenocytes/PBMC

An aliquot of BCG Pasteur prepared according to the section above was thawed. The dose of BCG for inoculation of the positive controls and splenocytes/PBMC was calculated as follows; the ideal TTP is 6.5 days, the inoculum size to achieve this TTP is calculated from the standard curve according to the equation TTP =mx+c. Each different stock of BCG will have a different inoculum volume. Duplicate positive MGIT control tubes (with PANTA/enrichment) are directly inoculated with BCG which is made up to 500µl with 7H9 media. These control tubes are placed in the MGIT 960 instrument until they register as being positive.

Duplicate BCG infected splenocyte/PBMC cultures were set up for each animal in micro-tubes by adding 600µl of MGIT RPMI with 10% FCS to $1x10^6$ cells and the calculated inoculum of BCG. If the calculated inoculum of BCG was greater than 10µl then the bacteria were centrifuged at 12000rpm for 10 minutes and re-suspended in the RPMI to remove the 7H9 media. The cultures were incubated at 37°C in a rotating tube holder for 96h. At the time of harvest the cultures were centrifuged at 12000rpm for 5 minutes and the supernatant removed. The cell pellet was re-suspended in 1ml of tissue culture water

to allow lysis of the mammalian cells for 15mins with intermittent vortexing. Cells were again pelleted by centrifugation at 12000rpm for 10mins before the supernatant was removed. The pellet was finally re-suspended in 500µl of 7H9 media (with PANTA/enrichment) and added to MGIT tubes (with PANTA/enrichment) before being placed in the MGIT 960 instrument until they registered as being positive.

2.7.3.3 Converting TTP values into GR values

The TTP values were converted into CFU counts so that the GR could be calculated for each sample as a measure of mycobacterial growth inhibition. As stated in section 2.7.3.1 a standard curve of TTP plotted against the inoculum volume had been produced. The standard curve was a logarithmic straight line and so obeyed the equation $y= m(\ln x)+c$ where y= TTP, m= slope, x= inoculum and c= the y axis intercept. Therefore the value of x can be found by rearranging the equation to $x=(y-c)/m$. The inoculum value in µl could then be converted to CFU counts by multiplying it by the CFU/µl value of the BCG stock as calculated from the agar plates. Finally the GR value for a sample is calculated by the following equation GR=CFU Sample (96h)/CFU positive controls.

2.8 Molecular biology

2.8.1 RNA extractions from mouse splenocytes

Between 1-2x10^6 mouse splenocytes were pelleted and RNA extractions were performed using the RNeasy mini kit according to the manufacturer's instructions, with the inclusion of a DNase digest. RNA integrity was assessed using the RNA nano kit and Bioanalyzer from Agilent technologies according to their instructions, a RNA integrity (RIN) value of above 7.0 was indicative of high quality RNA.

2.8.2 q-PCR SYBR-green

2.8.2.1 Reverse transcription with Omniscript

The following master mix in Table 2-2 was prepared to perform reverse transcription of RNA to produce cDNA:

Reagent	**Volume (µl)**
10 x buffer RT	2
dNTP mix (5mM each)	2
Oligo-dT primer (100ng/µl 15mer)	1
Omniscript reverse transcriptase	1
RNase-free water	4

Table 2-2 Master mix for reverse transcription for q-PCR

Once the master mix had been prepared 10µl was added to 10µl of template RNA and the mixture incubated at 37°C with gentle shaking in a heat block for 60mins. The cDNA was then ready to be used for q-PCR.

2.8.2.2 q-PCR using QuantiTect kit

cDNA transcripts were used to perform relative quantification of genes by q-PCR using the QuantiTect kit. A master mix for each gene of interest was prepared for each sample in triplicate according to Table 2-3 below:

Reagent	**Volume (µl)**
QuantiTect master mix	10
Forward primer (10pmol/µl)	1
Reverse primer (10pmol/µl)	1
Water	7

Table 2-3 Master mix for q-PCR reactions.
Primer sequences are provided in the appendix.

Once the master mix had been prepared it was dispensed into wells of a 96 well light cycler plate; 1µl of cDNA template was then added to each triplicate well. Each gene also had triplicate negative control wells which contained master mix but no template to assess non-specific amplification. Finally before running the samples the plate was centrifuged briefly to collect the entire sample at the bottom of the plate and was sealed with a transparent film ensuring all wells were individually sealed. The program cycle was as follows:

15 minutes	95°C	
15s	95°C	45 cycles
20s	60°C	
20s	72°C	

Finally a melt curve analysis was performed to assess purity of the amplified product.

2.8.3 BeadChip Microarrays

2.8.3.1 RNA amplification and labeling

RNA from mouse splenocytes was amplified and labeled using the Ambion-Illumina TotalPrep RNA Amplification kit according to the manufacturer's instructions; briefly, mRNA was reverse transcribed to produce cDNA using oligo (dT) primers containing a T7 promoter to enable *in vitro* transcription (IVT). The single stranded cDNA was converted to double stranded cDNA, before amplification and incorporation of biotin UTP (Uracil triphosphate) into the cRNA (mRNA). The resulting cRNA was assessed using the Bioanalyzer to check that the peak transcript length was between 1.0-1.4Kbp in length as a measure of transcript integrity.

2.8.3.2 Hybridisation of cRNA

Hybridisation of biotinylated cRNA to Illumina MouseRef-8 v2.0 BeadChips was performed according the manufacturer's instructions; briefly, 750ng of cRNA from each sample was hybridized for 16h within an Illumina hybridization chamber inside an illumina hybridization

oven at 58°C with rocking. Samples were loaded in a random order so that grouped samples were not all present on the same chip which held 8 arrays each. The chips underwent a series of washes in proprietary buffers followed by a 100% ethanol wash before being labeled with streptavidin-Cy3 to detect transcript abundance. Unbound streptavidin-Cy3 was removed by a final wash before the chips were dried in falcon tubes by centrifugation at 250xg for 4 minutes.

2.8.3.3 Scanning of BeadChip micro-arrays

BeadChips were scanned on the day of labeling using an iScan BeadArray reader (Illumina). Data files containing information about the levels of fluorescence for each gene on the arrays were produced using BeadStudio software (Illumina).

2.8.3.4 Quality control of arrays

All microarray data analysis using the software package R, was kindly performed by M. Kostov. Firstly array quality was assessed using the arrayQualityMetrics, a Bioconductor package which generates a report of quality metrics for microarrays. As the quality of all the arrays was good, they were all given the same weighting, meaning that each array had the same level of influence over the analysis. Principle component analysis (PCA) was performed to assess which variables had the most influence on gene expression levels across the arrays. Background correction aided by control probes, followed by quantile normalization was performed using the Neqc function of the Bioconductor package limma

(linear models for microarray) to normalize the arrays and correct differences in staining between them.

2.8.3.5 Data filtering

Genes that were not significantly ($p<0.05$) expressed above the background in any of the arrays were removed from the analysis; as were genes whose inter quartile range (IQR) was less than 0.3 across the arrays, as this indicated that their expression was not altered during this study.

2.8.3.6 Identification of differentially expressed genes

Limma from Bioconductor was used to identify differentially expressed genes by estimating the fold change between predefined groups by fitting a linear model, and using an empirical Bayes method to moderate standard errors of the estimated $\log_2$ fold change in expression for each gene. P-values from the resulting comparisons were adjusted for multiple testing using the Benjamini-Hochberg method with a false discovery rate of 0.05. Lists of differentially expressed genes were assessed for pathways enrichment using DAVID bioinformatics software.

2.8.3.7 Statistical analysis

MGIA and flow cytometry data were analysed using Prism 5 (GraphPad, software Inc). Statistical tests to assess the difference between two populations were performed using the non-parametric Wilcoxon matched pairs and Mann Whitney T tests and parametric paired

and un-paired T tests were performed. Correlations were assessed using SPSS Spearman's Rho and p-values and coefficients are reported.

Chapter 3

Assessment of cultured mycobacterial growth inhibition assay

3 Assessment of cultured MGIA

3.1 Introduction

3.1.1 What is a MGIA?

As previously mentioned in section 1.7, MGIAs can be thought of as *in vitro* challenge models for assessing efficacy of TB vaccines. Immune cells such as PBMC, taken from animals or humans after vaccination against TB, are assessed for their ability to reduce mycobacterial growth as compared to cells taken prior to vaccination. It is hypothesised that vaccine induced growth inhibition/killing of mycobacteria *in vitro* will correlate with protection against *M. tb* challenge/efficacy *in vivo*. Thus, it is hoped these assays could provide the illusive surrogate of protection, which could dramatically alter and inform the selection process for vaccine development.

3.1.2 Why are there so many different MGIAs?

Several MGIAs have been developed by different groups to suit the types of samples that they are able to obtain for their studies, such as whole blood and PBMC from humans or splenocytes from mice. Each of the published assays outlined previously in the introduction, have pros and cons that make them more or less suitable for use with different sample types. One key factor influencing the development of different MGIAs is

the reproducibility and ease of transferring methodologies of these assays between research groups.

3.1.3 Deciding which MGIA to test

The first aim of my project was to assess whether BCG vaccination would result in a reduction of mycobacterial growth *in vitro* in humans. For this, it was decided that the cultured MGIA developed by Worku *et al* [73] would be the most suitable; a schematic of the assay is provided below (

Fig. 3-1). The assay contains a 7 day mycobacterial antigen stimulation step, which aims to expand memory T cells induced by BCG vaccination. An advantage of this type of assay is that it can be performed on cryopreserved PBMC, so archived samples from clinical trials could be tested, which is not possible with the whole blood MGIA [154]. The mouse splenocyte MGIA [156] was unsuitable for my project as the plan was for me to work with human and NHP PBMC samples.

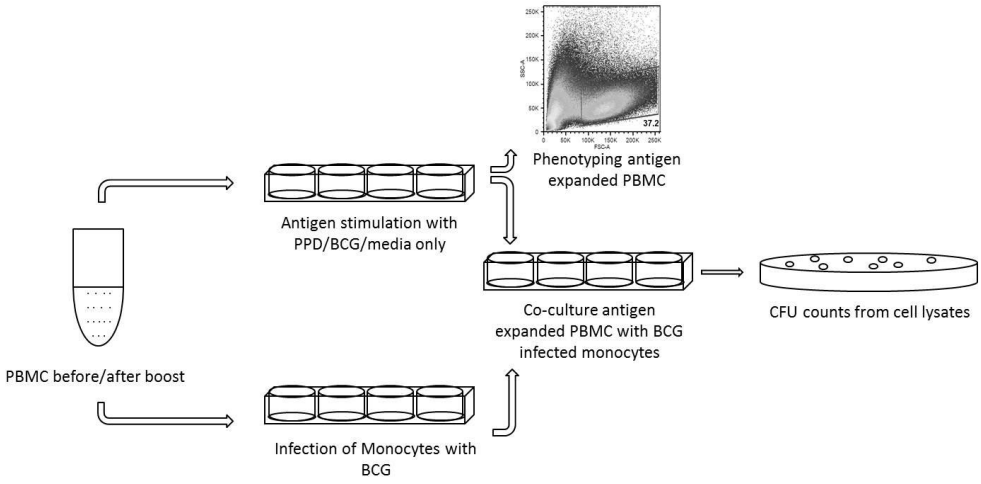

Fig. 3-1 Schematic outlining methodology of cultured MGIA.
PBMC taken from volunteers before and after BCG vaccination are stimulated with PPD, live BCG or media alone for 7 days, after which a proportion of the PBMC are analysed by flow cytometry. Autologous monocytes selected for by adherence are infected with BCG after 6 days culture. Antigen expanded PBMC and BCG infected monocytes are then co-cultured together to assess the ability of the PBMC to inhibit BCG growth in monocytes over 3 days as measured by CFU counts.

3.1.4 The need to optimise the cultured MGIA

Transferring the methodology for a MGIA is a challenging process, as these assays have many complex steps. This may explain why no other group has ever replicated previously published results from these assays. It was clear from the outset that alterations to the cultured MGIA were needed in order for me to successfully utilise this assay with cryopreserved PBMC. Many of the changes were made to improve cell viability as cell death was a major issue. All other alterations were concerned with the infection of monocytes with BCG and limiting variability of this process across assays.

3.1.5 Flow cytometric analysis

Flow cytometry was routinely used to investigate expansion of T cell populations in response to mycobacterial antigen stimulation. Prior to cell culture, PBMC were stained with CFSE, which incorporates into cells and is equally divided between daughter cells during proliferation. The decreasing fluorescent signal can therefore be used to measure cell division. The gating system that I used to identify distinct cell populations is detailed below (Fig. 3-2).

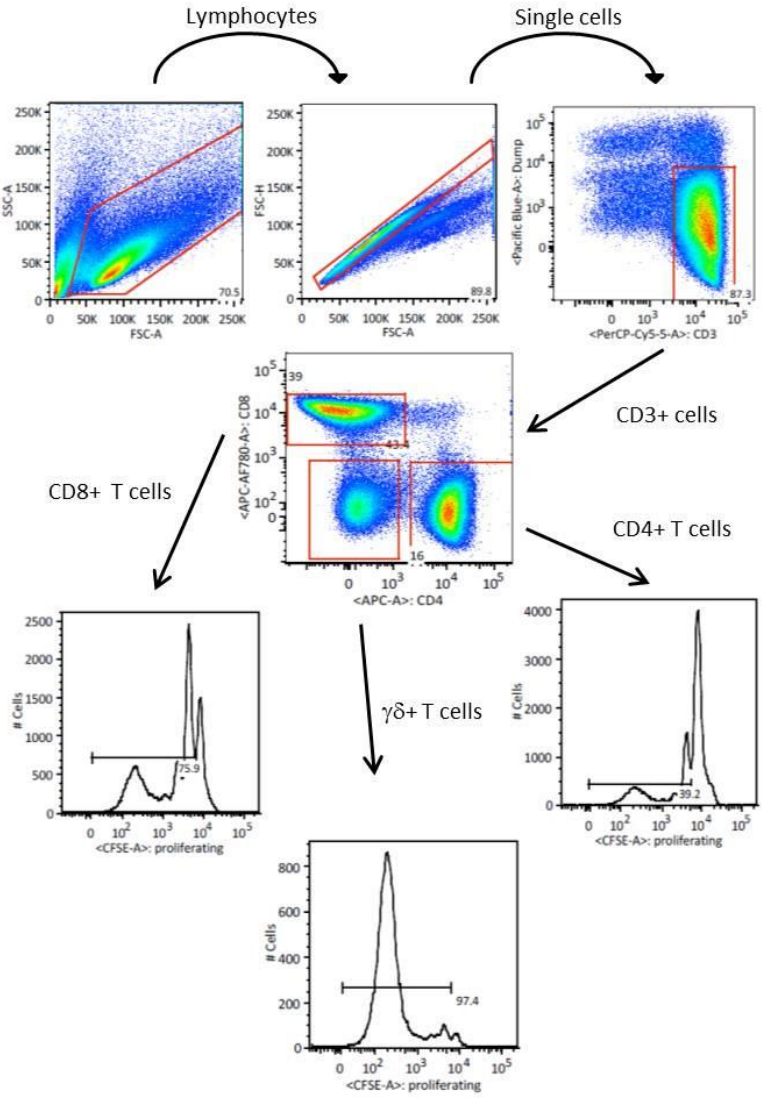

Fig. 3-2 Gating tree used throughout cultured MGIA.

PBMC were sorted by their physical size and complexity using forward and side scatter (respectively) to identify the lymphocyte population. Lymphocytes are further separated into single cells, $CD3^+$ cells are considered to be T cells and vivid dye was used to remove dead cells from the analysis. Finally the live T cells are separated into $CD4^+$, $CD8^+$ or $\gamma\delta^+$ T cells. The distinct T cell populations can then be gated for CFSE content to determine the level of proliferation.

3.2 Aims in this chapter

The aims of the experiments detailed in this chapter were as follows;

- Optimise expansion of PBMC with mycobacterial antigens for increased cell viability
- Assess different strains of BCG for their suitability for use in the MGIA
- Improve disaggregation of BCG for infection of monocytes
- Test the optimised MGIA on cryopreserved clinical trial samples to assess whether boosting BCG with a second dose of BCG enhances BCG growth inhibition *in vitro*
- Perform flow cytometry to phenotype the PBMC which have expanded in response to mycobacterial antigens, and determine whether this antigen expansion of T cell populations correlates with growth inhibition.

3.3 Results

3.3.1 Preliminary assessment of antigen stimulation method

Before attempting to perform the complete cultured MGIA, preliminary tests were carried out to check that all the separate processes involved in this complex assay worked independently. The first stage of the cultured MGIA is setting up the antigen stimulation of PBMC that are ultimately used for co-culture with BCG infected monocytes; this was where the preliminary experiments began.

Experiments to assess expansion of T cell populations by the mycobacterial antigens PPD and 85A were performed using cryopreserved PBMC from a BCG vaccinated volunteer (10 years previously), according to previously published methods [73]. The aims were to determine the levels of live cell recovery after 7 days culture, and ascertain whether stimulation with mycobacterial antigens would result in detectable proliferation of T cells in a BCG vaccinated individual.

Total cell counts were determined by flow cytometry for $CD4^+$, $CD8^+$ and $\gamma\delta^+$ T cell populations according to the gating tree outlined in Fig. 3-2. These counts were used to calculate the stimulation index for each T cell subset against each antigen (Fig. 3-3), stimulation index = counts antigen stim/counts media control. Unfortunately there did not

appear to be any perceivable expansion of $CD4^+$, $CD8^+$ or $\gamma\delta^+$ T cell populations in response to PPD or 85A as the stimulation index value of 1 means there has been no expansion; although this was only 1 volunteer and there were no replicates. A further limitation of this experiment was the omission of a positive control, such as concanavalin A, which would have made the interpretation of this apparent negative result easier interpret. However, The most interesting finding from this experiment, was that in all conditions, less than 40% of the starting PBMC were still viable after 7 days (PPD= 35%, 85A= 33% and media only= 28%). This would result in too few PBMC being available to perform the co-culturing step of the MGIA, so replicates would have to be dropped or suboptimal numbers of PBMC would have to be used. Therefore, rather than going on to evaluate proliferation in increased numbers of BCG-vaccinated subjects, I focussed at this point on optimising the culture conditions for increased PBMC viability during 7 day antigen stimulation.

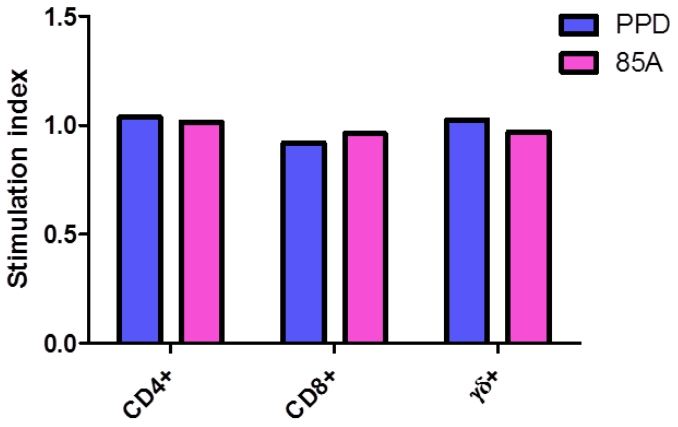

Fig. 3-3 Stimulation index for PPD and 85A stimulated T cells.
Flow cytometric data for a single BCG vaccinated volunteer where PBMC were stimulated with PPD (5μg/ml), 85A (2μg/ml) or media alone for 7 days. Bars represent the stimulation index (counts antigen stimulated/counts media control).

3.3.2 Comparison of cell culture medium

R10 media supplemented with human pooled AB serum was initially used for the 7 day culturing of PBMC according to published methods [73]. However, serum contains many immunological molecules with a broad spectrum of effects, including complement components involved in opsonisation of mycobacteria [40]. The effect of human sera upon PBMC taken from different donors is unlikely to be the same, and different batches of serum will result in some level of variability. AIM V, which is a proprietary serum free medium, was compared against R10 to establish which type of medium would result in the greatest yields of viable PBMC.

PBMC obtained from a single buffy coat were used to set up parallel cultures in triplicate using AIM V or R10 media with or without PPD. After 7 days culture, cells were analysed by flow cytometry to assess the frequency of viable T cells ($CD3^+$) (Fig. 3-4) for each culture condition. PBMC cultured in AIM V media contained significantly higher frequencies of live T cells after 7 days when compared to cells cultured in R10 media, regardless of antigen stimulation (PPD+ p=0.0023, PPD- p=0.0056). Values ranged from ≥ 35.7 ≤ 53.7% for AIM V cultured cells compared to ≥ 12.3 ≤ 26.2% for cells cultured in R10. Due to this result which was reproduced when the same cells were cultured using the same conditions in a separate experiment (data not shown); I decided that all future long-term PBMC culture would be performed using AIM V medium. The culturing of monocytes still had to be performed with R10, as AIM V media contains streptomycin and gentamicin, which would kill the mycobacteria used to infect the monocytes.

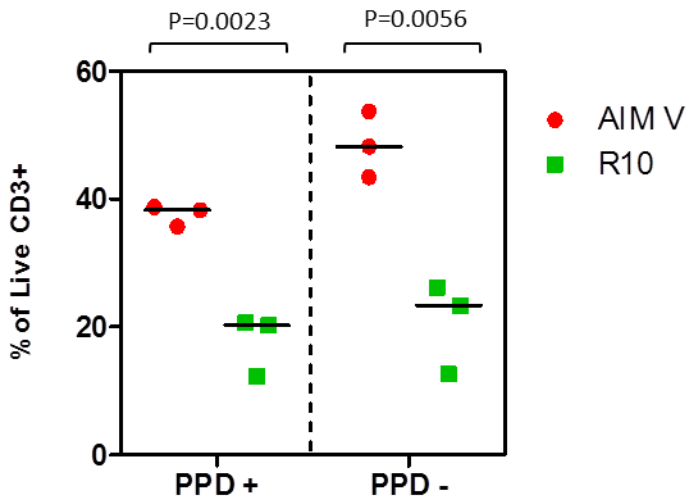

Fig. 3-4 Effect of different culture media on cell viability.
Flow cytometry data showing that long-term culture of PBMC in AIM V medium maintains T cell (CD3+) viability better than R10 medium. All data points are from a single buffy coat with tests carried out in triplicate. Bars represent the median % of live $CD3^+$ cells as a proportion of total number of cells in a sample. PPD+ indicates that PBMC were stimulated with 5µg/ml PPD, PPD- samples were cultured without any antigen. Data were analysed by 2 tailed unpaired T test.

3.3.3 Effect of cytokines on antigen stimulation of PBMC

Although there was an improvement in cell viability of PBMC when AIM V was used instead of R10, the number of live cells recovered from 7 day antigen stimulation was still consistently low. This would frequently result in insufficient cells being available to perform the co-culture step of the MGIA. The use of IL-2 and IL-7 is quite common practice during cell culture of cryopreserved primary cells [160, 161]. IL-7 is implicated in $CD4^+$ memory T cell survival and development [162, 163] and IL-2 has been shown to have both pro-proliferative and anti-apoptotic effects on $CD4^+$ and $CD8^+$ T cells [164]. I therefore went on to evaluate whether addition of these cytokines during antigen stimulation would increase

cell viability. The concentrations and time points used for the IL-2 and IL-7 stimulations had been previously optimised for use in cultured Elispot assays within our group; these were 20U/ml IL-7 on day 0, followed by 20U/ml of IL-7 and IL-2 on day 3 (Satti *et al*, unpublished data).

PBMC taken from 3 BCG vaccinated volunteers were stained with CFSE and used to assess antigen expansion of T cells cultured for 7 days with PPD, BCG or media rested in parallel with/without IL-2 and IL-7. The addition of IL-2 and IL-7 resulted in an approximately 10 fold increase in the number of live T cells recovered. This was significant for media rested $CD4^+$, $CD8^+$ and $\gamma\delta^+$ T cells (Fig. 3-5 graphs a, b and c respectively), and PPD stimulated $CD4^+$ T cells (a), p values ranged from 0.04-0.006 as determined by 2 tailed paired T test. Although there was a trend for increased live cell counts for all cultures where cytokines were present, the small number of volunteers meant that they were not significantly different ($p>0.05$).

IL-2 and IL-7 also induced non antigen specific proliferation in all the T cell populations studied; this can clearly be seen in the media only control cells (Fig. 3-5 graphs d-f) where there are high percentages of proliferating T cells in the antigen free control cells. This was an unexpected result as my hypothesis was that PBMC would undergo greater

expansion if both antigen and cytokines were present. PBMC cultured with antigen but without cytokines appeared to show slight expansion of $CD4^{+,}$ $CD8^{+}$ and $\gamma\delta^{+}$ T cells, but this was only significant for $\gamma\delta^{+}$ T cells stimulated with PPD (p=0.04) (f). Culturing without cytokines resulted in a dramatic loss of cell viability, making flow cytometric analysis and MGIA after 7 days antigen stimulation difficult to perform.

The question of whether to include IL-2 and IL-7 during antigen expansion was therefore difficult to resolve. On the one hand the addition of these cytokines significantly improved the viability of PBMC during 7 day culture with mycobacterial antigens, on the other, they induced strong non-specific proliferation in all the T cells studied, making it very difficult to determine the levels of expansion in response to antigen. I therefore decided to perform the antigen stimulations both with and without IL-2 and IL-7 in parallel during the MGIA, so that I could determine what effect, if any, they had on mycobacterial growth inhibition within this assay.

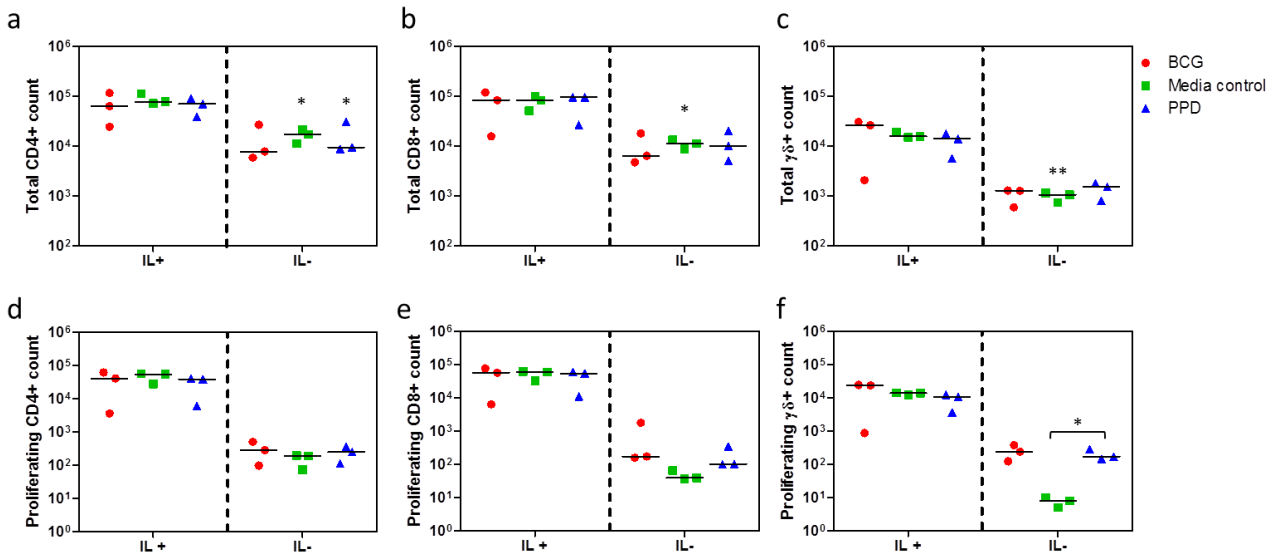

Fig. 3-5 IL-7 and IL-2 enhance T cell viability but also induce non antigen specific proliferation.
Graphs a-c show total number of live $CD4^+$, $CD8^+$ and $\gamma\delta^+$ T cells (respectively) present within a PBMC sample after 7 days culture with BCG 4000 CFU/2x10^5 PBMC, (red circles), media only control (green squares) or PPD 5µg/ml (blue triangles) (n=3). PBMC were also cultured with/without IL-2 and IL-7 20U/ml (IL+ or IL- respectively). Bars represent the median of 3 BCG vaccinated volunteers. * and ** indicate that live cell counts were significantly increased in cytokine cultured counterparts ($p<0.05$ and $p<0.01$ respectively) by 2 tailed paired T test. Graphs d-f show numbers of proliferating $CD4^+$, $CD8^+$ and $\gamma\delta^+$ T cells (respectively) as measured by CFSE intensity dilution, * indicates significant proliferation of PPD stimulated $\gamma\delta^+$ T cells as compared with media control.

3.3.4 Disaggregation of BCG

Mycobacteria are notoriously prone to aggregation due to their waxy cell wall which is hydrophobic; this is a problem when it comes to enumerating the bacteria using CFU counts; clumps of 100s of bacteria can be counted as a single colony on an agar plate. Aggregation of bacteria is also undesirable for infection of phagocytes as it has the potential to generate variability in the assay, as one phagocyte might take up 2 single bacteria, whereas another might engulf a particle containing many more. There are many

different methods available for disaggregation but for my studies the method would have to be suitable for use at containment level 3 for studies using *M. tb*.

Tests using a water bath sonicator for 5 minutes on BCG Danish cultures resulted in ineffective disaggregation of bacterial clumps as determined by colony morphology on 7H10 plates (personal observation); this method was therefore unsuitable for use with this stock of BCG. One method of removing large bacterial aggregates is to leave the bacteria to sediment for a short time before aspirating off the non sedimented bacteria. This method was used to test both BCG Pasteur and BCG Danish to assess which of these strains would be most suitable for use in the MGIA.

The colony morphology of my BCG Danish was still very rough, rose up from the surface of the plate and colony size was quite variable, which was most likely due to large numbers of bacteria starting a single colony. The BCG Pasteur on the other hand was a lot more uniform in size and shape, which is indicative of a more homogenous suspension. I therefore decided that BCG Pasteur would be used throughout the remainder of my studies, and the sedimentation method would be used during the cultured MGIA.

3.3.5 Cultured MGIA results

3.3.5.1 Effect of BCG boost on mycobacterial growth inhibition in vitro

Once the methods for antigen stimulation of PBMC and disaggregation of BCG Pasteur stocks had been optimised, it was possible to evaluate whether I could achieve similar cultured MGIA results to those already published [73]. The cultured MGIA had to distinguish between the ability of PBMC taken recently after BCG vaccination, and those taken before vaccination, to inhibit growth of BCG inside autologous monocytes *in vitro.* The levels of growth inhibition could then be correlated against the levels of proliferation of $CD4^{+,}$ $CD8^{+}$ and $\gamma\delta^{+}$ T cells in response to mycobacterial antigen stimulation and other immunological parameters such as Elispot responses.

Archived PBMC from one of the Jenner Institute's clinical trials (NCT00654316) [159] were utilised for the purpose of assessing the cultured MGIA with my optimisations. Volunteers, who had historically been vaccinated with BCG, received a second BCG vaccination (Danish SSI) (mean time between BCG vaccinations was 16 years). Cryopreserved PBMC from 7 volunteers taken 1 week prior to the BCG boost (W-1), and at weeks 4 and 24 post BCG boost were assessed for their ability to inhibit mycobacterial growth inside autologous monocytes *in vitro*. PBMC were first stained with CFSE and cultured for 7 days with PPD (tuberculin), BCG (Pasteur) or media alone to expand memory T cells prior to their co-culture with BCG infected monocytes. Parallel cultures were set up to assess the effects of IL-2 and IL-7 on antigen expansion whenever sufficient PBMC were available to do so.

The primary readout for the MGIA is CFU counts, which are displayed in Fig. 3-6, graphs a and b for PPD stimulated cultures with/without cytokines respectively and c and d for BCG stimulated cultures with/without cytokines respectively. The CFU counts were used to calculate the percentage inhibition of antigen stimulated PBMC in relation to the media controls (as done previously by Worku *et al.* 2002) according to the following calculation % inhibition = 100 - (100 x (CFU antigen stimulated/CFU media rested)).

PBMC taken from volunteers 4 weeks post BCG boost and stimulated with PPD plus cytokines or just BCG, were able to significantly inhibit mycobacterial growth *in vitro*, compared with PBMC taken prior to re-vaccination ($p=0.0313$ for PPD+ cytokine stimulation and $p=0.0469$ for BCG stimulation respectively (Fig. 3-7 graphs a and d). However, PBMC that were stimulated with PPD alone or with BCG plus cytokines did not show significant growth inhibition at any time point post BCG boost (Fig. 3-7. graphs b and c).

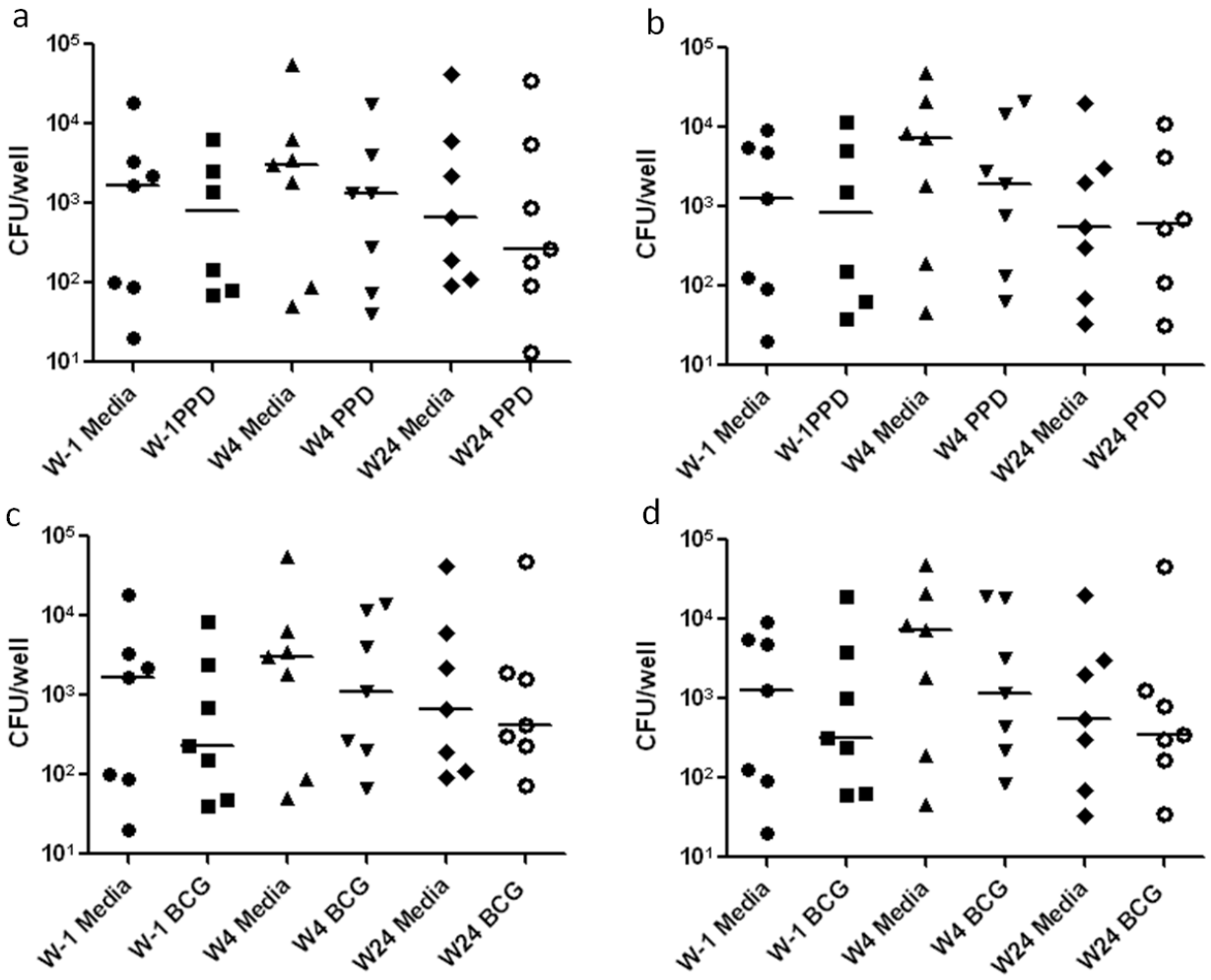

Fig. 3-6 Raw CFU counts for cultured MGIA

Graphs a and b show raw CFU data from PBMC stimulated with PPD (5ug/ml) and with/without cytokines (20U/ml) respectively (n=6-7). Graphs c and d show CFU data from PBMC cultured with whole BCG Pasteur ($3x10^4$/$1x10^6$ PBMC) and with/without cytokines respectively. The bars represent the median CFU value.

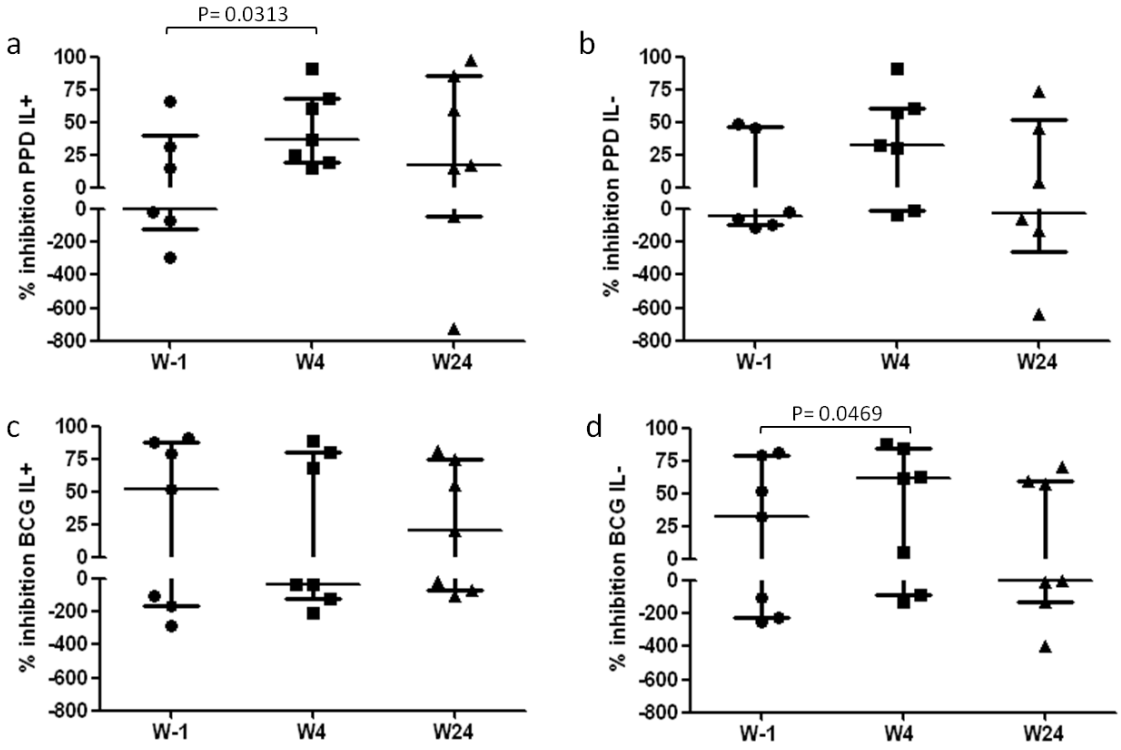

Fig. 3-7 Mycobacterial growth inhibition induced by BCG boost in human volunteers.
Graphs a and b show % growth inhibition data from PBMC stimulated with PPD (5ug/ml) and with/without cytokines (20U/ml) respectively (n=6-7). Graphs c and d show % inhibition data from PBMC cultured with whole BCG Pasteur ($3x10^4$/$1x10^6$ PBMC) and with/without cytokines respectively. The bars represent the median with interquartile range. Data were tested by Wilcoxon matched pairs T test.

3.3.5.2 Proliferation of T cell subsets in response to antigen stimulation

The same PBMC that had been antigen expanded or media rested for use in the MGIA were also assessed by flow cytometry. These cells had been stained with CFSE so that dividing cells could be identified, and therefore, the percentage of proliferating T cells in response to media only, PPD or BCG stimulation could be calculated for each T cell sub-

type (Fig. 3-8a-c). Data showing the effect of IL-2 and IL-7 (cytokines) on T cell proliferation are also provided (Fig. 3-8d-f).

In general there was a trend for greater proliferation of $CD4^+$ T cells in response to stimulation with PPD than with whole BCG when cytokines were not added to cultures, although this was not statistically significant (Fig. 3-8a). There was significant proliferation of $CD8^+$ T cells in samples taken 24 weeks post BCG boost when BCG was used as the stimulating antigen, which again, was only detected when cytokines were not added, $p=0.016$ (Fig. 3-8b). In contrast, in comparisons at weeks 4 and 24 between antigen stimulated and media rested PBMC, $\gamma\delta^+$ T cells showed significant expansion due to PPD and BCG ($p \leq 0.032$) (Fig. 3-8c). The week -1 data for these cells followed the same pattern and magnitude as for week 4 and 24, but there were only 4 data points available and so the antigen expansion is not significant. The BCG booster vaccination had no effect on the median levels of proliferation of any of the T cell populations studied.

As I have shown previously in Fig. 3-5, the addition of cytokines during the culture period resulted in unwanted non-specific proliferation of media rested cells (Fig. 3-8d-f). This meant that determining the levels of proliferation in response to antigen was impossible when IL-2 and IL-7 were used in cultures. When these cytokines were added to media

rested PBMC there was often significantly greater numbers of proliferating $CD4^+$ and $CD8^+$ T cells as compared to cultures where cytokines and PPD or BCG were present ($p \leq 0.032$) (Fig. 3-8d and e). This effect was absent in $\gamma\delta^+$ T cells cultured with cytokines (Fig. 3-8f) as the levels of proliferation in all conditions was close to 100%. The reason why I used Mann Whitney t tests for the analysis of the PBMC cultured without cytokines, was that a number of samples are missing due to insufficient numbers of cells available after the 7 day antigen stimulation. This meant that there was often not enough data to perform Wilcoxon matched pairs t tests, whereas this was not a problem when PBMC were cultured with cytokines.

The T cell proliferation and growth inhibition data from the MGIA were analysed for correlations against each other (non-parametric, spearman rank, pairwise correlations) and also against Elispot results obtained during the clinical trial from which the PBMC were taken (data shown in appendix), however, there were no significant correlations in any of the parameters tested.

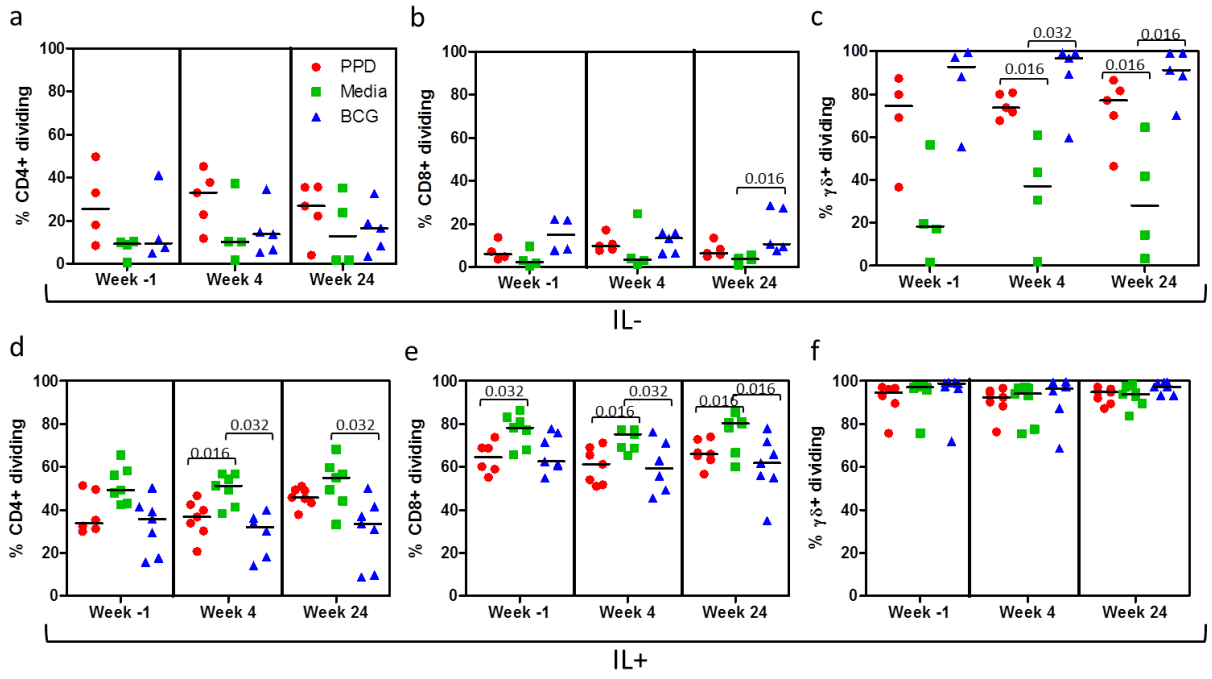

Fig. 3-8 Proliferation of T cells in response to mycobacterial antigens and cytokines.

Flow cytometry data from antigen stimulated PBMC used in MGIA (n=4-7). The graphs show % proliferation of distinct T cell populations within a PBMC sample taken 1 week prior to BCG boost (week -1), 4 and 24 weeks after BCG boost. (% dividing = 100 x (number of defined T cells in dividing gate/ total number of defined T cell)). PBMC were stimulated for 7 days with PPD 5μg/ml (red circles) BCG 6000 CFU/ 2 x 10^5 PBMC (Blue triangles) or media rested (green squares). Bars represent the median % proliferation. Graphs a-c show data from PBMC cultured without IL-2 and IL-7 with p-values determined by Mann Whitney t test. d-f show data for PBMC cultured with IL-2 and IL-7, p-values determined by Wilcoxon matched pairs t test.

3.4 Discussion

In 2002, D. Hoft *et al.* described a cultured MGIA where PBMCs taken from adult volunteers displayed enhanced ability to inhibit mycobacterial growth *in vitro* after re-vaccination with BCG [165]. This same study also assessed the *ex vivo* and whole blood MGIAs in parallel so comparisons could be drawn between the effectiveness of all three MGIAs against the same set of clinical trial samples. It is hoped that MGIAs might eventually provide a surrogate of protection against TB. In this present study, the cultured MGIA was used to assess cryopreserved PBMC from a clinical trial, where volunteers who had historically received BCG vaccination were re-vaccinated, thus, the samples were similar, although not identical to those used in the published cultured MGIA.

Mycobacterial growth inhibition was seen 4 weeks after BCG re-vaccination when PPD (with cytokines) or whole BCG was used as a stimulant, which generally concurs with the published data where mycobacterial growth inhibition was seen 8 and 24 weeks after BCG re-vaccination in humans [165]. However, mycobacterial growth inhibition was not seen 24 weeks after BCG re-vaccination in the present study. There are a number of reasons why this lack of growth inhibition could have occurred in these samples. One difference between the samples used for this study and those of the published studies, was that samples in this experiment had been cryopreserved; for assays such as Elispot and flow

cytometry, responses of cryopreserved cells have been shown to highly correlate with those of fresh cells [166, 167]. However, decreased cell viability has been correlated with decreased levels of proliferation in mononuclear cells [168]. There is no evidence from either the CFU counts (a measure of monocyte integrity) or the proliferation data to suggest that cell viability was an issue with the week 24 samples, so it is unlikely that cryopreservation accounts for the lack of mycobacterial growth inhibition at this time-point. One other important difference between the samples used in this study and those used for the published cultured MGIA, is the vaccine regime. Volunteers in the trial performed at the Jenner Institute received a BCG re-vaccination after an average interval of 16 years with 1 $x10^6$ CFU of BCG Danish; participants in the trial from which the published cultured MGIA data are taken were given their BCG re-vaccination 6 months after the initial vaccination and were immunized with $3x10^6$ CFU of Connaught BCG. There were therefore differences in the strain of BCG, the dose of BCG and the interval between BCG prime and re-vaccination. A Meta-analysis of the strains used in human efficacy trials suggests that the strain of BCG used does not have a significant impact upon protection [169], it is therefore unlikely that differences in BCG strain account for the differences seen in mycobacterial growth inhibition.

The shorter interval between BCG re-vaccination and higher dose of BCG used for the cultured MGIA could have a combined effect in producing greater T cell memory responses due to antigen persistence. There is evidence that immunogenicity of BCG vaccination is directly linked to dose and the number of viable mycobacteria [170]. However, the evidence for greater protection in response to antigen persistence is not so straight forward. Traditionally, immunological memory is thought to develop after antigen clearance in response to contraction of the effector population [171]. The persistence of BCG after vaccination is thought to prolong the effector phase and limit memory T cell development [172]. In an early study, it was found that resolution of a primary *M. tb* infection by isoniazid chemotherapy was necessary to generate $CD4^+$ memory T cells [173]. In contrast research has also demonstrated that *M. tb* strains engineered to be less virulent but more persistent in the host than BCG, offer increased protection from *M. tb* infection compared to BCG [123]. In the case of BCG vaccination, for example, it is well documented that heat-killed BCG, which does not persist in the host, provides significantly less protection than viable BCG against a TB challenge [174, 175]. It is therefore difficult to conclude whether greater antigen persistence could explain the differences in mycobacterial growth inhibition seen in the two different studies. It is possible that further assessment of the memory cell phenotypes present within the antigen stimulated cultures by multi-parameter flow cytometry, would reveal the memory-specific responses induced by mycobacterial antigens. It should

also be noted that although the cultured MGIA was shown to detect mycobacterial growth inhibition 8 and 24 weeks after BCG re-vaccination, the *ex-vivo* and whole blood MGIAs only detected growth inhibition 8 weeks after re-vaccination [165], which is in agreement with my findings. The authors of the study also investigated lymphoproliferative responses, IFN-γ secretion and $\gamma\delta^+$ T cell expansion at each time-point; between weeks 8 and 24 all three of these parameters decreased over time. These findings suggest that mycobacterial growth inhibition may only be detectable during a limited time period after vaccination, which corresponds with peak effector functions of T cells.

Although it is widely accepted that T_H1 immune responses activate macrophages to kill internalised mycobacteria, at this stage, the exact mechanisms behind mycobacterial growth inhibition *in vitro* is unknown. Some work by Worku *et al* 2003. points towards physical contact between PBMC and infected monocytes being essential to produce inhibition, suggestive that soluble mediators such as IFN-γ are not the main mechanism [73], this is in agreement with the finding that the addition of recombinant IFN-γ or TNF-α to *M. tb* infected monocyte cultures produces very little reduction in bacterial numbers, whereas, addition of PBMCs results in substantial decreases in CFU [153]. No significant correlations between IFN-γ secretion (*ex vivo* Elispot) and growth inhibition were seen during this study, which is in agreement with the observation that although IFN-γ is essential for mycobacterial

immunity [176], it is not directly responsible for mycobacterial killing *in vitro* [177, 178]. However, *ex-vivo* Elispot is a measure of T_{EM} responses, whereas the cultured MGIA also measures T_{CM} responses. This might account for the lack of correlation between mycobacterial growth inhibition and *ex-vivo* Elispot results. It is possible that cultured Elispot results would have been a more appropriate measure to correlate against mycobacterial growth inhibition.

Mycobacterial growth inhibition has been show to positively correlate with proliferation of $\gamma\delta^+$ T cells in response to stimulation with mycobacterial antigens [73]. Data from other MGIAs show that $CD4^+$ T cells are important for growth inhibition in mycobacteria sensitised individuals [153, 154]. The results presented here show that $CD4^+$ and $CD8^+$ T cells did not generally display significant levels of proliferation in response to PPD or BCG stimulation whereas $\gamma\delta^+$ T cells showed very significant proliferative responses. $\gamma\delta^+$ T cells can be activated in a MHC independent manner by non-peptidic antigens expressed by BCG [179-181]. This could account for the rapid and extensive proliferation of these cells in response to BCG/PPD. $CD4^+$ and $CD8^+$ T cells have to undergo MHC dependent antigen presentation from APC with co-receptors (naïve cells) in order to be activated and avoid becoming anergic. The extensive proliferation of $\gamma\delta^+$ T cells does not appear to be a memory response induced by the BCG boost, as proliferation levels remained similar across

pre and post boost time points. This is in contrast to the finding that BCG vaccination induces $\gamma\delta^+$ T cell memory responses, which correlate with mycobacterial growth inhibition [73, 165]. The way in which $\gamma\delta^+$ T cell expansion was calculated in these studies was to assess total numbers of $\gamma\delta^+$ T cells compared against $CD4^+$ and $CD8^+$ T cell numbers. Whereas, the calculations in this present study were on the proportion of $\gamma\delta^+$ T cells that were proliferating compared with the total $\gamma\delta^+$ T cell population. It is possible that measuring the strength of proliferation in terms of the number of divisions may have revealed memory responses of $\gamma\delta^+$ T cells in response to BCG re-vaccination. It is also possible that proliferation itself may not be the best measure of PBMC responses to stimulation, as the T cell proliferation data from this study did not correlate with growth inhibition. Investigation of activation markers and secreted immune mediators may be more appropriate for determining the role of different cell types in MGIAs.

Cell viability of cryopreserved PBMC over the course of the cultured MGIA was very low; the use of IL-7 and IL-2 as maintenance signals for long-term T cell culture is relatively common [3]. IL-7 is implicated in $CD4^+$ memory T cell survival and development [4, 5]; these cells have been shown to be important in other MGIA [153, 154]. There is growing evidence that apoptosis is a major cause of cell death in cryopreserved cells in humans and animals [161, 182, 183] and it is hypothesised that apoptosis is induced when

mitochondrial membranes are damaged during cryopreservation, the cause of which, has not been identified; this damage may lead to perturbation of the membrane potential of the mitochondria triggering the release of cytochrome c, caspase 3 and caspase 9 which induce apoptosis [161]. Studies have shown that blocking apoptosis not only increases cell viability, but also cell functionality [183]. The use of these cytokines had the desired effect of improving cell viability. However, IL-2 and IL-7 induced non-specific proliferation, therefore, antigen specific T cell proliferation could not be correlated against mycobacterial inhibition, as previously published [2]. It was surprising that addition of IL-7 and IL-2 resulted in non-specific proliferation of T cells during culture, as other studies have shown that naïve T cells do not proliferate in response to these cytokines *in vitro* when used at similar concentrations to ones I used [161, 184]. This difference could have been caused by the continued use of these cytokines throughout the culture period, instead of only using them for 12h to recover the thawed cells prior to their culture [161]. Also, the study in which these cytokines did not induce a proliferative effect on naïve cells only assessed $CD4^+$ T cells, all other PBMC had been depleted [184]; so there could have been a lack of monocyte derived cytokines such as TNF-α and IL-12, that were possibly present in my cultures, that influenced proliferation. It is noteworthy that the $CD4^+$ T cells had the weakest proliferative responses to IL-2 and IL-7 in my cultures, which suggests that naïve $CD4^+$ T cells do not strongly proliferate whereas naïve $\gamma\delta^+$ and $CD8^+$ T cells do. Given

these findings, the optimal use of IL-2 and IL-7 for improvement of PBMC viability, should possibly be limited to the thawing process, and not throughout the culture period. Although, the effect of a shorter incubation time with these cytokines would still need to be assessed for nonspecific proliferation. Another unexpected finding was that in cultures where cytokines but no antigen was present, there appeared to be significantly greater proportions of $CD4^+$ and $CD8^+$ cells proliferating than in cultures where both cytokines and antigen were present. This effect cannot be explained by differential levels of cell death between antigen stimulated and media rested cultures as dead cells were removed from the analysis as were B cells and monocytes, although it is possible that cells undergoing apoptosis which would be unresponsive to proliferation signals might not have been removed by gating on dead cells. The addition of antigens could also have inhibited proliferation of some T cells by the induction of anergy in response to suboptimal co-stimulation of naïve $CD4^+$ and $CD8^+$ T cells. Further multi-parametric flow cytometry with an apoptosis marker and cytokine staining could have been performed to resolve this question.

For an assay to be successfully utilised as a surrogate of protection, it must be reproducible and transferable between research institutes, particularly those in developing countries where efficacy trials for TB vaccines are conducted. Although significant mycobacterial growth inhibition in response to BCG re-vaccination was achieved during this

study, the range of these data are not consistent with what has been previously reported [73, 165]. These inconsistencies may have been due to the use of cryopreserved cells, although fresh PBMC samples from BCG vaccinated volunteers were not available for a direct comparison to be made. I believe the variability was caused by technical issues with infection of the monocyte layers, as raw CFU values from BCG infected monocytes differed greatly between volunteers even when no PBMC were added (monocyte only controls) (data shown in appendix); which suggests that either the volunteers had highly variable levels of innate growth inhibition in their monocytes, or the numbers of monocytes isolated and the levels of BCG infection were not uniform across volunteers or the different time-points. The cultured MGIA is the most technically challenging of all of the MGIAs and as such, transferability of this assay is perhaps limited, so it is unlikely that this assay would be suitable for use across multiple research institutes and in large scale clinical trials.

3.5 Chapter conclusions

- Culture of cryopreserved PBMC for 7 days with antigen results in extensive cell death, which is possibly caused by caspase driven apoptosis

- Culture in AIM V media instead of R10 improved cell viability
- Culture with IL-2 and IL-7 greatly enhanced cell viability but resulted in non-specific proliferation of T cells
- Strain of BCG used for vaccination/assay might be important and disaggregation is problematic
- BCG re-vaccination resulted in mycobacterial growth inhibition 4 weeks post boost compared with before boost
- T cell proliferation and *ex-vivo* Elispot results did not correlate with growth inhibition
- Variability of growth inhibition values between volunteers was substantial, resulting in reduced confidence in the results obtained

Chapter 4

Development of a novel MGIA

4 Developing a novel total PBMC infection MGIA

4.1 Introduction

4.1.1 Why develop a novel whole PBMC infection MGIA?

Due to the variability of the data obtained from the cultured MGIA (chapter 3) and an intrinsic problem with the suitability of this assay for use with samples where cell abundance was low, I decided to explore the use of an alternative MGIA for the remainder of my studies. As mentioned in section 1.7, a number of MGIAs have been published by different groups over the last decade. Unfortunately, each MGIA had characteristics that meant that they were not entirely suitable for use with cryopreserved human and NHP PBMC samples, which were available to use.

Data from the ex *vivo* MGIA [153] was for fresh PBMC and the assay had not been used to demonstrate BCG vaccine induced mycobacterial growth inhibition, therefore, I decided against using this assay for my work. The whole blood (WB) and MGIT MGIAs [154, 155] had only been demonstrated to be effective for fresh whole blood and not PBMC, so were not directly applicable to my studies, which planned to use cryopreserved PBMC from both NHP and human samples. The murine MGIA [156] was not suitable, as it required the use of splenocytes and bone marrow derived macrophages neither of which are readily available

from humans or NHP. Unfortunately, none of the published MGIA appeared to be suited for use with cryopreserved PBMC; I therefore decided to use this opportunity to develop a novel MGIA that would be simple to perform, require fewer cells and be suitable for a range of different cell types.

4.1.2 The total PBMC infection MGIA

4.1.2.1 Infection of total PBMC with BCG

The most likely main causes of variability that I witnessed with the cultured MGIA, were the cell viability of antigen expanded T cells and differences in the quality of the monocyte layers infected with BCG. The WB and MGIT MGIAs [154, 155] do not involve the separation and infection of monocyte layers with BCG, instead, mycobacteria are added to WB cultures at a low dose and are left to incubate for 96h. These assays therefore do not suffer from monocyte layer variability, so I decided to use this infection strategy in my novel MGIA. I also adopted a 96h incubation period, as this duration was also used for the WB and MGIT MGIA.

One of the problems with this infection strategy is that it is not known whether the bacteria are phagocytosed or are living extracellularly within cultures. It is therefore impossible to ascertain whether growth inhibition is caused by macrophage activation, or some other cell population, mechanism or artefact in the blood. The novel MGIA would be performed on

PBMC; I could therefore infect the PBMC (all mononuclear cells including monocytes), and then wash away non-phagocytosed mycobacteria after 4h by pelleting the PBMC and removing the supernatant. The aim was that by removing extracellular bacteria, I would enhance the sensitivity of the assay and ensure that any perceived mycobacterial growth inhibition was due to intracellular killing of the bacteria.

4.1.2.2 Total PBMC infection MGIA overview

Mycobacteria were used to infect total PBMCs for 4 hours, after which, PBMC were pelleted using a duration and speed that would not pellet free mycobacteria and the supernatant was discarded. PBMC were washed 3 times in this manner to remove non-cell associated bacteria before being split into 6 equal samples. Three of 6 of these samples were immediately harvested (T0) by prolonged centrifugation at high speed to pellet all PBMC and any extracellular mycobacteria. Pellets were lysed and the CFU determined by plating out serial dilutions on 7H10 agar. The remaining 3 samples were cultured for 96h before harvesting (T96) and plating out for CFU.

CFU counts were used to calculate the growth ratio (GR= CFU T96/CFU T0). As the T96 CFU counts are compared against matched T0 values, any variability in the infection level between individuals is normalised. I hypothesised that PBMC taken from BCG vaccinated humans/animals, would result in lower GR values than those achieved by naïve PBMC.

4.2 Aims of this chapter

The aims of the experiments detailed in this chapter were as follows;

- Perform preliminary tests to assess suitability of total PBMC infection method
- Optimise methods for the total PBMC infection MGIA
- Assess variability of this assay
- Assess the ability of this assay to differentiate between naïve PBMC and those taken post BCG vaccination

4.3 Results

4.3.1 Total PBMC infection method

As this assay had not been performed before, I wanted to determine if infection of total PBMC with BCG, followed by washing, resulted in recovery of sufficient numbers of bacteria from the cultures as well as the removal of non-phagocytosed BCG. The first assessment was performed using cryopreserved PBMC taken from 6 healthy volunteers. Samples were processed as outlined in **Error! Reference source not found.**, but in an attempt to determine the phenotypic cell association of the BCG left behind after washing; I stained the BCG with CFSE and took a proportion of the infected PBMC at T0 and T96 for flow cytometric analysis.

4.3.1.1 Growth kinetics of BCG Pasteur in PBMC culture

As the name implies, a MGIA should be a measure of mycobacterial growth inhibition, therefore, there had to be some bacterial growth over the course of the 96h culture period for this assay to be effective. Mycobacterial growth was observed in all 6 of the volunteers with fairly similar kinetics (Fig. 4-1), as determined by CFU counts obtained at T0 and at T96 (mean CFU $8.1x10^4$ and $1.7x10^5$ respectively). Between volunteers, there was considerable variability in the T0 CFU counts even though all of the samples were infected with the same inoculum; some cultures had more than twice that of others.

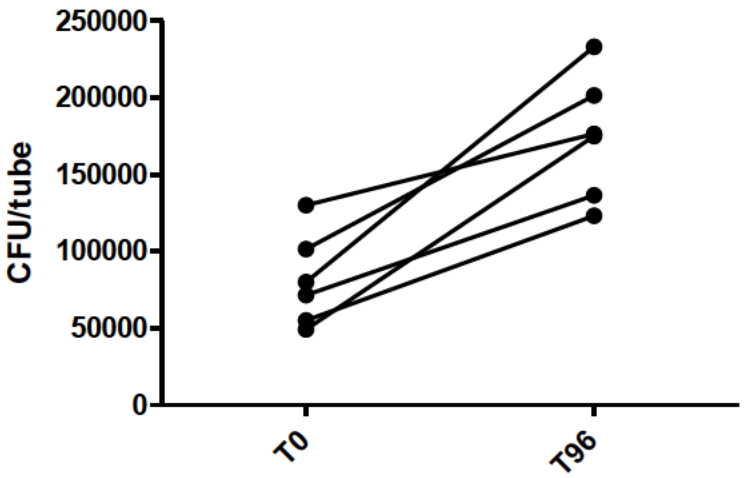

Fig. 4-1 BCG Pasteur growth in total PBMC infection MGIA.
Data shown are CFU/tube counts taken from PBMC cultures infected with BCG at a MOI of 3:1 BCG per monocyte (10% total PBMC), and washed after 4h. Data points represent the median CFU from triplicate cultures for each individual. T0 and T96 indicate that cultures were harvested immediately following washing or after 96h of cell culture respectively.

4.3.1.2 BCG retention after washing

The effectiveness of the BCG infection method can be expressed as the percentage of BCG remaining after infection as compared to the starting inoculum and is calculated as % retention = 100 x (CFU T0/ CFU inoculum). For this experiment the starting inoculum was $6x10^5$ for all samples, and BCG retention rates ranged from 8.2 - 21.7% (Table 4-1).

Volunteer	CFU T0	CFU inoculum	% BCG retention
1	49333	$6x10^5$	8.2
2	55000	$6x10^5$	9.2
3	71666	$6x10^5$	11.9
4	80000	$6x10^5$	13.3
5	130000	$6x10^5$	21.7
6	101666	$6x10^5$	16.9

Table 4-1 % BCG retained after PBMC infection.
PBMC from 6 healthy volunteers were infected at a MOI of 3:1 BCG per monocyte (10% total PBMC), and washed x3 after 4h. CFU counts taken immediately after washing (T0) were used to calculate the % BCG retention = 100 x (CFU T0/ CFU inoculum).

4.3.1.3 Localisation of BCG in PBMC

BCG infected PBMC from 3 volunteers were also assessed by flow cytometry (Fig. 4-2) to determine whether mycobacteria were co-localised with monocytes ($CD14^+$), which were the primary target cells. BCG was stained with CFSE prior to infection of PBMC; median fluorescent intensity (MFI) of CFSE could then be used as an indicator of BCG localisation to $CD14^+$ or $CD14^-$ cells; the higher the MFI the more bacteria were localised to a cell population. Data from the 3 volunteers showed that the MFI of CFSE was significantly higher in $CD14^+$ cells as compared to $CD14^-$ cells at T0 and approaching significance at T96 ($p=0.003$ and $p=0.09$ respectively) (Fig. 4-3). This finding indicates that there is a preferential localisation of the CFSE stained BCG towards $CD14^+$ cells, and this localisation was maintained throughout the 96h culture period.

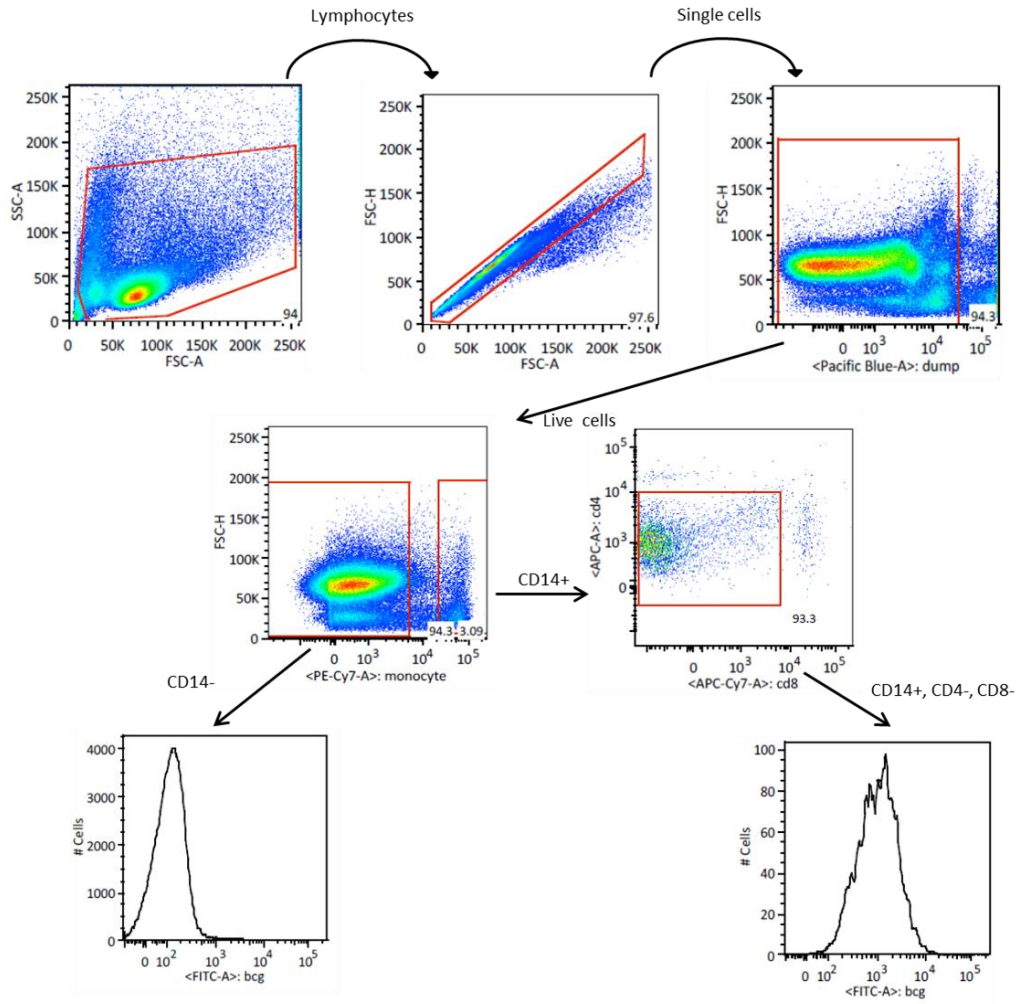

Fig. 4-2 Gating tree for BCG localisation.

Lymphocytes were selected for by side and forward scatter before selection of single cells. Dead cells were removed before gates were applied to $CD14^+$ (monocytes) and $CD14^-$ (all other lymphocytes). $CD4^+$ and $CD8^+$ cells were removed from the $CD14^+$ gate and the MFI for CFSE (FITC channel) was determined.

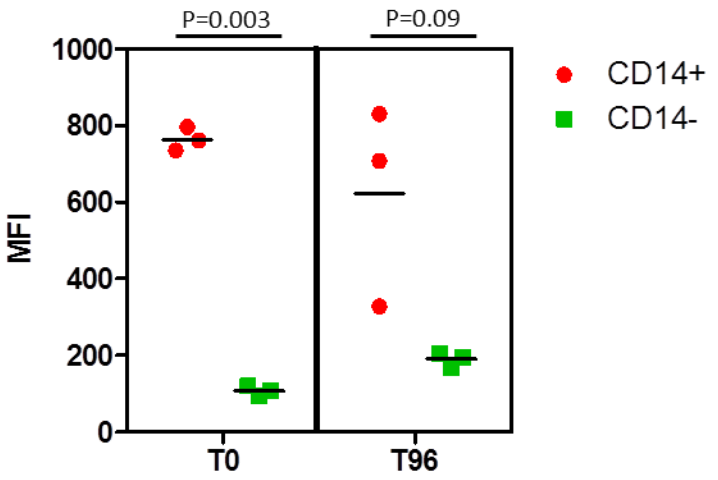

Fig. 4-3 MFI of CFSE in $CD14^+$ and $CD14^-$ PBMC.
BCG stained with CFSE was used to infect PBMC from 3 healthy volunteers at a MOI of 3:1 BCG per monocyte (10% total PBMC), followed by washing after 4h. T0 and T96 indicate that cultures were harvested immediately following washing or after 96h of cell culture respectively. Bars represent the median MFI of CFSE for $CD14^+$ and $CD14^-$ cells (red and green bars respectively). Data were analysed by 2 tailed paired T test.

4.3.2 Removal of BCG aggregates

In order to infect mammalian cells with BCG, the mycobacterial growth media had to be removed before reconstitution of the bacteria in R10 media. When previously performing the cultured MGIA, I had noticed that re-suspension of BCG Pasteur stocks in R10 media resulted in the formation of a "precipitate like" substance. The substance was clearly visible both under the light microscope (Fig. 4-4) and even by the naked eye. This had also been a problem when performing the cultured MGIA, but the majority of the substance was usually removed during the washing of the BCG infected monocyte layers. However, it was a significant problem when performing the total PBMC MGIA, as the washing method

involved centrifugation; this resulted in the substance being pelleted along with the PBMC. As I did not know what the substance was, I was unsure what effect it might have on the MGIA, therefore I decided to investigate what it was, and how best to remove it.

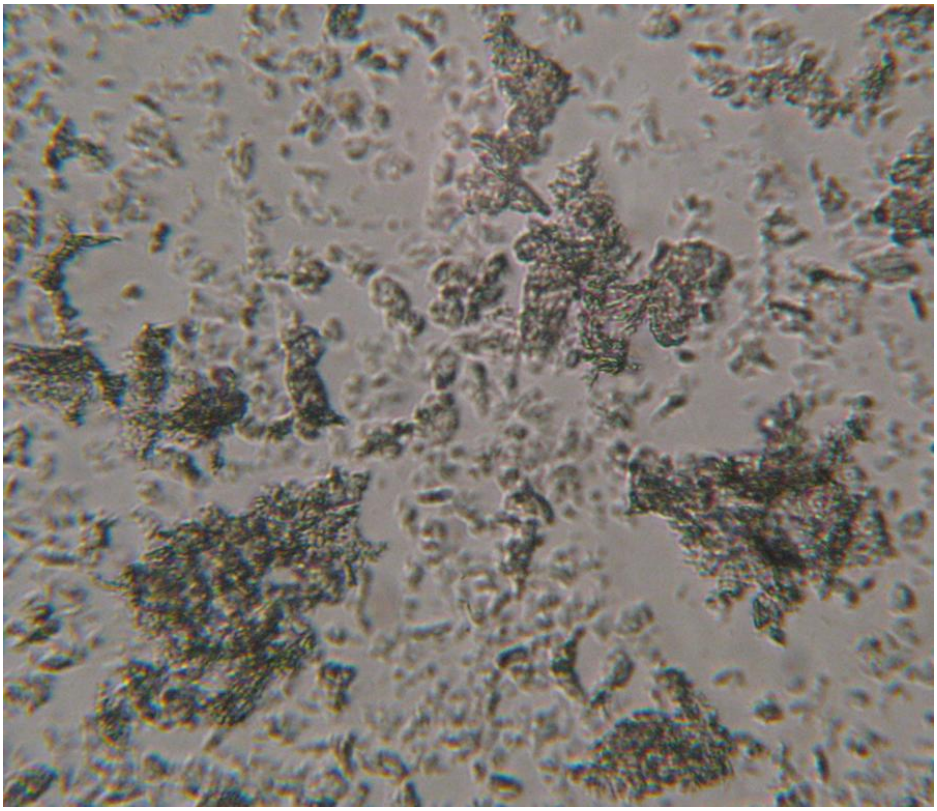

Fig. 4-4 The "precipitate like" substance.
Photograph of the substance formed when BCG Pasteur was reconstituted in R10 media (20x magnification) using a light microscope.

4.3.2.1 Identification of the "precipitate like" substance

Although I did not know what the substance was, I hypothesised that it was large aggregates of BCG. To test this theory, I removed the 7H9 media from 1 vial of BCG and re-suspended the pelleted bacteria in 1 ml of R10 media. Immediately, the precipitate like substance was formed. I gently pelleted the substance in a microfuge (1000 rpm for 30s) and removed the supernatant (containing non aggregated BCG). I suspended the pellet in a small amount of PBS and heat fixed it to a microscope slide for acid fast staining.

The stain revealed that the substance contained BCG that had formed very large aggregates (Fig. 4-5). This had great implications not only for the infection method in the novel MGIA but also for the cultured MGIA as well; these aggregates contain vast quantities of BCG, if just one is present in the PBMC culture then it could drastically alter the CFU count and thus completely alter the perceived level of mycobacterial growth inhibition.

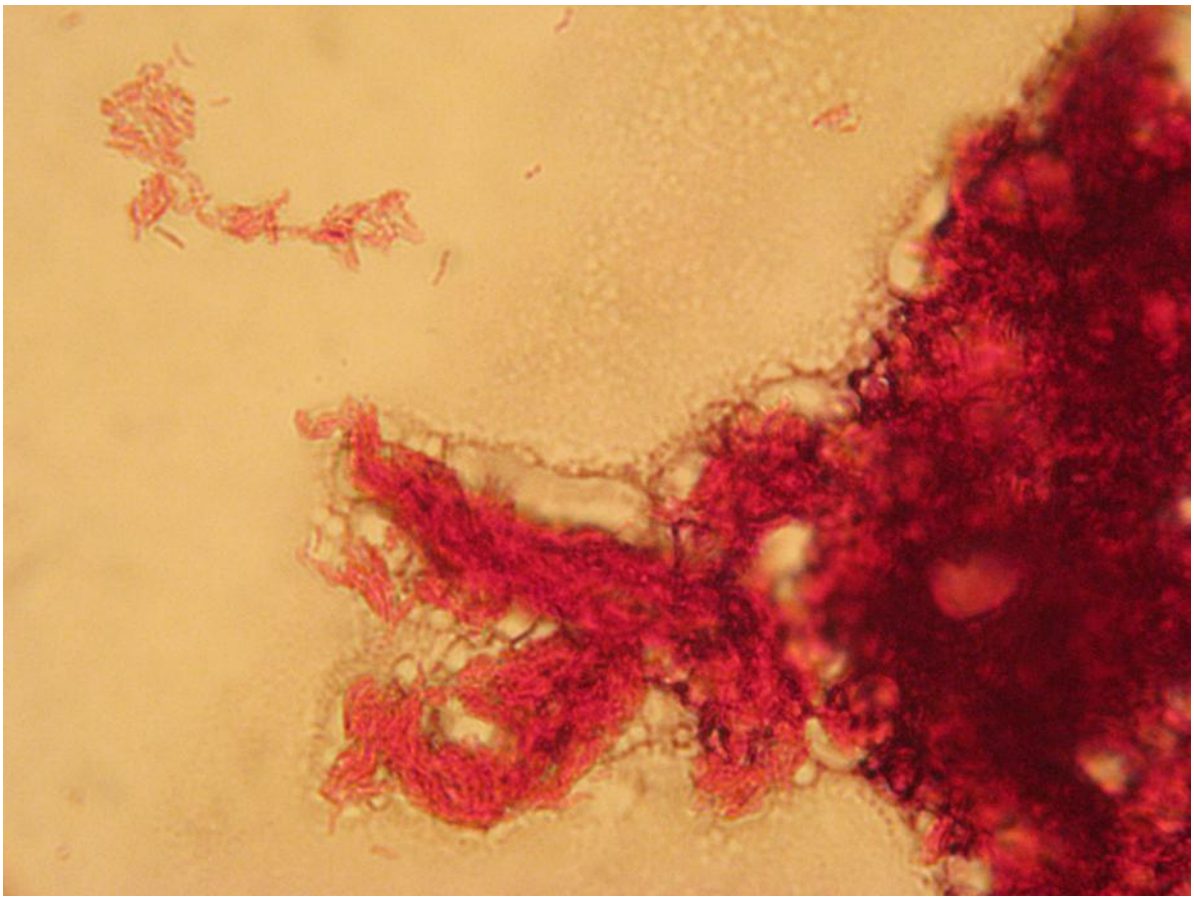

Fig. 4-5 BCG aggregates upon reconstitution in R10 media.
Photograph taken at 100x magnification (oil immersion) using a light microscope showing acid fast bacilli present in a large aggregate as well as individual acid fast bacteria.

4.3.2.2 Testing 5µm filters to remove mycobacterial aggregates

The general consensus for performing mycobacterial infection of mammalian cells *in vitro,* is that mycobacteria are disaggregated before being reconstituted in mammalian cell culture medium [73, 153, 156, 185]. As I have shown, this does not prevent aggregation of the bacteria once they are reconstituted in cell culture media. I assessed the feasibility of using 5µm syringe filters to remove these aggregates after reconstitution of the bacteria in

R10 media. Briefly, the results were that after filtering there were no large aggregates of BCG visible in the R10 media under the microscope and although there was a reduced number of bacteria remaining after the filtering, there was still enough to perform the infections; this filtering method therefore replaced the sedimentation procedure used throughout the cultured MGIA experiments detailed in section 3.3.5.

4.3.3 Assessment of total PBMC infection MGIA using NHP PBMC

From the results detailed in section 4.3.1, I was confident that the total PBMC infection method delivered a suitable dose of BCG that was preferentially associated with $CD14^+$ cells. The level of mycobacterial growth during the 96h culture was also encouraging as it was in a similar range to the published data for the whole blood and MGIT MGIAs [154, 155]. The next step was to assess the ability of this assay to discriminate between mycobacterial growth in PBMC taken pre and post BCG vaccination. Cryopreserved PBMC samples from NHP were utilised for this purpose.

4.3.3.1 Cynomolgus macaques given different vaccine regimes

Six cynomolgus macaques were vaccinated with clinical grade BCG using the same dose and route as is used for humans (100µl of SSI BCG reconstituted in 1ml Sauton's media via intradermal (i.d) injection). Two of these animals also received a mucosal BCG boost 5 weeks after the initial BCG prime using an endotracheal catheter (~$1x10^6$ CFU), while 2 different animals received an unknown experimental protein/adjuvant TB vaccine at weeks

23 and 26 after BCG prime. PBMC isolated before, and at least 12 weeks after BCG prime (includes samples after BCG/protein boosts) were used in the novel MGIA. Lower GR values are indicative of mycobacterial growth inhibition.

Log transformed GR values are displayed for all animals as pre and post vaccination only, as there were only 2 animals in each vaccination group (Fig. 4-6). There was no significant difference between pre and post vaccination GR values (mean log transformed GR values 0.45, and 0.40 respectively) although 4 out of 6 animals did have lower GR values following vaccination. PBMC taken from the 2 animals that received a mucosal BCG boost (blue data points) did not have lower GR values than animals that received only 1 BCG vaccination (red data points); both animals that received the protein/adjuvant boosts (purple data points) appeared to show enhanced mycobacterial growth inhibition after vaccination.

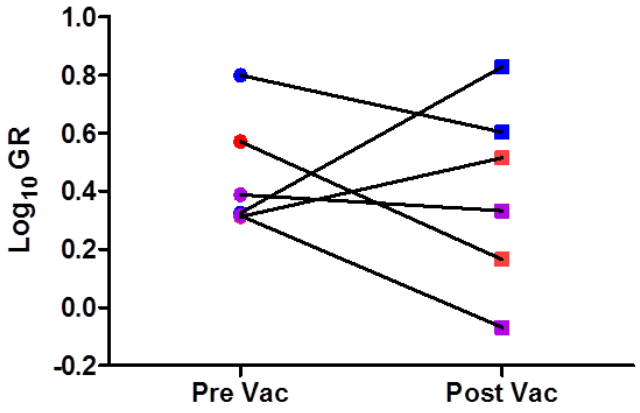

Fig. 4-6 GR values for vaccinated NHP using different regimes.
Graph shows log transformed GR data from 6 cynomolgus macaques before and after vaccination with clinical grade SSI BCG (100µl i.d) (red data points). 2/6 animals also received a mucosal BCG boost after 5 weeks ($1x10^6$ CFU) (blue data points) and 2/6 received 2 doses of an unknown subunit vaccine at weeks 23 and 26 post BCG prime (GSK) (purple data points). Post vaccination samples were obtained 12, 13 and 30 weeks after the initial BCG vaccination for animals given single BCG, BCG mucosal boost and subunit vaccine boost respectively. GR= CFU T96/CFU T0.

4.3.3.2 Cynomolgus macaques given just BCG

Initial assessment of the total PBMC infection MGIA in NHP was complicated by the fact that there were 3 different vaccine regimens for only 6 animals, with varying intervals between vaccinations and PBMC isolations. The following experiment was performed using cryopreserved PBMC from 10 cynomolgus macaques, taken before and after (16 week interval) a single i.d BCG vaccination (100µl of SSI BCG reconstituted in 1ml Sauton's media). A new stock of BCG Pasteur was used for the PBMC infections, as the one used for experiments detailed in sections 4.3.1.1 and 4.3.3.1 had ran out. The stock was prepared in exactly the same way as the previous batch and was derived from the same seed stock.

There was no significant difference between the GR values obtained before and after BCG vaccination (Fig. 4-7). Some of the animals had higher GR values after vaccination, whereas others had lower values. In general, all of the GR values were lower than I had obtained in previous experiments, with mean log transformed GR values of 0.04 and 0.09 for pre and post BCG samples respectively; these values indicate that there was very little

mycobacterial growth during the 96h culture period. This lack of growth was most likely caused by the change in the stock of BCG used for the assay, as all other equipment and conditions were the same as used previously.

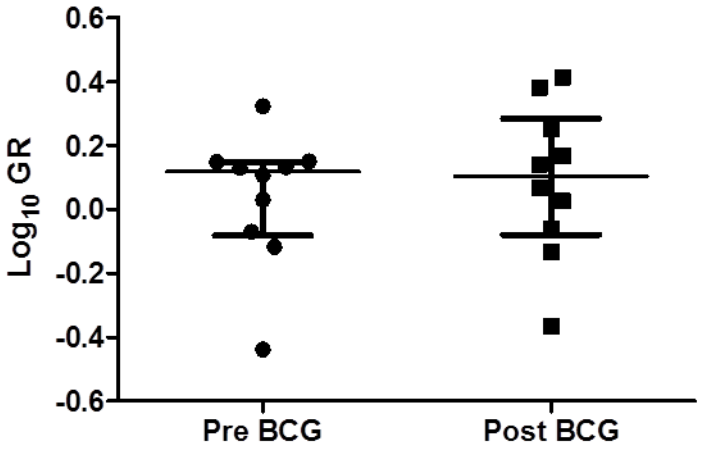

Fig. 4-7 GR values for BCG vaccinated NHP.
Graph shows log transformed GR data from 10 cynomolgus macaques pre and post vaccination with clinical grade SSI BCG (100µl i.d). Bars represent the median with inter quartile range. GR= CFU T96/CFU T0.

4.3.4 Increasing GR values by using starter cultures

One of the methods by which I tried to improve the growth rate of the mycobacteria was to infect PBMC with bacteria from a 72h starter culture. Frozen stocks of mycobacteria have a lag period before they regain full metabolism; this can be seen when comparing growth rates of mycobacteria in liquid or solid cultures from fresh and frozen stocks. The doubling time of BCG/*M. tb* is approximately 20 hours so over the course of 96h a maximum of 5

divisions is possible, which will be less if there is a significant lag period. I hypothesised that by using bacteria from 72h cultures I eliminate the lag period in bacterial growth and achieve greater GR values.

The experiment was performed using cryopreserved PBMC from volunteers and naïve NHP using mycobacteria from a starter culture or cryopreserved stocks from a -80°C freezer. The mean log transformed GR value for cultures infected with BCG from cryopreserved stocks was -0.75 compared with -0.08 when the BCG was taken from a 72h starter culture p=0.06 (Fig. 4-8) This result was close to being significant but the GR values were still very low suggesting there was very little growth, and in most cases, a reduction in the number of bacteria over the 96h culture period was observed. This result pointed towards increased survival of BCG when taken from starter cultures, but no improvement in growth.

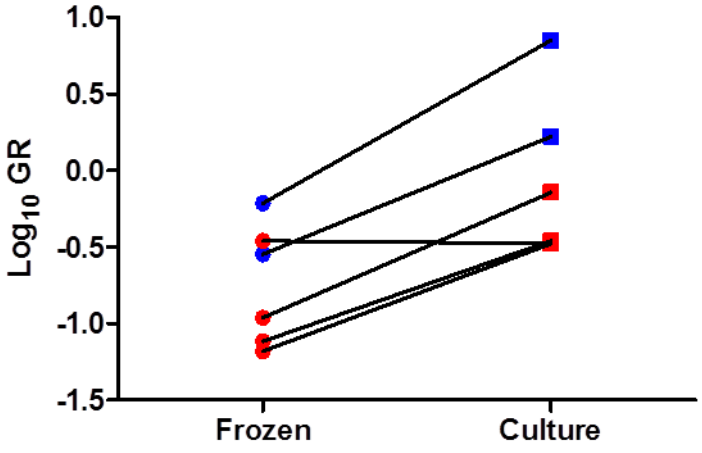

Fig. 4-8 Starter cultures improve survival of BCG in total PBMC infection MGIA.
Graph showing log transformed GR values for 4 volunteers (red data points) and 2 NHP (blue data points). PBMC were infected with BCG from cryopreserved stocks (frozen) or from 72h starter cultures (culture) P=0.06 Wilcoxon matched-pairs t test. GR= CFU T96/CFU.

4.3.5 Effect of shaking in whole blood and PBMC cultures

All previous experiments using the total PBMC infection MGIA had been performed using cryopreserved PBMC in 5ml polystyrene tubes that were stationary during a 96h culture period. The whole blood (WB) and MGIT MGIAs [154, 155] in contrast both use WB with mixing of the cultures throughout the culture period. I decided to test whether gentle shaking (orbital swirling in 24 well plates) of the cultures would improve mycobacterial growth during the novel MGIA, whilst also assessing the differences in growth ratios between WB, fresh PBMC and cryopreserved PBMC from 4 naïve rhesus macaques. The PBMC samples were infected and washed as normal, but this could not be done for the WB samples as I wanted to maintain all of the different components of the blood. I therefore infected WB cultures (diluted 1:1 with R10) with an intended dose of $1x10^6$ CFU/ml and did not perform any washes.

As the BCG Pasteur stocks that I had made were not growing well, I also decided to evaluate the H37Rv strain of *M. tb* as the infecting organism instead of BCG. My hypothesis was that as H37Rv is a pathogenic strain of *M. tb,* it would display superior

intracellular growth, which would result in greater GR values, thus making the assay a more stringent test of growth inhibition; and ultimately perhaps, more indicative of *in vivo* protection. As I had achieved higher GR values by using bacteria from starter cultures (4.3.4) the H37Rv used for the infections was prepared in a 72h starter culture. CFU counts were determined for all of the cultures on day 0, day 4 and day 7 after infection (D0, D4 and D7 respectively). The fresh samples were processed in 2 batches, animals D41 and D74 were processed together as were animals C87 and X21, whereas the frozen PBMC samples were all processed together. Flow cytometry was performed on the frozen PBMC cultures to assess whether shaking had any effect on the functionality of T cells.

4.3.5.1 Effect of shaking on Growth kinetics of H37Rv

As shown in Fig. 4-9a and b, the CFU counts from the stationary WB cultures were very similar to their shaken counterparts during the first 4 days of culture, although the shaking did appear to improve mycobacterial growth between day 4 and day 7 of culture in all 4 animals. CFU data for the fresh PBMC cultures are displayed in Fig. 4-9c and d and show very high levels of mycobacterial growth between day 0 and day 4 in the stationary cultures, but unfortunately, the shaken cultures yielded very little CFU counts, so many of the data points are missing. However, there are data for both stationary and shaken cultures for the cryopreserved PBMC which are displayed in Fig. 4-9e and f which show that there is possibly a slight increase in mycobacterial growth when cultures are shaken

but the CFU counts were very similar to the stationary cultures. From these data it would appear that mycobacteria are able to grow equally as well in PBMC as they are in WB, if not better; and although the levels of growth were not as great in the cryopreserved PBMC as they were in the fresh samples, there was still good growth for 3 out of the 4 animals in the stationary and shaking cultures.

As can be seen in Fig. 4-9a-d, there was a large degree of variation in the day 0 CFU counts between animals in the fresh samples, which could have been caused by the fact that they were processed in 2 different batches and so were infected with H37Rv from 2 different starter cultures. However, this was still a problem in the frozen PBMC where all of the samples were processed together in a single batch, so the starter culture could not be the cause of variability in those samples.

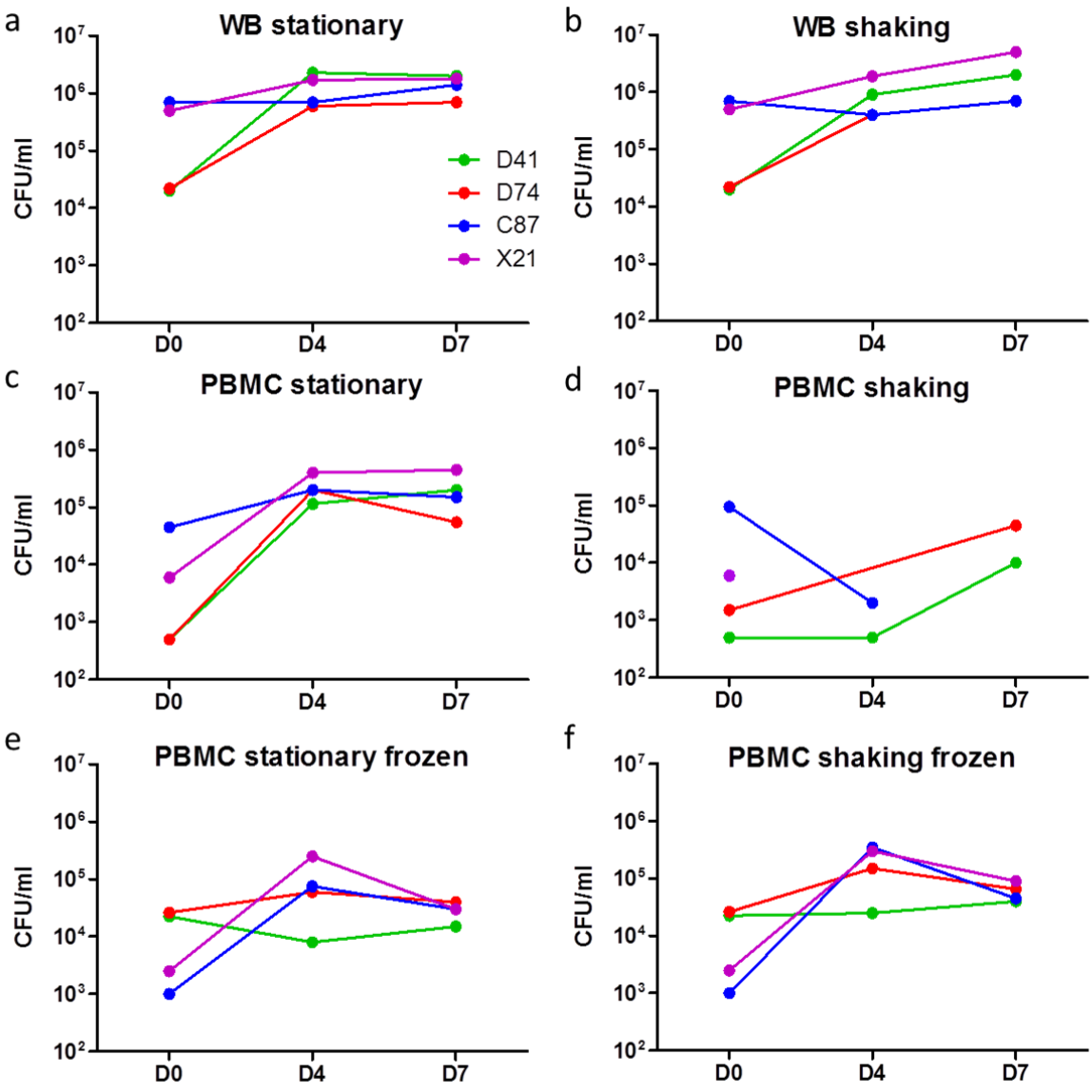

Fig. 4-9 Effect of shaking on growth of H37Rv in WB, fresh PBMC and frozen PBMC cultures.
Graphs showing CFU data for 4 naïve rhesus macaques D41, D74, C87 and X21 (green, red, blue and violet data sets respectively). CFU counts were measured on day 0, day 4 and day 7 after infection with H37Rv (D0, D4 and D7 respectively). (a) whole blood culture without shaking, (b) whole blood culture with shaking, (c) PBMC culture without shaking, (d) PBMC culture with shaking, (e) cryopreserved PBMC without shaking, (f) Cryopreserved PBMC with shaking.

4.3.5.2 Variability of GR values in individual animals

Variability in CFU counts at day 0 could potentially have a profound effect on the GR values for these animals as seen in Fig. 4-10. Animals with the highest GR values in the fresh PBMC cultures generally had lower GR values in the frozen PBMC cultures and *vice versa*. This disparity in mycobacterial growth inhibition of fresh and frozen PBMC taken from the same animal could be due to the effects of cryopreservation, however I believe it is due to the variation in the day 0 CFU counts as by day 4 and day 7 the CFU counts are similar for each animal across the fresh and frozen assays (Fig. 4-9c and e). Some of the GR values appear to be implausibly high considering the doubling time for *M. tb* is approximately 20h, so the maximum GR value should be around 25. Clearly the CFU estimation must be inaccurate for some of these samples, although it is impossible to tell whether the day 0 CFU counts are too low, the day 4 and 7 are too high, or a combination of both.

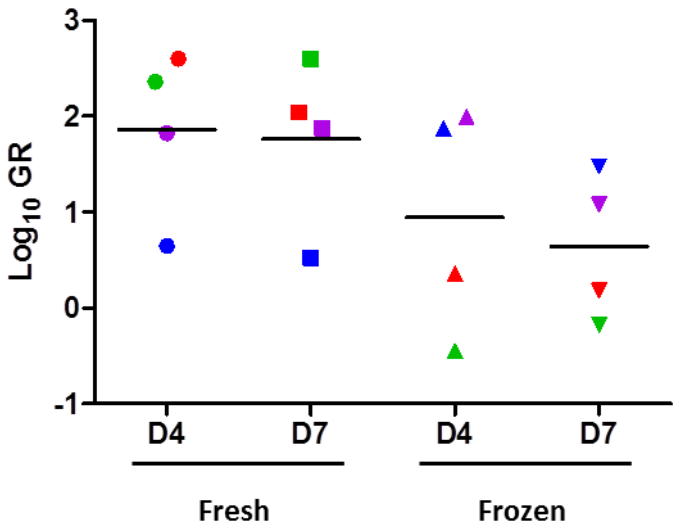

Fig. 4-10 Variability in GR values between fresh and frozen PBMC.
Graphs showing log transformed GR data for 4 naïve rhesus macaques D41, D74, C87 and X21 (green, red, blue and violet data sets respectively). GR values were calculated at day 4 and day 7 after infection with H37Rv (D4 and D7 respectively) in fresh and frozen PBMC without any shaking. GR = CFU D4 or D7/CFU D0. Bars represent the mean log transformed GR value.

4.3.5.3 Shaking has no effect on T cell viability

In order for the total PBMC MGIA to be effective, there needed to be a careful balance between ensuring mycobacteria could grow, whilst maintaining PBMC viability within cultures. I needed to establish whether the shaking of PBMC would result in increased cell death, so I performed multifunctional flow cytometry on the cryopreserved PBMC taken from the MGIA.

Gentle shaking of the cultures did not affect the viability of T cells as seen in Fig. 4-11. Graph (a) shows the percentage of live T cells as compared to total lymphocytes from stationary cultures and (b) shows the same data for shaken cultures which are almost

identical for all animals. T cell viability was maintained very well between day 0 and day 4 for stationary and shaken cultures (mean D0 = 44.93, mean D4 = 43.43 and 44.70 respectively). T cell viability waned by day 7 of culture in both still and shaken cultures (mean = 34.73 and 37.30 respectively) although this was not significantly lower than the day 0 values.

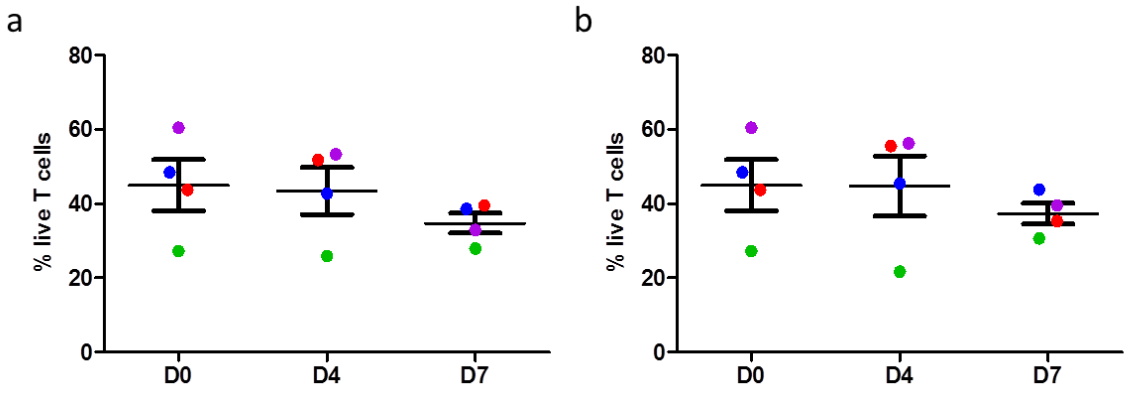

Fig. 4-11 Shaking does not affect T cell viability.
Graphs show flow cytometry data for 4 naïve rhesus macaques D41, D74, C87 and X21 (green, red, blue and violet data sets respectively). Cryopreserved PBMC used in the novel MGIA were sampled at the point of harvest on day 0 (same for stationary and shaken cultures), 4 or 7 (D0, D4 and D7 respectively). Bars represent the mean with SEM. (a) samples from stationary cultures, (b) samples from shaken (orbital) cultures.

4.3.5.4 Shaking does not alter functionality of T cells

As well as the cell viability analysis detailed in the previous section, T cells were also assessed for their ability to express IFN-γ, TNF-α and IL-2 in response to culture with H37Rv using flow cytometry. Spice plots displaying data in pie charts and bar charts are

shown in Fig. 4-12; (a) shows data from $CD4^+$ T cells; there were no significant differences between the shaking and stationary cultures for any of the cytokines on day 4 or 7. Data for $CD8^+$ T cells are shown in (b); again there were no significant differences between the shaking and stationary cultures. The third sub set of T cells studied, were considered to be a mixture of NK and $\gamma\delta^+$ T cells ($CD3^+$, $CD4^-$ and $CD8^-$), data for these cells are displayed in (c). These were the most responsive cells by far, especially on day 0 (overnight stimulation due to brefeldin treatment), where greater than 60% were triple positive. Again there were no significant differences in cytokine expression between stationary and shaking cultures.

Most of the samples contained very low numbers of responding cells and there was quite a lot of variation between animals with animal D41 hardly responding at all in any T cell type, these factors could explain why there were no significant differences between the shaking and stationary cultures.

a

Day: D0
Agitation: still
Day: D4
Agitation: shake
Day: D4
Agitation: still
Day: D7
Agitation: shake
Day: D7
Agitation: still
10^2.0 -
10^1.0 -
10^0.0 -
10^-1.0 -
10^-2.0 -
IFNg
IL-2
TNF
Pie Slice
Bar Chart Legend
Day: D0
Agitation: still
Day: D4
Agitation: shake
Day: D4
Agitation: still
Day: D7
Agitation: shake
Day: D7
Agitation: still

b
Day: D0
Agitation: still
Day: D4
Agitation: shake
Day: D4
Agitation: still
Day: D7
Agitation: shake
Day: D7
Agitation: still
Bar Chart Legend
Day: D0
Agitation: still
Day: D4
Agitation: shake
Day: D4
Agitation: still
Day: D7
Agitation: shake
Day: D7
Agitation: still
10^2.0 -
10^1.0 -
10^0.0 -
10^-1.0 -
10^-2.0 -
IFNg
IL-2
TNFa
Pie Slice

C

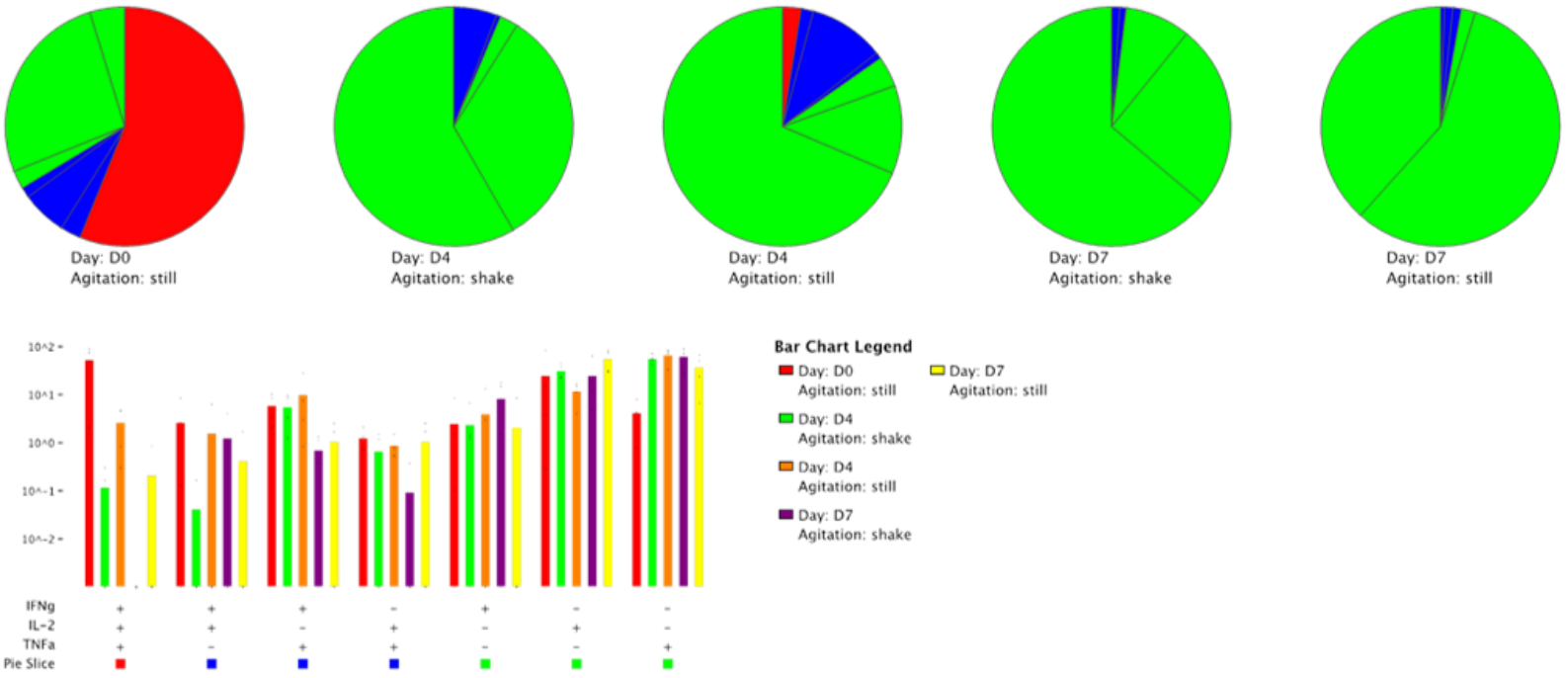
Day: D0
Agitation: still
Day: D4
Agitation: shake
Day: D4
Agitation: still
Day: D7
Agitation: shake
Day: D7
Agitation: still
10^2
10^1
10^0
10^-1
10^-2
IFNg
IL-2
TNFa
Pie Slice
Bar Chart Legend
Day: D0
Agitation: still
Day: D4
Agitation: shake
Day: D4
Agitation: still
Day: D7
Agitation: shake
Day: D7
Agitation: still

Fig. 4-12 Shaking does not alter functionality of T cells.
Spice plots show flow cytometry data for 4 naïve rhesus macaques D41, D74, C87 and X21. Cryopreserved PBMC used in the novel MGIA were sampled at the point of harvest on day 0 (same for still and shaken cultures), 4 or 7 (D0, D4 and D7 respectively). Pie charts display the mean percentage of triple positive (red) double positive (blue) or single positive (green) cells for all animals. Bars represent the mean percentage of cytokine positive cells with points representing each animal, for day 0 (red), Day 4 shaking (green), day 4 still (orange), day 7 shaking (purple) and day 7 still (yellow). (a) data for $CD4^+$ T cells, (b) data for $CD8^+$ T cells and (c) NK and $\gamma\delta^+$ T cells.

4.3.6 Assessing the level of variability of the total PBMC infection MGIA

As seen in section 4.3.5.2 there appeared to be considerable variation between the GR values for fresh and cryopreserved PBMC taken from the same animal. I wanted to assess whether this variability was caused by cryopreservation of PBMC or if it was due to the total PBMC infection MGIA being performed on different days. Cryopreserved PBMC taken from 4 naïve rhesus macaques were used to perform the MGIA 3 times on the same samples on different days. PBMC were harvested on day 0, 4, 5, 6 and 7 to assess the levels of variability in GR values at these different time-points.

The GR values (Fig. 4-13) were generally quite low with the exception of Assay 2, some data points for assay 1 are missing due to a lack of recovery of CFU counts for some time-points (c and d). Even though all of the samples had been treated the same across the 3 different assays the levels of variability were substantial for all 4 animals (graphs a-d). Mean coefficient of variance values for all 4 animals were 121, 83, 49 and 89% across

the 3 assays for days 4, 5, 6 and 7 respectively. So clearly there was a significant amount of variation when performing the MGIA on different days.

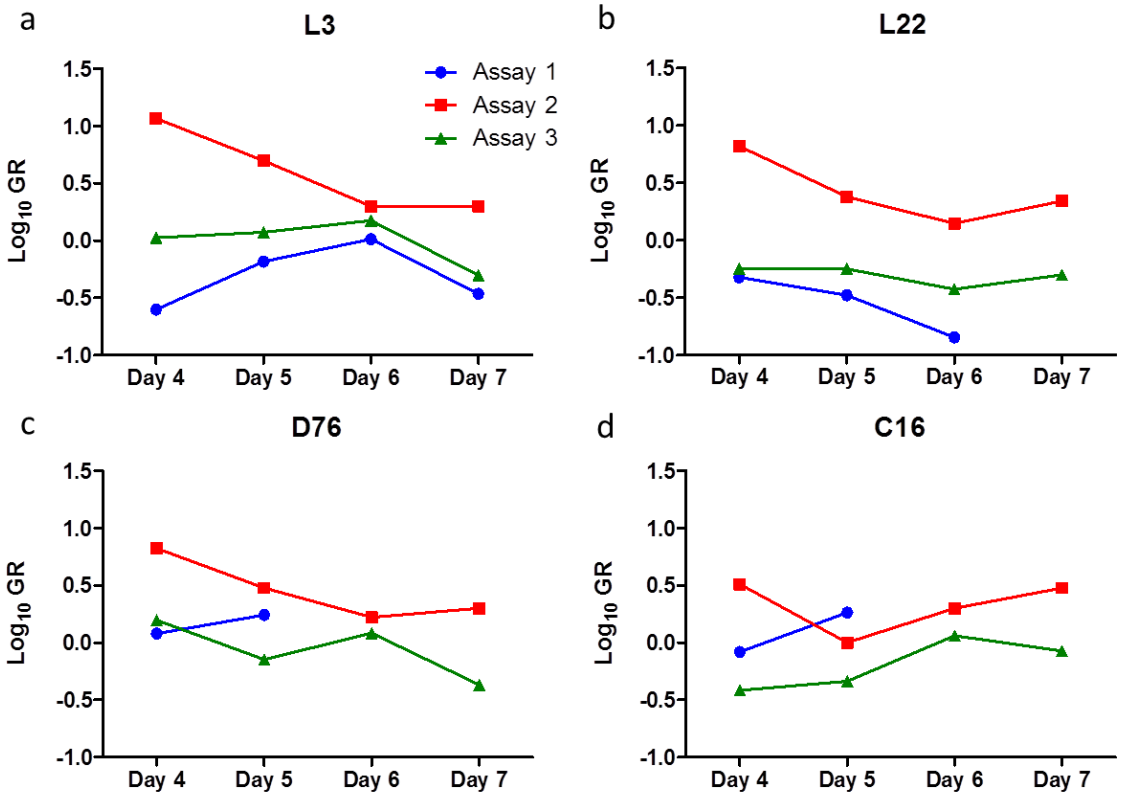

Fig. 4-13 Day to day variability of total PBMC MGIA.
Graphs show log transformed GR data for cryopreserved PBMC taken from 4 naïve rhesus macaques L3, L22, D76 and C16 (a-d respectively). The MGIA was performed 3 times on separate days (blue, red and green data points). Cells were harvested for CFU counts at day 0, 4, 5, 6 and 7. GR = CFU day (4-7)/CFU day 0.

4.3.7 Does washing really help?

The total PBMC infection MGIA contained a washing step to remove non-phagocytosed mycobacteria with the rationale that this would improve sensitivity. However it was possible that the washing procedure was not effective and was a contributory cause to the variation in the infection process. I decided to determine the levels of mycobacteria that were present in adherent cells (monocytes) and non-adherent cells after infection and washing of PBMC. Cryopreserved PBMC from 3 volunteers were rested overnight with benzonase and 25U/ml of IL-2 to improve cell viability then infected with BCG, due to logistical reasons H37Rv was not used. Following infection and washing (4.1.2.2) PBMC were incubated in 24 well plates. T0 cultures were incubated for 2 hours to allow adhesion of monocytes, before non-adherent cells were gently washed off with warm R10 and directly plated out for CFU counts. Adherent cells were lysed before also being plated out for CFU counts; T96 cultures were also processed in this manner.

CFU data are displayed in Fig. 4-14 showing that following the washing step of the MGIA, there was a mean CFU count of $2.3x10^4$/ml at T0 for the adherent cells (graph a) and $2.2x10^4$/ml in the non-adherent cells (graph b). Over the course of the 96h culture there was a decrease in the numbers of bacteria recovered from the adherent cells with a mean CFU count of $2.3x10^3$/ml, but the numbers present in the non-adherent fraction remained

fairly constant with a mean CFU count of $2.5x10^4$/ml. The washing step therefore did not remove all non-phagocytosed BCG and around half the bacteria present within cultures did not appear to be associated with adherent cells. So I decided that in future, I would infect cultures using a low inoculum of mycobacteria and not perform any washing steps, in an attempt to reduce variability caused by washing.

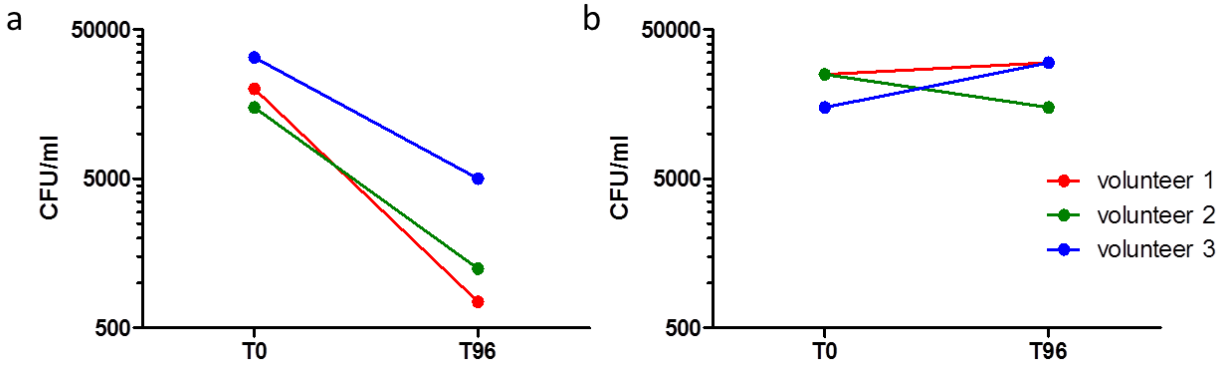

Fig. 4-14 Effectiveness of washing step in the total PBMC infection MGIA.
Graphs showing CFU counts for (a) adhered monocytes and (b) non-adhered PBMC taken from 3 volunteers (red, green and blue data sets). Cultures were harvested after 2h (T0) and 96h (T96).

4.3.8 Assessment of mouse splenocytes

After I had performed optimisations of the total PBMC infection MGIA, I went on to assess whether it could differentiate between mycobacterially naïve and BCG vaccinated individuals. For this experiment, splenocytes from 8 naïve and 8 BCG vaccinated C57BL/6 mice were used to perform the MGIA all on the same day. The rationale behind using mouse

splenocytes to assess the novel MGIA was that BCG is known to confer reliable and consistent protection against *M. tb* challenge in mice. The aim of my project was to establish an *in vitro* assay that measures this protection against *M. tb.* Samples from BCG vaccinated humans and NHP were limited, so I reasoned that evaluating the assay in BCG vaccinated vs. naïve mice was the best way forward.

Mice were vaccinated sub cutaneously with $1x10^5$ CFU BCG Pasteur with an interval of 16 weeks before the MGIA was performed. The infecting organism used for the MGIA was *M. tb* H37Rv and I did not perform the washing procedure, instead I inoculated the splenocytes with a low dose of bacteria (approximate MOI of 1:200 bacteria/splenocyte).

The levels of infection at T0 were very similar across all animals, and bacterial growth was seen in all samples over the 96h culture period (Fig. 4-15a and b). There was no significant difference in the growth ratios between the naïve and BCG vaccinated mice (graph c) Mean log transformed GR= 0.359 and 0.369 for naïve and BCG vaccinated mice respectively. The BCG vaccination was shown to be effective in group matched mice vaccinated at the same time as those used for my studies; these mice were challenged with *M. tb* and were shown to be protected as compared with naïve mice Poyntz *et al.*unpublished work.

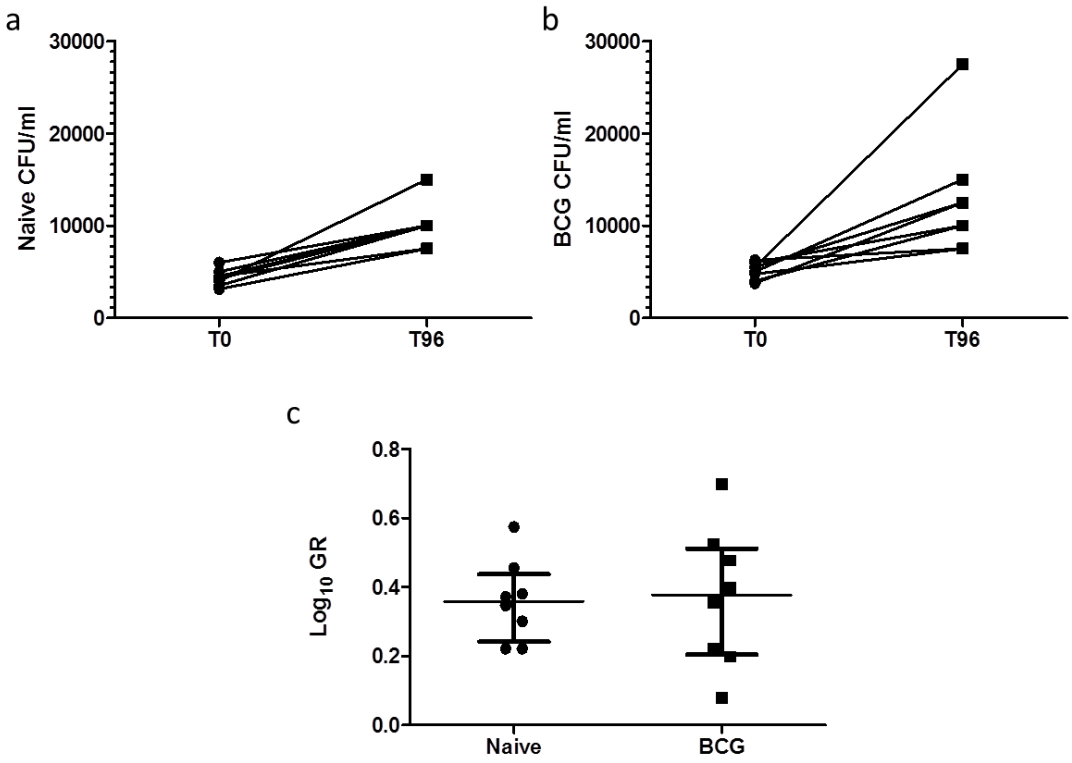

Fig. 4-15 Mouse splenocytes in total PBMC infection MGIA.

Splenocytes taken from naïve and BCG vaccinated C57BL/6 mice were used to perform the novel MGIA. Vaccinated mice received $1x10^5$ CFU BCG Pasteur sub cutaneously with a 16 week interval before being used for the MGIA. (a) CFU data for Naïve mice at time 0 (T0) and time 96h (T96), (b) CFU data for BCG vaccinated mice at T0 and T96 and (c) log transformed GR data for naïve and BCG vaccinated animals. Bars represent the median with inter quartile range. GR= CFU T96/CFU T0.

4.4 Discussion

Many assays where monocytes are infected with bacteria involve the isolation of monocytes by adhesion [40, 73, 153, 156, 157, 185]. In the previous chapter, the problems of using cryopreserved PBMC for isolation of monocyte layers and the extremely high levels of variability were discussed. The total PBMC infection MGIA was designed to eliminate the variability in monocyte layer quality with a total PBMC infection strategy. This assay was optimised for use with cryopreserved PBMCs and was assessed for the ability to discriminate between naïve and BCG vaccinated PBMC/splenocyte samples.

Washing PBMC to remove non-phagocytosed BCG was ineffective and introduced variability rather than increasing sensitivity. The cultured, murine, cattle and *ex-vivo* MGIAs all utilised washing steps to remove extracellular mycobacteria to improve sensitivity [73, 153, 156, 185]. However, these assays all involved the infection of adherent monocyte layers, so any mycobacteria that were attached to the surface of the monocytes would most likely be phagocytosed throughout the period of culture and would therefore be susceptible to intracellular killing and growth inhibition; this may not have been the case for the total PBMC infection MGIA as mycobacteria that were attached to non-phagocytic cells may not become internalised. Although I had shown that BCG was preferentially associated with $CD14^+$ cells after infection of total PBMC samples; the pelleting of PBMC during wash steps

may have aided the attachment of extracellular mycobacteria to cells other than monocytes, making removal of non-phagocytosed bacteria more difficult; this, combined with the act of filtering mycobacteria to remove aggregates resulted in levels of inter and intra assay variability that were much greater than what has been reported for other MGIAs [73, 153-156, 185]. Amikacin is an antibiotic that has been shown to kill extracellular mycobacteria whilst leaving internalised bacteria intact [186]. It is possible that removal of extracellular mycobacteria would have been much more effective had this method been used during my studies and thus, assay variability may have been reduced to a more acceptable level and sensitivity to detect mycobacterial growth inhibition would have been enhanced.

In an MGIA study performed using whole blood from BCG vaccinated neonates (whole blood MGIA), control samples were taken from adults at the beginning and end of the study which showed no change in the levels of growth inhibition over time [154], whereas the total PBMC infection MGIA was highly variable when identical samples were processed on different days. Intra assay variability is generally quite high in all of the MGIAs that have been reported; this is especially true when human samples are used as opposed to those from inbred animal species. When the washing step was removed from the total PBMC infection MGIA, levels of inter and intra assay variability were greatly reduced, although the

use of inbred mice for these experiments will also have contributed to this decrease in variability.

Although the total PBMC infection MGIA was optimised to the point where inter and intra assay variability were within the limits of similar published MGIAs [154, 155] it was still unable to discriminate between naïve and BCG vaccinated samples. This finding is in disagreement with murine MGIA studies performed in the same species of mouse with the same vaccination regime [156, 157], which suggests that the total PBMC infection assay was in some way flawed. The effectiveness of the BCG vaccinations was assessed separately *in vivo* by *M. tb* challenge of experimentally matched mice, so failure of the BCG immunisations to protect these mice can be ruled out as the reason for the assay's failure. It is possible that further study of the functionality/phenotypes of the mouse splenocytes that were utilised for this experiment may have yielded data that could then have been correlated against the GR values for each animal, this may have shown that animals with low or high GR values also have low or high ELIspot/ICS responses respectively; had this been the case then it could be concluded that the total PBMC infection MGIA may be a measure of immunogenicity as opposed to a correlate of protection. As previously mentioned in section 1.7.5, the murine MGIA is technically very similar to the cultured MGIA, but uses bone marrow as a source of monocytes and does not involve antigen

expansion of memory cells. The use of bone marrow derived macrophages is not feasible during clinical trials and NHP studies and due to the similarity of this type of MGIA with the cultured assay previously described in chapter 3, this assay was deemed to be unsuitable for use during this study.

The total PBMC infection MGIA most closely resembles the WB and MGIT MGIAs [154, 155] (WB is directly inoculated with BCG) except for the techniques used for enumeration of mycobacteria and mixing of co-cultures. The mixing of co-cultures may be required for ensuring that mycobacteria are effectively phagocytosed and that memory T cells come into contact with their cognate antigens in these types of MGIA. Growth inhibition was not affected by gentle orbital shaking during my studies, however, a more vigorous mixing technique such as those used in the whole blood [154] (rocking in bijous) or the MGIT [155] (360^{o} rotation) MGIAs may have been more effective in ensuring that cells were thoroughly mixed throughout the culture period. The experiment in which mixing was assessed in the present study was primarily designed to determine whether levels of mycobacterial growth could be improved; it was therefore performed using blood from naïve NHP only, in order to establish what the maximum GR values would be. This study therefore does not demonstrate whether or not mixing improves mycobacterial growth

inhibition; head to head comparisons between naïve and BCG vaccinated samples would have to be assessed in order to answer this question.

One other important factor that may have contributed to the failure of the total PBMC infection MGIA to discriminate between naïve and BCG vaccinated samples, could have been masking of adaptive responses by innate immune responses. It is generally accepted that a small proportion of individuals who are exposed to *M. tb,* clear the infection without the induction of adaptive immunity [3], which suggests that strong innate immune responses are capable of protecting against *M. tb* infection. The effects of innate immunity on BCG vaccination have been studied in Malawian adolescents where BCG vaccination has been shown to have 0% efficacy [102]. The authors found that in comparison to UK adolescents, the Malawian volunteers had higher pro (TNF-α) and anti-inflammatory (IL-10) responses to PPD stimulation prior to vaccination [187], suggestive that innate immune responses might play a role in the variability of BCG efficacy between geographical regions. If this is true, then it is possible that innate immunity could also affect *in vitro* growth levels of BCG during MGIAs. It would be interesting to see if naïve blood samples from volunteers in different countries had varying levels of mycobacterial growth inhibition in an MGIA. There is also direct evidence that innate responses are induced during MGIAs. In TST- individuals, peripheral blood lymphocytes (PBMC minus adherent cells) have been shown to

limit growth of *M. tb* inside infected monocytes [153] and levels of mycobacterial growth inhibition vary considerably between volunteers prior to vaccination with BCG [73, 154]. In cattle, percentage growth inhibition in naïve animals was found to be just under 60% (10:1 lymphocytes to monocytes) as compared to just under 80% in BCG vaccinated animals [185] and naïve mouse splenocytes have been shown to kill *M. tb* inside infected macrophages during the first 4 days of co-culture [156].

In this present study it was found that overnight stimulation of PBMC taken from mycobacterially naïve macaques with live *M .tb* resulted in high levels of triple positive $CD3^+CD4^-CD8^-$ cells expressing IL-2, TNF-α and IFN-γ, in contrast, both $CD4^+$ and $CD8^+$ T cells had very low responses. The highly responsive $CD3^+CD4^-CD8^-$ T cells most probably contained $\gamma\delta^+$ T cells and possibly NKT cells; although the exact composition of this population was not determined due to limitations in the number of fluorochromes used. $\gamma\delta^+$ T cells have been linked to *in vitro* mycobacterial growth inhibition in the cultured MGIA [73], the cattle MGIA [185] and by the work outlined in chapter 3. There is a large body of evidence that $\gamma\delta^+$ T cells are actively involved in the immune response against *M. tb* in humans [188, 189], NHP [72] and mice [190]. These T cells are thought to be important during the early stages of *M. tb* infection, and have been shown to preferentially respond to live mycobacteria where $CD4^+$ T cells do not [191], which concurs with my findings in NHP

PBMC infected with live *M. tb.* IFN-γ expression by $\gamma\delta^+$ T cells and NK cells could result in innate activation of macrophages, resulting in growth inhibition. Further work was needed to evaluate the effect of innate immunity; this was done using T cell depletion studies and microarrays which are described in chapters 5 and 6 respectively.

4.5 Chapter conclusions

- The novel total PBMC infection method resulted in variable CFU counts between samples at T0
- Removing the wash step of the novel MGIA reduced inter-sample variability in CFU counts at T0
- Using mycobacteria from starter cultures improved bacterial survival during the MGIA
- Shaking in 24 well plates did not improve mycobacterial growth, T cell viability or T cell functionality
- The novel MGIA could not distinguish between PBMC taken from naïve and BCG vaccinated cynomolgus macaques
- The novel MGIA could not distinguish between splenocytes taken from naïve and BCG vaccinated mice

Chapter 5

Mycobacterial growth indicator tube assay

5 Mycobacterial growth indicator tube assay (MGIT)

5.1 Introduction

5.1.1 The MGIT assay

5.1.1.1 BACTEC™ system

As discussed in the previous results chapters, I had not found a MGIA that could reliably detect vaccine induced mycobacterial growth inhibition, which was also suitable for use in preclinical studies of TB vaccine efficacy. I therefore assessed a third MGIA that used a different methodology to those previously described in chapters 3 and 4. The MGIT assay was developed by R. Wallis *et al*. [155], and has been used to demonstrate mycobacterial growth inhibition in WB taken from human volunteers after receiving BCG vaccination(s). The way the MGIT assay differs from other MGIAs, is that it utilises the BACTEC™ system for quantification of mycobacteria instead of CFU counts.

Mycobacteria are inoculated into MGIT tubes that contain a fluorochrome that is quenched by oxygen. As the bacteria multiply and respire, oxygen in the tube is depleted; the fluorochrome is no longer quenched and so fluoresces. Once a tube reaches a determined level of fluorescence it is registered as being positive. The time to positivity (TTP) is the

read out for this assay and is inversely proportional to the starting inoculum of mycobacteria. The TTP relates not only to the number of bacteria but also to their rate of metabolism.

5.1.1.2 Rationale for using mouse splenocytes in MGIT assay

To date, all published MGIT data for mycobacterial growth inhibition have been obtained using human whole blood [155]. I hypothesised that splenocytes taken from mice would also be suitable for this assay. The use of murine samples allows the advantage of being able to show that *in vitro* growth inhibition using this assay corresponds with *in vivo* protection using the well-defined mouse *M. tb* challenge model. If this assay could be shown to distinguish between splenocytes from BCG vaccinated and naïve animals, then this would potentially allow me to use cryopreserved PBMC from NHP/humans in this assay.

5.2 Aims of this chapter

The aims of the experiments detailed in this chapter were as follows;

- Assess the ability of the MGIT assay to discriminate between mycobacterial growth inhibition in splenocytes taken from naïve and BCG vaccinated mice.
- Establish if *in vitro* growth inhibition seen in the MGIT assay corresponds with *in vivo* protection from *M. tb* challenge in the mouse model.
- Investigate the cell populations responsible for BCG induced mycobacterial growth inhibition in the MGIT assay.
- Assess the ability of the MGIT assay to discriminate between mycobacterial growth inhibition in cryopreserved PBMC taken from naïve and BCG/BCG-MVA85A vaccinated NHP.
- Establish if growth inhibition seen in the MGIT assay correlates with *in vivo* survival and other clinical parameters from *M. tb* challenge in the NHP model.

5.3 Results

5.3.1 MGIT assay vs. the total PBMC infection MGIA using mouse splenocytes

For this experiment age matched naïve and BCG vaccinated ($1x10^6$ CFU Pasteur) C57bl/6 mice (8 in each group) were used to perform the total PBMC infection MGIA and the MGIT assay in a head to head comparison. There was a 6 week interval between BCG vaccinations and the removal of spleens for use in the MGIAs. CFU values from the novel MGIA were obtained by counting colonies on agar plates, whereas CFU values for the MGIT assay were calculated from TTP values using the BACTEC™ machine.

The total PBMC infection MGIA was unable to detect differences in mycobacterial growth inhibition between the naïve and BCG vaccinated groups as seen in **Error! Reference source not found.**a. However, when the same splenocytes were used to perform the MGIT assay, there was a significant ($p=0.024$) $0.1\log_{10}$ reduction in mycobacterial growth in the BCG vaccinated animals as compared to naïve animals (**Error! Reference source not found.**b). There was no relationship between how each animal performed across the assays, for example, the naïve animal represented by the black data point has the highest GR value in the total PBMC infection MGIA and the lowest GR value in the MGIT assay.

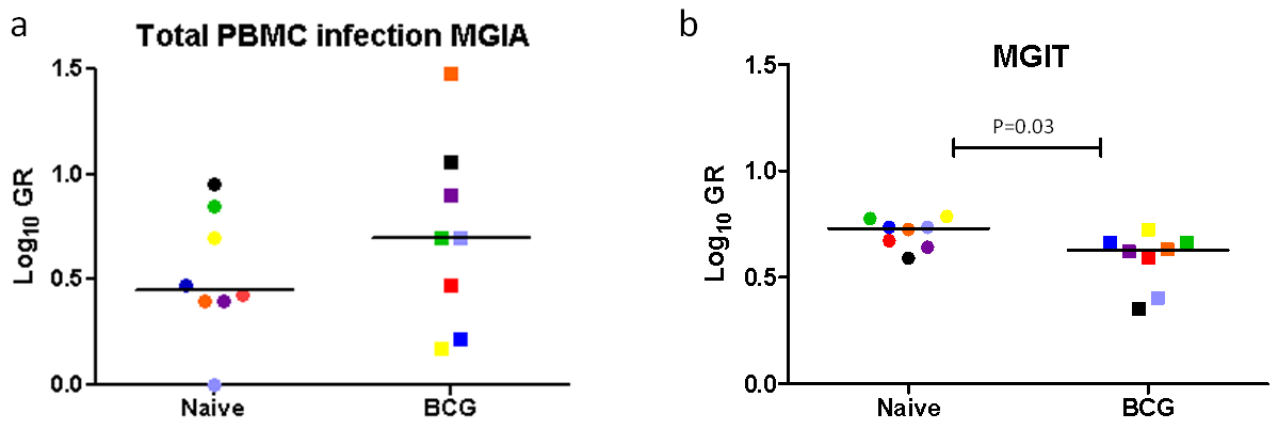

Fig. 5-1 Effectiveness of the total PBMC infection MGIA and MGIT assay using mouse splenocytes.
Data shown are log_{10} transformed GR values for naïve and BCG vaccinated ($1x10^6$ CFU s.c) C57bl/6 mice. Spleens were harvested 6 weeks after vaccination and used for head to head comparison in both MGIAs. Graph (a) shows data from the novel MGIA (GR= CFU day 4/CFU day 0) and (b) shows data from the MGIT assay where TTP is converted to CFU counts (GR=CFU day 4 sample tubes/ CFU control tubes). Individual animals are indicated by the colour of the data points within the naïve or BCG groups between the different assays. Bars represent the median values, n=8, Mann Whitney t tests were used to analyse the data.

5.3.2 Growth inhibition in vitro corresponds with in vivo protection in mice

Having successfully demonstrated that BCG vaccination in mice resulted in a reduction of BCG growth *in vitro* as measured by the MGIT assay, I now set out to assess whether this growth inhibition corresponded with *in vivo* protection against *M. tb* challenge. Although there is a large body of evidence that BCG vaccination protects mice from *M. tb* challenge [115, 156, 192]; I needed to show that the dose of BCG, route of administration and time-course that I used for mice in the MGIT assay, would also be protective *in vivo.*

As the MGIT assay is performed using splenocytes it was not possible to use the same animals for this assay and the *M. tb* challenge, so animals were placed into matched groups for parallel study with 10 animals in each group as outlined in Fig. 5-2. Animals were sacrificed for use in the MGIT assay in the same week as the *M. tb* challenge was performed. The challenge dose was estimated to be 230 CFU/mouse as determined by plating out lung homogenates from 2 extra naïve mice the day after challenge.

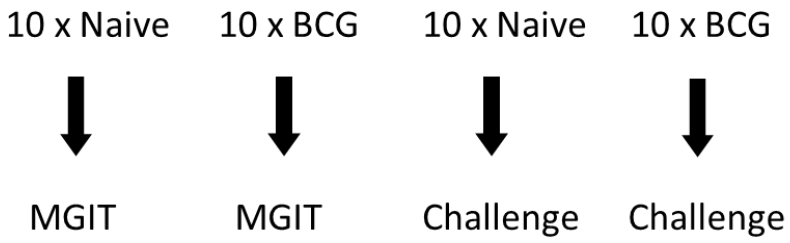

Fig. 5-2 Organisation for groups of mice used for parallel study of MGIT assay and *M. tb* challenge.
Age matched C57bl/6 mice were left as naïve or were vaccinated with BCG Pasteur ($1x10^6$ s.c). At 6 weeks post vaccination, naïve and vaccinated groups were divided in half for use in the MGIT assay or for *M. tb* challenge.

5.3.2.1 BCG vaccination induced mycobacterial growth inhibition in mice

BCG vaccination induced a significant ($p=0.0013$) reduction in mycobacterial growth in mouse splenocytes as measured by the MGIT assay (Fig. 5-3). There was a $0.2\log_{10}$ reduction between the naïve and BCG vaccinated animals with $\log_{10}$ transformed data ranges of 0.55 - 0.90 and 0.37 - 0.61 respectively.

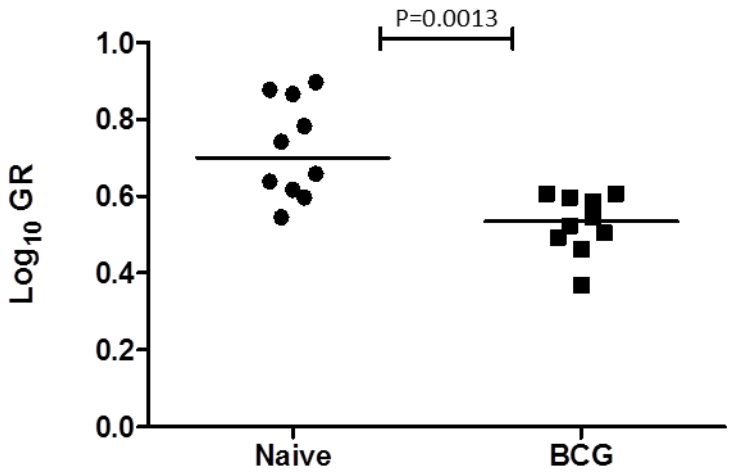

Fig. 5-3 BCG induced mycobacterial growth inhibition in mouse splenocytes.
Data shown are log_{10} transformed GR values for naïve and BCG vaccinated ($1x10^6$ CFU s.c) C57bl/6 mice. Spleens were harvested 6 weeks after vaccination for the MGIT assay. Bars represent the median, n=10, Mann Whitney t test was used to analyse the data. TTP values were converted to CFU, GR=CFU day 4 sample tubes/ CFU control tubes.

5.3.2.2 BCG vaccination protects mice against M. tb challenge

BCG vaccinated mice had significantly lower levels of *M. tb* in their lungs (p=0.0002) and spleens (p=0.0003) compared with naïve animals, following *M. tb* challenge (Fig. 5-4). The level of protection afforded was a 0.76 log_{10} and 0.6 log_{10} reduction in the median CFU/ml counts in the lungs and spleens of the animals respectively.

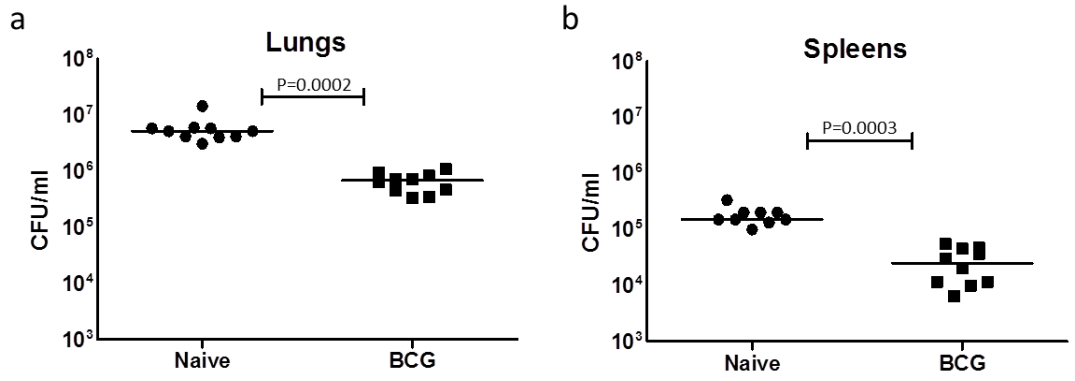

Fig. 5-4 BCG vaccination protects mice against *M. tb* challenge.
Graphs show CFU/ml data for C57bl/6 mice that were aerogenically challenged with 230 CFU of *M. tb* Erdman. Mice were naïve or had received BCG vaccination ($1x10^6$ CFU Pasteur, s.c) 6 weeks prior to challenge. Lungs and spleens were harvested from all animals 28 days after challenge. Graph (a) shows CFU/ml data from lungs and graph (b) shows CFU/ml data from spleens. Bars represent the median values, n=10, p-values determined by Mann Whitney t tests.

5.3.3 Effect of T cell depletions on mycobacterial growth inhibition

I hypothesised that the mycobacterial growth inhibition seen in the MGIT assay was T_H1 cell mediated. In order to test this theory, I performed $CD4^+$ and $CD8^+$ T cell depletions on splenocytes taken from naïve and BCG vaccinated mice, and used the depleted cells to perform the MGIT assay. The effectiveness of the depletions was 67-90% for $CD4^+$ and 89-98% for $CD8^+$ T cells. The gating strategy used for estimation of cell depletion percentages is displayed in Fig. 5-5. As the MGIT tubes are expensive to use, this experiment was performed using CFU counts on 7H9 agar plates instead. All splenocyte-BCG co-cultures contained $1x10^6$ splenocytes so that depleted samples were not affected by a reduction in the number of cells. The splenocytes used for this experiment were

taken from the same animals as described in section 5.3.2.1. The GR values from the non-depleted samples almost significantly correlated with the MGIT GR values (p=0.07 data not shown) for the mice, so I am confident that that the CFU counts, overall, gave a good approximation of how these samples would have performed had I used the BACTEC™ system.

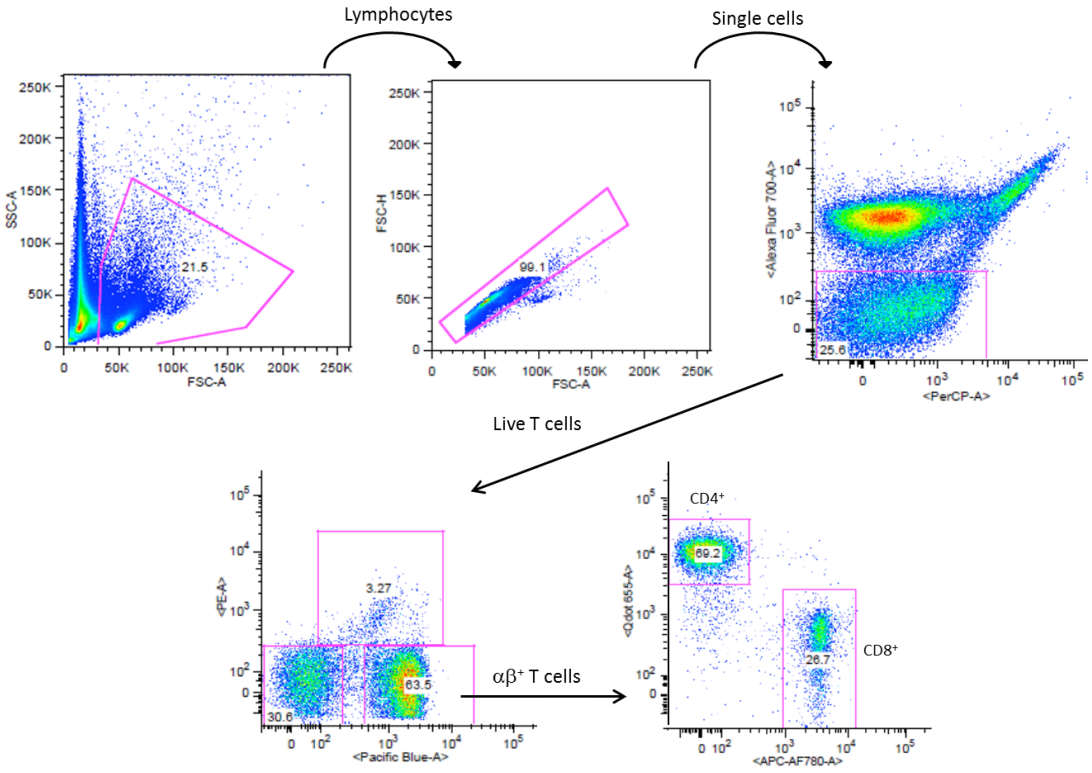

Fig. 5-5 Gating tree for mouse splenocytes.

Diagram describes the gating strategy used for mouse splenocytes. The lymphocyte population was selected for and single cells identified. B cells and dead cells were excluded from the analysis and cells that were positive for TCR-αβ were selected. The $CD4^+$ and $CD8^+$ T cells were then identified within this population.

The results were surprising as the levels of mycobacterial growth were less when the $CD4^+$ and $CD8^+$ T cells were depleted as compared with the non-depleted controls (Fig. 5-6), although this was not significant in any of the groups. A trend for lower GR values was seen in the $CD4^+$ depleted samples as compared to the non-depleted controls in naïve and BCG vaccinated animals (p=0.125 and p=0.125 respectively). The same trend was seen in the $CD8^+$ depleted samples in naïve and BCG vaccinated animals (p=0.06 and p=0.125 respectively). There was also a trend for lower GR values in BCG vaccinated animals compared to the naïve animals in the non-depleted controls and in the $CD4^+$ T cell depleted samples although this was not significant (p=0.22 and p=0.34 respectively).

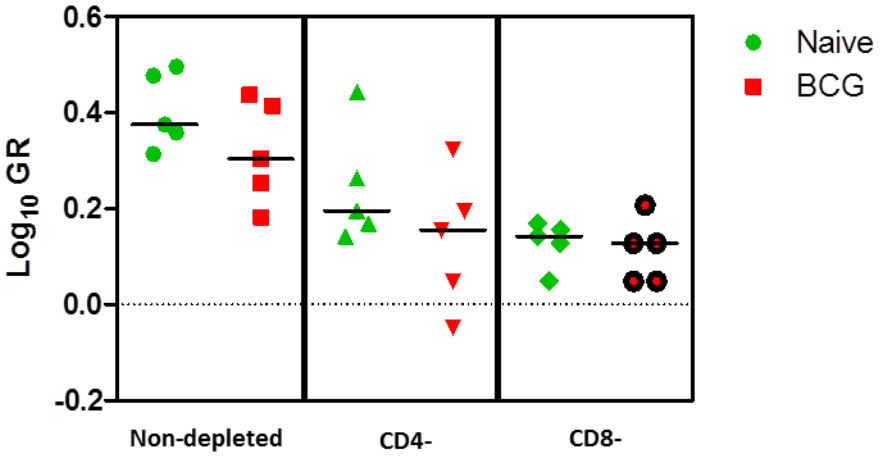

Fig. 5-6 Effect of $CD4^+$/$CD8^+$ T cell depletions on mycobacterial growth inhibition.
The graph shows Log_{10} transformed GR values for non-depleted, $CD4^+$ and $CD8^+$ T cell depleted splenocytes. Splenocytes taken from naïve and BCG vaccinated ($1x10^6$ CFU) mice are displayed with green and red data points respectively. The bars represent the median values. Data were analysed by Mann Whitney (BCG vs. naïve) and Wilcoxon matched pairs T tests.

5.3.4 MGIT assay using PBMC from NHP

Cryopreserved PBMC from a vaccination-challenge experiment using rhesus macaques were available for use with the MGIT assay. Precise details of the study are described elsewhere [158]. PBMC samples from 5 BCG vaccinated (group B) and 5 BCG-MVA85A (group A) vaccinated animals were utilised for my study. PBMC taken before vaccination and 1 week prior to *M. tb* challenge were used for each animal. These time-points were chosen so that naïve growth inhibition responses could be compared with those most likely to correspond to *in vivo M. tb* challenge responses (Fig. 5-7).

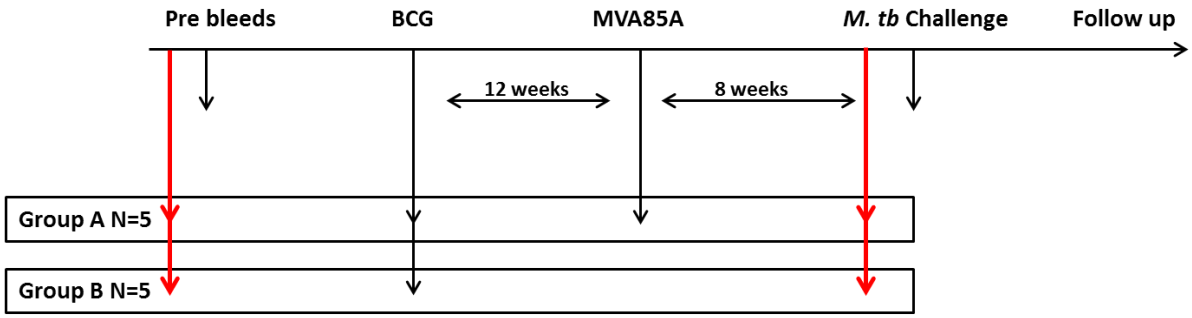

Fig. 5-7 Schematic diagram of NHP vaccination-challenge regime.
Ten rhesus macaques were all vaccinated with BCG (100µl BCG Danish i.d), 5 out of 10 of the animals received a MVA85A boost ($5x10^8$ PFU) 12 weeks later. At 21 weeks post BCG vaccination all animals were aerosol challenged with between 40-65 CFU of *M. tb* Erdman. The red arrows indicate time-points at which the PBMC used for my studies were taken. Each animal had a pre vaccination sample and a sample that was taken 1 week prior to the challenge.

5.3.4.1 BCG & BCG-MVA85A induced mycobacterial growth inhibition in NHP PBMC

BCG and BCG-MVA85A vaccination resulted in a significant decrease in the levels of mycobacterial growth when both groups were combined (p=0.0098) (Fig. 5-8). The log_{10} transformed data ranged from 0.17 - 0.87 in the pre vaccination samples and from -0.26 - 0.51 in the post vaccination samples (median values were 0.75 and 0.15 respectively).

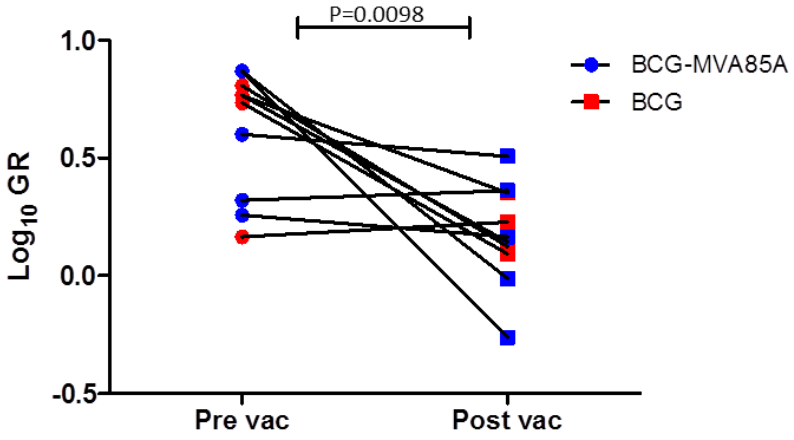

Fig. 5-8 BCG/BCG-MVA85A induced mycobacterial growth inhibition in cryopreserved PBMC from NHP. Graph shows the log_{10} transformed GR values for 5 BCG (100µl BCG Danish i.d) and 5 BCG-MVA85A (100µl BCG Danish i.d, $5x10^8$ PFU) vaccinated rhesus macaques (red and blue data points respectively). Time-points are from pre vaccination and post vaccination (1 week prior to *M. tb* challenge). TTP values were converted to CFU, GR=CFU day 4 sample tubes/ CFU control tubes. N=10, Wilcoxon matched pairs t test was performed on the data.

I also analysed the MGIT data from group A and B separately to see if there were any differences in the levels of mycobacterial growth inhibition between them. There were no significant differences between the groups (Fig. 5-9). There were also no significant differences between the pre and post vaccination GR values in either of the groups alone, although there was a trend for lower GR values post vaccination in both groups.

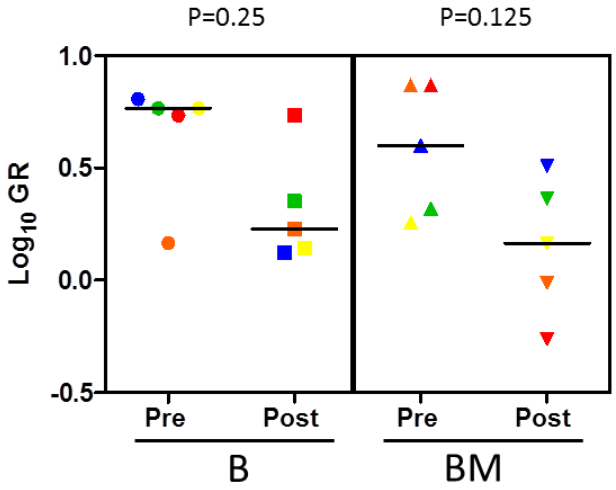

Fig. 5-9 MGIT results for individual groups of NHP.
Graph shows the log_{10} transformed GR values for BCG (B) and BCG-MVA85A (BM) vaccinated rhesus macaques. Time-points are from pre vaccination and post vaccination (1 week prior to *M. tb* challenge). Individual animals in each group are identified by the colour of the data points between the pre and post vaccination samples. Bars represent the median values. TTP values were converted to CFU, GR=CFU day 4 sample tubes/ CFU control tubes. Wilcoxon matched pairs t test was performed on the data.

5.3.4.2 Correlation of clinical parameters with MGIT assay results

Clinical data from the vaccinated-challenged NHP were available for correlation against pre and post vaccination GR values. Some of the clinical parameters analysed, included, duration of survival, lung CFU counts, lesion volume:lung volume ratio, lesion counts and Elispot data from pre vaccination, 1 week before challenge and 2 weeks after challenge. The only parameter that significantly correlated with the GR values was the lung score, which correlated positively in the naïve (p=0.03) (Fig. 5-10a), and negatively with the vaccinated (p=0.02) GR values (Fig. 5-10b). The lung score was calculated by scoring each lobe based on the number and type (severity) of lesion between 1-5 and adding the scores together for a maximum of 25.

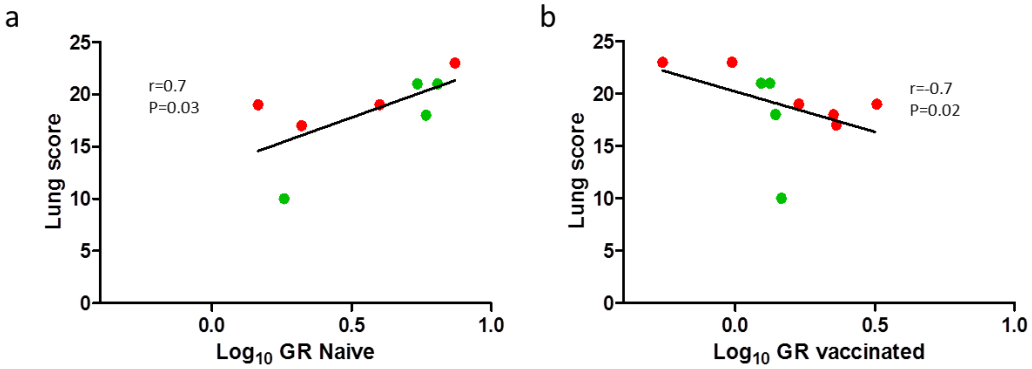

Fig. 5-10 Correlation of lung score with GR values pre and post vaccination in NHP.
Graphs represent correlations between log_{10} transformed GR values pre (graph a) and post (graph b) vaccination with BCG/BCG-MVA85A against lung scores for the animals post *M. tb* challenge at the point of necropsy. Red data points indicate animals that met humane end points before the end of study. Green data points indicate animals that survived until the end of the study 52 weeks post challenge. Correlations were performed using spearman rho.

5.4 Discussion

The mouse *M. tb* challenge model is a well characterised system used to evaluate the protective efficacy of novel TB vaccines [98, 115, 156]. BCG vaccination is known to provide an approximate 1-2$\log_{10}$ reduction in *M. tb* CFU in the lungs and spleens of challenged animals. Thus, if mycobacterial growth inhibition *in vitro* does correlate with *in vivo* protection, then the mouse model is an ideal system to prove this and 'validates' the MGIT assay as measuring what it is intended to. The MGIT assay, developed by R. Wallis *et al* [155] has been shown to detect improved mycobacterial growth inhibition in human WB cultures in response to BCG vaccination. To date, this assay has not been performed using samples obtained from mice. Since it is technically challenging to consistently obtain sufficient WB from mice to perform the MGIT assay (600µl), splenocytes taken from naïve and BCG vaccinated mice were used to assess the MGIT assay.

In repeated MGIT assays performed using mouse splenocytes, the levels of mycobacterial growth were significantly reduced in BCG vaccinated animals compared with naïve controls. One of the most striking features of the MGIT data was the low level of variability between the animals in each group. The data were much tighter than was seen in the total PBMC infection MGIA when identical samples were used for both MGIAs. The levels of variability and reproducibility seen in the MGIT assay indicate that this is a robust assay, capable of

detecting small (0.1-0.2 $\log_{10}$) differences between groups of animals. The sensitivity of this MGIA to detect such small differences is very encouraging; this means that it should be able to distinguish between BCG and improved TB vaccines/boosted samples, although this was not assessed during the course of these studies. It would be very interesting to see whether splenocytes taken from BCG-MVA85A boosted animals have improved levels of mycobacterial growth inhibition over BCG alone splenocytes, as this heterologous booster vaccine that was developed at the Jenner Institute has been shown to be more efficacious than BCG alone in the mouse and guinea pig *M. tb* challenge model [115, 116].

Mice that were experimentally matched to those used for the MGIT assay were challenged with *M. tb* to establish whether there was an association between mycobacterial growth inhibition in the MGIT assay and protection *in vivo.* The level of protection seen in this study is in accordance with what has been previously reported [115, 156, 192], although it is slightly less than 1 log, which could be due to the relatively large challenge dose of 230 CFU/mouse, however, it was nonetheless highly significant. The challenge data are also very tight with little variation between the animals in each group, which concurs with the low levels of variance seen in the MGIT data. There appears to be a temporal association between enhanced mycobacterial growth inhibition seen in the MGIT assay, and protection from *M. tb* challenge, but due to the fact that different mice had to be used between the

MGIT assay and the *M. tb* challenge, it was not possible to directly correlate GR values *in vitro* with mycobacterial burden *in vivo.* The way this could be achieved in mice, would be to test multiple vaccination regimes that induce significantly different levels of protection from *M. tb* challenge within different groups, the median group CFU values from challenge could then be correlated against the median group inhibition values in the MGIT assay, as was done for the murine MGIA in which mycobacterial growth inhibition correlated with protection for a number of candidate TB vaccines [156]. If the MGIT assay could be performed using a very small amount of blood (<100µl from each mouse) then it could also be possible to perform the MGIT assay and challenge in the same mouse.

The levels of BCG vaccine induced mycobacterial growth inhibition were more modest in the MGIT assay than was seen in the published murine MGIA (1log reduction in CFU), in which the same strain of mouse and vaccine regime were used. However it is worth noting that the levels of *in vivo* protection were also greater in the murine MGIA than was seen in this present study, which perhaps suggests that the vaccinations were less effective during these experiments, which may have contributed to the lower levels of mycobacterial growth inhibition seen in the MGIT MGIA. Another contributing factor could have been the difference in the methods used to infect the co-cultures. Infection of monocyte layers with a low MOI (1:100) of mycobacteria followed by washing away free bacteria (murine MGIA),

is the most efficient method of obtaining phagocytosed mycobacteria. It is generally thought that MGIAs are a measure of intracellular killing, therefore, if the majority of bacteria are phagocytosed prior to the start of co-culture with PBMC/Splenocytes, then intracellular killing can begin immediately. In contrast, when mycobacteria are inoculated into splenocyte/WB/PBMC cultures they may persist extracellularly for a prolonged period of time, perhaps even the full duration of the assay (4 days) as no studies have been conducted to assess the efficiency of phagocytosis in MGIAs that use this method of infection. It is possible that extracellular survival of mycobacteria throughout the MGIT assay could reduce the sensitivity of this assay to detect mycobacterial growth inhibition/killing.

When a direct comparison of the MGIT and total PBMC infection MGIAs was performed using identical splenocyte samples the MGIT assay appeared to be effective where the total PBMC infection MGIA was not. Differences between these assays included the vessel and conditions used during splenocyte-BCG culture as well as the method by which the growth of BCG was measured. The action of rotating the splenocyte-BCG cultures in polypropylene micro-tubes (MGIT assay) may have a number of effects on mycobacterial growth. Firstly, rotating the cultures means that memory T cells are more likely to make physical contact with macrophages or DC containing BCG/mycobacterial antigens; physical

contact between BCG infected monocytes and lymphocytes has been shown to mediate intracellular mycobacterial growth inhibition [73, 153]. In contrast, when splenocytes/PBMCs are cultured in stationary tissue culture plates (total PBMC infection MGIA) they are unlikely to make contact with memory cells that are not in their immediate vicinity. Secondly, aeration of the cultures may also improve the growth of the mycobacteria which is essential if growth inhibition is to be detected (as opposed to mycobacterial killing). One way to assess if the rotation is important would be to set up cultures in parallel with half rotating and half remaining stationary and seeing if there was a difference in mycobacterial growth between them. The ability of macrophages to adhere to the culture vessel may be important for their functionality. A study by Barker *et al* [193] has shown that cultures of non-adherent human monocytes were able to kill *M. smegmatis* whereas adhered monocytes could not. So the use of polypropylene micro-tubes which permit very limited monocyte adherence could enhance mycobacterial growth inhibition in the MGIT assay, although the effect has not yet been demonstrated for BCG or *M. tb*.

A possible reason why the MGIT assay has low variability, good reproducibility and is able to detect small differences in mycobacterial growth levels, is the method by which the bacteria are quantified. Serial dilutions of mycobacteria are prone to errors from pipetting, clumping and adherence of bacteria to plastic-ware; all of which lead to errors in the

estimation of CFU. The MGIT system does not require serial dilution of samples and the readout is determined by a computer, so there is little investigator error/bias. Clumping is a major limitation of CFU estimation using 7H10 agar plates, and there is no way of knowing whether a colony has arisen from a single bacterium or many. CFU counts do not measure the health of the bacteria that are being counted, a damaged bacterium may grow slowly producing a small colony, but all colonies count as 1, regardless of their size. A major advantage of the MGIT system is that oxygen depletion is the factor that indicates the level of mycobacterial growth inhibition. Oxygen levels in MGIT cultures are not influenced by clumping, but they are affected by the number of bacteria and their metabolism. The MGIT system is possibly sensitive enough to detect differences in mycobacterial growth rates and not just the number of viable organisms, it is therefore perhaps a more accurate method for measuring mycobacterial growth in a MGIA.

Due to the significant cost of using MGIT tubes in the BACTEC^{TM} system, the T cell depletion studies outlined in section 5.3.3 were performed using 7H10 agar plates, which, although are not as sensitive as the BACTEC^{TM} system, would permit the assessment of the roles of $CD4^+$ and $CD8^+$ T cells in mycobacterial growth inhibition in the MGIT assay. Although the number of animals was small (n=5 per group) a trend for reduced mycobacterial growth in the $CD4^+$ or $CD8^+$ depleted splenocytes was seen. The apparent

improvement in growth inhibition upon removal of the $CD4^+$ T cells was not expected as T_H1 cell mediated immunity is known to be important for protection against TB in mice [98]. One limitation of this experiment was that splenocyte numbers were kept the same between depleted and non-depleted samples in order to remove any effects due to lower cell numbers, however, this will have had the effect of artificially increasing the abundance of all other cell populations. Perhaps a more effective method of assessing the role of memory $CD4^+$ and $CD8^+$ T cells would have been to top up depleted samples from BCG vaccinated mice with naïve $CD4^+$ and $CD8^+$ T cells respectively. Taking into account the aforementioned limitations of this study the results do concur with the findings of other MGIA T cell depletion studies; such as those using human WB in the MGIT assay, where depletion of either $CD4^+$ or $CD8^+$ T cells did not significantly increase the growth levels of the avirulent H37Ra strain of *M. tb*, however the depletion of both $CD4^+$ and $CD8^+$ T cells did [155]. Similarly, when PBMC samples that were enriched for $CD4^+$ or $CD8^+$ T cells were used to perform the cultured MGIA, there was no significant improvement in BCG growth inhibition [73]. However, there is evidence that $CD4^+$ T cell depletion in PBMC samples from TST positive individuals does significantly reduce their ability to inhibit virulent *M. tb* growth *in vitro,* this effect was not seen in TST negative individuals or for either group when $CD8^+$ T cells were depleted [153]. Although it is not implicitly stated that the TST+ individuals were latently infected with *M. tb,* it is implied that perhaps exposure to *M.*

tb is required to produce effective $CD4^+$ T cell responses that are capable of inhibiting intracellular growth of *M. tb.* It could also be the case that $CD4^+$ T cells are required for inhibiting the growth of virulent strains of *M. tb* but are not necessary for growth inhibition of avirulent strains or BCG, which may possibly be mediated through differences in the expression of virulence factors/antigenic targets that $CD4^+$ T cells recognise e.g. ESAT-6. If this is the case, then it is important that the MGIT assay results which have so far been obtained using BCG strains as the infectious organism are validated against virulent *M. tb*. This has already been done for the murine MGIA where mycobacterial growth inhibition in response to various TB vaccines has been correlated with *in vivo* protection against *M. tb* challenge when either *M. tb* or BCG was used as the infectious organism in the MGIA [156].

Although not significant, there was also a trend for lower GR values in BCG vaccinated mice compared to naïve controls in the non-depleted and $CD4^+$ T cell depleted cultures, suggestive of a BCG vaccine effect; this, combined with the fact that all cultures had the same number of splenocytes, points towards a relative increase in the abundance of a cell type other than $CD4^+$/$CD8^+$ T cells being important for mycobacterial growth inhibition in this assay. Possible cell types that could have an involvement in the MGIT assay include, NK cells, monocytes, neutrophils and B cells, however, the most likely cell type is perhaps $\gamma\delta^+$ T

cells as these cells have been previously identified as being important during MGIAs [73, 185, 194, 195]. $\gamma\delta^+$ T cells have both innate and adaptive properties. They undergo receptor gene rearrangement, which is a defining feature of the T cells of the adaptive immune response, but their gene rearrangement is limited. They do not need to undergo clonal expansion to respond to antigens they encounter; nor do they need antigens to be presented by MHC molecules. Mouse studies have shown that these cells are implicated in early control of *M. tb* infection [69] and that they are capable of secreting IFN-γ [70] and IL-17 [71]. The subject of whether these cells exhibit a memory phenotype is controversial, with evidence both for a memory phenotype in humans and NHP [72, 194] and against in mice [190]. One important factor in this debate is that mice do not express the Vδ9Vδ2 homologue that has been identified as having a memory phenotype in humans and macaques, and no functional equivalent has yet been found. $\gamma\delta^+$ T cells have been shown to produce IFN-γ and TNF-α [196, 197] which activate macrophages to kill phagocytosed BCG. In contrast to humans or macaques, mouse macrophages can be effectively activated to kill internalised mycobacteria by stimulation with exogenous IFN-γ [198]. The response of $\gamma\delta^+$ cells to produce IFN-γ is more rapid than that of the $CD4^+/CD8^+$ T cells as they do not require MHC presentation of antigens to become activated [199] and in the mouse this could account for the greater mycobacterial growth inhibition seen upon $CD4^+/CD8^+$ T depletion. The MGIT data in mice clearly show that BCG vaccination results

in a memory response that can be detected by mycobacterial growth inhibition; the mechanism behind this perceived inhibition is unclear. Although there was a trend for lower GR values in $CD4^+$ T cell depleted splenocytes from BCG vaccinated mice, this was not significant and so the existence of a memory response in the absence of $CD4^+$ has not been proven with this study. Further investigation of the mechanisms involved in BCG growth inhibition in the MGIT assay is described in chapter 6.

The successful use of mouse splenocytes indicated that PBMC would also be a suitable sample type for use with the MGIT assay. NHP are thought to be the most relevant animal model of human TB as they display similar pathologies such as highly ordered granulomas and many reagents used for assessment of immune responses are common to humans. Unlike humans, NHP can be challenged with *M. tb* and so preclinical TB vaccine efficacy can be assessed in this model. Cryopreserved PBMC taken from rhesus macaques before and after BCG or BCG-MVA85A vaccination were available for use in the MGIT assay. The animals had also been challenged with *M. tb* and so survival outcomes and clinical data were available for correlation against the MGIT assay results. This was the first time that the MGIT assay had been performed using cryopreserved PBMC and was the first time that an MGIA has been performed using samples from NHP. Mycobacterial growth inhibition was seen in response to BCG or BCG-MVA85A vaccination when data

from all of the monkeys were grouped together. Although this result remains to be repeated, it was very encouraging to see that the assay was successful in this cell type, as a wealth of cryopreserved PBMC are available from numerous clinical and NHP studies. The ability of the MGIT assay to be performed using WB, PBMC or splenocytes will facilitate its use in animal studies as well as clinical trials. The spread of the data was a lot greater than that which was seen using mouse splenocytes. This could have been due to greater heterogeneity in the monkeys, as variability of the data was also quite large when this assay was performed in humans [155]. The cryopreservation of PBMC could also have had an effect on the health and functionality of these cells, which could also contribute to variability; a comparison of the variability between animals when fresh or cryopreserved PBMC are used would inform whether this was the case. In the study where the MGIT assay was used to assess human WB samples, the authors suggested that the volunteers could be grouped by their responses to the primary BCG immunisation and subsequent BCG re-vaccination. Some of the volunteers displayed mycobacterial growth inhibition in response to the primary vaccination, others only responded after the BCG re-vaccination and some volunteers did not respond at all [155]. In the NHPs, 8 out 10 of the monkeys vaccinated against TB (BCG/BCG-MVA85A) displayed enhanced mycobacterial growth inhibition, which is a higher proportion of responders than was previously found in humans, possibly due to less heterogeneity in these animals than is

seen in humans. It would be interesting to investigate different time points after vaccination in these NHP to see how the kinetic of mycobacterial growth inhibition changes over time, especially in response to the MVA85A boost, as this was not done during the course of this study. Unlike mice, the use of WB would also be possible with NHP, so a direct comparison between monkeys and humans in response to BCG/BCG-MVA85A could also be performed as is possible with assays such as Elispot.

Attempts to correlate the MGIT assay data to the clinical outcomes of the *M. tb* challenge experiment from which the NHP PBMC samples were obtained were limited by the fact that there were no significant differences in the survival times between any of the three groups (naïve, BCG and BCG-MVA85A vaccinated animals) after challenge [158]. This indicates that the use of survival as a measure of protective efficacy of TB vaccines in NHP is perhaps not suitable. This idea is supported by a number of studies where BCG has been shown to be efficacious when fixed term study end-points were used [200, 201]. Bearing this limitation in mind, it is not surprising that the MGIT data did not correlate with post challenge survival. The only clinical parameter from the challenge study that did discriminate between the naïve and vaccinated animals was the lesion volume:lung volume ratio, which was determined using MRI scans with stereology at the end of the study; although this parameter also did not correlate with the MGIT assay data. The apparent

lack of correlation between the MGIT assay and survival/lesion:lung ratio scores could also be due to the sample time-points used. The post vaccination time-point of 20 weeks post BCG was chosen as it was thought that this would best represent the responses of the animals as they would occur during the challenge that took place 1 week after this time-point, but it could be that peak growth inhibition responses occurred at a different time-point, as work in humans suggests that the levels of growth inhibition vary over the months following vaccination with a peak at 8 weeks post after primary BCG vaccination. In a separate NHP *M. tb* challenge study that assessed the protective efficacy of BCG and BCG-MVA85A, significant differences were seen between the vaccinated and naïve animals in clinical parameters including weight loss, lung X-ray scores and bacterial burden in the lungs [201]. The *M. tb* infection for this study was performed by intra-tracheal instillation and the endpoint of the study was set at 16 weeks post challenge, so survival was not the endpoint. Therefore, there is evidence that BCG and BCG-MVA85A vaccination in NHP can be protective against *M. tb* challenge *in vivo* and the MGIT assay may possibly be proven to correlate with protection in this model.

5.5 Chapter conclusions

- BCG vaccination induces reproducible mycobacterial growth inhibition in mouse splenocytes that can be detected by the MGIT assay
- Vaccine induced mycobacterial growth inhibition *in vitro* corresponds with *in vivo* protection from *M. tb* aerosol challenge in mice
- The mechanism behind vaccine induced mycobacterial growth inhibition is yet to be determined
- BCG and BCG-MVA85A vaccination induces mycobacterial growth inhibition in cryopreserved NHP PBMC that can be detected by the MGIT assay
- Correlation between *in vitro* growth inhibition in NHP PBMC has yet to be correlated with *in vivo* protection from *M. tb challenge*

Chapter 6

Investigation of immune mechanisms involved in inhibition of mycobacterial growth

6 Differential gene expression in naïve and BCG vaccinated mouse splenocytes

6.1 Introduction

6.1.1 Rationale for using microarrays

The results in chapter 5 showed that BCG vaccination in mice resulted in increased mycobacterial growth inhibition (i.e. less growth) in mouse splenocytes. In this chapter, I describe differential gene expression (DGE) studies that were performed with splenocyte cells from the same mice used for the MGIT assay described in section 5.3.2. The aim of this experiment was to gain insight into the mechanisms behind mycobacterial growth inhibition in mouse splenocytes.

6.1.2 The Illumina MouseRef-8 v2.0 BeadChip

The Illumina MouseRef-8 BeadChip contains 19,100 unique genes and enables the interrogation of 8 separate samples on a single slide. The genes on the MouseRef-8 BeadChip are derived from the NIH reference sequence (RefSeq) database, which is a collection of non-redundant, well-annotated gene sequences. The BeadArray technology developed by Illumina consists of beads that have 1000's of copies of a gene (probe) bound to the surface of a bead, and each bead has at least 5 replicates in each array (Fig. 6-1).

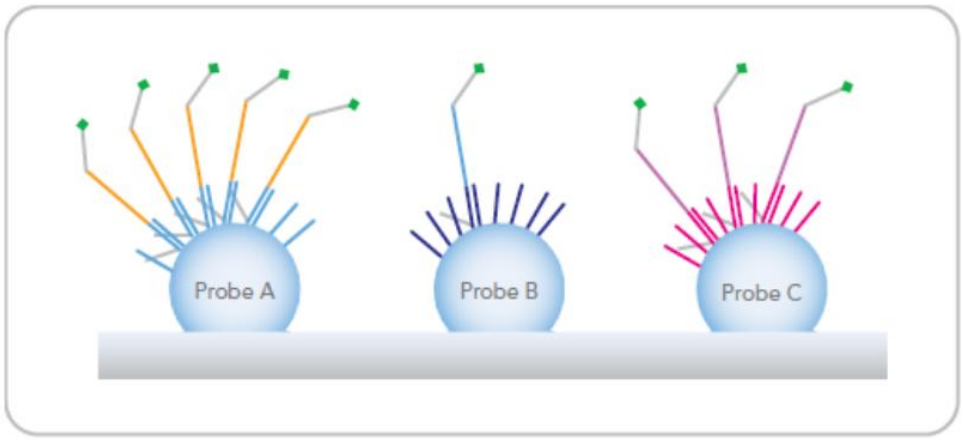

Fig. 6-1 Diagram of BeadChip array surface.
Diagram taken from Illumina "whole genome gene expression direct hybridisation assay guide". The fluorescent signal from probe (A) will be 5 times that of Probe (B) and directly relates to the level of transcription of each gene (probe).

6.1.3 q-PCR

RNA from splenocytes was used to perform q-PCR for the genes IFN-γ and TNF-α, using the house keeping gene HPRT to normalise the data across different samples. HPRT is ubiquitously expressed in mammalian cells and its expression does not change in response to stimulation, it can therefore be used to normalise against differences in the amount of total RNA across samples. The cycle threshold (CT) value is the number of polymerase chain reaction cycles required for a gene to be detected above background level. The CT value is inversely proportional to the abundance of a gene within a sample. Assuming PCR efficiency is 100%, then each difference in CT value of 1, is equal to a 2 fold change (FC) in the abundance of a gene (e.g. a difference in CT value of 3 is equal to a FC

value of 8). From the CT value the FC value can be calculated using the equation y =1.3826ln(x) + 0.083 where y=CT value and x = FC value. The fold change of a gene due to stimulation with antigen is calculated using the following calculation;

$$FC = \frac{\text{target gene (Stimulated/HPRT)}}{\text{target gene (Un-stimulated/HPRT)}}$$

6.2 Aims of this chapter

- Determine the dose of BCG to use for *ex vivo* stimulation of mouse splenocytes
- Use microarrays to evaluate splenocytes from naïve and BCG vaccinated mice to produce lists of differentially expressed genes
- investigate the functionality and biological pathway involvement of differentially expressed genes
- Correlate differentially expressed genes against GR values from MGIT assay (5.3.2)

6.3 Results

6.3.1 Determining the dose of BCG to use for stimulation of splenocytes

To maximise the likelihood of detecting differences in the gene expression of splenocytes from BCG vaccinated compared to naïve mice, I extracted RNA from splenocytes cultured overnight with media alone (un-stimulated), or with BCG (stimulated). Two different doses of BCG were compared in overnight stimulation to determine which concentration would result in optimum gene expression. For this stimulation I planned to use the same dose of BCG used for the MGIT assay, so the experiments would be comparable. However, the dose of BCG used to infect splenocytes for the MGIT assay was very low, between 2800-9000 CFU/1x10^6 splenocytes, and typically a dose of 1x10^6 CFU is routinely used in our lab to induce an immune response *in vitro*. I used q-PCR to assess if the low dose of BCG would be sufficient for inducing a change in gene expression that could be detected by DNA microarray.

For this experiment, splenocytes from 2 naïve and 2 BCG vaccinated mice were stimulated overnight with a low or high dose of BCG (5000 or 1x10^6 CFU/1x10^6 splenocytes respectively) or left un-stimulated as controls. All results are relative quantifications, as standards were not used for this experiment, so absolute quantities of genes are unknown. With only 2 animals in each group, statistical analysis of these data could not be

performed. However, the use of the higher dose of BCG was clearly required to detect a difference in gene expression, as incubation with the lower dose did not increase the expression of either TNF-α or IFN-γ (Fig 6-2a and b). The levels of TNF-α expression appeared to be the same between naïve and BCG vaccinated mice regardless of whether the low or high dose of BCG was used for the *ex-vivo* stimulation (Fig. 6-2a). However, the expression level of IFN-γ was elevated only in BCG vaccinated animals (Fig. 6-2b).

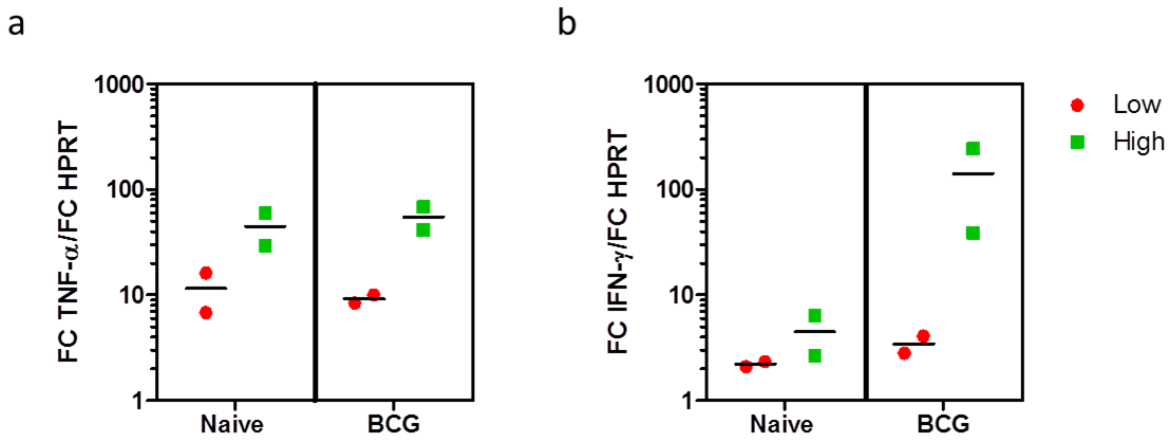

Fig. 6-2 Differential gene expression in response to varying doses of BCG stimulation.
Graphs display HPRT normalised FC values for (a) TNF-α (b) and IFN-γ. Low dose BCG (5000 CFU) and high dose BCG ($1x10^6$ CFU) samples are indicated by red and green data points respectively. Bars represent the median values, n=2.

6.3.2 Quality assessment of RNA for microarrays

RNA integrity is of great importance when it comes to achieving good quality microarray data. I analysed RNA quality using the Agilent Bioanalyzer system, which produces a

number of readouts including the RNA integrity number (RIN), a value between 7.0 - 10.0 indicates that RNA transcripts are intact and of good quality [202].

RNA was extracted from splenocytes taken from 10 (5 x naïve and 5 x BCG vaccinated) of the animals used to perform the MGIT assay detailed in section 5.3.2. Each animal had splenocytes that were either un-stimulated or BCG stimulated in overnight culture (20 samples in total). A total of 16 arrays were available for use in this experiment so both un-stimulated and BCG stimulated samples from 4 of the naïve and 4 BCG vaccinated mice were selected (based on the highest RIN values) for hybridisation to the array. The data from the Agilent Bioanalyzer are displayed in Fig. 6-3. Of the 10 animals, 2 had a BCG stimulated RNA RIN value less than 7.0, most likely due to the low quantity of RNA isolated from these 2 samples, so these animals were removed from further study (N5 and B4). However, the quantity and quality of RNA from the remaining samples was sufficient to progress to the amplification and hybridisation stages with median RNA concentrations of 25ng/µ and 27ng/µl for un-stimulated and stimulated samples respectively as measured using the Nanodrop (data ranges of 20.3-31.7 and 13.2-33.6 respectively).

The maximum volume of 11µl of RNA from each sample was used for amplification and biotinylation of the RNA transcripts using the Ambion TotalPrep kit. The amplified RNA was

quantified using Nanodrop to ensure that there was sufficient RNA for microarray hybridisation. The median concentration of amplified RNA for the un-stimulated and stimulated samples was 214.5ng/µl and 215.5ng/µl respectively (data ranges of 180-261ng/µl and 200-246ng/µl respectively). The quality of the amplified RNA samples was also assessed using the Agilent Bioanalyzer, the results of which are displayed in Fig. 6-4.

A peak transcript length between 1000-2000 base pairs is considered to be good quality. Some of the samples do appear slightly degraded with sharp peaks around the 1000 base pair mark, but they were still within the range of being good quality, so the samples were all adjusted to the same concentration (750ng/5µl) and hybridised to the MouseRef-8 v2.0 BeadChips.

a

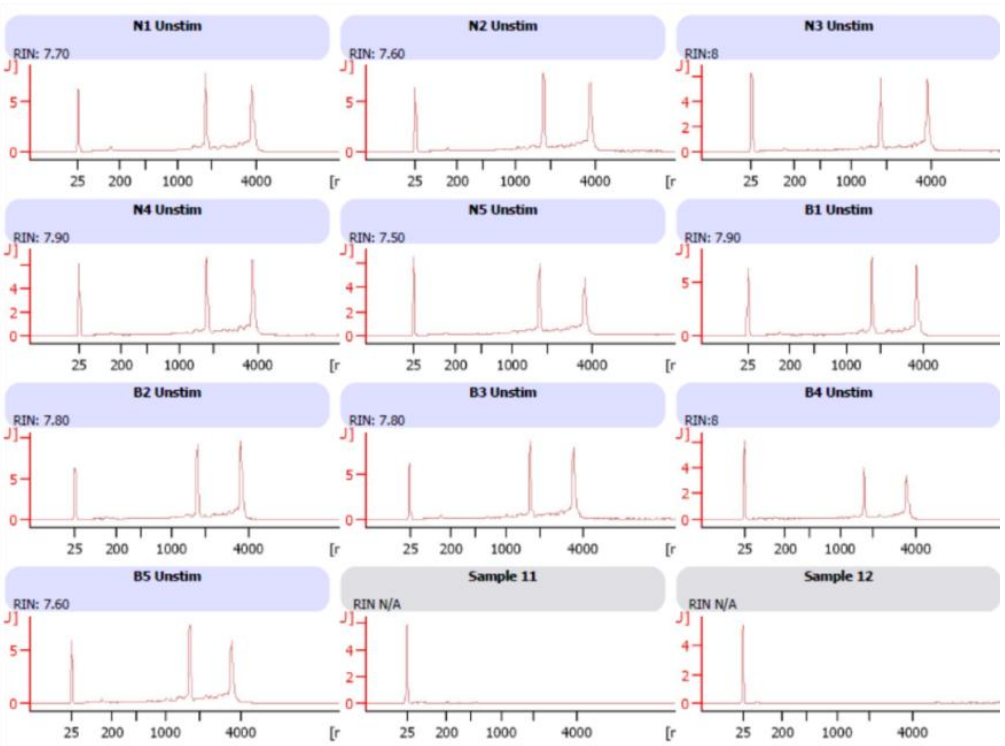
N1 Unstim
RIN: 7.70
N2 Unstim
RIN: 7.60
N3 Unstim
RIN:8
N4 Unstim
RIN: 7.90
N5 Unstim
RIN: 7.50
B1 Unstim
RIN: 7.90
B2 Unstim
RIN: 7.80
B3 Unstim
RIN: 7.80
B4 Unstim
RIN:8
B5 Unstim
RIN: 7.60
Sample 11
RIN N/A
Sample 12
RIN N/A

b

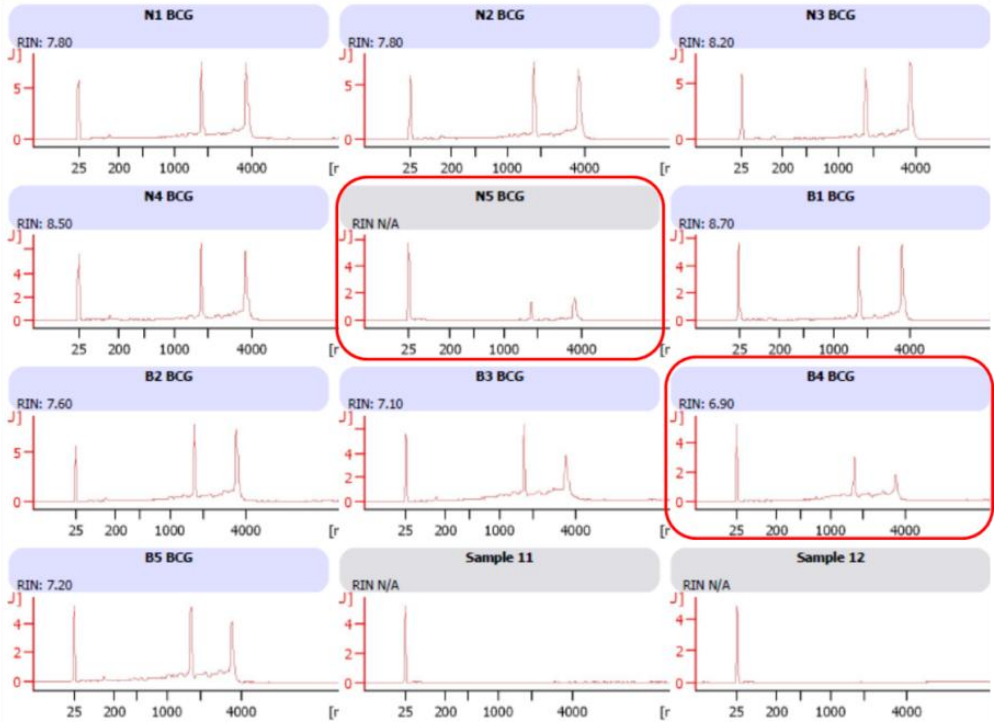
N1 BCG
RIN: 7.80
N2 BCG
RIN: 7.80
N3 BCG
RIN: 8.20
N4 BCG
RIN: 8.50
N5 BCG
RIN N/A
B1 BCG
RIN: 8.70
B2 BCG
RIN: 7.60
B3 BCG
RIN: 7.10
B4 BCG
RIN: 6.90
B5 BCG
RIN: 7.20
Sample 11
RIN N/A
Sample 12
RIN N/A

Fig. 6-3 Bioanalyzer electropherogram charts for RNA used for amplification.

Electropherograms showing the peaks for 28s, 18s and marker RNA from the right to the left of the graphs respectively. Graphs in panel (a) are from control (un-stimulated) samples, graphs in panel (b) are from BCG stimulated samples ($1x10^6$ CFU/$1x10^6$ splenocytes). The letters N and B indicate that samples were from naïve or BCG vaccinated mice respectively. The RIN value for each sample is displayed in the sample name panel above each electropherogram. Red boxes indicate that the sample had a RIN value below 7.0 and so was unsuitable for use in the microarray.

a

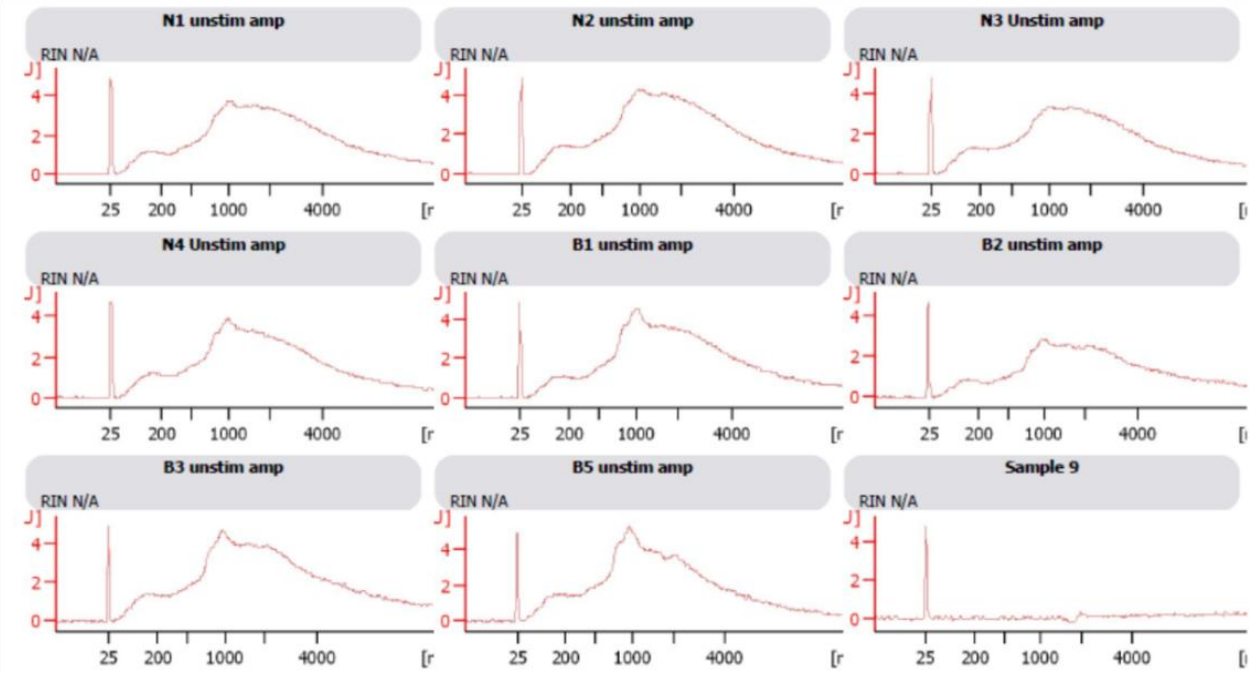
N1 unstim amp
RIN N/A
N2 unstim amp
RIN N/A
N3 Unstim amp
RIN N/A
N4 Unstim amp
RIN N/A
B1 unstim amp
RIN N/A
B2 unstim amp
RIN N/A
B3 unstim amp
RIN N/A
B5 unstim amp
RIN N/A
Sample 9
RIN N/A
25 200 1000 4000

b

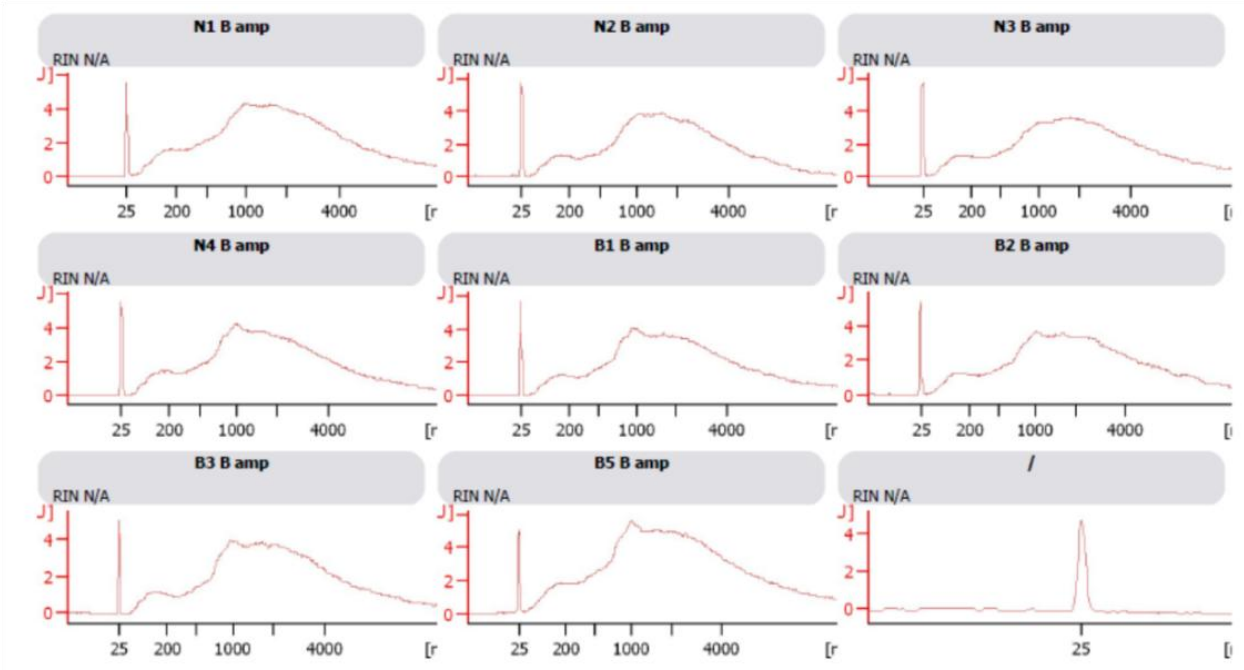
N1 B amp
RIN N/A
N2 B amp
RIN N/A
N3 B amp
RIN N/A
N4 B amp
RIN N/A
B1 B amp
RIN N/A
B2 B amp
RIN N/A
B3 B amp
RIN N/A
B5 B amp
RIN N/A
/
RIN N/A
25 200 1000 4000

Fig. 6-4 Bioanalyzer electropherogram charts for amplified RNA used for microarray
Electropherograms showing the peak transcript length of amplified RNA samples. Graphs in panel (a) are from control (un-stimulated) samples, graphs in panel (b) are from BCG stimulated samples ($1x10^6$ CFU/$1x10^6$ splenocytes). The letters N and B indicate that samples were from naïve or BCG vaccinated mice respectively.

6.3.3 Microarray normalisation

To ensure that discrepancies in hybridisation efficiency between the arrays and chips (8 arrays on each chip) did not impact upon the DGE analysis, the data were quantile normalised. Arrays 1-8 were on chip 1 and arrays 9-16 were on chip 2 (Table 6-1). Before normalisation, there was clearly a chip effect seen across the arrays (Fig. 6-5a), with chip 2 having greater levels of fluorescence than chip 1. Whereas after normalisation, all the arrays were centred around the same point, so that the data between arrays and across the different chips were comparable (Fig. 6-5b).

Array number	Sample
1	Naïve 1 unstim
2	Naïve 3 unstim
3	BCG 2 stim
4	Naïve 2 stim
5	BCG 3 unstim
6	Naïve 4 unstim
7	Naïve 3 stim
8	BCG 1 unstim
9	BCG 3 stim
10	BCG 2 unstim
11	Naïve 1 stim
12	Naïve 2 unstim
13	BCG 1 stim
14	BCG 5 stim
15	Naive 4 stim
16	BCG 5 unstim

Table 6-1 Table showing which samples were hybridised to each array.

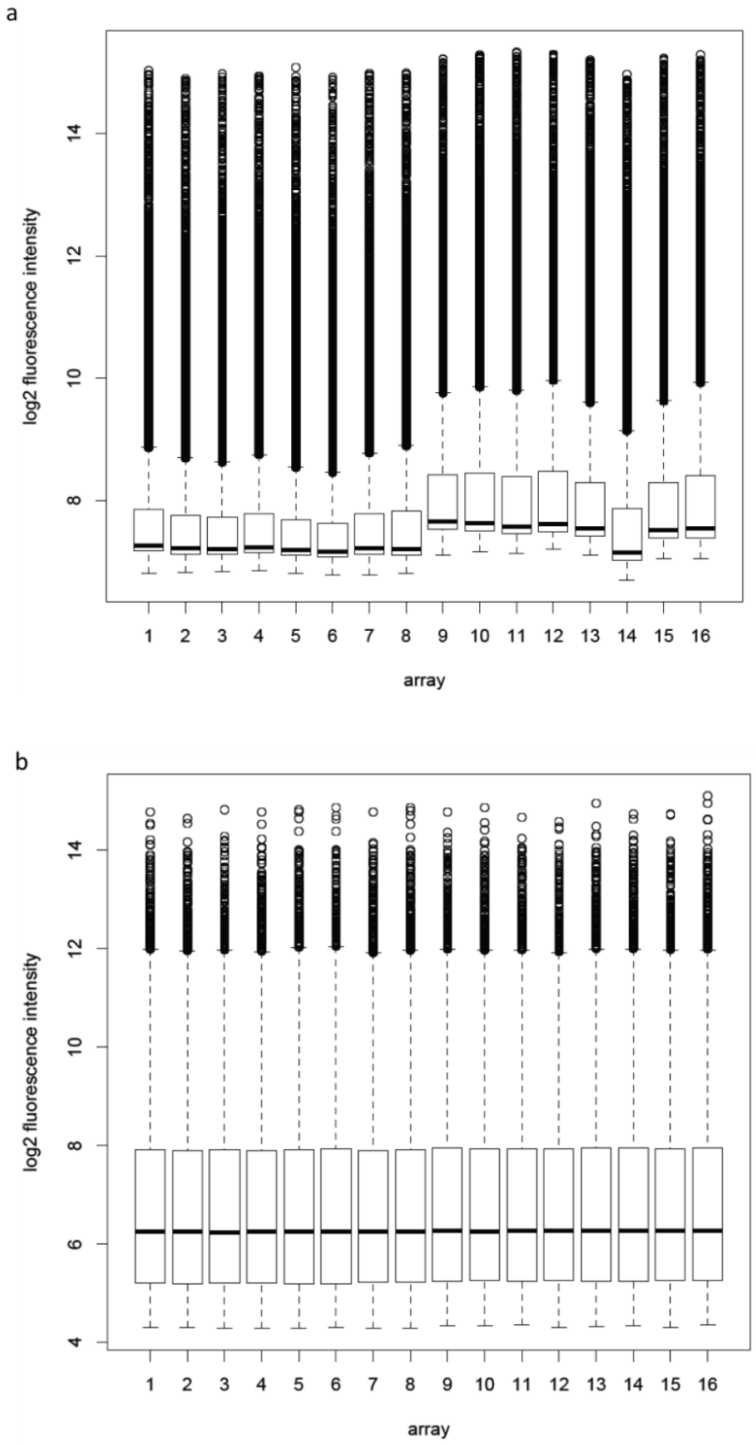

Fig. 6-5 Boxplot showing $\log_2$ fluorescent intensities of arrays.

Data showing the $\log_2$ fluorescent intensities across the arrays before quantile normalisation using limma (a) and after normalisation (b). Bars represent the median values, boxes represent the inter-quartile range, whiskers indicate the range of data and the black circles represent outliers which were removed from the analysis.

6.3.4 DGE in splenocytes taken from naïve and BCG vaccinated mice

Once the arrays had been normalised and genes with low expression levels or unchanging expression levels were removed, the data were compared between groups for DGE using a linear model in limma. In naïve mice, 1285 genes were differentially expressed (at a false discovery rate (FDR) p-value of 0.05) between BCG stimulated and un-stimulated splenocytes (Fig. 6-6 green circle) whereas in BCG vaccinated mice, 2229 genes were differentially expressed (at an FDR p-value of 0.05) (Fig. 6-6 red circle). A total of 1153 genes were specifically differentially expressed in BCG vaccinated animals shown in Table 6-2 and 1150 genes were differentially expressed in both naïve and BCG vaccinated animals in response to BCG stimulation (Table 6-3).

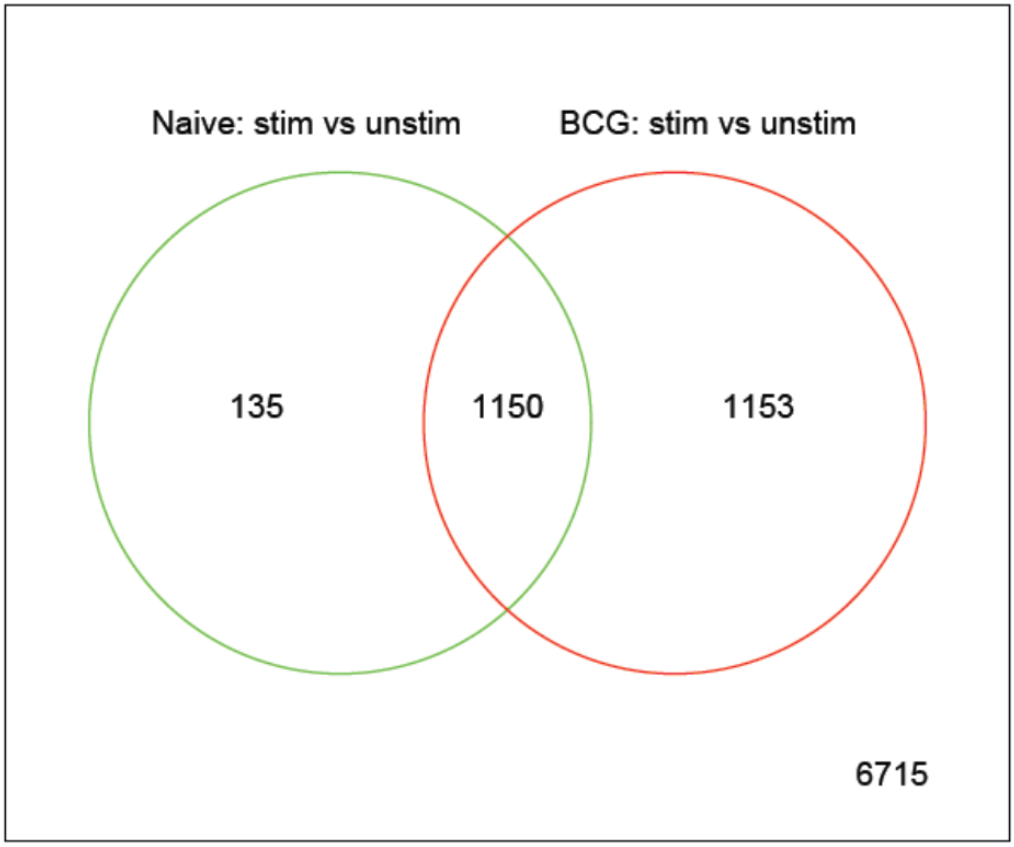

Fig. 6-6 Venn diagram of differentially expressed genes in response to BCG stimulation.
The diagram shows the number of genes that were differentially expressed when comparisons were made between groups. The green circle represents genes that were significantly ($p<0.05$) differentially expressed in splenocytes taken from naïve mice in response to *ex-vivo* stimulation with BCG compared with control splenocytes. The red circle represents genes that were significantly differentially expressed in splenocytes taken from BCG vaccinated mice in response to *ex-vivo* stimulation with BCG compared with control splenocytes. Differential gene expression was determined using an empirical Bayes model using limma.

Gene	Log_2 FC	Adj. p-value
Timp1	1.11800305	4.00E-06
Nos2	1.684894953	7.00E-06
Gpr31c	1.267404095	1.20E-05
Zbtb32	1.43072801	1.30E-05
Ccl9	-0.854684547	2.80E-05
Cryl1	-0.905844483	3.20E-05
Rbpj	0.934595352	3.40E-05
4732429D16Rik	-0.690589339	3.70E-05
Etv6	0.927024179	4.10E-05
Timp1	1.01354004	4.20E-05

Table 6-2 Top 10 differentially expressed genes in splenocytes from BCG vaccinated mice but not naïve mice. The table contains genes that were differentially expressed in splenocytes taken from BCG vaccinated mice but not in naïve mice (unstim vs. stim). The log_2FC column indicates the level of differential expression of a gene. p-values from the resulting comparisons were adjusted for multiple testing using the Benjamini-Hochberg method with a false discovery rate of 0.05. Repeated genes indicate separate probes for a single gene and negative FC values indicate down regulation of a gene.

Gene	Log_2 FC Naïve	Log_2 FC BCG	F value	Adj. p-value
Retnlg	-4.796291675	-4.902506384	587.08	< 1.00E-05
Il1a	4.562543078	4.874453183	532.47	< 1.00E-05
Ifng	5.483340409	7.982658266	493.21	< 1.00E-05
Il1b	4.260231228	4.129665895	448.03	< 1.00E-05
Serpina3f	5.742116957	6.309558787	446.87	< 1.00E-05
Edn1	3.940546938	4.549758991	426.35	< 1.00E-05
Ifng	4.352347956	6.920407478	413.06	< 1.00E-05
Lyz2	-3.168908934	-3.510703958	400.82	< 1.00E-05
Gbp2	3.48271623	3.565803138	370.61	< 1.00E-05
Lyz	-2.564696933	-2.822467898	361.19	< 1.00E-05
Cxcl9	5.151930651	5.851429717	340.13	< 1.00E-05
Lyzs	-3.146398113	-3.40058282	325.94	< 1.00E-05
Tnf	3.87556112	4.236357094	308.82	< 1.00E-05
Ccl3	3.280567232	3.594409956	308.47	< 1.00E-05
Ltf	-3.202540575	-3.595910681	283.24	< 1.00E-05
Csf2	2.702213029	4.318917009	268.89	< 1.00E-05
Cxcl1	5.392271384	4.908723736	258.35	< 1.00E-05
Igf1	-2.813543834	-3.102879586	257.88	< 1.00E-05
AA467197	2.605918564	3.428774827	252.24	< 1.00E-05
Il1rn	3.331620414	3.981897701	247.56	< 1.00E-05

Table 6-3 Top 20 differentially expressed genes in splenocytes from BCG vaccinated and naïve mice.
The table contains genes that were differentially expressed in splenocytes re-stimulated with BCG in both the BCG vaccinated and naive mice (unstim vs. stim). The log_2FC column indicates the level of differential expression of a gene. F=variance of the group means / mean of within group variances using ANOVA. p-values from the resulting comparisons were adjusted for multiple testing using the Benjamini-Hochberg method with a false discovery rate of 0.05. Repeated genes indicate separate probes for a single gene and negative FC values indicate down regulation of a gene.

6.3.5 Pathway analysis of differentially expressed genes

6.3.5.1 BCG vaccine specific differentially expressed genes

All genes (1153) that were specifically differentially expressed in BCG vaccinated mice were used to perform pathways analysis using the open source functional annotation tool from DAVID bioinformatics [203]. Genes that were enriched for specific biological pathways were grouped together and used to produce functional annotation charts from the Kyoto encyclopaedia of genes and genomes (KEGG) database. Charts were ranked according to the number of genes present in each pathway compared to that expected for the total number of genes by p-value. The top chart was for the lysosome pathway displayed in Fig. 6-7 which had a p-value of 0.008 (at a false discovery rate (FDR) p-value of 0.05) with 20 genes present. The second most significant chart was the cytokine-cytokine receptor interaction chart which had a p-value of 0.01 with 23 genes present Fig. 6-8.

6.3.5.2 Differentially expressed genes in naïve and BCG vaccinated mice

The 1150 genes that were differentially expressed in both naïve and BCG vaccinated mice were also used to create annotation charts. The top chart was the Cytokine-cytokine receptor pathway with a p-value of 2.5 E-06 and 40 genes present (Fig. 6-9). The second chart was the Toll like receptor signalling pathway displayed in Fig. 6-10 with a p-value of 6.0E-06 (at a false discovery rate (FDR) p-value of 0.05) with 23 genes present and the

third top chart was again the lysosome pathway (Fig. 6-11) (with a p-value of 0.0001 (at a false discovery rate (FDR) p-value of 0.05) with 23 genes present.

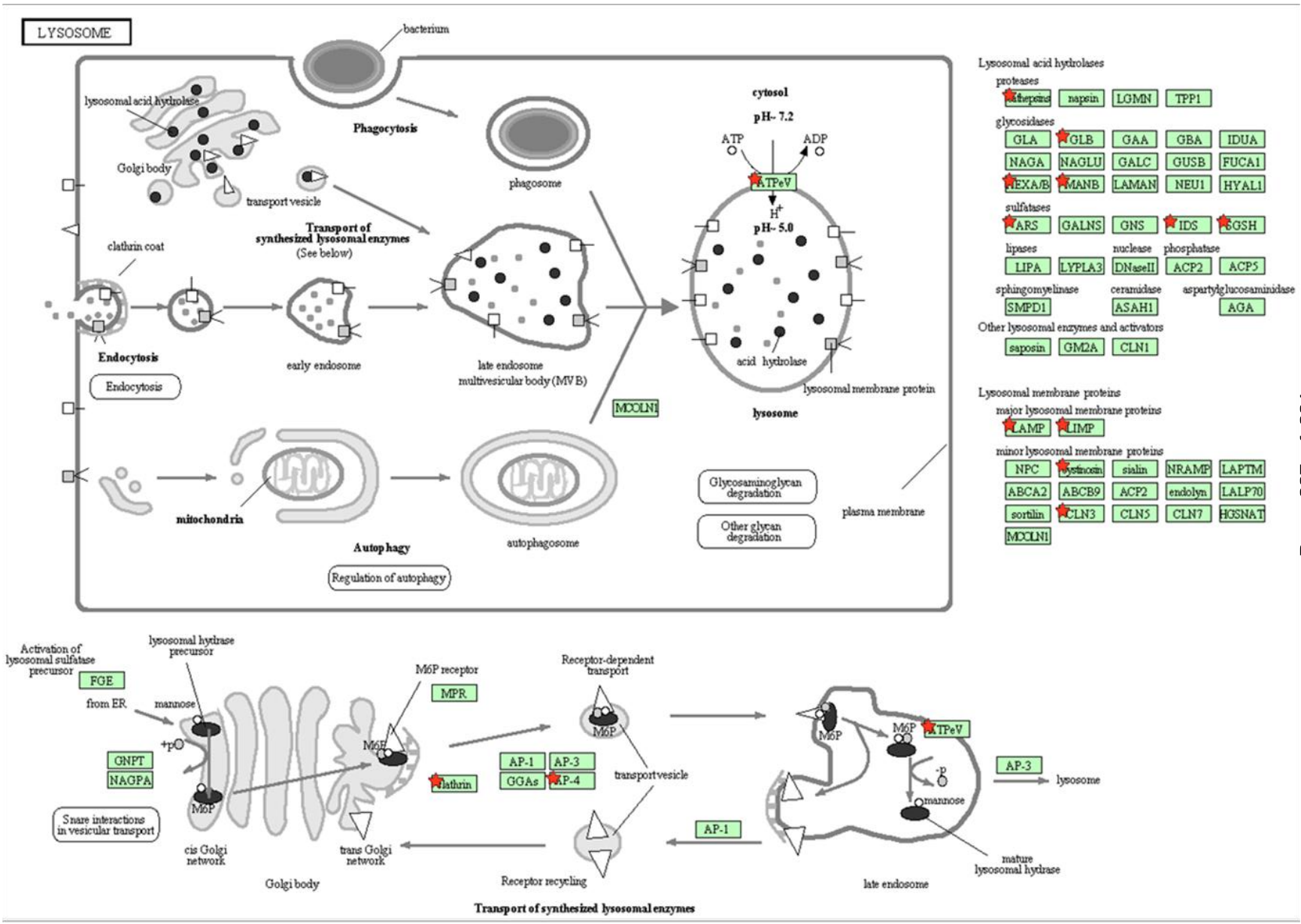
LYSOSOME
bacterium
lysosomal acid hydrolase
Phagocytosis
Golgi body
transport vesicle
phagosome
cytosol
pH~ 7.2
ATP
ADP
ATPeV
H+
pH~ 5.0
Transport of synthesized lysosomal enzymes
(See below)
clathrin coat
Endocytosis
early endosome
late endosome
multivesicular body (MVB)
MCOLN1
acid hydrolase
lysosomal membrane protein
lysosome
Endocytosis
mitochondria
Autophagy
autophagosome
Regulation of autophagy
Glycosaminoglycan degradation
Other glycan degradation
plasma membrane
Lysosomal acid hydrolases
proteases
cathepsins
napsin
LGMN
TPP1
glycosidases
GLA
GLB
GAA
GBA
IDUA
NAGA
NAGLU
GALC
GUSB
FUCA1
HEXA/B
MANB
LAMAN
NEU1
HYAL1
sulfatases
ARS
GALNS
GNS
IDS
SGSH
lipases
nuclease
phosphatase
LIPA
LYPLA3
DNaseII
ACP2
ACP5
sphingomyelinase
ceramidase
aspartylglucosaminidase
SMPD1
ASAH1
AGA
Other lysosomal enzymes and activators
saposin
GM2A
CLN1
Lysosomal membrane proteins
major lysosomal membrane proteins
LAMP
LIMP
minor lysosomal membrane proteins
NPC
cystinosin
sialin
NRAMP
LAPTM
ABCA2
ABCB9
ACP2
endolyn
LALP70
sortilin
CLN3
CLN5
CLN7
HGSNAT
MCOLN1
Activation of lysosomal sulfatase precursor
FGE
lysosomal hydrase precursor
from ER
mannose
+pO
GNPT
NAGPA
M6P
M6P receptor
MPR
M6P
clathrin
AP-1
AP-3
GGAs
AP-4
Receptor-dependent transport
transport vesicle
Snare interactions in vesicular transport
cis Golgi network
trans Golgi network
Golgi body
Receptor recycling
AP-1
M6P
M6P
ATPeV
-p
mannose
AP-3
lysosome
mature lysosomal hydrase
late endosome
Transport of synthesized lysosomal enzymes

Fig. 6-7 BCG vaccine specific differentially expressed genes in the lysosome Pathway.
Differentially expressed genes from BCG vaccinated mice in response to BCG stimulation (stim vs. unstim) are denoted in the KEGG pathway by a red star.

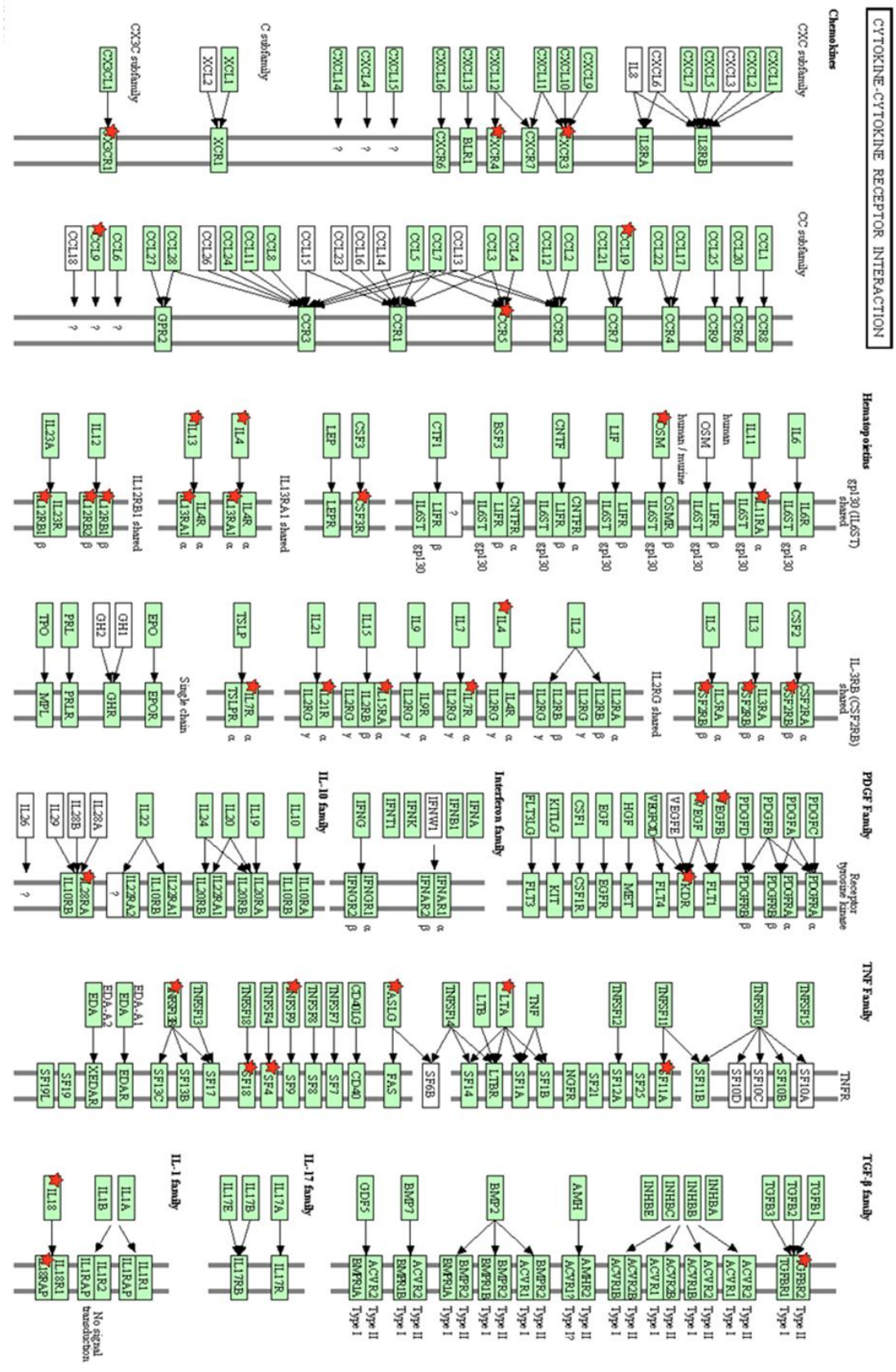
CYTOKINE-CYTOKINE RECEPTOR INTERACTION
Chemokines
CXC subfamily
CC subfamily
C subfamily
CX3C subfamily
Hematopoietins
gp130 (IL6ST) shared
human / murine
human
IL2RG shared
IL12RB1 shared
IL13RA1 shared
Single chain
IL-3RB (CSF2RB) shared
PDGF Family
Receptor tyrosine kinase
Interferon family
IL-10 family
TNF Family
TNFR
TGF-β family
IL-17 family
IL-1 family
No signal transduction

Fig. 6-8 BCG vaccine specific differentially expressed genes in the cytokine-cytokine receptor Pathway.
Differentially expressed genes from BCG vaccinated mice in response to BCG stimulation (stim vs. unstim) are denoted in the KEGG pathway by a red star.

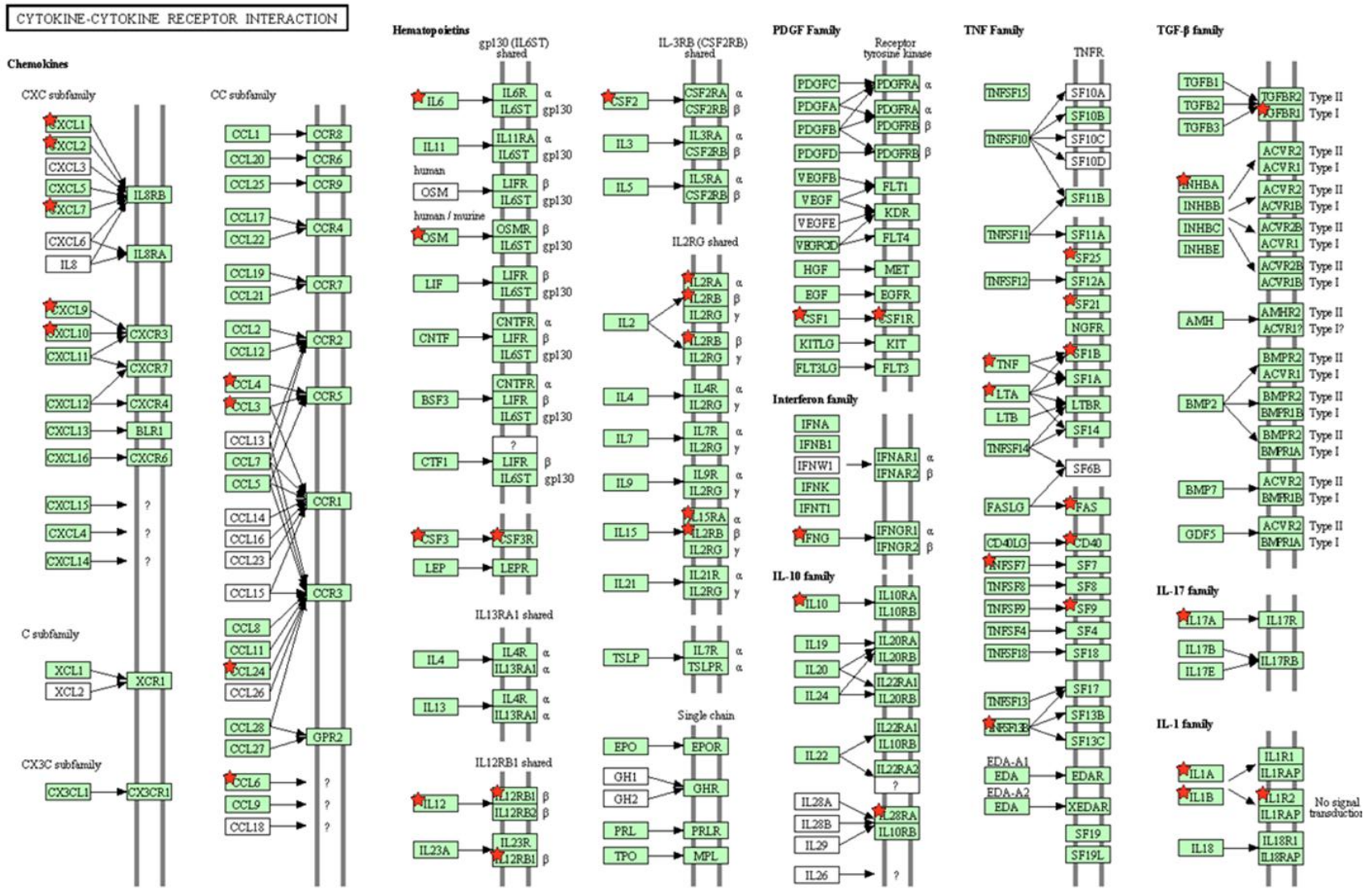
CYTOKINE-CYTOKINE RECEPTOR INTERACTION
Chemokines
CXC subfamily
CC subfamily
CXCL1
CXCL2
CXCL3
CXCL5
CXCL7
CXCL6
IL8
IL8RB
IL8RA
CXCL9
CXCL10
CXCL11
CXCR3
CXCR7
CXCL12
CXCR4
CXCL13
BLR1
CXCL16
CXCR6
CXCL15
CXCL4
CXCL14
C subfamily
XCL1
XCL2
XCR1
CX3C subfamily
CX3CL1
CX3CR1
CCL1
CCL20
CCL25
CCL17
CCL22
CCL19
CCL21
CCL2
CCL12
CCL4
CCL3
CCL13
CCL7
CCL5
CCL14
CCL16
CCL23
CCL15
CCL8
CCL11
CCL24
CCL26
CCL28
CCL27
CCL6
CCL9
CCL18
CCR8
CCR6
CCR9
CCR4
CCR7
CCR2
CCR5
CCR1
CCR3
GPR2
Hematopoietins
gp130 (IL6ST) shared
IL6
IL11
human
OSM
human / murine
OSM
LIF
CNTF
BSF3
CTF1
CSF3
LEP
IL6R
IL11RA
LIFR
OSMR
CNTFR
?
CSF3R
LEPR
α
β
gp130
IL13RA1 shared
IL4
IL13
IL4R
IL13RA1
IL12RB1 shared
IL12
IL23A
IL12RB1
IL12RB2
IL23R
IL-3RB (CSF2RB) shared
CSF2
IL3
IL5
CSF2RA
CSF2RB
IL3RA
IL5RA
IL2RG shared
IL2
IL4
IL7
IL9
IL15
IL21
IL2RA
IL2RB
IL2RG
IL4R
IL7R
IL9R
IL15RA
IL21R
γ
Single chain
TSLP
TSLPR
EPO
GH1
GH2
PRL
TPO
EPOR
GHR
PRLR
MPL
PDGF Family
Receptor tyrosine kinase
PDGFC
PDGFA
PDGFB
PDGFD
VEGFB
VEGF
VEGFE
VEGFC/D
HGF
EGF
CSF1
KITLG
FLT3LG
PDGFRA
PDGFRB
FLT1
KDR
FLT4
MET
EGFR
CSF1R
KIT
FLT3
Interferon family
IFNA
IFNB1
IFNW1
IFNK
IFNT1
IFNG
IFNAR1
IFNAR2
IFNGR1
IFNGR2
IL-10 family
IL10
IL19
IL20
IL24
IL22
IL28A
IL28B
IL29
IL26
IL10RA
IL10RB
IL20RA
IL20RB
IL22RA1
IL22RA2
IL28RA
TNF Family
TNFR
TNFSF15
TNFSF10
TNFSF11
TNFSF12
TNF
LTA
LTB
TNFSF14
FASLG
CD40LG
TNFSF7
TNFSF8
TNFSF9
TNFSF4
TNFSF18
TNFSF13
TNFSF13B
EDA-A1
EDA
EDA-A2
EDA
SF10A
SF10B
SF10C
SF10D
SF11B
SF11A
SF25
SF12A
SF21
NGFR
SF1B
SF1A
LTBR
SF14
SF6B
FAS
CD40
SF7
SF8
SF9
SF4
SF18
SF17
SF13B
SF13C
EDAR
XEDAR
SF19
SF19L
TGF-β family
TGFB1
TGFB2
TGFB3
INHBA
INHBB
INHBC
INHBE
AMH
BMP2
BMP7
GDF5
TGFBR2
TGFBR1
ACVR2
ACVR1
ACVR2B
ACVR1B
AMHR2
ACVR1?
BMPR2
BMPR1B
BMPR1A
Type II
Type I
IL-17 family
IL17A
IL17B
IL17E
IL17R
IL17RB
IL-1 family
IL1A
IL1B
IL18
IL1R1
IL1RAP
IL1R2
IL18R1
IL18RAP
No signal transduction

Fig. 6-9 Genes from naive and BCG vaccinated mice present in cytokine-cytokine receptor pathway.
Differentially expressed genes from BCG vaccinated and naïve mice in response to BCG stimulation (stim vs. unstim) are denoted in the KEGG pathway by a red star.

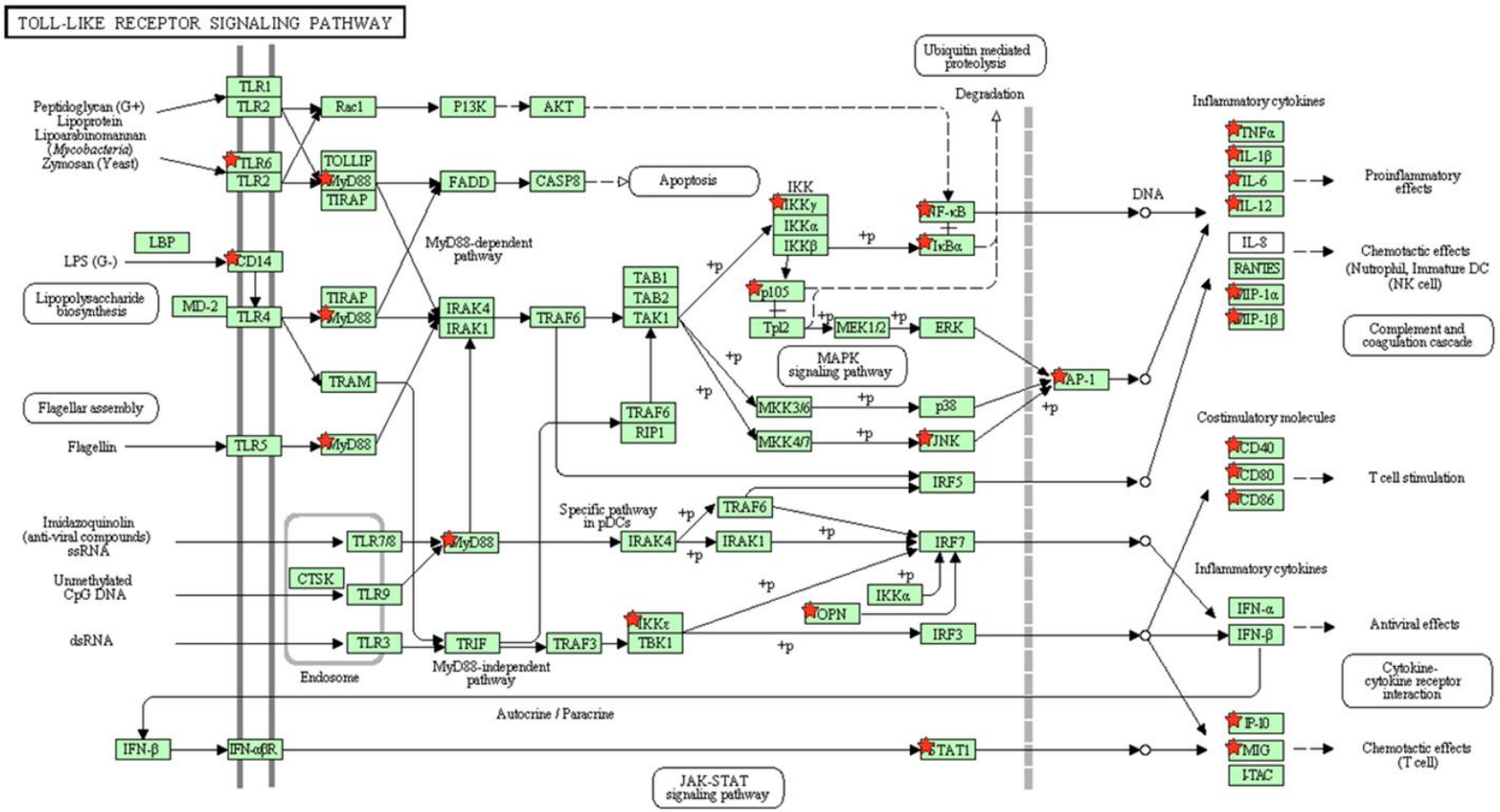
TOLL-LIKE RECEPTOR SIGNALING PATHWAY
Peptidoglycan (G+)
Lipoprotein
Lipoarabinomannan (Mycobacteria)
Zymosan (Yeast)
TLR1
TLR2
TLR6
TLR2
Rac1
P13K
AKT
TOLLIP
MyD88
TIRAP
FADD
CASP8
Apoptosis
Ubiquitin mediated proteolysis
Degradation
IKK
IKKγ
IKKα
IKKβ
NF-κB
IκBα
DNA
Inflammatory cytokines
TNFα
IL-1β
IL-6
IL-12
Proinflammatory effects
IL-8
RANTES
MIP-1α
MIP-1β
Chemotactic effects (Nutrophil, Immature DC (NK cell)
Complement and coagulation cascade
LBP
LPS (G-)
CD14
Lipopolysaccharide biosynthesis
MD-2
TLR4
TIRAP
MyD88
MyD88-dependent pathway
IRAK4
IRAK1
TRAF6
TAB1
TAB2
TAK1
p105
Tpl2
MEK1/2
ERK
MAPK signaling pathway
TRAM
AP-1
Flagellar assembly
Flagellin
TLR5
MyD88
TRAF6
RIP1
MKK3/6
p38
MKK4/7
JNK
Costimulatory molecules
CD40
CD80
CD86
T cell stimulation
IRF5
Imidazoquinolin (anti-viral compounds) ssRNA
Unmethylated CpG DNA
dsRNA
TLR7/8
CTSK
TLR9
TLR3
MyD88
TRIF
Endosome
MyD88-independent pathway
Specific pathway in pDCs
TRAF6
IRAK4
IRAK1
IRF7
IKKα
OPN
IKKε
TBK1
TRAF3
IRF3
Inflammatory cytokines
IFN-α
IFN-β
Antiviral effects
Cytokine-cytokine receptor interaction
Autocrine / Paracrine
IFN-β
IFN-αβR
STAT1
IP-10
MIG
ITAC
Chemotactic effects (T cell)
JAK-STAT signaling pathway
+p

Fig. 6-10 Genes from naive and BCG vaccinated mice present in the Toll like receptor pathway.
Differentially expressed genes from BCG vaccinated and naïve mice in response to BCG stimulation (stim vs. unstim) are denoted in the KEGG pathway by a red star.

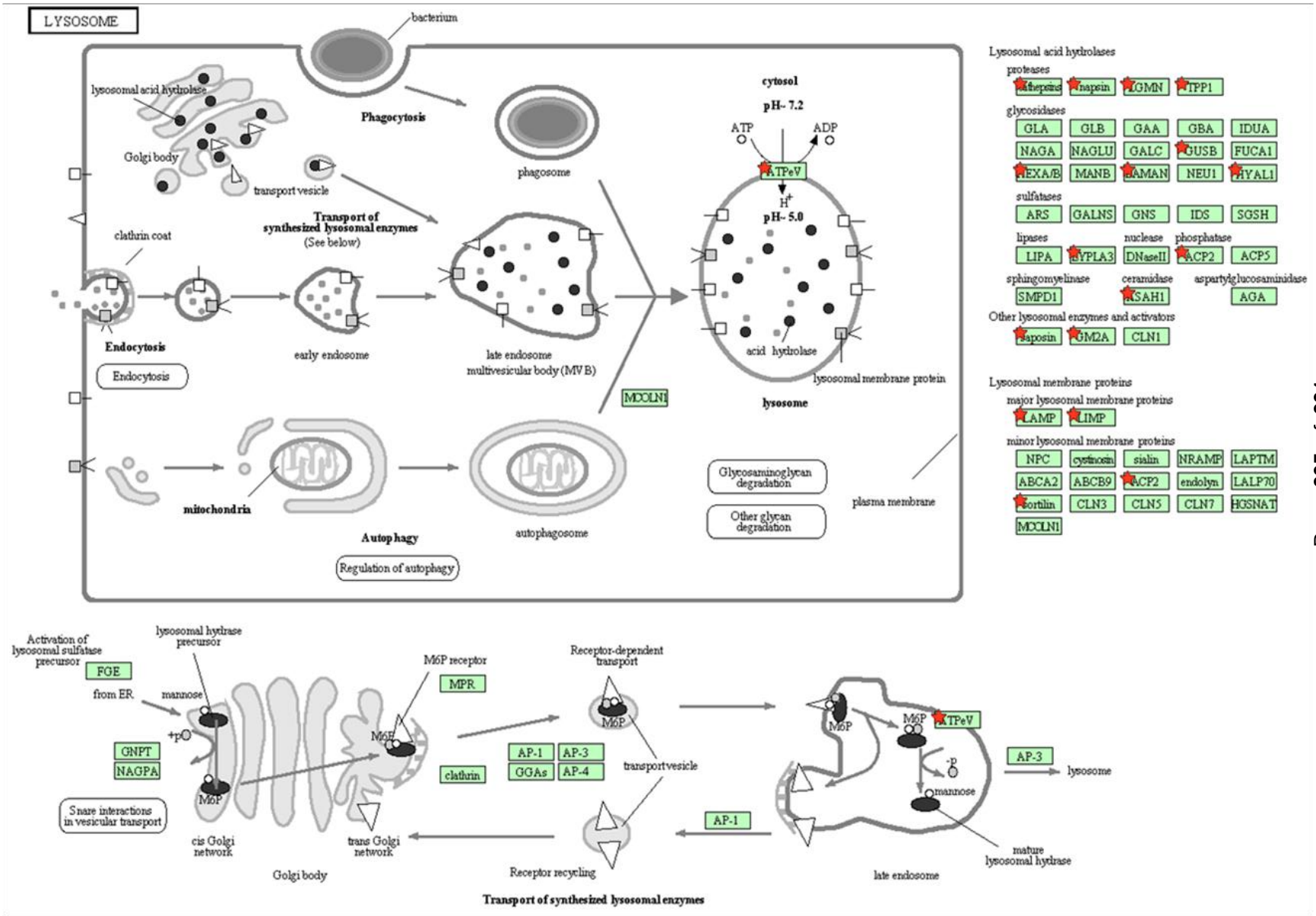
LYSOSOME
bacterium
lysosomal acid hydrolase
Golgi body
transport vesicle
Phagocytosis
phagosome
Transport of synthesized lysosomal enzymes
(See below)
clathrin coat
Endocytosis
Endocytosis
early endosome
late endosome
multivesicular body (MVB)
MCOLN1
cytosol
pH~ 7.2
ATP
ADP
ATPeV
H+
pH~ 5.0
acid hydrolase
lysosomal membrane protein
lysosome
mitochondria
Autophagy
Regulation of autophagy
autophagosome
Glycosaminoglycan degradation
Other glycan degradation
plasma membrane
Lysosomal acid hydrolases
proteases
Cathepsins
Napsin
AGMN
TPP1
glycosidases
GLA
GLB
GAA
GBA
IDUA
NAGA
NAGLU
GALC
GUSB
FUCA1
HEXA/B
MANB
AMAN
NEU1
HYAL1
sulfatases
ARS
GALNS
GNS
IDS
SGSH
lipases
nuclease
phosphatase
LIPA
PLA3
DNaseII
ACP2
ACP5
sphingomyelinase
ceramidase
aspartylglucosaminidase
SMPD1
ASAH1
AGA
Other lysosomal enzymes and activators
Saposin
GM2A
CLN1
Lysosomal membrane proteins
major lysosomal membrane proteins
LAMP
LIMP
minor lysosomal membrane proteins
NPC
cystinosin
sialin
NRAMP
LAPTM
ABCA2
ABCB9
ACP2
endolyn
LALP70
Sortilin
CLN3
CLN5
CLN7
HGSNAT
MCOLN1
Activation of lysosomal sulfatase precursor
FGE
lysosomal hydrase precursor
from ER
mannose
+pO
GNPT
NAGPA
M6P
M6P receptor
MPR
clathrin
AP-1
AP-3
GGAs
AP-4
Receptor-dependent transport
transport vesicle
Snare interactions in vesicular transport
cis Golgi network
trans Golgi network
Golgi body
Receptor recycling
AP-1
AP-3
lysosome
-P
mannose
mature lysosomal hydrase
late endosome
Transport of synthesized lysosomal enzymes

Fig. 6-11 Genes from naive and BCG vaccinated mice present in the lysosome pathway.
Differentially expressed genes from BCG vaccinated and naïve mice in response to BCG stimulation (stim vs. unstim) are denoted in the KEGG pathway by a red star.

6.3.6 Correlations between DGE and MGIT assay in mice

As the mice used to perform the microarray experiments were also used to perform the MGIT assays described in section 5.3.2, it was possible to perform correlations between gene expression levels and mycobacterial growth inhibition for these mice. In order to produce a gene list for the correlations, direct comparison between the two BCG stimulated conditions (stimulated naïve mice versus stimulated vaccinated mice) was performed. This resulted in a much smaller list of 56 differentially expressed genes, as sensitivity to detect differential expression was reduced in this cross-group analysis, the surviving genes were those with the greatest differential expression between BCG vaccinated and naïve mice, and are provided in the appendix. These genes were used to perform correlations between BCG stimulated gene expression values in naïve and BCG vaccinated mouse splenocytes, and $\log_{10}$ GR values from the MGIT assay.

The genes found to significantly correlate ($p<0.05$) were IFN-γ, IFI205, GPr83 and RAD541 which are displayed in Table 6-4. CCR5 and CCl24 were close to being significantly correlated (p-values of 0.086 and 0.058 respectively). Higher expression levels of these

genes correlated with lower GR values from the MGIT assay. When un-stimulated gene expression values for naïve and BCG vaccinated mice were correlated against the GR values, no significant ($p<0.05$) correlations were found. All of the genes found to correlate with the GR values also all correlated with IFN-γ, suggestive of an IFN-γ mediated pathway.

			GR	Ifng	Ifng	Ccl24	Ccr5	Ccr5	Ifi205	Gpr83	Rad54l
Spearman's rho	GR	Correlation Coefficient	1.000	-.690	-.738*	-.690	-.643	-.643	-.714*	-.714*	-.738*
		Sig. (2-tailed)	.	.058	.037	.058	.086	.086	.047	.047	.037
		N	8	8	8	8	8	8	8	8	8
	Ifng	Correlation Coefficient	-.690	1.000	.976**	.929**	.786*	.786*	.976**	.881**	.786*
		Sig. (2-tailed)	.058	.	.000	.001	.021	.021	.000	.004	.021
		N	8	8	8	8	8	8	8	8	8
	Ifng	Correlation Coefficient	-.738*	.976**	1.000	.905**	.857**	.857**	.952**	.833*	.810*
		Sig. (2-tailed)	.037	.000	.	.002	.007	.007	.000	.010	.015
		N	8	8	8	8	8	8	8	8	8
	Ccl24	Correlation Coefficient	-.690	.929**	.905**	1.000	.690	.690	.976**	.881**	.762*
		Sig. (2-tailed)	.058	.001	.002	.	.058	.058	.000	.004	.028
		N	8	8	8	8	8	8	8	8	8
	Ccr5	Correlation Coefficient	-.643	.786*	.857**	.690	1.000	1.000**	.762*	.548	.905**
		Sig. (2-tailed)	.086	.021	.007	.058	.	.	.028	.160	.002
		N	8	8	8	8	8	8	8	8	8
	Ccr5	Correlation Coefficient	-.643	.786*	.857**	.690	1.000**	1.000	.762*	.548	.905**
		Sig. (2-tailed)	.086	.021	.007	.058	.	.	.028	.160	.002
		N	8	8	8	8	8	8	8	8	8
	Ifi205	Correlation Coefficient	-.714*	.976**	.952**	.976**	.762*	.762*	1.000	.857**	.810*
		Sig. (2-tailed)	.047	.000	.000	.000	.028	.028	.	.007	.015
		N	8	8	8	8	8	8	8	8	8
	Gpr83	Correlation Coefficient	-.714*	.881**	.833*	.881**	.548	.548	.857**	1.000	.643
		Sig. (2-tailed)	.047	.004	.010	.004	.160	.160	.007	.	.086
		N	8	8	8	8	8	8	8	8	8
	Rad54l	Correlation Coefficient	-.738*	.786*	.810*	.762*	.905**	.905**	.810*	.643	1.000
		Sig. (2-tailed)	.037	.021	.015	.028	.002	.002	.015	.086	.
		N	8	8	8	8	8	8	8	8	8

*. Correlation is significant at the 0.05 level (2-tailed).

**. Correlation is significant at the 0.01 level (2-tailed).

Table 6-4 correlations between differential gene expression and GR values from MGIT assay.
Data presented in this table are from BCG stimulated splenocytes taken from naïve (n=4) and BCG vaccinated (n=4) mice together. The $\log_{10}$ GR values were obtained for each mouse as described in section 5.3.2. Only genes that were approaching significance or below 0.05 are displayed. P-values were determined by spearman's rho. Repeated genes indicate separate probes for a single gene.

6.4 Discussion

The high throughput nature of microarrays means that they can easily be affected by variation in the quality of starting RNA, amplified RNA, hybridisation conditions, chips, and washing steps. All of the quality measures that were carried out indicated that the RNA used for the arrays was of good quality, both before and after amplification. The normalisation procedure was successful in removing the chip effect, so comparisons could be made between samples across the chips with confidence. The purpose of these experiments was to identify genes/biological pathways that were differentially expressed in response to BCG stimulation between naïve and BCG vaccinated mice. These genes may indicate which mechanisms are involved in mycobacterial growth inhibition *in vitro* and also during *in vivo* protection in mice if the same mechanisms are involved in both of these processes.

Out of the 19,100 different genes that were present on the arrays 2438 were differentially expressed in the naïve and BCG vaccinated mice. Of these genes, those that were differentially expressed in both naïve and BCG vaccinated mice (stim vs. unstim), and those specific to BCG vaccinated mice (stim vs. unstim) were of interest, as these genes represent common innate responses and BCG vaccine induced responses respectively. A number of genes known to be important in immunity against *M. tb,* were differentially

expressed in *ex-vivo* splenocytes from both naïve and BCG vaccinated mice, including IFN-γ, TNF-α, and IL-17 [98, 204-206]. These genes were all up-regulated in response to *ex-vivo* BCG stimulation in all animals, but more so in BCG vaccinated mice. This great deal of overlap in the response to BCG stimulation in splenocytes taken from naïve and BCG vaccinated mice indicates that in the mouse model, innate immune mechanisms are important for the control of mycobacterial growth. This finding is supported by the fact that different strains of naïve mice have inherently different levels of susceptibility to *M. tb* challenge [207] and the C57bl/6 mice used throughout this study have been shown have high levels of resistance against *M. tb* challenge. The innate responses in this present study support the suggestion made in chapter 5 that innate immune responses may have contributed to the failure of the total PBMC infection MGIA to discriminate between naïve and BCG vaccinated samples due to masking of adaptive responses in vaccinated animals.

A large number of genes were specifically differentially expressed in BCG vaccinated mice, indicating that BCG vaccination broadens the immune response to *in vitro* re-stimulation with BCG. These genes included NOS2 and TIMP1. The fold change levels in these genes were not as pronounced as those seen to be differentially expressed in naïve and BCG vaccinated mice, possibly due to more potent effects or lower levels of sensitivity to activation, as is the case for NOS2 which is induced by IFN-γ that itself had a 32 fold

increase in naïve mice without induction of NOS2 transcription. It is possible that further genes involved in *M. tb* immunity have not been detected in this analysis due to low abundance, insufficient sensitivity of the microarray or because of the low number of samples (n=4 naïve and n=4 BCG vaccinated mice). The fact that the mice used for these experiments were an inbred strain (C57bl/6) means that there was very little variability between mice in each group, so many differentially expressed genes were detected, but perhaps not as many as would have been found had larger sample sizes been used. Some of the interesting genes and pathways that were significantly differentially expressed are discussed below.

IFN-γ was up-regulated in splenocytes from both naïve and BCG vaccinated animals, but more so by approximately 6 fold in BCG vaccinated mice compared with naïve mice, demonstrating that BCG vaccination induces memory T cells that can produce greater quantities of IFN-γ than naïve T cells. Increased expression of IFN-γ in BCG vaccinated mice was expected, so this finding was confirmation that the microarray study would enable detection of BCG vaccine mediated DGE between vaccinated and naïve mice. It is well known that BCG vaccination in mice results in increased IFN-γ secretion in response to mycobacterial antigens [208, 209] as measured by Elispot and flow cytometry. IFN-γ was also identified in two separate microarray studies as being differentially expressed in the

lungs between naive and BCG vaccinated mice after *M. tb* challenge [152, 192]. One limitation of microarrays is that they do not indicate which cells within the sample the DGE is taking place in. There are a number of adaptive cells that express IFN-γ including $CD4^+$, $CD8^+$, $\gamma\delta^+$ T cells and NK^+ T cells, so any, or all of these cells may have contributed to the increased abundance of this gene in this present study and those that have been published. Flow cytometry is routinely used at the Jenner Institute to measure IFN-γ in the splenocytes of BCG vaccinated mice and typically is found to be expressed largely in $CD4^+$ T cells with a low level of expression in $CD8^+$ T cells although as discussed in chapter 4 it was also found to be expressed by $\gamma\delta^+$ T cells in PBMC from naïve NHP.

NOS2 is produced by murine granulocytes and macrophages in response to IFN-γ [56]. This gene was only up-regulated in splenocytes taken from BCG vaccinated mice, which fits with the enhanced levels of IFN-γ expression seen in BCG vaccinated animals. RNS production in mice has clearly been shown to be involved in protection against *M. tb* challenge *in vivo* [56, 210] and has been identified in a separate microarray study as being up-regulated upon infection of mice with *M. tb* [211]. This could indicate that higher levels of IFN-γ which are only present in BCG vaccinated mice are required to initiate NOS2 expression and induce mycobacterial growth inhibition by damaging bacterial DNA, proteins and lipids [212]. Together, this damage impairs mycobacterial metabolism and could

ultimately inhibit replication. This could potentially be a mechanism involved in mycobacterial growth inhibition seen in the MGIT assay. Another gene that was only up-regulated in BCG vaccinated mice was TIMP1 (Tissue inhibitor of metalloproteinase 1). The protein encoded by this gene inhibits the action of MMP-9 which has a role in attracting lymphocytes to the site of *M. tb* infection and development of granulomas but is also implicated in tissue destruction, cavitation and lung pathology of TB [213]. Macrophages that phagocytose *M. tb* or even inert latex beads up-regulate their levels of TIMP1, but this gene has also been shown to be induced by IL-1 action through NF-κβ signalling [214]. The specific up-regulation of this gene in BCG vaccinated mice could indicate that TIMP1 has a role in limiting tissue destruction during *M. tb* infection. Although it is unlikely that TIMP1 will be a major contributing factor to growth inhibition in the MGIT assay as there are no extracellular matrices for MMP-9 to destroy and thus TIMP1 cannot mediate its effects.

The genes IL-17a and IL-17f were both up-regulated in BCG vaccinated mice compared with naïve mice. These cytokines are pro-inflammatory and have been linked to DTH responses. IL-17 has also been linked with memory mediated protection against *M. tb* in mice [215]. The relationship between IL-17 and BCG infection is perhaps not a simple one, with studies suggesting that IFN-γ down regulates IL-17 in BCG infected DCs [216].

This is in contrast to my findings that both IFN-γ and IL-17 were up-regulated in splenocytes from BCG vaccinated and naïve mice in response to BCG stimulation, but more so in BCG vaccinated animals. The reasons for this disparity could be due to the fact that Cruz *et al,* used DC from IFN-γ knock-out mice, which may have aberrated responses to BCG, and the cells utilised in the present study were splenocytes not DCs, so other cellular interactions may influence IL-17 expression. IL-17a and IL-17f along with IFN-γ, have also been identified as being differentially expressed between naive and BCG vaccinated mice in *M. tb* challenged animals [152], and unpublished flow cytometry data within our group also show increased levels of IL-17 in Balb/c mice that have been BCG vaccinated K. Griffiths *et al.* IL-17 responses have also been associated with protection in cattle following viral vectored vaccination against *M. tb* [217], so there is a growing body of evidence that enhanced T_H17 responses are important for protection and the array data in this present study concur with this theory.

CSF2, also known as granulocyte-macrophage colony stimulating factor, controls the production, differentiation and function of granulocytes and macrophages. Macrophages are believed to be the final effector cell responsible for killing or restricting the growth of mycobacteria under the influence of lymphokines including IFN-γ [218, 219]. CSF2 has been shown to activate macrophages to restrict the growth of *M. tb* in human macrophages

[220], and be important for control of *M. tb* growth in mice [221]. As was the case with IFN-γ and IL-17, this gene was up-regulated in naïve and vaccinated mouse splenocytes in response to BCG stimulation, but more so in BCG vaccinated animals and could therefore be involved in the enhanced mycobacterial growth inhibition activity of splenocytes from BCG vaccinated mice.

The Hamp gene encodes for the hormone hepcidin which is produced in the liver to control iron homeostasis, but also plays a key role in iron recycling within the macrophage. Hepcidin mediates the destruction of the iron transporter protein ferroportin, resulting in an increase in iron levels within macrophages. My findings show that BCG stimulation increases iron levels in macrophages (favoured by mycobacteria). Iron is essential for mycobacterial growth and so it was not surprising to see increased expression of hepcidin in BCG infected splenocytes, but it was surprising to see that it was specifically differentially expressed in the BCG vaccinated mice, as these mice can better control the growth of mycobacteria. However, hepcidin has been shown to be antimicrobial [222, 223], and up-regulated in macrophages from humans and mice in response to mycobacteria and IFN-γ [224, 225]. So perhaps the up-regulation of hepcidin under the influence of IFN-γ has an anti-mycobacterial effect and contributes to BCG mediated protection against *M. tb* challenge

in mice, which can explain why this gene was only differentially expressed in the BCG vaccinated animals.

Pathways analysis is used to analyse large numbers of genes for their presence within biological pathways. In this way, genes are no longer analysed individually, but are instead looked at as being functionally grouped. Differentially expressed genes specific to BCG vaccinated but also in both naïve and BCG vaccinated mice were found to be significantly enriched for the lysosome and cytokine-cytokine receptor pathways. The lysosome pathway is involved in the development of phagolysosomes which destroy phagocytosed mycobacteria contained within them. Lysosomes also combine with autophagosomes which may contain mycobacteria and thus mediate their destruction [76]. This pathway was the most significant pathway identified in BCG vaccinated mice, but surprisingly, the majority of the genes were actually down-regulated in response to BCG stimulation. To maximise the likelihood of detecting differences in the gene expression of splenocytes of BCG vaccinated compared to naïve mice, splenocytes were stimulated with a high dose of BCG (MOI 1:1). One explanation for this apparent down regulation of the lysosome pathways which is a very significant anti-mycobacterial mechanism, is that the BCG used for the stimulation was actively inhibiting this pathway, as BCG, like *M. tb*, expresses ManLAM [226] which has been shown to disrupt phagolysosome maturation [53]. The dose of BCG used to infect

splenocytes during the MGIT assay was very low, between 2800-9000 CFU/1x10^6 splenocytes, so if the down-regulation of the lysosome pathway was linked to the high dose of BCG used for stimulation then it may not be as pronounced during the MGIT assay, or it may be absent. Another limiting factor of this study is that only one time-point after stimulation was assessed (12 hours) and it may be that down-regulation of the lysosome pathway would eventually be overcome by activation with IFN-γ. Microarray studies of DGE in the lungs of mice challenged with *M. tb* did not identify the lysosome pathway as being down regulated [152, 192], although this was a different organ and different time points were assessed than in this present study. Further study of DGE during the time course of the MGIT assay with varying doses of BCG would further help in identifying the exact mechanisms of mycobacterial growth inhibition *in vitro*.

The cytokine-cytokine receptor pathways contain a number of cytokine families divided into individual pathways; it is large and all-encompassing for inflammatory responses. As with the lysosome pathway, BCG vaccinated animals had more differentially expressed genes present in these pathways than naïve animals, which indicates an enhanced immune response against BCG stimulation in BCG vaccinated animals. In particular, IFN-γ, IL-12 receptors, IL-18, CCR5 which are all involved in T_H1 immune responses were all up-regulated to a greater extent in BCG vaccinated animals. Cytokines of the T_H1 axis were

also identified as being differentially expressed in vaccinated mice that were challenged with *M. tb* compared with naïve challenged mice by microarray [152, 192, 227]. There is a growing amount of microarray data that support the theory that BCG vaccination works by producing enhanced T_H1 responses primarily mediated by increased production of IFN-γ. However, IFN-γ alone does not correlate with protection and it is clear from microarray and other intricate studies that the effects of IFN-γ are very broad and far reaching resulting in activation of the lysosome pathway [228], NOS2 production [56], induction of autophagy [76], production of hepcidin [225] and many other processes that have anti-mycobacterial actions. So it is perhaps to be expected that IFN-γ itself does not correlate with protection as it is not directly anti-mycobacterial, it must act upon a multitude of complex processes in concert to elicit its effects. The present study was designed to address the question of what differences there were between naïve and BCG vaccinated mice in terms of their responses to *ex vivo* stimulation with BCG, as this is the stimulation present in the MGIT assay. There are therefore limitations to how relevant these responses are in terms of *in vivo* challenge or *in vitro* stimulation with *M. tb.* If *M. tb* were to be used during the MGIT assay then separate study of the splenocyte responses of naïve and BCG vaccinated mice to *M. tb* stimulation would be warranted. It would be very interesting to see if the DGE response to *M. tb* challenge *in vivo* was the same as that seen during *in vitro* stimulation as this would further validate the MGIT assay as measuring protective responses.

The TLR pathway was the most significant pathway identified in BCG stimulated splenocytes from both naïve and BCG vaccinated mice. The activation of PRR by bacterial products leads to NF-κB activation and the secretion of IFN-γ which would enhance the ability of innate immune cells to clear a mycobacterial infection. In naïve and BCG vaccinated mice there was evidence of activation of TLR-6 and MyD88 which is involved in the signal cascade to activate NF-κB and thus initiate an immune response. TLR-6 interacts with TLR-2 which has been shown to respond to LAM in mycobacterial cell walls [229]. Unfortunately, the expression of TLR-2 could not be assessed as this gene was not present on the microarray. The great deal of overlap in this pathway between naïve and BCG vaccinated animals was expected as TLR signalling is part of the immediate innate immune response to pathogens.

One of the primary objectives of performing the microarray study was to try to identify which processes were responsible for mycobacterial growth inhibition seen in the MGIT assay. Correlations between DGE and growth inhibition values could therefore help to identify genes that were most important for growth inhibition. Of the 56 genes found to be differentially expressed between BCG vaccinated and naïve Mice (BCG stim vs. naive stim), only 4 gene probes significantly correlated with the MGIT data (IFN-γ, IFI205, GPr83 and

RAD541) with CCR5 and CCL24 approaching significance. All of these genes also strongly correlated with IFN-γ which indicated that IFN-γ mediated responses were strongly associated with growth inhibition, a finding that has been found previously in mouse *M. tb* challenge microarray studies [192, 227]. The small number of animals used for this present study limits the power to detect correlates of growth inhibition and it is possible that the use of greater numbers of animals would have resulted in greater power to identify further correlates. If genes involved in the downstream anti-mycobacterial processes that are under the control of IFN-γ (e.g.NOS2) were shown to correlate with growth inhibition, then this could help to identify which mechanisms are responsible for growth inhibition *in vitro*.

Although the sample size was small, genes/pathways associated with the control of mycobacterial growth were identified. In both naïve and BCG vaccinated mice IFN-γ appeared to be highly important for limiting mycobacterial growth. IFN-γ is important for initiating a number of anti-mycobacterial processes. BCG vaccination, which is known to be protective in the mouse model, clearly enhances the secretion of IFN-γ from memory T cells and this augments the activation of innate immune cells and enhances clearance of mycobacteria. $CD4^+$ T cells are known to be important for immunity against *M. tb* [135-140], but here is also growing evidence that $\gamma\delta^+$ T cells are involved in host defence against *M. tb* in mice, cattle and in humans [69, 73, 185] as they are thought to be

involved in the early host response to *M. tb*. $CD4^+$ and $\gamma\delta^+$ T cells are both capable of producing the cytokines IFN-γ and IL-17, which have been implicated in protection against TB [98, 150]. The very nature of MGIAs is to assess functional responses of immune mechanisms as a whole, which makes identification of the exact underlying mechanisms responsible for growth inhibition difficult. However the present microarray study indicates that T_H1 and T_H17 mediated responses are responsible for the differences seen in mycobacterial growth inhibition between naïve and BCG vaccinated mice. The identification of NOS2 induction in BCG vaccinated mice alone, suggests that IFN-γ induced production of RNS contributes towards mycobacterial growth inhibition in BCG vaccine mice. Further work needs to be conducted in order to identify whether $CD4^+$, $\gamma\delta^+$ or both T cell types are responsible for IFN-γ mediated mycobacterial growth inhibition in the MGIT assay. This study was also limited to DGE in mice, whereas the MGIT assay has been shown to detect BCG vaccine induced mycobacterial growth inhibition in humans [155] and also in NHP (chapter 5). It may not be the case that the mechanisms involved in mycobacterial growth in mice are the same as those measured by the MGIT assay in humans and NHP. In particular, there is debate as to the importance and induction of NOS2 in human phagocytes [57]. Further study of the mechanisms behind mycobacterial growth between different species is therefore required.

6.5 Chapter conclusions

- A high dose of BCG was required to produce differential gene expression of IFN-γ in splenocytes taken from naïve and BCG vaccinated mice
- Approximately half of the genes that were differentially expressed between control and BCG stimulated splenocytes were specific to BCG vaccinated mice
- The Lysosome and cytokine-cytokine receptor pathway were the most significant pathways identified in BCG vaccinated mice. These pathways were also identified using differentially expressed genes common to naïve and BCG vaccinated mice. TLR signalling was only identified in naïve plus BCG vaccinated mice.
- Correlations of DGE and MGIT assay found IFN-γ to correlate directly with growth inhibition
- The mechanism behind mycobacterial growth inhibition seen in the MGIT assay appears to be T_H1 dependent, with increased magnitude of IFN-γ in BCG vaccinated animals playing a vital role in growth inhibition. Although the cells responsible for the increased expression of this cytokine were not identified in this study, previous studies in our lab have identified $CD4^+$ T cells as the primary source of IFN-γ following vaccination with BCG. It is possible that IL-17 and IFN-γ are acting synergistically and induction of NOS2 is important for inhibiting mycobacterial growth.

Chapter 7

Concluding remarks and future directions

7. Concluding remarks and future directions

7.1 Summary

An improved vaccine against *M. tb* is urgently required to prevent almost 2 million deaths from TB per annum. One of the most challenging aspects of developing an improved TB vaccine, is efficacy testing. At present, the only reliable measure of efficacy is large scale field trials in TB endemic areas; these trials take years to carry out in thousands of subjects; and cost millions of pounds to perform. Surrogates of protection expedite the process of assessing vaccines for immunogenicity in animal models and early clinical trials.

So far, no single parameter has been found to robustly correlate with protection against TB in various preclinical or clinical models [129, 130]. It is currently thought that systems measuring a whole host of cellular mechanisms such as functional assays might provide the elusive surrogate of protection. One such functional assay is the MGIA which can be thought of as an *in vitro* challenge model for assessing vaccine efficacy. All MGIAs have one principle in common, which is, samples taken after vaccination against TB should be better able to inhibit growth of mycobacteria in cell culture, as compared to samples from unvaccinated controls.

Throughout this project a number of different MGIAs were assessed, using different cell types from animal models and humans. Problems were encountered with both inter and intra assay variability during the first two MGIAs that were assessed (cultured and novel MGIA), which meant these assays were unsuitable for pre-clinical vaccine efficacy assessment. The final MGIA (MGIT assay) that was assessed had much better reproducibility, and far less variability making it suitable for vaccine efficacy testing. The MGIT assay was able to discriminate between splenocytes and PBMC taken from naïve and BCG vaccinated mice and NHP respectively. A microarray experiment was then performed to elucidate the mechanisms behind BCG vaccine induced mycobacterial growth inhibition seen in the mouse MGIT assay.

7.2 Main findings

Samples from volunteers who had historically received BCG vaccination and were given a BCG re-vaccination were used to assess the cultured MGIA. PBMC taken 4 weeks after BCG re-vaccination had significantly higher levels of mycobacterial growth inhibition compared with matched samples taken prior to BCG re-vaccination. Variation between volunteers was considerable with many negative values, which indicated that antigen stimulated PBMC were less capable of inhibiting mycobacterial growth than media rested

PBMC. From these experiments it appeared that $\gamma\delta^+$ T cells were the cell type most likely to demonstrate functional responses and survive the culture period of this MGIA.

In comparison to the cultured MGIA the total PBMC infection MGIA was relatively simple to perform and did not bias cellular responses by culturing with antigens, however, variability was a continuing problem throughout the development and optimisation of this assay. Ultimately, even with the optimisation experiments that were performed for this assay, no significant differences in mycobacterial growth inhibition were seen between naïve and BCG vaccinated animals, (mouse splenocytes or NHP PBMC), in any of the experiments where this assay was performed. $\gamma\delta^+$ T cells/NK^+ cells ($CD3^+$, $CD4^-$ and $CD8^-$) from naïve rhesus macaques responded very strongly to overnight stimulation with *M. tb* H37Rv producing IFN-γ, TNF-α and IL-2. $CD4^+$ and $CD8^+$ T cells did not respond strongly even after 4 or 7 days *ex-vivo* stimulation in naïve animals. This finding supports the results from the cultured MGIA in humans where the $\gamma\delta^+$ t cells, where the most abundant activated cell type following cell culture.

In contrast to the cultured and total PBMC infection MGIAs, the MGIT MGIA is very simple to perform, which makes it easier to implement across numerous vaccine trial sites. Experiments using the MGIT assay with mouse splenocytes showed that BCG vaccination

results in improved mycobacterial growth inhibition. This improved growth inhibition coincides with *in vivo* protection from *M. tb* challenge in the lungs and spleens of experimentally matched mice. $CD4^+$ and $CD8^+$ T cell depletion studies revealed a trend for enhanced mycobacterial growth inhibition when these cells were absent, indicating a possible role for $\gamma\delta^+$ T cells within this assay. PBMC from BCG and BCG-MVA85A vaccinated NHP also showed enhanced mycobacterial growth inhibition compared with pre vaccination samples.

DGE studies in the mice used for the MGIT assay revealed that BCG vaccination had primed a broader immune response in these animals, but there were also strong innate immune responses that could have an impact upon mycobacterial growth inhibition. The small sample size also meant that there was little power to perform correlations between the MGIT assay and DGE data, however IFN-γ and genes that this cytokine induces correlated with mycobacterial growth. NOS2 was only differentially expressed in BCG vaccinated mice, and so RNS could contribute for the enhanced mycobacterial growth inhibition seen in BCG vaccinated animals.

7.3 Future directions

7.3.1 Evaluate BCG-MVA85A vaccination in MGIT assay

Although the MGIT assay has been shown in this thesis and by R. Wallis *et al,* [155] to differentiate between naïve and BCG vaccinated mice and humans respectively; it has not been shown to differentiate between BCG and an improved vaccine against TB. MVA85A is the most clinically advanced novel TB vaccine candidate, and can enhance BCG efficacy against *M. tb* challenge in mice, guinea pigs, NHP and cattle [115, 116, 201, 217]. Thus if mycobacterial growth inhibition in the MGIT assay does correlate with protection, then BCG-MVA85A vaccinated mice should have lower GR values than BCG vaccinated mice.

7.3.2 Correlating GR values from MGIT assay with in vivo protection

Direct correlations between mycobacterial growth inhibition in the MGIT assay and protection from *M. tb* challenge are not possible in mice due to limited blood availability for use in the MGIT assay, necessitating the use of splenocytes. Experiments evaluating multiple vaccination regimes that induce significantly different levels of protection from *M. tb* challenge could be used to perform correlations; the median group CFU values from challenge could be correlated against median group GR values in the MGIT assay. If the MGIT assay could be performed using a very small volume of blood (<100µl from each mouse) then it could be possible to perform the MGIT assay and challenge using the same animal. Experiments could be performed to assess the minimum volume of blood required

to perform the MGIT assay. Another option could be to use the guinea pig model of TB, where blood volumes are not so restrictive, so the same animals could be used for the MGIT assay and *M. tb* challenge, and the cost of guinea pig experiments is still relatively inexpensive. It would also be advantageous to be able to use WB in the MGIT assay for TB vaccine efficacy studies in NHP.

7.3.3 Elucidation of the mechanisms in MGIT assay

The T cell depletion and microarray experiments I performed could be extended to further identify the precise mechanism(s) involved in BCG vaccine induced mycobacterial growth inhibition. Further studies involving T cell depletions and flow cytometry on splenocytes used to perform the MGIT assay might uncover which cell type(s) are responsible. Perturbation studies of RNS production, autophagy and macrophage activation could indicate the relative importance of these mechanisms within the MGIT assay. However, there is also the possibility that by blocking these processes there will be an increase in cell death which will affect the MGIT assay. The use of fluorescence microscopy with a reporter strain of BCG would enable the intracellular location of the bacteria to be confirmed. Thus, the importance of phagolysosome maturation and autophagy could be assessed. The importance of RNS in mice in relation to mycobacterial growth inhibition is well known [56] but its importance in human macrophages is controversial [57]. It would be interesting to

compare the mechanisms involved in mycobacterial growth inhibition between mice, humans and even NHP possibly by using microarrays.

7.3.4 Overall

The MGIT assay has been shown to detect BCG vaccine induced mycobacterial growth inhibition in WB from humans [155] and in this study, it has also been shown to be effective using splenocytes and PBMC from mice and NHP respectively. In mice this assay corresponded with protection from aerosol challenge with *M. tb* and therefore has the potential to be used to accelerate TB vaccine efficacy testing in mice and ultimately in humans.

8. Appendix

8.1 Electronic files

8.1.1 Non-human primate clinical data from M. tb challenge

8.1.2 Microarray data files

8.2 Elispot data TB006 BCG-BCG

T006	**BCG-BCG.....PPD**										
	PPD										
	volunteer	screen	BCG vacc	**1**	**2**	**4**	**8**	**12**	**24**	**52**	
		0	1	2	3	5	9	13	25		
	6	367	476	867	620	977	653	**no blood**	407		6
	7	63	163	840	747	850	1053	610	657	433	7
	8	83	30	527	230	477	170	123	127	57	8
	9	160	340	503	720	953	597	147	400	87	9
	10	267	800	1077	1147	777	563	657	447	533	10
	12	253	237	337	543	713	420	467	497	467	12
	14	130	250	213	407	1130	**no blood**	933	170	273	14

8.3 Monocyte only control wells cultured MGIA TB006

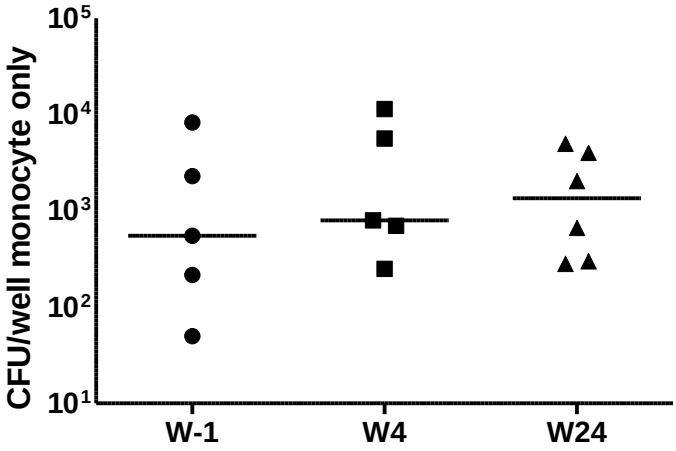

Figure 8-1 Positive control CFU counts from monocyte only wells of cultured MGIA.
Graph shows CFU data for the monocyte only control wells from the cultured MGIA using PBMC taken 1 week prior to BCG re-vaccination (W-1) 4 and 24 weeks post vaccination (W4 and W24 respectively). Bars represent the median CFU per monocyte only well.

8.4 Primers for q-PCR

All of the primers used for the q-PCR experiment in this thesis had been designed and established as being effective by Dr H. Fletcher prior to my studies.

Mouse HPRT forward 5' AGCCTAAGATGAGCGCAAGT 3'
Mouse HPRT reverse 5' TTACTAGGCAGATGGCCACA 3'

Mouse IFN-γ forward 5' GGGTTGTTGACCTCAAACTTGGCA 3'
Mouse IFN-γ reverse 5' CAGGCCATCAGCAACAACAT 3'

Mouse TNF-α forward 5' GATGAGAAGTTCCCAAATGG 3'
Mouse TNF-α reverse 5' GAAGATGATCTGAGTGTGAG 3'

8.5 Genes from direct comparison of stimulated splenocytes from naïve and BCG vaccinated mice

Symbol	Name	log2FC	adj.P.Val
Ifng	Interferon gamma	2.520	2.480E-05
Ifng	Interferon gamma	2.432	3.890E-05
Il17f	Interleukin 17f	1.896	5.956E-03
Csf2	Colony stimulating factor 2	1.534	2.639E-04
2010005H15Rik	Riken cDNA	1.434	2.292E-02
Ccl24	Chemokine (c-c) motif 24 ligand	1.376	7.326E-03
Hamp	Hepcidin	1.329	4.001E-04
Il17a	Interleukin 17a	1.301	1.100E-02
Il4	Interleukin 4	1.202	3.179E-02
Nos2	Nitric oxide synthase 2	1.179	7.326E-03
Upp1	Uridine phosphorylase 1	1.147	4.000E-02
Gpr83	Probable G-protein coupled receptor 83	1.145	3.228E-02
Oasl1	2'-5' oligoadenylate synthetase-like 1	1.142	2.542E-02
Rad51	RAD51	1.121	1.173E-02
Batf2	basic leucine zipper transcription factor, ATF-like 2	1.042	4.645E-02
Zbtb32	zinc finger and BTB domain containing 32	1.040	1.100E-02
Upp1	Uridine phosphorylase 1	1.028	4.184E-02
Ccr5	C-C chemokine receptor type 5	1.013	1.100E-02
Lta	Lymphotoxin-alpha	0.987	2.680E-02
Ffar2	Free fatty acid receptor 2 (FFA2)	0.981	3.515E-02
Il27	Interleukin 27	0.978	4.667E-03
Timp1	tissue inhibitor of metaloproteases	0.977	8.002E-03
Ifi205	interferon activated gene 205	0.969	1.664E-02
Tbx21	T-box 21	0.961	2.292E-02
Schip1	schwannomin interacting protein 1	0.953	2.542E-02
Gpr31c	G protein coupled receptor	0.932	9.973E-03

AA467197	NMES1	0.874	1.100E-02
Oasl2	2'-5' oligoadenylate synthetase-like 2	0.872	3.515E-02
Pabpc4	poly(A) binding protein, cytoplasmic 4	0.867	3.515E-02
Il12rb1	interleukin 12 receptor-b 1	0.848	1.100E-02
Fcgr1	Fc receptor, IgG, high affinity I	0.848	3.515E-02
Cetn4	centrin 4	0.845	4.714E-02
Ccr5	C-C chemokine receptor type 5	0.844	1.184E-02
Il2ra	Interleukin 2 receptor a	0.770	4.177E-02
Mlkl	mixed lineage kinase domain-like	0.769	4.990E-02
Rad54l	Rad45 like	0.769	3.515E-02
Arg2	arginase type II	0.735	3.515E-02
P2ry14	purinergic receptor P2Y, G-protein coupled, 14	0.699	3.664E-02
Slc12a7	solute carrier family 12 member	-0.89963	0.022922
Rapgef4	Rap guanine nucleotide exchange factor (GEF) 4	-0.709682	0.025421
Tcf7	Transcription factor 7	-0.740722	0.025421
Brwd1	Bromodomain and WD containing	-0.803949	0.025421
Tcf7	Transcription factor 7	-0.846548	0.025421
Sspn	sarcospan	-0.563973	0.035152
Ar	androgen receptor	-0.738328	0.035152
Arhgef4	Rho guanine nucleotide exchange factor (GEF) 4	-0.749908	0.035152
Galnt9	Galnt9	-0.775531	0.035152
Matk	megakaryocyte-associated tyrosine kinase	-0.778604	0.035152
Ovgp1	oviduct specific glycoprotein	-0.794286	0.03919
Dtx4	Deltex 4	-0.838741	0.041306
Zfp69	Zinc finger protein 69	-0.822251	0.041839
Nt5e	5' nucleotidase	-0.846981	0.049901
Scml4	sex comb mid leg (drosophila)	-0.855546	0.049901

Table 8-1 Differentially expressed genes between BCG vaccinated and naïve mice by direct comparison.

References

1. Hershkovitz, I., et al., *Detection and molecular characterization of 9,000-year-old Mycobacterium tuberculosis from a Neolithic settlement in the Eastern Mediterranean.* PLoS ONE, 2008. 3(10): p. e3426.
2. Bloom, B.R., *Tuberculosis: pathogenesis, protection, and control*. 1994: ASM Press.
3. Bhatt, K. and P. Salgame, *Host innate immune response to Mycobacterium tuberculosis.* J Clin Immunol, 2007. 27(4): p. 347-62.
4. Corbett, E.L., et al., *The growing burden of tuberculosis: global trends and interactions with the HIV epidemic.* Arch Intern Med, 2003. 163(9): p. 1009-21.
5. Girardi, E., et al., *Impact of the HIV epidemic on the spread of other diseases: the case of tuberculosis.* AIDS, 2000. 14 Suppl 3: p. S47-56.
6. WHO. *Tuberculosis factsheet n°104*. 2010 [cited 2011 22/03/11]; Available from: http://www.who.int/mediacentre/factsheets/fs104/en/index.html.
7. Maartens, G., P.A. Willcox, and S.R. Benatar, *Miliary tuberculosis: rapid diagnosis, hematologic abnormalities, and outcome in 109 treated adults.* Am J Med, 1990. 89(3): p. 291-6.
8. Slavin, R.E., T.J. Walsh, and A.D. Pollack, *Late generalized tuberculosis: a clinical pathologic analysis and comparison of 100 cases in the preantibiotic and antibiotic eras.* Medicine (Baltimore), 1980. 59(5): p. 352-66.
9. *Emergence of Mycobacterium tuberculosis with extensive resistance to second-line drugs--worldwide, 2000-2004.* MMWR Morb Mortal Wkly Rep, 2006. 55(11): p. 301-5.
10. *Extensively drug-resistant tuberculosis (XDR-TB): recommendations for prevention and control.* Wkly Epidemiol Rec, 2006. 81(45): p. 430-2.
11. Gandhi, N.R., et al., *Extensively drug-resistant tuberculosis as a cause of death in patients co-infected with tuberculosis and HIV in a rural area of South Africa.* Lancet, 2006. 368(9547): p. 1575-80.
12. Raviglione, M.C. and I.M. Smith, *XDR tuberculosis--implications for global public health.* N Engl J Med, 2007. 356(7): p. 656-9.
13. Migliori, G.B., et al., *First tuberculosis cases in Italy resistant to all tested drugs.* Euro Surveill, 2007. 12(5): p. E070517 1.
14. Velayati, A.A., et al., *Emergence of new forms of totally drug-resistant tuberculosis bacilli: super extensively drug-resistant tuberculosis or totally drug-resistant strains in iran.* Chest, 2009. 136(2): p. 420-5.

15. WHO. *Estimated TB incidence rates 2009*. 2010 [cited 2011 23/03/2011]; Available from: http://gamapserver.who.int/mapLibrary/app/searchResults.aspx.
16. Saikingaku, T.S., *Toda's bacteriology*, 2007: Tokyo.
17. Brosch, R., et al., *A new evolutionary scenario for the Mycobacterium tuberculosis complex.* Proc Natl Acad Sci U S A, 2002. 99(6): p. 3684-9.
18. de Jong, B.C., et al., *Progression to active tuberculosis, but not transmission, varies by Mycobacterium tuberculosis lineage in The Gambia.* J Infect Dis, 2008. 198(7): p. 1037-43.
19. Cole, S.T., et al., *Deciphering the biology of Mycobacterium tuberculosis from the complete genome sequence.* Nature, 1998. 393(6685): p. 537-44.
20. Gheorghiu, M., J. Augier, and P.H. Lagrange, *Maintenance and Control of the French Bcg Strain 1173-P2 (Primary and Secondary Seed-Lots).* Bulletin De L Institut Pasteur, 1983. 81(3): p. 281-288.
21. Behr, M.A. and P.M. Small, *Has BCG attenuated to impotence?* Nature, 1997. 389(6647): p. 133-4.
22. Dubos, R.J. and C.H. Pierce, *Differential characteristics in vitro and in vivo of several substrains of BCG. IV. Immunizing effectiveness.* Am Rev Tuberc, 1956. 74(5): p. 699-717.
23. Grange, J.M. and J.A. Gibson, *Strain to strain variation in the immunogenicity of BCG.* Dev Biol Stand, 1986. 58 (Pt A): p. 37-41.
24. Lagranderie, M.R., et al., *Comparison of immune responses of mice immunized with five different Mycobacterium bovis BCG vaccine strains.* Infect Immun, 1996. 64(1): p. 1-9.
25. Ritz, N., et al., *Influence of BCG vaccine strain on the immune response and protection against tuberculosis.* FEMS Microbiol Rev, 2008. 32(5): p. 821-41.
26. Milstien, J.B. and J.J. Gibson, *Quality control of BCG vaccine by WHO: a review of factors that may influence vaccine effectiveness and safety.* Bull World Health Organ, 1990. 68(1): p. 93-108.
27. Shapiro, C., et al., *A case-control study of BCG and childhood tuberculosis in Cali, Colombia.* Int J Epidemiol, 1985. 14(3): p. 441-6.
28. Behr, M.A., *BCG--different strains, different vaccines?* Lancet Infect Dis, 2002. 2(2): p. 86-92.
29. Zhu, B.L., et al., *BCG vaccines Their mechanisms of attenuation and impact on safety and protective efficacy.* Human Vaccines, 2009. 5(2): p. 70-78.
30. Beharka, A.A., et al., *Pulmonary surfactant protein A up-regulates activity of the mannose receptor, a pattern recognition receptor expressed on human macrophages.* J Immunol, 2002. 169(7): p. 3565-73.

31. Gaynor, C.D., et al., *Pulmonary surfactant protein A mediates enhanced phagocytosis of Mycobacterium tuberculosis by a direct interaction with human macrophages.* J Immunol, 1995. 155(11): p. 5343-51.
32. Ernst, J.D., *Macrophage receptors for Mycobacterium tuberculosis.* Infect Immun, 1998. 66(4): p. 1277-81.
33. Liu, T., et al., *Differences in expression of toll-like receptors and their reactivities in dendritic cells in BALB/c and C57BL/6 mice.* Infect Immun, 2002. 70(12): p. 6638-45.
34. Moreno, C., et al., *Lipoarabinomannan from Mycobacterium tuberculosis induces the production of tumour necrosis factor from human and murine macrophages.* Clin Exp Immunol, 1989. 76(2): p. 240-5.
35. Abel, B., et al., *Toll-like receptor 4 expression is required to control chronic Mycobacterium tuberculosis infection in mice.* J Immunol, 2002. 169(6): p. 3155-62.
36. Stenger, S. and R.L. Modlin, *Control of Mycobacterium tuberculosis through mammalian Toll-like receptors.* Curr Opin Immunol, 2002. 14(4): p. 452-7.
37. Divangahi, M., et al., *NOD2-deficient mice have impaired resistance to Mycobacterium tuberculosis infection through defective innate and adaptive immunity.* J Immunol, 2008. 181(10): p. 7157-65.
38. Gandotra, S., et al., *Nucleotide-binding oligomerization domain protein 2-deficient mice control infection with Mycobacterium tuberculosis.* Infect Immun, 2007. 75(11): p. 5127-34.
39. Lamhamedi-Cherradi, S., C. de Chastellier, and J.L. Casanova, *Growth of Mycobacterium bovis, Bacille Calmette-Guerin, within human monocytes-macrophages cultured in serum-free medium.* J Immunol Methods, 1999. 225(1-2): p. 75-86.
40. Schlesinger, L.S., et al., *Phagocytosis of Mycobacterium tuberculosis is mediated by human monocyte complement receptors and complement component C3.* J Immunol, 1990. 144(7): p. 2771-80.
41. Gatfield, J. and J. Pieters, *Essential role for cholesterol in entry of mycobacteria into macrophages.* Science, 2000. 288(5471): p. 1647-50.
42. Flannagan, R.S., G. Cosio, and S. Grinstein, *Antimicrobial mechanisms of phagocytes and bacterial evasion strategies.* Nat Rev Microbiol, 2009. 7(5): p. 355-66.
43. Armstrong, J.A. and P.D. Hart, *Response of cultured macrophages to Mycobacterium tuberculosis, with observations on fusion of lysosomes with phagosomes.* J Exp Med, 1971. 134(3 Pt 1): p. 713-40.

44. Armstrong, J.A. and P.D. Hart, *Phagosome-lysosome interactions in cultured macrophages infected with virulent tubercle bacilli. Reversal of the usual nonfusion pattern and observations on bacterial survival.* J Exp Med, 1975. 142(1): p. 1-16.
45. Clemens, D.L. and M.A. Horwitz, *The Mycobacterium tuberculosis phagosome interacts with early endosomes and is accessible to exogenously administered transferrin.* J Exp Med, 1996. 184(4): p. 1349-55.
46. Sturgill-Koszycki, S., U.E. Schaible, and D.G. Russell, *Mycobacterium-containing phagosomes are accessible to early endosomes and reflect a transitional state in normal phagosome biogenesis.* EMBO J, 1996. 15(24): p. 6960-8.
47. Russell, D.G., J. Dant, and S. Sturgill-Koszycki, *Mycobacterium avium- and Mycobacterium tuberculosis-containing vacuoles are dynamic, fusion-competent vesicles that are accessible to glycosphingolipids from the host cell plasmalemma.* J Immunol, 1996. 156(12): p. 4764-73.
48. Sturgill-Koszycki, S., et al., *Lack of acidification in Mycobacterium phagosomes produced by exclusion of the vesicular proton-ATPase.* Science, 1994. 263(5147): p. 678-81.
49. Clemens, D.L., B.Y. Lee, and M.A. Horwitz, *Deviant expression of Rab5 on phagosomes containing the intracellular pathogens Mycobacterium tuberculosis and Legionella pneumophila is associated with altered phagosomal fate.* Infect Immun, 2000. 68(5): p. 2671-84.
50. Vergne, I., et al., *Mycobacterium tuberculosis phagosome maturation arrest: mycobacterial phosphatidylinositol analog phosphatidylinositol mannoside stimulates early endosomal fusion.* Mol Biol Cell, 2004. 15(2): p. 751-60.
51. Kusner, D.J., *Mechanisms of mycobacterial persistence in tuberculosis.* Clin Immunol, 2005. 114(3): p. 239-47.
52. Chua, J., et al., *A tale of two lipids: Mycobacterium tuberculosis phagosome maturation arrest.* Curr Opin Microbiol, 2004. 7(1): p. 71-7.
53. Fratti, R.A., et al., *Mycobacterium tuberculosis glycosylated phosphatidylinositol causes phagosome maturation arrest.* Proc Natl Acad Sci U S A, 2003. 100(9): p. 5437-42.
54. Webb, J.L., et al., *Macrophage nitric oxide synthase associates with cortical actin but is not recruited to phagosomes.* Infect Immun, 2001. 69(10): p. 6391-400.
55. Miller, B.H., et al., *Mycobacteria inhibit nitric oxide synthase recruitment to phagosomes during macrophage infection.* Infect Immun, 2004. 72(5): p. 2872-8.

56. Bogdan, C., *Nitric oxide and the immune response.* Nat Immunol, 2001. 2(10): p. 907-16.
57. Weinberg, J.B., *Nitric oxide production and nitric oxide synthase type 2 expression by human mononuclear phagocytes: a review.* Mol Med, 1998. 4(9): p. 557-91.
58. May, M.E. and P.J. Spagnuolo, *Evidence for activation of a respiratory burst in the interaction of human neutrophils with Mycobacterium tuberculosis.* Infect Immun, 1987. 55(9): p. 2304-7.
59. Witko-Sarsat, V., et al., *Presence of proteinase 3 in secretory vesicles: evidence of a novel, highly mobilizable intracellular pool distinct from azurophil granules.* Blood, 1999. 94(7): p. 2487-96.
60. Masson, P.L., J.F. Heremans, and E. Schonne, *Lactoferrin, an iron-binding protein in neutrophilic leukocytes.* J Exp Med, 1969. 130(3): p. 643-58.
61. Rivas-Santiago, B., et al., *Expression of cathelicidin LL-37 during Mycobacterium tuberculosis infection in human alveolar macrophages, monocytes, neutrophils, and epithelial cells.* Infect Immun, 2008. 76(3): p. 935-41.
62. Martineau, A.R., et al., *Neutrophil-mediated innate immune resistance to mycobacteria.* J Clin Invest, 2007. 117(7): p. 1988-94.
63. Keller, C., et al., *Genetically determined susceptibility to tuberculosis in mice causally involves accelerated and enhanced recruitment of granulocytes.* Infect Immun, 2006. 74(7): p. 4295-309.
64. D'Avila, H., et al., *Neutrophils recruited to the site of Mycobacterium bovis BCG infection undergo apoptosis and modulate lipid body biogenesis and prostaglandin E production by macrophages.* Cell Microbiol, 2008. 10(12): p. 2589-604.
65. Bodnar, K.A., N.V. Serbina, and J.L. Flynn, *Fate of Mycobacterium tuberculosis within murine dendritic cells.* Infect Immun, 2001. 69(2): p. 800-9.
66. Tailleux, L., et al., *Constrained intracellular survival of Mycobacterium tuberculosis in human dendritic cells.* J Immunol, 2003. 170(4): p. 1939-48.
67. Brill, K.J., et al., *Human natural killer cells mediate killing of intracellular Mycobacterium tuberculosis H37Rv via granule-independent mechanisms.* Infect Immun, 2001. 69(3): p. 1755-65.
68. Roy, S., et al., *NK cells lyse T regulatory cells that expand in response to an intracellular pathogen.* J Immunol, 2008. 180(3): p. 1729-36.
69. Ladel, C.H., et al., *Protective role of gamma/delta T cells and alpha/beta T cells in tuberculosis.* Eur J Immunol, 1995. 25(10): p. 2877-81.

70. Garcia, V.E., et al., *Single-cell cytokine analysis of gamma delta T cell responses to nonpeptide mycobacterial antigens.* J Immunol, 1997. 159(3): p. 1328-35.
71. Peng, M.Y., et al., *Interleukin 17-producing gamma delta T cells increased in patients with active pulmonary tuberculosis.* Cell Mol Immunol, 2008. 5(3): p. 203-8.
72. Shen, Y., et al., *Adaptive immune response of Vgamma2Vdelta2+ T cells during mycobacterial infections.* Science, 2002. 295(5563): p. 2255-8.
73. Worku, S. and D.F. Hoft, *Differential effects of control and antigen-specific T cells on intracellular mycobacterial growth.* Infect Immun, 2003. 71(4): p. 1763-73.
74. Beckman, E.M., et al., *Recognition of a lipid antigen by CD1-restricted alpha beta+ T cells.* Nature, 1994. 372(6507): p. 691-4.
75. Sieling, P.A., et al., *CD1-restricted T cell recognition of microbial lipoglycan antigens.* Science, 1995. 269(5221): p. 227-30.
76. Gutierrez, M.G., et al., *Autophagy is a defense mechanism inhibiting BCG and Mycobacterium tuberculosis survival in infected macrophages.* Cell, 2004. 119(6): p. 753-66.
77. O'Garra, A., *Cytokines induce the development of functionally heterogeneous T helper cell subsets.* Immunity, 1998. 8(3): p. 275-83.
78. Hsieh, C.S., et al., *Development of TH1 CD4+ T cells through IL-12 produced by Listeria-induced macrophages.* Science, 1993. 260(5107): p. 547-9.
79. Murphy, K.M. and S.L. Reiner, *The lineage decisions of helper T cells.* Nat Rev Immunol, 2002. 2(12): p. 933-44.
80. Mosmann, T.R. and R.L. Coffman, *TH1 and TH2 cells: different patterns of lymphokine secretion lead to different functional properties.* Annu Rev Immunol, 1989. 7: p. 145-73.
81. Le Gros, G., et al., *Generation of interleukin 4 (IL-4)-producing cells in vivo and in vitro: IL-2 and IL-4 are required for in vitro generation of IL-4-producing cells.* J Exp Med, 1990. 172(3): p. 921-9.
82. Scott, P., *IFN-gamma modulates the early development of Th1 and Th2 responses in a murine model of cutaneous leishmaniasis.* J Immunol, 1991. 147(9): p. 3149-55.
83. Seder, R.A., et al., *The presence of interleukin 4 during in vitro priming determines the lymphokine-producing potential of CD4+ T cells from T cell receptor transgenic mice.* J Exp Med, 1992. 176(4): p. 1091-8.
84. Swain, S.L., et al., *IL-4 directs the development of Th2-like helper effectors.* J Immunol, 1990. 145(11): p. 3796-806.

85. Constant, S.L. and K. Bottomly, *Induction of Th1 and Th2 CD4+ T cell responses: the alternative approaches.* Annu Rev Immunol, 1997. 15: p. 297-322.
86. Amsen, D., et al., *Instruction of distinct CD4 T helper cell fates by different notch ligands on antigen-presenting cells.* Cell, 2004. 117(4): p. 515-26.
87. Kamath, A.B., et al., *Cytolytic CD8+ T cells recognizing CFP10 are recruited to the lung after Mycobacterium tuberculosis infection.* J Exp Med, 2004. 200(11): p. 1479-89.
88. Lazarevic, V. and J. Flynn, *CD8+ T cells in tuberculosis.* Am J Respir Crit Care Med, 2002. 166(8): p. 1116-21.
89. Lazarevic, V., D. Nolt, and J.L. Flynn, *Long-term control of Mycobacterium tuberculosis infection is mediated by dynamic immune responses.* J Immunol, 2005. 175(2): p. 1107-17.
90. Sad, S., D. Kagi, and T.R. Mosmann, *Perforin and Fas killing by CD8+ T cells limits their cytokine synthesis and proliferation.* J Exp Med, 1996. 184(4): p. 1543-7.
91. Gonzalez-Juarrero, M., et al., *Temporal and spatial arrangement of lymphocytes within lung granulomas induced by aerosol infection with Mycobacterium tuberculosis.* Infect Immun, 2001. 69(3): p. 1722-8.
92. Vordermeier, H.M., et al., *Increase of tuberculous infection in the organs of B cell-deficient mice.* Clin Exp Immunol, 1996. 106(2): p. 312-6.
93. Maglione, P.J., J. Xu, and J. Chan, *B cells moderate inflammatory progression and enhance bacterial containment upon pulmonary challenge with Mycobacterium tuberculosis.* J Immunol, 2007. 178(11): p. 7222-34.
94. Maglione, P.J., et al., *Fc gamma receptors regulate immune activation and susceptibility during Mycobacterium tuberculosis infection.* J Immunol, 2008. 180(5): p. 3329-38.
95. Ordway, D., et al., *The cellular immune response to Mycobacterium tuberculosis infection in the guinea pig.* J Immunol, 2007. 179(4): p. 2532-41.
96. Fuller, C.L., J.L. Flynn, and T.A. Reinhart, *In situ study of abundant expression of proinflammatory chemokines and cytokines in pulmonary granulomas that develop in cynomolgus macaques experimentally infected with Mycobacterium tuberculosis.* Infect Immun, 2003. 71(12): p. 7023-34.
97. Rhoades, E.R., A.M. Cooper, and I.M. Orme, *Chemokine response in mice infected with Mycobacterium tuberculosis.* Infect Immun, 1995. 63(10): p. 3871-7.
98. Cooper, A.M., et al., *Disseminated Tuberculosis in Interferon-Gamma Gene-Disrupted Mice.* Journal of Experimental Medicine, 1993. 178(6): p. 2243-2247.

99. Sprent, J. and C.D. Surh, *T cell memory.* Annu Rev Immunol, 2002. 20: p. 551-79.
100. Zinkernagel, R.M. and H. Hengartner, *Protective 'immunity' by pre-existent neutralizing antibody titers and preactivated T cells but not by so-called 'immunological memory'.* Immunological Reviews, 2006. 211: p. 310-319.
101. Sallusto, F., et al., *Two subsets of memory T lymphocytes with distinct homing potentials and effector functions.* Nature, 1999. 401(6754): p. 708-712.
102. Colditz, G.A., et al., *Efficacy of BCG vaccine in the prevention of tuberculosis. Meta-analysis of the published literature.* JAMA, 1994. 271(9): p. 698-702.
103. Sutherland, I. and I. Lindgren, *The protective effect of BCG vaccination as indicated by autopsy studies.* Tubercle, 1979. 60(4): p. 225-31.
104. Soysal, A., et al., *Effect of BCG vaccination on risk of Mycobacterium tuberculosis infection in children with household tuberculosis contact: a prospective community-based study.* Lancet, 2005. 366(9495): p. 1443-51.
105. Rodrigues, L.C., V.K. Diwan, and J.G. Wheeler, *Protective effect of BCG against tuberculous meningitis and miliary tuberculosis: a meta-analysis.* Int J Epidemiol, 1993. 22(6): p. 1154-8.
106. Fine, P.E., et al., *Delayed-type hypersensitivity, mycobacterial vaccines and protective immunity.* Lancet, 1994. 344(8932): p. 1245-9.
107. Cooper, A.M., *Cell-mediated immune responses in tuberculosis.* Annu Rev Immunol, 2009. 27: p. 393-422.
108. Pathak, S.K., et al., *Direct extracellular interaction between the early secreted antigen ESAT-6 of Mycobacterium tuberculosis and TLR2 inhibits TLR signaling in macrophages.* Nat Immunol, 2007. 8(6): p. 610-8.
109. Brodin, P., et al., *High content phenotypic cell-based visual screen identifies Mycobacterium tuberculosis acyltrehalose-containing glycolipids involved in phagosome remodeling.* PLoS Pathog. 6(9): p. e1001100.
110. Rodrigues, L.C., et al., *Effect of BCG revaccination on incidence of tuberculosis in school-aged children in Brazil: the BCG-REVAC cluster-randomised trial.* Lancet, 2005. 366(9493): p. 1290-5.
111. Brandt, L., et al., *The protective effect of the Mycobacterium bovis BCG vaccine is increased by coadministration with the Mycobacterium tuberculosis 72-kilodalton fusion polyprotein Mtb72F in M. tuberculosis-infected guinea pigs.* Infect Immun, 2004. 72(11): p. 6622-32.
112. Tsenova, L., et al., *Evaluation of the Mtb72F polyprotein vaccine in a rabbit model of tuberculous meningitis.* Infect Immun, 2006. 74(4): p. 2392-401.

113. Langermans, J.A., et al., *Protection of macaques against Mycobacterium tuberculosis infection by a subunit vaccine based on a fusion protein of antigen 85B and ESAT-6.* Vaccine, 2005. 23(21): p. 2740-50.
114. Olsen, A.W., et al., *Protective effect of a tuberculosis subunit vaccine based on a fusion of antigen 85B and ESAT-6 in the aerosol guinea pig model.* Infect Immun, 2004. 72(10): p. 6148-50.
115. Goonetilleke, N.P., et al., *Enhanced immunogenicity and protective efficacy against Mycobacterium tuberculosis of bacille Calmette-Guerin vaccine using mucosal administration and boosting with a recombinant modified vaccinia virus Ankara.* J Immunol, 2003. 171(3): p. 1602-9.
116. Williams, A., et al., *Boosting with poxviruses enhances Mycobacterium bovis BCG efficacy against tuberculosis in guinea pigs.* Infect Immun, 2005. 73(6): p. 3814-6.
117. Radosevic, K., et al., *Protective immune responses to a recombinant adenovirus type 35 tuberculosis vaccine in two mouse strains: CD4 and CD8 T-cell epitope mapping and role of gamma interferon.* Infect Immun, 2007. 75(8): p. 4105-15.
118. Abel, B., et al., *The novel tuberculosis vaccine, AERAS-402, induces robust and polyfunctional CD4+ and CD8+ T cells in adults.* Am J Respir Crit Care Med, 2010. 181(12): p. 1407-17.
119. Grode, L., et al., *Increased vaccine efficacy against tuberculosis of recombinant Mycobacterium bovis bacille Calmette-Guerin mutants that secrete listeriolysin.* J Clin Invest, 2005. 115(9): p. 2472-9.
120. Horwitz, M.A. and G. Harth, *A new vaccine against tuberculosis affords greater survival after challenge than the current vaccine in the guinea pig model of pulmonary tuberculosis.* Infect Immun, 2003. 71(4): p. 1672-9.
121. Sambandamurthy, V.K., et al., *Long-term protection against tuberculosis following vaccination with a severely attenuated double lysine and pantothenate auxotroph of Mycobacterium tuberculosis.* Infect Immun, 2005. 73(2): p. 1196-203.
122. Sambandamurthy, V.K., et al., *A pantothenate auxotroph of Mycobacterium tuberculosis is highly attenuated and protects mice against tuberculosis.* Nat Med, 2002. 8(10): p. 1171-4.
123. Martin, C., et al., *The live Mycobacterium tuberculosis phoP mutant strain is more attenuated than BCG and confers protective immunity against tuberculosis in mice and guinea pigs.* Vaccine, 2006. 24(17): p. 3408-19.

124. Rubakova, E., et al., *Specificity and efficacy of dendritic cell-based vaccination against tuberculosis with complex mycobacterial antigens in a mouse model.* Tuberculosis (Edinb), 2007. 87(2): p. 134-44.
125. Okada, M., et al., *Evaluation of a novel vaccine (HVJ-liposome/HSP65 DNA+IL-12 DNA) against tuberculosis using the cynomolgus monkey model of TB.* Vaccine, 2007. 25(16): p. 2990-3.
126. Li, Y.P., et al., *Mycobacterium vaccae vaccine to prevent tuberculosis in high risk people: A meta-analysis.* Journal of Infection, 2010. 60(5): p. 320-330.
127. Qin, L., et al., *A framework for assessing immunological correlates of protection in vaccine trials.* J Infect Dis, 2007. 196(9): p. 1304-12.
128. Andrews, N., R. Borrow, and E. Miller, *Validation of serological correlate of protection for meningococcal C conjugate vaccine by using efficacy estimates from postlicensure surveillance in England.* Clin Diagn Lab Immunol, 2003. 10(5): p. 780-6.
129. Kagina, B.M., et al., *Specific T cell frequency and cytokine expression profile do not correlate with protection against tuberculosis after bacillus Calmette-Guerin vaccination of newborns.* Am J Respir Crit Care Med, 2010. 182(8): p. 1073-9.
130. Buddle, B.M., et al., *Identification of immune response correlates for protection against bovine tuberculosis.* Vet Immunol Immunopathol, 2005. 108(1-2): p. 45-51.
131. Elias, D., H. Akuffo, and S. Britton, *PPD induced in vitro interferon gamma production is not a reliable correlate of protection against Mycobacterium tuberculosis.* Trans R Soc Trop Med Hyg, 2005. 99(5): p. 363-8.
132. Mittrucker, H.W., et al., *Poor correlation between BCG vaccination-induced T cell responses and protection against tuberculosis.* Proc Natl Acad Sci U S A, 2007. 104(30): p. 12434-9.
133. Hope, J.C., et al., *Identification of surrogates and correlates of protection in protective immunity against Mycobacterium bovis infection induced in neonatal calves by vaccination with M. bovis BCG Pasteur and M. bovis BCG Danish.* Clin Vaccine Immunol, 2011. 18(3): p. 373-9.
134. Andersen, P. and B. Smedegaard, *CD4(+) T-cell subsets that mediate immunological memory to Mycobacterium tuberculosis infection in mice.* Infect Immun, 2000. 68(2): p. 621-9.
135. Caruso, A.M., et al., *Mice deficient in CD4 T cells have only transiently diminished levels of IFN-gamma, yet succumb to tuberculosis.* J Immunol, 1999. 162(9): p. 5407-16.

136. Cowley, S.C. and K.L. Elkins, *CD4+ T cells mediate IFN-gamma-independent control of Mycobacterium tuberculosis infection both in vitro and in vivo.* J Immunol, 2003. 171(9): p. 4689-99.
137. Feng, C.G. and W.J. Britton, *CD4+ and CD8+ T cells mediate adoptive immunity to aerosol infection of Mycobacterium bovis bacillus Calmette-Guerin.* J Infect Dis, 2000. 181(5): p. 1846-9.
138. Ladel, C.H., S. Daugelat, and S.H. Kaufmann, *Immune response to Mycobacterium bovis bacille Calmette Guerin infection in major histocompatibility complex class I- and II-deficient knock-out mice: contribution of CD4 and CD8 T cells to acquired resistance.* Eur J Immunol, 1995. 25(2): p. 377-84.
139. Saunders, B.M., et al., *CD4 is required for the development of a protective granulomatous response to pulmonary tuberculosis.* Cell Immunol, 2002. 216(1-2): p. 65-72.
140. Scanga, C.A., et al., *Depletion of CD4(+) T cells causes reactivation of murine persistent tuberculosis despite continued expression of interferon gamma and nitric oxide synthase 2.* J Exp Med, 2000. 192(3): p. 347-58.
141. Jones, B.E., et al., *Relationship of the manifestations of tuberculosis to CD4 cell counts in patients with human immunodeficiency virus infection.* Am Rev Respir Dis, 1993. 148(5): p. 1292-7.
142. Chen, C.Y., et al., *A critical role for CD8 T cells in a nonhuman primate model of tuberculosis.* PLoS Pathog, 2009. 5(4): p. e1000392.
143. Giri, P.K., I. Verma, and G.K. Khuller, *Enhanced immunoprotective potential of Mycobacterium tuberculosis Ag85 complex protein based vaccine against airway Mycobacterium tuberculosis challenge following intranasal administration.* FEMS Immunol Med Microbiol, 2006. 47(2): p. 233-41.
144. Agger, E.M., et al., *Protective immunity to tuberculosis with Ag85B-ESAT-6 in a synthetic cationic adjuvant system IC31.* Vaccine, 2006. 24(26): p. 5452-60.
145. Goletti, D., et al., *Region of difference 1 antigen-specific CD4+ memory T cells correlate with a favorable outcome of tuberculosis.* J Infect Dis, 2006. 194(7): p. 984-92.
146. Steinman, L., *A brief history of T(H)17, the first major revision in the T(H)1/T(H)2 hypothesis of T cell-mediated tissue damage.* Nat Med, 2007. 13(2): p. 139-45.
147. Khader, S.A., et al., *IL-23 and IL-17 in the establishment of protective pulmonary CD4+ T cell responses after vaccination and during Mycobacterium tuberculosis challenge.* Nat Immunol, 2007. 8(4): p. 369-77.

148. Khader, S.A. and A.M. Cooper, *IL-23 and IL-17 in tuberculosis.* Cytokine, 2008. 41(2): p. 79-83.
149. Khader, S.A., et al., *IL-23 compensates for the absence of IL-12p70 and is essential for the IL-17 response during tuberculosis but is dispensable for protection and antigen-specific IFN-gamma responses if IL-12p70 is available.* J Immunol, 2005. 175(2): p. 788-95.
150. Lockhart, E., A.M. Green, and J.L. Flynn, *IL-17 production is dominated by gammadelta T cells rather than CD4 T cells during Mycobacterium tuberculosis infection.* J Immunol, 2006. 177(7): p. 4662-9.
151. Umemura, M., et al., *IL-17-mediated regulation of innate and acquired immune response against pulmonary Mycobacterium bovis bacille Calmette-Guerin infection.* J Immunol, 2007. 178(6): p. 3786-96.
152. Aranday Cortes, E., et al., *Mycobacterium bovis-BCG vaccination induces specific pulmonary transcriptome biosignatures in mice.* PLoS ONE, 2010. 5(6): p. e11319.
153. Silver, R.F., et al., *Lymphocyte-dependent inhibition of growth of virulent Mycobacterium tuberculosis H37Rv within human monocytes: requirement for CD4+ T cells in purified protein derivative-positive, but not in purified protein derivative-negative subjects.* J Immunol, 1998. 160(5): p. 2408-17.
154. Kampmann, B., et al., *Novel human in vitro system for evaluating antimycobacterial vaccines.* Infect Immun, 2004. 72(11): p. 6401-7.
155. Cheon, S.H., et al., *Bactericidal activity in whole blood as a potential surrogate marker of immunity after vaccination against tuberculosis.* Clin Diagn Lab Immunol, 2002. 9(4): p. 901-7.
156. Parra, M., et al., *Development of a murine mycobacterial growth inhibition assay for evaluating vaccines against Mycobacterium tuberculosis.* Clin Vaccine Immunol, 2009. 16(7): p. 1025-32.
157. Kolibab, K., et al., *A practical in vitro growth inhibition assay for the evaluation of TB vaccines.* Vaccine, 2009. 28(2): p. 317-22.
158. Sharpe, S.A., et al., *Establishment of an aerosol challenge model of tuberculosis in rhesus macaques and an evaluation of endpoints for vaccine testing.* Clin Vaccine Immunol, 2010. 17(8): p. 1170-82.
159. Whelan, K.T., et al., *Safety and immunogenicity of boosting BCG vaccinated subjects with BCG: comparison with boosting with a new TB vaccine, MVA85A.* PLoS ONE, 2009. 4(6): p. e5934.
160. Bejon, P., et al., *Immunogenicity of the candidate malaria vaccines FP9 and modified vaccinia virus Ankara encoding the pre-erythrocytic antigen ME-TRAP*

in 1-6 year old children in a malaria endemic area. Vaccine, 2006. 24(22): p. 4709-15.

161. Sarkar, S., V. Kalia, and R.C. Montelaro, *Caspase-mediated apoptosis and cell death of rhesus macaque CD4+ T-cells due to cryopreservation of peripheral blood mononuclear cells can be rescued by cytokine treatment after thawing.* Cryobiology, 2003. 47(1): p. 44-58.
162. Kondrack, R.M., et al., *Interleukin 7 regulates the survival and generation of memory CD4 cells.* J Exp Med, 2003. 198(12): p. 1797-806.
163. Li, J., G. Huston, and S.L. Swain, *IL-7 promotes the transition of CD4 effectors to persistent memory cells.* J Exp Med, 2003. 198(12): p. 1807-15.
164. Miyazaki, T., et al., *Three distinct IL-2 signaling pathways mediated by bcl-2, c-myc, and lck cooperate in hematopoietic cell proliferation.* Cell, 1995. 81(2): p. 223-31.
165. Hoft, D.F., et al., *Investigation of the relationships between immune-mediated inhibition of mycobacterial growth and other potential surrogate markers of protective Mycobacterium tuberculosis immunity.* J Infect Dis, 2002. 186(10): p. 1448-57.
166. Weinberg, A., et al., *Optimization and limitations of use of cryopreserved peripheral blood mononuclear cells for functional and phenotypic T-cell characterization.* Clin Vaccine Immunol, 2009. 16(8): p. 1176-86.
167. Maecker, H.T., et al., *Impact of cryopreservation on tetramer, cytokine flow cytometry, and ELISPOT.* BMC Immunol, 2005. 6: p. 17.
168. Weinberg, A., et al., *Viability and functional activity of cryopreserved mononuclear cells.* Clin Diagn Lab Immunol, 2000. 7(4): p. 714-6.
169. Brewer, T.F. and G.A. Colditz, *Relationship between bacille Calmette-Guerin (BCG) strains and the efficacy of BCG vaccine in the prevention of tuberculosis.* Clin Infect Dis, 1995. 20(1): p. 126-35.
170. Edwards, L.B., World Health Organization. Tuberculosis Research Office., and C.E. Palmer, *BCG vaccination ; studies by the WHO Tuberculosis Research Office, Copenhagen*. 1953, Geneva,: World Health Organization. 307 p.
171. Masopust, D., et al., *The role of programming in memory T-cell development.* Curr Opin Immunol, 2004. 16(2): p. 217-25.
172. Henao-Tamayo, M.I., et al., *Phenotypic definition of effector and memory T-lymphocyte subsets in mice chronically infected with Mycobacterium tuberculosis.* Clin Vaccine Immunol, 2010. 17(4): p. 618-25.
173. Orme, I.M., *Characteristics and specificity of acquired immunologic memory to Mycobacterium tuberculosis infection.* J Immunol, 1988. 140(10): p. 3589-93.

174. Orme, I.M., *Induction of nonspecific acquired resistance and delayed-type hypersensitivity, but not specific acquired resistance in mice inoculated with killed mycobacterial vaccines.* Infect Immun, 1988. 56(12): p. 3310-2.
175. Haile, M., et al., *Immunization with heat-killed Mycobacterium bovis bacille Calmette-Guerin (BCG) in Eurocine L3 adjuvant protects against tuberculosis.* Vaccine, 2004. 22(11-12): p. 1498-508.
176. Newport, M.J., et al., *A mutation in the interferon-gamma-receptor gene and susceptibility to mycobacterial infection.* N Engl J Med, 1996. 335(26): p. 1941-9.
177. Douvas, G.S., et al., *Gamma interferon activates human macrophages to become tumoricidal and leishmanicidal but enhances replication of macrophage-associated mycobacteria.* Infect Immun, 1985. 50(1): p. 1-8.
178. Rook, G.A., et al., *Activation of macrophages to inhibit proliferation of Mycobacterium tuberculosis: comparison of the effects of recombinant gamma-interferon on human monocytes and murine peritoneal macrophages.* Immunology, 1986. 59(3): p. 333-8.
179. Constant, P., et al., *Stimulation of human gamma delta T cells by nonpeptidic mycobacterial ligands.* Science, 1994. 264(5156): p. 267-70.
180. Constant, P., et al., *The antituberculous Mycobacterium bovis BCG vaccine is an attenuated mycobacterial producer of phosphorylated nonpeptidic antigens for human gamma delta T cells.* Infect Immun, 1995. 63(12): p. 4628-33.
181. Lang, F., et al., *Early activation of human V gamma 9V delta 2 T cell broad cytotoxicity and TNF production by nonpeptidic mycobacterial ligands.* J Immunol, 1995. 154(11): p. 5986-94.
182. Baust, J.M., B. Van, and J.G. Baust, *Cell viability improves following inhibition of cryopreservation-induced apoptosis.* In Vitro Cell Dev Biol Anim, 2000. 36(4): p. 262-70.
183. Matsushita, T., et al., *Apoptotic cell death and function of cryopreserved porcine hepatocytes in a bioartificial liver.* Cell Transplant, 2003. 12(2): p. 109-21.
184. Geginat, J., F. Sallusto, and A. Lanzavecchia, *Cytokine-driven proliferation and differentiation of human naive, central memory, and effector memory CD4(+) T cells.* J Exp Med, 2001. 194(12): p. 1711-9.
185. Carpenter, E., L. Fray, and E. Gormley, *Cellular responses and Mycobacterium bovis BCG growth inhibition by bovine lymphocytes.* Immunol Cell Biol, 1997. 75(6): p. 554-60.
186. Balu, S., et al., *A novel human IgA monoclonal antibody protects against tuberculosis.* J Immunol, 2011. 186(5): p. 3113-9.

187. Weir, R.E., et al., *Mycobacterial purified protein derivatives stimulate innate immunity: Malawians show enhanced tumor necrosis factor alpha, interleukin-1beta (IL-1beta), and IL-10 responses compared to those of adolescents in the United Kingdom.* Infect Immun, 2004. 72(3): p. 1807-11.
188. Kabelitz, D., et al., *The primary response of human gamma/delta + T cells to Mycobacterium tuberculosis is restricted to V gamma 9-bearing cells.* J Exp Med, 1991. 173(6): p. 1331-8.
189. De Libero, G., et al., *Selection by two powerful antigens may account for the presence of the major population of human peripheral gamma/delta T cells.* J Exp Med, 1991. 173(6): p. 1311-22.
190. Griffin, J.P., et al., *Kinetics of accumulation of gamma delta receptor-bearing T lymphocytes in mice infected with live mycobacteria.* Infect Immun, 1991. 59(11): p. 4263-5.
191. Havlir, D.V., et al., *Selective expansion of human gamma delta T cells by monocytes infected with live Mycobacterium tuberculosis.* J Clin Invest, 1991. 87(2): p. 729-33.
192. Rodgers, A., K.M. Whitmore, and K.B. Walker, *Potential correlates of BCG induced protection against tuberculosis detected in a mouse aerosol model using gene expression profiling.* Tuberculosis (Edinb), 2006. 86(3-4): p. 255-62.
193. Barker, K., et al., *Nonadherent cultures of human monocytes kill Mycobacterium smegmatis, but adherent cultures do not.* Infect Immun, 1996. 64(2): p. 428-33.
194. Hoft, D.F., R.M. Brown, and S.T. Roodman, *Bacille Calmette-Guerin vaccination enhances human gamma delta T cell responsiveness to mycobacteria suggestive of a memory-like phenotype.* J Immunol, 1998. 161(2): p. 1045-54.
195. Hoft, D.F. and J.M. Tennant, *Persistence and boosting of bacille Calmette-Guerin-induced delayed-type hypersensitivity.* Ann Intern Med, 1999. 131(1): p. 32-6.
196. Casetti, R. and A. Martino, *The plasticity of gamma delta T cells: innate immunity, antigen presentation and new immunotherapy.* Cell Mol Immunol, 2008. 5(3): p. 161-70.
197. Gioia, C., et al., *Different cytokine production and effector/memory dynamics of alpha beta+ or gamma delta+ T-cell subsets in the peripheral blood of patients with active pulmonary tuberculosis.* Int J Immunopathol Pharmacol, 2003. 16(3): p. 247-52.

198. Flesch, I.E. and S.H. Kaufmann, *Mechanisms involved in mycobacterial growth inhibition by gamma interferon-activated bone marrow macrophages: role of reactive nitrogen intermediates.* Infect Immun, 1991. 59(9): p. 3213-8.
199. Morita, C.T., et al., *Direct presentation of nonpeptide prenyl pyrophosphate antigens to human gamma delta T cells.* Immunity, 1995. 3(4): p. 495-507.
200. Sugawara, I., et al., *Protective efficacy of recombinant BCG Tokyo (Ag85A) in rhesus monkeys (Macaca mulatta) infected intratracheally with H37Rv Mycobacterium tuberculosis.* Tuberculosis (Edinb), 2009. 89(1): p. 62-7.
201. Verreck, F.A., et al., *MVA.85A boosting of BCG and an attenuated, phoP deficient M. tuberculosis vaccine both show protective efficacy against tuberculosis in rhesus macaques.* PLoS ONE, 2009. 4(4): p. e5264.
202. Schroeder, A., et al., *The RIN: an RNA integrity number for assigning integrity values to RNA measurements.* BMC Mol Biol, 2006. 7: p. 3.
203. Huang da, W., B.T. Sherman, and R.A. Lempicki, *Systematic and integrative analysis of large gene lists using DAVID bioinformatics resources.* Nat Protoc, 2009. 4(1): p. 44-57.
204. Algood, H.M., et al., *TNF influences chemokine expression of macrophages in vitro and that of CD11b+ cells in vivo during Mycobacterium tuberculosis infection.* J Immunol, 2004. 172(11): p. 6846-57.
205. Flynn, J.L., et al., *IL-12 increases resistance of BALB/c mice to Mycobacterium tuberculosis infection.* J Immunol, 1995. 155(5): p. 2515-24.
206. Tufariello, J.M., J. Chan, and J.L. Flynn, *Latent tuberculosis: mechanisms of host and bacillus that contribute to persistent infection.* Lancet Infect Dis, 2003. 3(9): p. 578-90.
207. Chackerian, A.A. and S.M. Behar, *Susceptibility to Mycobacterium tuberculosis: lessons from inbred strains of mice.* Tuberculosis (Edinb), 2003. 83(5): p. 279-85.
208. Minassian, A.M., et al., *Preclinical development of an in vivo BCG challenge model for testing candidate TB vaccine efficacy.* PLoS ONE, 2011. 6(5): p. e19840.
209. Power, C.A., et al., *A valid ELISPOT assay for enumeration of ex vivo, antigen-specific, IFNgamma-producing T cells.* J Immunol Methods, 1999. 227(1-2): p. 99-107.
210. MacMicking, J.D., et al., *Identification of nitric oxide synthase as a protective locus against tuberculosis.* Proc Natl Acad Sci U S A, 1997. 94(10): p. 5243-8.

211. Gonzalez-Juarrero, M., et al., *Immune response to Mycobacterium tuberculosis and identification of molecular markers of disease.* Am J Respir Cell Mol Biol, 2009. 40(4): p. 398-409.
212. De Groot, M.A., Fang, F. G., ed. *Nitric oxide and infection*. Kluwer Academic-Plenum, New York. 1999.
213. Elkington, P.T., C.M. O'Kane, and J.S. Friedland, *The paradox of matrix metalloproteinases in infectious disease.* Clin Exp Immunol, 2005. 142(1): p. 12-20.
214. Wilczynska, K.M., et al., *A novel mechanism of tissue inhibitor of metalloproteinases-1 activation by interleukin-1 in primary human astrocytes.* J Biol Chem, 2006. 281(46): p. 34955-64.
215. Cooper, A.M. and S.A. Khader, *The role of cytokines in the initiation, expansion, and control of cellular immunity to tuberculosis.* Immunological Reviews, 2008. 226: p. 191-204.
216. Cruz, A., et al., *Cutting edge: IFN-gamma regulates the induction and expansion of IL-17-producing CD4 T cells during mycobacterial infection.* J Immunol, 2006. 177(3): p. 1416-20.
217. Vordermeier, H.M., et al., *Viral booster vaccines improve Mycobacterium bovis BCG-induced protection against bovine tuberculosis.* Infect Immun, 2009. 77(8): p. 3364-73.
218. Prasad, H.K., R. Singh, and I. Nath, *Radiolabelled M. leprae resident in human macrophage cultures as an in vitro indicator of effective immunity in human leprosy.* Clin Exp Immunol, 1982. 49(3): p. 517-22.
219. Walker, L. and D.B. Lowrie, *Killing of Mycobacterium microti by immunologically activated macrophages.* Nature, 1981. 293(5827): p. 69-71.
220. Denis, M. and E. Ghadirian, *Granulocyte-macrophage colony-stimulating factor restricts growth of tubercle bacilli in human macrophages.* Immunol Lett, 1990. 24(3): p. 203-6.
221. Szeliga, J., et al., *Granulocyte-macrophage colony stimulating factor-mediated innate responses in tuberculosis.* Tuberculosis (Edinb), 2008. 88(1): p. 7-20.
222. Park, C.H., et al., *Hepcidin, a urinary antimicrobial peptide synthesized in the liver.* J Biol Chem, 2001. 276(11): p. 7806-10.
223. Zasloff, M., *Antibiotic peptides as mediators of innate immunity.* Curr Opin Immunol, 1992. 4(1): p. 3-7.
224. Sow, F.B., et al., *Expression and localization of hepcidin in macrophages: a role in host defense against tuberculosis.* Journal of Leukocyte Biology, 2007. 82(4): p. 934-945.

225. Sow, F.B., et al., *Mycobacterium tuberculosis components stimulate production of the antimicrobial peptide hepcidin.* Tuberculosis, 2011. 91(4): p. 314-321.
226. Prinzis, S., D. Chatterjee, and P.J. Brennan, *Structure and antigenicity of lipoarabinomannan from Mycobacterium bovis BCG.* J Gen Microbiol, 1993. 139(11): p. 2649-58.
227. Mollenkopf, H.J., K. Hahnke, and S.H. Kaufmann, *Transcriptional responses in mouse lungs induced by vaccination with Mycobacterium bovis BCG and infection with Mycobacterium tuberculosis.* Microbes Infect, 2006. 8(1): p. 136-44.
228. Darnell, J.E., Jr., I.M. Kerr, and G.R. Stark, *Jak-STAT pathways and transcriptional activation in response to IFNs and other extracellular signaling proteins.* Science, 1994. 264(5164): p. 1415-21.
229. Means, T.K., et al., *The CD14 ligands lipoarabinomannan and lipopolysaccharide differ in their requirement for Toll-like receptors.* J Immunol, 1999. 163(12): p. 6748-55.